REGULATION OF CD38 BY IRF4 IN CHRONIC LYMPHOCYTIC LEUKAEMIA

A thesis submitted in part requirement for the
degree of Doctor of Philosophy

Helen Marr

Northern Institute for Cancer Research,
Faculty of Medical Sciences,
Newcastle University

January 2016

ABSTRACT

Genome-wide association analysis identified rs872071, a common variant in the 3'UTR of IRF4, as tagging a risk allele for chronic lymphocytic leukaemia (CLL). The risk allele is significantly associated with expression of CD38, a poor prognostic marker in CLL. IRF4 is a transcription factor with pleiotropic roles in the regulation of B cell development, and interrogation of the *CD38* gene identified a number of putative binding sites for IRF4, suggesting that CD38 may be transcriptionally regulated by IRF4.

Chromatin immunoprecipitation (ChIP) demonstrated significant IRF4-*CD38* binding at two composite ETS/IRF consensus element (EICE) sites in SU-DHL-6 and MEC-1 mature B cell lines. Furthermore, there was evidence of IRF4-*CD38* binding at these EICE sites in primary CLL lymphocytes in some, but not all, cases. ChIP studies using markers of histone methylation suggested increased transcriptional activation at the IRF4-*CD38* binding sites in MEC-1 cells with IRF4 knockdown. In contrast, transcriptional activity at these sites appeared to be reduced in SU-DHL-6 cells with IRF4 knockdown.

Co-culture of primary CLL lymphocytes on a CD40L-expressing monolayer led to an upregulation of IRF4 expression, but no consistent effect on CD38 expression. In addition, ChIP studies using markers of histone methylation were suggestive of reduced transcriptional activity at the IRF4-*CD38* binding site after CD40L co-culture, suggesting that IRF4 may be a negative regulator of CD38 in CLL.

Taken together, the evidence indicates that IRF4 binds to the *CD38* locus. However, direct experimental evidence for an effect on CD38 expression is lacking. It is necessary to consider that the interaction between IRF4 and CD38 is unlikely to be a linear signal transduction pathway. Indeed the prevailing evidence regarding the function of IRF4 in B cells suggests a complex signalling network involving numerous other transcription factors and cytokines.

Furthermore, IRF4 has been suggested as a putative therapeutic target in haematological malignancies including myeloma. Transient IRF4 knockdown using RNA

interference (RNAi) techniques was tolerated by SU-DHL-6, MEC-1 and lymphoblastoid TK6 cell lines, though cell proliferation in TK6 and SU-DHL-6 was significantly impaired. Long-term stable knockdown was also tolerated in TK6 cells, but not in MEC-1 cells, suggesting an essential role for IRF4 in maintenance of MEC-1 cells. Targeted knockdown of IRF4 also sensitised TK6 B cells and MEC-1 CLL cells to the growth inhibitory effects of fludarabine, a nucleoside analogue used in the treatment of CLL. These findings indicate that IRF4 is necessary to the maintenance of MEC-1 cells, which represent a CLL cell line model.

A greater understanding of the role of IRF4 in the development and maintenance of CLL may indicate new therapeutic targets in CLL. Indeed, a recently developed novel mouse model of CLL has indicated that deficient IRF4 expression predisposes to the development of CLL. However, the role of IRF4 in the maintenance of CLL cells is yet to be determined. The heterogeneous nature of IRF4 expression in primary CLL lymphocytes determined here, and its potentially pleiotropic role in the transcriptional regulation of CD38 in B cells at different stages of differentiation, suggest that if IRF4 is a key player in the maintenance of the leukaemic clone, its role may be context or patient specific, and dependent on other signalling components or somatic genetic abnormalities.

ACKNOWLEDGEMENTS

Firstly, I would like to thank Bright Red and the Medical Research Council for their generous funding of my PhD studies.

I am extremely grateful to Dr Reuben Tooze, (Leeds Institute of Molecular Medicine, University of Leeds) who kindly made available unpublished data which is discussed in Chapter 3 of this thesis. Dr Tooze gave a fascinating presentation about IRF4 in B cell lymphoma at the Northern Institute of Cancer Research during the second year of my PhD, and this was extremely helpful in informing a successful change of tack in my ChIP studies.

I would like to thank Dr Andy Rawstron (Haematological Malignancy Diagnostic Service, Leeds) for supplying the flow cytometry data with regard to TK6 cell line surface marker expression, featured in Chapter 3. I would also like to thank Dr Chris Pepper for supplying the CD40L-expressing and non-expressor fibroblast cell lines, for use in co-culture studies of primary CLL lymphocytes.

I am very grateful to Dr Sue Tudhope who was extremely helpful and patient in assisting me with flow cytometry and primary CLL lymphocyte co-culture work in the first year of my PhD when I was still finding my feet.

I am also grateful to Dr Jonathan Wallis and to the patients of the Freeman Hospital CLL clinic who enabled me to obtain a regular supply of patient samples for work on primary CLL cells.

I would like to thank my colleagues in the Molecular Carcinogenesis group for their support throughout my PhD. In particular, Dr Sarah Fordham and Dr Nicola Sunter have provided me with an enormous amount of practical help, moral support and friendship, throughout my project. Dr Fordham provided data pertaining to TK6 puromycin and polybrene sensitivity, discussed in Chapters 2 and 4. It has also been a great pleasure to work alongside Mohammed Nahari as he has been studying for his PhD.

I would like to thank my supervisors: Professor James Allan, Dr Elaine Willmore and Dr Luke Gaughan. Dr Gaughan has provided essential instruction and supervision in ChIP work throughout the project. Dr Willmore has provided access to patient samples, and supervisory support particularly in the setting up of the primary cell co-culture work. Finally, Professor Allan has been unendingly approachable and good-humoured in his role as my PhD supervisor, and I am extremely grateful to him for his patience, guidance and support.

TABLE OF CONTENTS

Chapter 1. Introduction 1

1.1 B-cell biology and differentiation 2

1.1.1 Basic B-cell function 2

1.1.2 B cell maturation 2

1.1.3 B cell differentiation in the germinal centre 2

1.2 IRF4 6

1.2.1 Discovery of IRF4 6

1.2.2 Structure and function of IRF4 8

1.2.3 Expression of IRF4 10

1.2.4 IRF4 and B cell maturation 11

1.2.5 IRF4 in the germinal centre 12

1.2.5.a IRF4 and class switch recombination (CSR) 14

1.2.5.b IRF4 and plasma cell differentiation 15

1.2.5.c IRF4 coordinates CSR and plasma cell differentiation 15

1.2.5.d IRF4 and the initiation of the germinal centre reaction 16

1.2.6 Interaction of IRF4 and IRF8 18

1.3 CD38 19

1.3.1 Distribution and function of CD38 19

1.3.2 CD38 and B cells 20

1.3.3 CD38 enzyme function 21

1.4 Chronic Lymphocytic Leukaemia (CLL) 21

1.4.1 Monoclonal B cell lymphocytosis 23

1.4.2 Staging of CLL 23

1.4.3 Somatic prognostic markers 24

1.4.3.a *IGHV* mutation 24

1.4.3.b CD38 expression 24
1.4.3.c ZAP70 25
1.4.3.d Cytogenetics 26
1.4.3.e Somatic gene mutations 28
1.4.3.f CD49d 30
1.4.3.g Telomere length 30
1.4.4 Aetiology and maintenance of CLL 30
1.4.4.a CLL cell of origin 30
1.4.4.b BCR signalling 31
1.4.4.c Tumour microenvironment 33
1.4.4.d Nurse-like cells 34
1.4.4.e Homing CLL cells to lymph nodes 36
1.4.4.f T cell interactions 37
1.4.5 CD38 and CLL aetiology 38
1.4.6 CLL Therapy 40
1.4.6.a Novel agents in CLL 42
1.4.7 Constitutional genetics in CLL 44
1.4.7.a *IRF4* carries a common risk allele for CLL incidence 46
1.4.7.b IRF4 risk allele is associated with CD38 positivity 48
1.5 Hypothesis 48
1.6 Aims 49

Chapter 2. Materials and Methods 50

2.1 Chemicals and Reagents 51

2.2 Cell Lines 51

2.3 General Cell Culture Methods 51

2.3.1 Routine Cell Culture 51

2.3.2 Cell counting and determination of cell density for suspension cell lines 53

2.3.3 Passage of suspension cell lines 53

2.3.4 Passage of adherent mouse fibroblast cell lines 53

2.3.5 Cryopreservation of cell stocks 54

2.3.6 Resuscitation of frozen cell stocks 54

2.3.7 Preparation of cell pellets 54

2.3.8 Setting up cell growth curves 55

2.3.9 Setting up cytotoxic growth inhibition assays 55

2.4 Western immunoblotting 57

2.4.1 Cytosol preparation 57

2.4.2 Estimation of protein concentration by Pierce BCA assay 57

2.4.3 SDS polyacrylamide gene electrophoresis (PAGE) and electrophoretic transfer 57

2.4.4 Antibody detection and visualisation of bound proteins 58

2.5 Generation of knockdown cell lines deficient in IRF4 using short interfering and short hairpin RNA-mediated gene knockdown 60

2.5.1 siRNA constructs, controls and reagents 60

2.5.2 siRNA transfection 62

2.5.3 shRNA constructs, controls and reagents 63

2.5.4 Assessment of puromycin sensitivity 63

2.5.5 Assessment of hexadimethrine bromide sensitivity 65

2.5.6 Lentiviral transduction 67

2.5.7 Transfer of transduced cells in to puromycin-containing media 68

2.5.8 Establishing transduced cell clones with uniform IRF4 protein knockdown 68

2.6 Chromatin immunoprecipitation 70

2.6.1 Immunoprecipitation to optimise antibody for ChIP 70

2.6.2 Preparation of chromatin for ChIP 73

2.6.2.a Cross-linking chromatin 73

2.6.2.b Lysis of the cellular and nuclear membranes to isolate nuclear material 73

2.6.2.c Sonication of chromatin to generate fragments 74

2.6.2.d Determining DNA concentration in chromatin preparation 74

2.6.2.e Confirmation of chromatin fragment length prior to ChIP 74

2.6.3 Manual ChIP procedure 75

2.6.3.a Preparation of magnetic beads with ChIP antibody 75

2.6.3.b Preparation of sonicated chromatin samples for ChIP, and preparation of the input sample 76

2.6.3.c Chromatin immunoprecipitation step 76

2.6.3.d Elution and cross-link reversal of ChIP and input samples 77

2.6.3.e DNA extraction 78

2.6.4 Robotic ChIP procedure 78

2.6.5 Real time PCR set up 78

2.6.6 Analysis of ChIP results 79

2.7 Flow cytometry 80

2.7.1 Flow cytometry antibodies 81

2.7.2 Determining CD38 expression in cell lines and primary leukaemic lymphocytes 81

2.7.3 Determining CD40L expression in co-culture fibroblast monolayer 84

2.8 Culture of primary leukaemic lymphocytes 86

2.8.1 Collection and separation of primary leukaemic lymphocytes from whole blood samples 86

2.8.2 Cryopreservation of primary lymphocytes 86

2.8.3 Preparing fibroblast monolayer for co-culture of leukaemic lymphocytes 87

2.8.4 Co-culture of primary lymphocytes on fibroblast layer 87

2.8.5 Harvest of leukaemic lymphocytes from co-culture 87

2.8.6 CFSE labelling and measurement to demonstrate proliferation of primary leukaemic lymphocytes 88

Chapter 3. Binding of IRF4 to *CD38* **90**

3.1 Introduction **91**

3.1.1 IRF4 consensus binding site 91

3.1.2 Interrogation of the CD38 upstream flanking sequence and 5'UTR reveals six putative binding sites for IRF4 91

3.1.3 Chromatin immunoprecipitation (ChIP) 93

3.2 Aims of chapter 3 ..... **93**

3.3 Results **94**

3.3.1 Initial ChIP work in TK6 B-lymphoblastoid cell line 94

3.3.1.a Immunoprecipitation to identify a functional IRF4 antibody suitable for ChIP 94

3.3.1.b Primer design for amplification of IRF4 binding sites in the *CD38* 5'UTR and upstream flanking sequence 98

3.3.1.c Establishment of ChIP using an antibody to histone as a positive control 101

3.3.1.d IRF4 does not bind at the *CD38* 5'UTR or upstream flanking sequences in TK6 105

3.3.2 Cell lines and expression of IRF4 binding partners 109

3.3.3 Genome wide ChIP binding data across the CD38 locus 118

3.3.4 Investigation by ChIP of IRF4-CD38 intron 1 binding in SU-DHL-6 and MEC-1 cell lines 123

3.3.4.a Validation of primers to elements 1 and 2, and to *CD38* 5'UTR 123

3.3.4.b Evidence of IRF4-*CD38* binding in SU-DHL-6 and MEC-1 cells 127

3.4 Discussion **134**

3.4.1 IRF4-CD38 binding 134

3.4.2 Technical issues in the interpretation of ChIP data 138

3.4.2.a Excessive non-specific antibody-chromatin binding 138

3.4.2.b Inter-assay variability within cell lines 139

3.5 Summary of chapter 3 ..... **140**

Chapter 4. Investigation of the relationship between IRF4 and CD38 using *in vitro* B-cell model systems 141

4.1 Introduction 142

4.1.1 The function of IRF4 as a transcription factor 142

4.1.2 RNA interference techniques 144

4.2 Aims of chapter 4 146

4.3 Results 148

4.3.1 siRNA-mediated knockdown of IRF4 in TK6 cell line 148

4.3.1.a Flow cytometry analysis of CD38 expression in TK6 cells with siRNA-mediated transient IRF4 knockdown 148

4.3.2 siRNA-mediated knockdown of IRF4 in MEC-1 cell line 153

4.3.2.a Flow cytometry analysis of CD38 expression in MEC-1 cells with siRNA-mediated transient IRF4 knockdown 153

4.3.3 siRNA-mediated knockdown of IRF4 in DHL6 cell line 157

4.3.3.a Flow cytometry analysis of CD38 expression in SU-DHL-6 cells with siRNA-mediated transient IRF4 knockdown 157

4.3.4 shRNA-mediated knockdown of IRF4 in TK6 cell line 161

4.3.4.a TK6 cell populations generated with constitutive IRF4 knockdown, by shRNA transduction 161

4.3.4.b TK6 cell clones generated with uniform IRF4 knockdown 161

4.3.4.c CD38 expression by flow cytometry in TK6 cell clones with shRNA-mediated IRF4 knockdown 164

4.3.5 shRNA-mediated knockdown of IRF4 in MEC-1 and SUDHL-6 cell lines 166

4.3.5.a MEC-1 shRNA transduction and cell cloning 166

4.3.5.b SU-DHL-6 shRNA transduction 166

4.3.6 Effect of siRNA-mediated transient IRF4 knockdown on IRF4-CD38 binding 167

4.3.6.a ChIP in MEC-1 cells with siRNA-mediated IRF4 knockdown 167

4.3.6.b ChIP in SU-DHL-6 cells with siRNA-mediated IRF4 knockdown 170

4.4 Discussion 172

4.4.1 Generating cells with IRF4 knockdown 172

4.4.2 CD38 expression in cells with IRF4 knockdown 174

4.4.3 ChIP in MEC-1 and SU-DHL-6 cells with siRNA-induced IRF4 knockdown 176

4.5 Summary of chapter 4 179

Chapter 5. Effect of IRF4 knockdown on cell growth, and sensitivity to cytotoxic agents using *in vitro* B cell model systems 180

5.1 Introduction 181

5.1.1 IRF4 in B cell malignancies 181

5.1.2 Cytotoxic agents currently used for the treatment of CLL 182

5.2 Aims of chapter 5 183

5.3 Results 184

5.3.1 Effect of siRNA-mediated IRF4 knockdown on cell growth in MEC-1 cells 184

5.3.2 Effect of siRNA-mediated IRF4 knockdown on sensitivity to cytotoxic agents in MEC-1 cells 184

5.3.2.a Fludarabine 186

5.3.2.b Ibrutinib 186

5.3.3 Effect of siRNA-mediated IRF4 knockdown on cell growth in SU-DHL-6 cells 190

5.3.4 Effect of siRNA-mediated IRF4 knockdown on sensitivity to cytotoxic agents in SU-DHL-6 cells 190

5.3.4.a Fludarabine 190

5.3.5 Effect of shRNA-mediated constitutive IRF4 knockdown on cell growth in TK6 cells 194

5.3.6 Effect of shRNA-mediated constitutive IRF4 knockdown on sensitivity to cytotoxic agents in TK6 B cells 194

5.3.6.a Fludarabine 196

5.3.6.b Bendamustine 199

5.4 Discussion 202

5.4.1 IRF4 knockdown and growth kinetics in B cells 202

5.4.2 IRF4 knockdown and sensitivity to anti-leukemic chemotherapy 205

5.5 Summary of chapter 5 206

Chapter 6. The role of IRF4 as a regulator of *CD38* in primary CLL lymphocytes cultured *ex vivo* 207

6.1 Introduction 208

6.2 Aims of chapter 6 208

6.3 Results 210

6.3.1 Primary CLL lymphocytes express IRF4 210

6.3.2 Primary CLL lymphocytes co-culture on a CD40L monolayer 210

6.3.2.a Primary CLL lymphocytes demonstrate upregulation of IRF4 protein expression on CD40L co-culture 210

6.3.2.b Primary CLL lymphocyte proliferation on CD40L monolayer 214

6.3.2.c CD38 expression in primary CLL lymphocytes co-cultured on CD40L monolayer 216

6.3.3 ChIP using primary leukaemic lymphocytes 218

6.3.3.a IRF4-*CD38* binding in primary *ex vivo* CLL lymphocytes prior to co-culture 218

6.3.3.b Investigation of IRF4-*CD38* binding in primary *ex vivo* CLL lymphocytes after CD40L monolayer co-culture 220

6.3.3.c IRF4-*CD38* binding in primary *ex vivo* CLL lymphocytes after CD40L co-culture 222

6.3.3.d *CD38* binding by histone methylation marks after CD40L monolayer co-culture 225

6.4 Discussion 230

6.4.1 Technical issues in primary CLL lymphocyte ChIP 230

6.4.2 IRF4 expression in primary CLL lymphocytes before and after CD40L monolayer co-culture 232

6.4.3 IRF4 expression in CLL 232

6.4.4 CD38 expression in primary CLL lymphocytes after CD40L co-culture 233

6.4.5 ChIP in primary CLL lymphocytes 234

6.5 Summary 235

Chapter 7. Concluding Discussion **237**

7.1 Discussion **238**

7.2 Further work **244**

References **245**

LIST OF FIGURES

Figure 1.1 B cell maturation 3

Figure 1.2 B cell differentiation through the germinal centre 5

Figure 1.3 IRF4 protein structure 9

Figure 1.4 IRF4 is essential to the germinal centre reaction 13

Figure 1.5 Graded expression of IRF4 coordinates class switch recombination (CSR) and plasmacytic differentiation through a model of 'kinetic control' 17

Figure 1.6 rs872071 risk allele in IRF4 47

Figure 2.1 Optimising CD38 antibody concentration for use in primary CLL lymphocytes 83

Figure 2.2 Using flow cytometry to assess CD38 expression in primary CLL lymphocytes 85

Figure 3.1 Six putative IRF4 binding sites are found in the CD38 5'UTR and upstream flanking sequence 92

Figure 3.2 TK6 cell line expresses IRF4 protein 96

Figure 3.3 A goat polyclonal IRF4 antibody (Santa Cruz, M17, sc-6059) was used in an immunoprecipitation (IP) experiment in TK6 cells, to assess its suitability for ChIP 97

Figure 3.4 Chromatin fragments obtained from TK6 cells for ChIP using antibody to histone 3 (H3) 103

Figure 3.5 Successful establishment of manual ChIP protocol in TK6 cells using antibody to histone 3 (H3) 104

Figure 3.6 Chromatin fragments obtained from TK6 cells for ChIP using IRF4 antibody 106

Figure 3.7 ChIP using antibody to IRF4 in TK6 cells 107

Figure 3.8 Dissociation curves for CD38 primer set 5 108

Figure 3.9 Wildtype oligonucleotide probes used in electrophoretic mobility shift assays (EMSAs) to investigate the DNA binding domains of the PU.1/ IRF4 complex 110

Figure 3.10 Western immunoblots demonstrating the expression of IRF4 and its common binding partners in a panel of cell lines 112

Figure 3.11 Composite Ets/IRF consensus element (EICE) binding sites in CD38 upstream flanking sequence and 5'UTR 113

Figure 3.12 Comparison of IRF4, PU1 and CD38 mRNA expression by cell lines 115

Figure 3.13 IRF4, PU.1 and CD38 mRNA expression by MEC-1 cell line 116

Figure 3.14 Flow cytometry histogram plots: CD38 expression in TK6, SU-DHL-6 and MEC-1 cell lines 117

Figure 3.15 Element 1 binding: ChIP sequencing (ChIP seq) data demonstrates binding in CD38 by IRF4, PU.1 and SPI-B in OCI-LY3 and OCI-LY10 lymphoma cell lines 120

Figure 3.16 Element 2 binding: ChIP sequencing data demonstrates binding in CD38 by IRF4, PU.1 and SPI-B in OCI-LY3 and OCI-LY10 lymphoma cell lines 121

Figure 3.17 CD38 gene and potential IRF4 binding sites 122

Figure 3.18 SU-DHL-6 and MEC-1 chromatin fragment size after sonication 128

Figure 3.19 ChIP in SU-DHL-6 using IRF4 antibody to determine IRF4-CD38 binding 130

Figure 3.20 ChIP in MEC-1 using IRF4 antibody to determine IRF4-CD38 binding 131

Figure 3.21 ChIP in TK6 using IRF4 antibody to determine IRF4-CD38 binding 132

Figure 4.1 Protein knockdown by RNA interference (RNAi) using short interfering (siRNA) and short hairpin (shRNA) constructs 147

Figure 4.2 IRF4 protein knockdown in TK6 using Combination siRNA 149

Figure 4.3 Comparing IRF4 knockdown achieved in TK6 cells using 500nM or 1μM concentration Combination siRNA 150

Figure 4.4 CD38 expression in TK6 cells with transient siRNA-mediated IRF4 knockdown 151

Figure 4.5 IRF4 protein knockdown in MEC-1 using IRF4 Combination siRNA 154

Figure 4.6 CD38 expression in MEC-1 cells with siRNA-mediated transient IRF4 knockdown 155

Figure 4.7 Transient siRNA-mediated IRF4 knockdown in SU-DHL-6 cells 158

Figure 4.8 CD38 expression in SU-DHL-6 cells with transient siRNA-mediated IRF4 knockdown 159

Figure 4.9 TK6 cell populations generated after transduction with shRNA constructs targeted against IRF4 162

Figure 4.10 TK6 cells cloned from cell populations transduced with off target shRNA or shRNA construct 6, targeted to IRF4 163

Figure 4.11 ChIP using IRF4 and H3K4me3 antibodies in MEC-1 cells with siRNA-mediated IRF4 knockdown 169

Figure 4.12 ChIP using IRF4 and H3K9me3 antibodies in SU-DHL-6 cells with siRNA-mediated IRF4 knockdown 171

Figure 5.1 Proliferation of MEC-1 cells with transient siRNA-mediated IRF4 knockdown 185

Figure 5.2 Effect of DMSO on siRNA treated MEC-1 cells 187

Figure 5.3 Fludarabine cytotoxicity in MEC-1 cells with siRNA-mediated IRF4 knockdown 188

Figure 5.4 Ibrutinib cytotoxicity in MEC-1 cell line with transient IRF4 knockdown 189

Figure 5.5 Proliferation of SU-DHL-6 cells with transient IRF4 knockdown 191

Figure 5.6 Effect of DMSO on siRNA-treated SU-DHL-6 cells 192

Figure 5.7 Fludarabine cytotoxicity in SU-DHL-6 cells with siRNA-mediated IRF4 knockdown 193

Figure 5.8 Proliferation of TK6 cell clones with shRNA-mediated constitutive IRF4 knockdown 195

Figure 5.9 Effect of DMSO on TK6 cells with shRNA-mediated constitutive IRF4 knockdown 197

Figure 5.10 Growth inhibition with fludarabine (0-10μM) in TK6 cell clones with shRNA-mediated constitutive IRF4 knockdown 198

Figure 5.11 Growth inhibition with fludarabine (0-15μM) in TK6 cell clones with shRNA-mediated constitutive IRF4 knockdown 200

Figure 5.12 Bendamustine cytotoxicity in TK6 cells with stable shRNA-mediated IRF4 knockdown 201

Figure 6.1 IRF4 expression by western immunoblotting in primary lymphocytes from 11 CLL patients 212

Figure 6.2 IRF4 expression in primary CLL lymphocytes after culture on CD40L-expressing fibroblast monolayer 213

Figure 6.3 Proliferation of CLL lymphocytes cultured on CD40L monolayer 215

Figure 6.4 CD38 expression in primary CLL lymphocytes from a CD38+ CLL patient, after co-culture on a CD40L monolayer 217

Figure 6.5 IRF4-CD38 binding in primary CLL cells: patient 6 219

Figure 6.6 Agarose gel electrophoresis of chromatin fragments obtained from primary CLL lymphocytes from 3 patients, after CD40L monolayer co-culture 223

Figure 6.7 IRF4-CD38 binding in primary CLL lymphocytes from 3 patients after co-culture on CD40L monolayer 224

Figure 6.8 ChIP investigating IRF4-CD38 binding in primary CLL lymphocytes from patient 3 after co culture on NTL or CD40L monolayers 226

Figure 6.9 ChIP in patient 3 investigating binding by IRF4, H3K9me3 (repressive histone mark) and H3K4me3 (activating histone mark) antibody in CD38 227

Figure 6.10 ChIP using antibody to H3K9me3 (repressive histone mark) in primary CLL lymphocytes from patient 9 after co-culture on CD40L monolayer 229

LIST OF TABLES

Table 1.1 Discovery of IRF4 7

Table 1.2 Matute scoring system for CLL diagnosis; Binet and Rai scoring systems for staging disease 22

Table 1.3 Incidence of common acquired cytogenetic abnormalities in CLL and their impact on survival 27

Table 1.4 Risk alleles for CLL identified in genome wide association studies (GWAS) 45

Table 2.1 Cell lines 52

Table 2.2 Preparation of cytotoxic agents for growth inhibition assays 56

Table 2.3 Primary and secondary antibodies used in western immunoblotting 59

Table 2.4 siRNA constructs for knockdown of *IRF4* 61

Table 2.5 Mission® shRNA constructs used to target IRF4 in a panel of lymphoid cell lines 64

Table 2.6 Establishing the sensitivity of cell lines to puromycin 66

Table 2.7 Antibodies used in chromatin immunoprecipitation (ChIP) 71

Table 2.8 Antibodies used in flow cytometry 82

Table 3.1 TK6 expresses surface CD38 95

Table 3.2 *CD38* 5'UTR and upstream flanking sequence primer sets 99

Table 3.3 Efficiency of CD38 primer sets 1-5 100

Table 3.4 Chromatin used in initial ChIP experiments in TK6 102

Table 3.5 CD38 expression in TK6, SU-DHL-6 and MEC-1 cell lines 117

Table 3.6 Primer sets to putative IRF4 binding sites in CD38 element 1 and element 2 124

Table 3.7 Efficiency of primer sets to elements 1 and 2 in CD38 intron 1 125

Table 3.8 Efficiency of new primer sets to CD38 5'UTR 126

Table 3.9 Chromatin used for ChIP in SU-DHL-6, MEC-1 and TK6 cells, with IRF4 antibody 129

Table 4.1 IRF4 acts as a dichotomous regulator of target genes 145

Table 4.2 Flow cytometry histogram statistics demonstrating CD38 expression in TK6 cells with transient siRNA-mediated IRF4 knockdown 152

Table 4.3 Flow cytometry histogram statistics demonstrating CD38 expression in MEC-1 cells with transient siRNA-mediated IRF4 knockdown 156

Table 4.4 Flow cytometry histogram statistics demonstrating CD38 expression in SU-DHL-6 cells with transient siRNA-mediated IRF4 knockdown 160

Table 4.5 Flow cytometry histogram statistics demonstrating CD38 expression in TK6 cells with shRNA-induced constitutive IRF4 knockdown 165

Table 5.1 Effect of IRF4 on proliferation of a range of B cell lines 204

Table 6.1 Patient characteristics 211

Table 6.2 CD38 expression in primary CLL lymphocytes after co-culture on CD40L monolayer 217

Table 6.3 DNA yield from chromatin fragments after sonication: a comparison of DNA yield from primary CLL cells cultured on CD40L monolayer with cells cultured on NTL monolayer 221

LIST OF EQUATIONS

Equation 2.1 *Determining the volume of shRNA construct required to achieve required MOI* 67

Equation 2.2 *Formula 3.1* 79

Equation 2.3 *Determining the adjusted input Ct value* 80

Equation 2.4 *Calculating the % input achieved using ChIP antibodies* 80

ABBREVIATIONS

APRIL	A proliferation-inducing ligand
ADP	Adenosine diphosphate
ADPr	Adenosine disphosphate ribose
AID	Activation-induced cytidine deaminase
ANOVA	Analysis of variance
APC	Allophycocyanin
APC	Antigen presenting cell
AR	Autoregulatory
ATM	ataxia telangiectasia mutated
BCA	Bicinchoninic acid assay
BAFF	B-cell activating factor of the tumour necrosis family
BCR	B cell receptor
Bp	Base pair
BTK	Bruton's tyrosine kinase
C terminal	Carboxyl terminal
CAT	Chloramphenicol acetyl-transferase
CD (5, 19 etc)	Cluster of differentiation
CD40L	CD40 ligand
CDS	Coding domain sequence
CFSE	Carboxyfluorescein succinimidyl ester
ChIP	Chromatin immunoprecipitation
CLL	Chronic lymphocytic leukaemia
CSR	Class switch recombination
cADPR	cyclic ADPR
Del	Deletion

DMSO	Dimethyl sulfoxide
DNA	Deoxyribonucleic acid
ECL	Enhanced chemiluminescence
EDTA	Ethylenediaminetetraacetic acid
EGTA	Ethylene glycol tetraacetic acid
EICE	Ets/Interferon consensus element
Eκ3'	3' enhancer of the immunoglobulin kappa light chain
EMSA	Electrophoretic mobility shift assay
EλB	B domain of the immunoglobulin lambda light chain enhancer
FBS	Fetal bovine serum
FCR	Fludarabine cyclophosphamide rituximab chemoimmunotherapy
FDC	Follicular dendritic cell
FISH	Fluorescence in situ hybridisation
FITC	Fluorescein isothiocyanate
GC	Germinal centre
GWAS	Genome wide association study
HCDR	Heavy chain complementarity determining region
HEVs	High endothelial venules
HR	Hazard ratio
HMEC-1	Human microvascular endothelial cell line
HUVECs	Human umbilical vein endothelial cells
IAD	Interferon activation domain
ICSAT	Interferon consensus sequence binding protein in T cell leukaemia
iEK	Intronic kappa light chain enhancer
Ig	Immunoglobulin
IGHV	Variable region of the heavy chain genes

IHC	Immunohistochemistry
IL (-2, -4, -7)	Interleukin
IP3	Inositol triphosphate
ISG15	Interferon stimulated gene 15
IP	Immunoprecipitation
IRF (1,2,4,8)	Interferon regulatory factor
ISRE	Interferon stimulated response element
LB (1,2,3)	Lysis buffer
LiCL	Lithium chloride
LPS	Lipopolysaccharide
LSIRF	Lymphoid-restricted IRF
M	Molar
MAF	Minor allele frequency
MSCs	Marrow stromal cells
MMP-9	Matrix-metalloproteinase-9
MBL	Monoclonal B cell lymphocytosis
MAPK	Mitogen-activated protein kinase pathway
mg	Milligram
MOI	Multiplicity of infection
N terminal	Amino terminal
Na deoxycholate	Sodium deoxycholate
NAD	Nicotinamide adenine dinucleotide
NF-EM5	Nuclear factor enhancer motif 5
NFκB	Nuclear factor kappa B
nM	Nanomolar
NTC	Non template control
NTL	Non CD40L-expressing murine fibroblast line

NLC	Nurse-like cell
OS	Overall survival
PBS	Phosphate buffered saline
PCR	Polymerase chain reaction
PE	Phycoerythrin
PercP	Peridinin chlorophyll
PEST	Proline, glutamic acid, serine, threonine
PFS	Progression free survival
PI3-K	Phosphoinositide 3-kinase
Pip	PU.1 dependent protein
PRDM1	PR domain zinc finger protein 1
pre-BCR	Pre B cell receptor
PVDF	Polyvinylidene fluoride
qPCR	Quantitative PCR
RISC	RNA-induced silencing complex
RNA	Ribonucleic acid
RNAi	RNA interference
rtPCR	Real time PCR
SDS	Sodium dodecyl sulfate
SDS-PAGE	Sodium dodecyl sulphate polyacrylamide gel electrophoresis
SF3B1	Splicing factor 3b subunit 1
SHM	Somatic hypermutation
shRNA	Short hairpin RNA
siRNA	Short interfering RNA
SNP	Single nucleotide polymorphism
SDF-1	Stromal-derived-growth factor 1
T-ALL	T cell acute lymphoblastic leukaemia

TBS	Tris-buffered saline
T_H	T helper cells
TP53	Tumour protein 53
H3K4me3	Trimethylated histone 3 lycine 4
H3K9me3	Trimethylated histone 3 lycine 9
TRIS	Tris(hydroxymethyl)aminomethane
Tu	Viral titres
UTR	Untranslated region
V	Volts
V(D)J	Variable diversity joining region
VCAM-1	Vascular cell adhesion molecule-1
VLA-4	Very late antigen-4
ZAP70	Zeta-associated protein of 70kDa
µg	Microgram
µM	Micromolar

Chapter 1. Introduction

1.1 B-cell biology and differentiation

1.1.1 Basic B-cell function

B cells can be distinguished from other lymphocytes by the presence of the B cell receptor (BCR) which comprises the membrane-bound immunoglobulin (Ig) and associated heterodimeric CD79 molecule. Through the B cell receptor, B cells have the capacity to recognise foreign antigens and to secrete specific antibodies, and are therefore vital in the provision of humoral immunity.

1.1.2 B cell maturation

B cells are generated from haematopoietic stem cells in the bone marrow. Their maturation is characterised by random rearrangement of the variable (V) diversity (D) joining (J) antibody gene loci. (Carsetti, 2000)

Progenitor B cells (pro-B cells) first undergo rearrangement of the heavy chain immunoglobulin locus. Once the heavy chain μ protein appears in the cytoplasm, it is paired with surrogate light chains to form a pre-B cell receptor (pre-BCR), along with signalling molecules Igα and Igβ. Autonomous signalling via the pre-BCR stimulates proliferation and survival, and these large pre-B cells therefore undergo a brief clonal expansion before the pre-BCR is downregulated. The cells are then able to exit the cell cycle and enter a resting phase as small pre-B cells, and the immunoglobulin light chain locus is rearranged. Rearranged light chains are then assembled with heavy chains into a mature B cell receptor which is expressed on the cell surface as an IgM molecule. (Figure 1.1)

The B cells then leave the marrow to complete their final development to mature cells in the periphery. Carsetti (2000)

1.1.3 B cell differentiation in the germinal centre

The germinal centre (GC) is the main source of memory B cells and plasma cells: antibody-secreting B cells which are produced in response to stimulation by an exogenous antigen. (Klein and Dalla-Favera, 2008) (Figure 1.2)

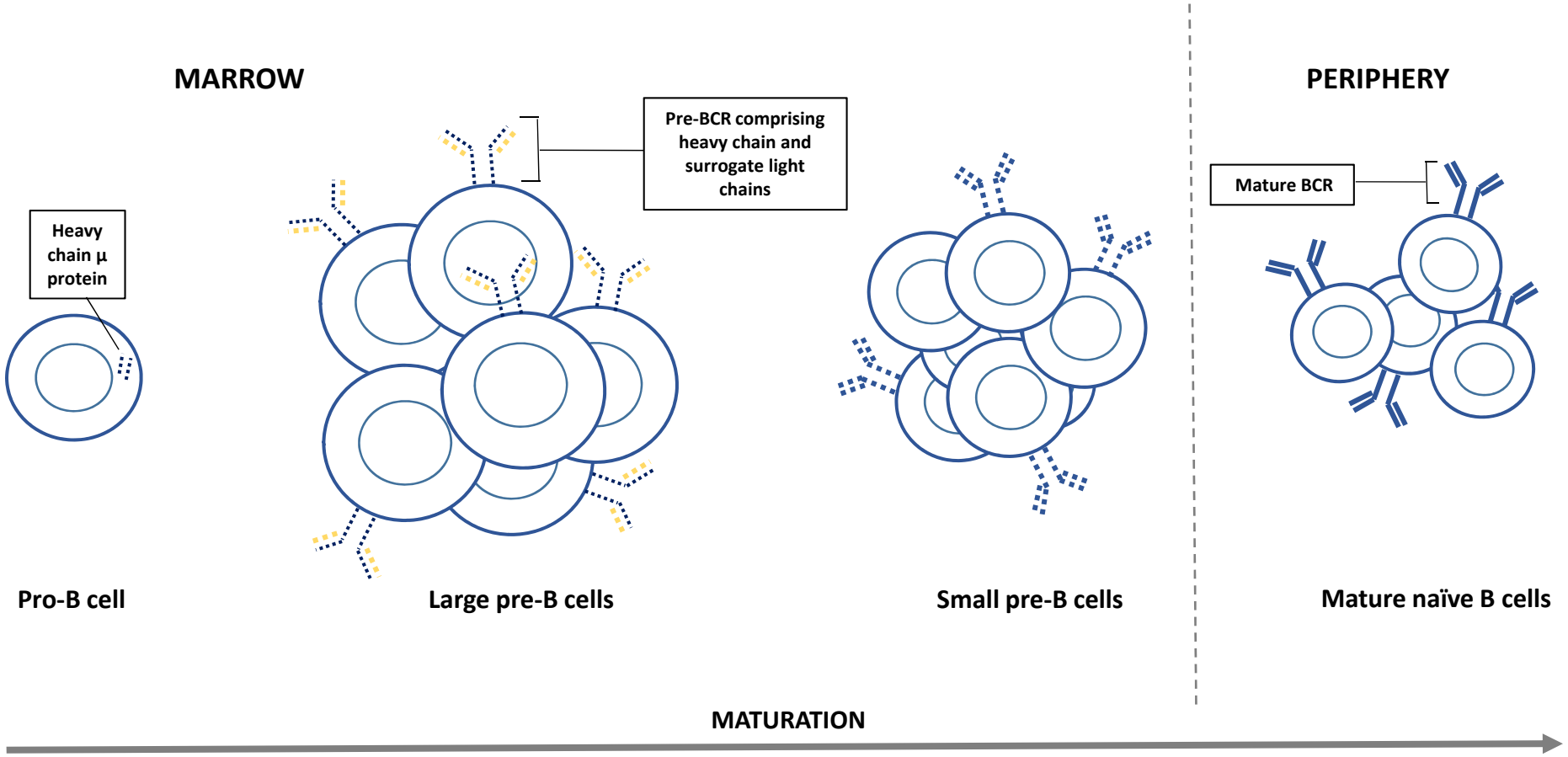

Figure 1.1 B cell maturation

B cell development in the bone marrow features sequential heavy and then light chain rearrangement and maturation of the B cell receptor (BCR). The heavy chain immunoglobulin locus is rearranged in pro-B cells. When the heavy chain μ protein is expressed in the cytoplasm, it is paired with surrogate light chains to form the pre-BCR. Autonomous signalling via the pre-BCR leads to a short-lived clonal expansion of these large pre-B cells. The pre-BCR is then downregulated and the cells exit the cell cycle and enter a resting phase as small pre-B cells. The immunoglobulin light chain locus is rearranged. Rearranged light chains combine with heavy chains to form the mature BCR which is expressed as IgM on the surface of B cells which exit the bone marrow and complete their maturation in the periphery. (Carsetti, 2000)

The germinal centre reaction occurs within peripheral lymphoid tissues, in the lymph nodes, tonsils, spleen and Peyer's patches. After encountering a foreign antigen carried by an antigen presenting cell (APC), naïve B cells migrate to the T cell rich zone of the lymphoid tissue. There, they are activated by the interaction of their CD40 surface receptor with the CD40 ligand, CD154, which is expressed by T helper cells (T_H), and by a number of other ligand interactions with T_H cells and APCs. The germinal centre reaction is thus initiated. Some of these activated B cells develop directly into antibody secreting cells (terminally differentiated plasma cells or dividing plasmablasts) after exiting the germinal centre. (Klein and Dalla-Favera, 2008)

Others develop into GC precursor B cells and move to the primary follicle which is populated by IgM+IgD+ B cells and stromal follicular dentritic cells (FDCs) which can present an unprocessed antigen on their long dendrites. The precursor B cells, called centroblasts, proliferate rapidly making up the dark zone of the GC. They push the IgM+IgD+ B cells and FDCs aside into a surrounding structure known as the light zone. During proliferation, centroblasts undergo somatic hypermutation (SHM) which allows them to diversify the variable region of their surface immunoglobulins by non-random mutations in the V(D)J regions of the immunoglobulin variable region of both the heavy and light chains. This ensures the production of an antibody with a high affinity for the exogenous antigen. In the light zone of the GC, T_H cells and FDCs help to select centrocytes with the best antigen affinity. Some centrocytes also undergo class switch recombination (CSR), the DNA-level mechanism by which the constant heavy chain region of the immunoglobulin switches isotype from IgM and IgD to IgG, IgA or IgE. In this way, the effector function – determined by the class or isotype of the antibody- of the resultant antibody is optimised, without affecting the variable antigen-binding region. Centrocytes that have been selected for their antigen-binding capacity can then differentiate into plasma cells or memory B cells. Overall, centrocytes are very heterogeneous compared to centroblasts, and the presence of somatic hypermutation indicates a B cell that has experienced T cell exposure and a germinal centre reaction.

Germinal centre cells are very prone to apoptosis, unless rescued by anti-apoptotic signals, and this allows for the rapid elimination of cells which do not bear an

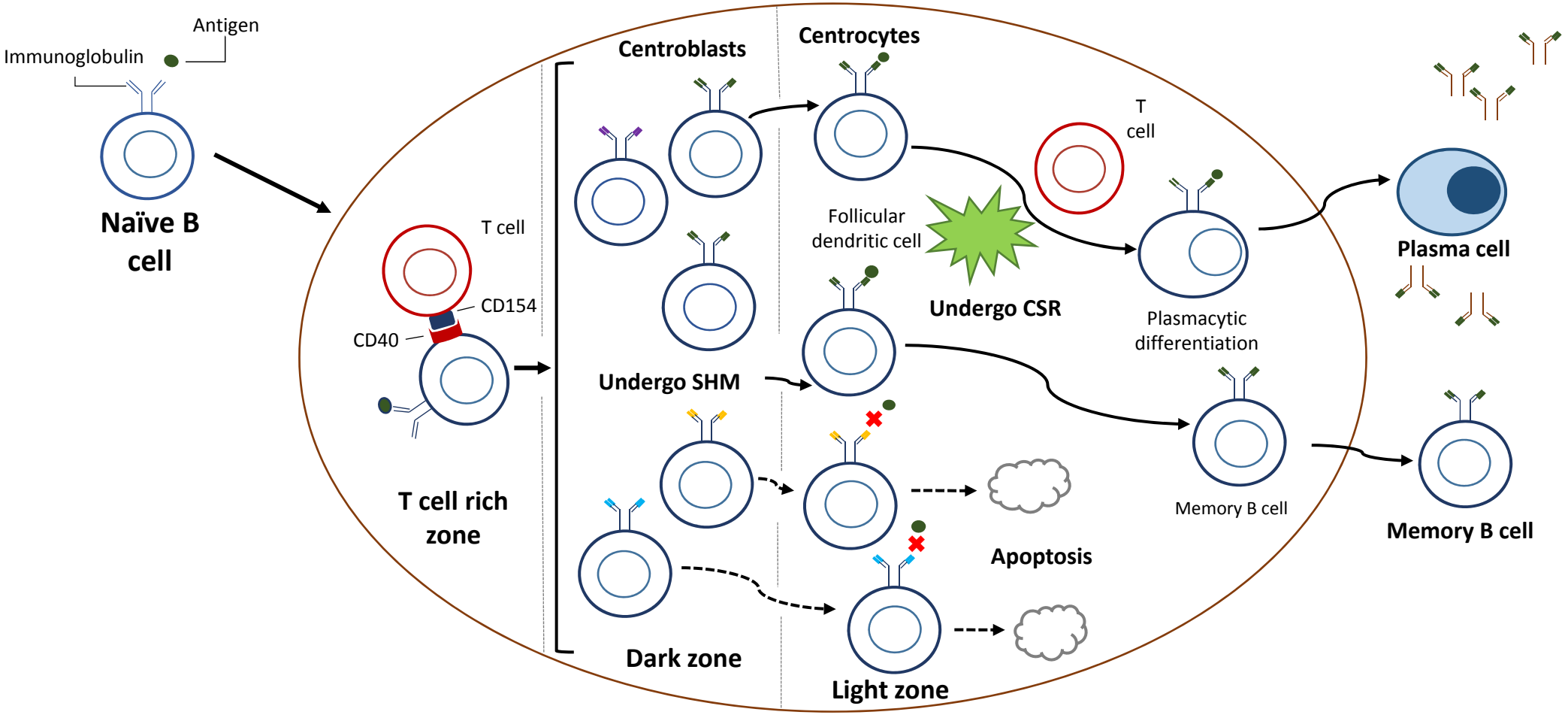

Figure 1.2 B cell differentiation through the germinal centre
After encountering an antigen, naïve B cells are activated by their interactions in the T cell rich zone of the lymph node, and the germinal centre reaction is initiated. B cells proliferate rapidly as centroblasts in the dark zone of the lymph node. These cells undergo somatic hypermutation (SHM) to diversify the heavy and light chain regions of their surface immunoglobulins. In the light zone, rapid proliferation slows down and some of these centrocytes undergo class switch recombination (CSR) of their immunoglobulin isotype. Interactions with T cells and follicular dendritic cells select the cells with highest antigen affinity which then differentiate to plasma cells or memory B cells. Figure modified from Klein and Dalla-Favera, 2008.

effective or functional antibody. (Klein and Dalla-Favera, 2008)

1.2 IRF4

IRF4 (interferon regulatory factor 4) is a critical regulator of B cell maturation and differentiation. It is one of the family of interferon regulatory transcription factors, which were originally defined as a group of transcription factors induced by both type I and type II interferons and other cytokines in response to viral infections. The IRFs bind to interferon stimulated response elements (ISRE) elements within interferon-inducible genes, thus playing an essential role in primary host immunity. (Nguyen et al., 1997; Marecki and Fenton, 2002) The IRFs all share significant homology at the N-terminal 115 amino acids, where a tryptophan-repeat sequence is found (five tryptophans repeated at 10-18 amino acid intervals). The DNA binding domain is located at this region, through which the IRFs are able to bind to the ISRE in their target genes. (Nguyen et al., 1997; Mamane et al., 1999) IRF4 shares closest structural homology with family member, IRF8. (Lu, 2008)

IRF4 is unique amongst its transcription factor family as its expression is primarily regulated, not by interferon, but by pathways of lymphocyte activation including BCR signalling by anti-IgM. (Shaffer et al., 2009)

1.2.1 Discovery of IRF4

IRF4 was discovered in the 1990s in a number of guises, by independent investigators. (Table 1.1) IRF4 was first identified incidentally, when it was determined that Ets transcription factor PU.1 recruited a second protein to bind to the 3' enhancer in the murine immunoglobulin kappa light chain (Eκ3'). (Pongubala et al., 1992) This second protein was initially named NF-EM5 (nuclear factor enhancer motif 5). Eisenbeis *et al* subsequently also identified a PU.1-containing protein complex binding to the B domain of the murine immunoglobulin lambda light chain enhancer (EλB). They named the protein that bound PU.1 in this complex, Pip. (PU.1 dependent protein) (Eisenbeis et al., 1993; Eisenbeis et al., 1995) Simultaneously, Matsuyama *et al* screened murine spleen DNA by PCR and identified IRF4 as a new member of the IRF

Name		Reference
NF-EM5 (nuclear factor enhancer motif 5)	Bound with PU.1 to 3'enhancer of murine kappa light chain (Eκ'3)	(Pongubala *et al.*, 1992)
Pip (PU.1-dependent protein)	Bound with PU.1 to the B domain of the murine immunoglobulin lambda light chain enhancer (EλB)	(Eisenbeis *et al.*, 1993; Eisenbeis *et al.*, 1995)
LSIRF (lymphoid-restricted interferon regulatory factor)	Found on a screen of murine spleen DNA; expressed in B and T cell lineages but absent from other haemopoetic cells	(Matsuyama *et al.*, 1995)
ICSAT (interferon consensus sequence binding protein in T cell leukaemia cells)	Bound to the 5' proximal promoter region of the human interleukin-5 gene (*IL5*) in a human adult T cell leukaemia cell line	(Yamagata *et al.*, 1996)

Table 1.1 Discovery of IRF4
IRF4 was first identified in a number of different guises, binding to murine kappa and lambda light chains in a heterodimer with PU.1, and to the human interleukin-5 gene in a T cell leukaemia line. Its expression was thought at first to be restricted to lymphoid haemopoietic lineages.

family. They noted it to be present in B and T cell lines but absent from other haemopoetic lineages and named it lymphoid-restricted IRF (LSIRF). (Matsuyama et al., 1995) Finally, Yamagata *et al* identified a factor binding to the 5' proximal promoter region of the human interleukin-5 gene (IL5) in a human adult T cell leukaemia cell line. They noted the significant homology of its N terminal region with other IRF family members, and named it ICSAT (interferon consensus sequence binding protein in T cell leukaemia cells). (Yamagata et al., 1996)

Using the coding region of murine LSIRF to screen a human lymphocyte library, the human homologue gene was mapped by FISH to chromosome 6.(Grossman et al., 1996)

1.2.2 Structure and function of IRF4

IRF4 protein comprises two important, independent regions: the N terminal DNA binding domain (Pongubala et al., 1992; Eisenbeis et al., 1995; Grossman et al., 1996) and the C terminal regulatory domain, separated by a flexible linker. (Brass et al., 1999) In addition, a putative IRF activation domain (IAD) is found within the carboxyl terminus of some of the IRFs including IRF4, via which the IRFs can interact with other proteins including other members of the IRF family. (Marecki and Fenton, 2002) (Figure 1.3)

The IRF4 C terminal regulatory domain has a number of important roles. It contains an autoinhibitory region, which allows only weak DNA binding by IRF4 on its own. (Brass et al., 1996) However, this autoinhibition is relieved when the C terminal regulatory domain of IRF4 interacts with phosphorylated PU.1 protein via a PU.1 PEST domain (a region rich in proline (P), glutamic acid (E), serine (S), threonine (T)) allowing ternary complex formation (Pongubala et al., 1993) (Brass 1996). This interaction specifically requires the phosphorylation of PU.1 at Ser148 (Pongubala et al., 1992; Pongubala et al., 1993) Some interaction between PU.1 and IRF4 also occurs via their respective DNA binding domains (Pongubala et al., 1992; Brass et al., 1999).

Importantly, the C terminal region of IRF4 also includes an activation domain, which allows it to behave as a transcriptional activator of downstream gene targets

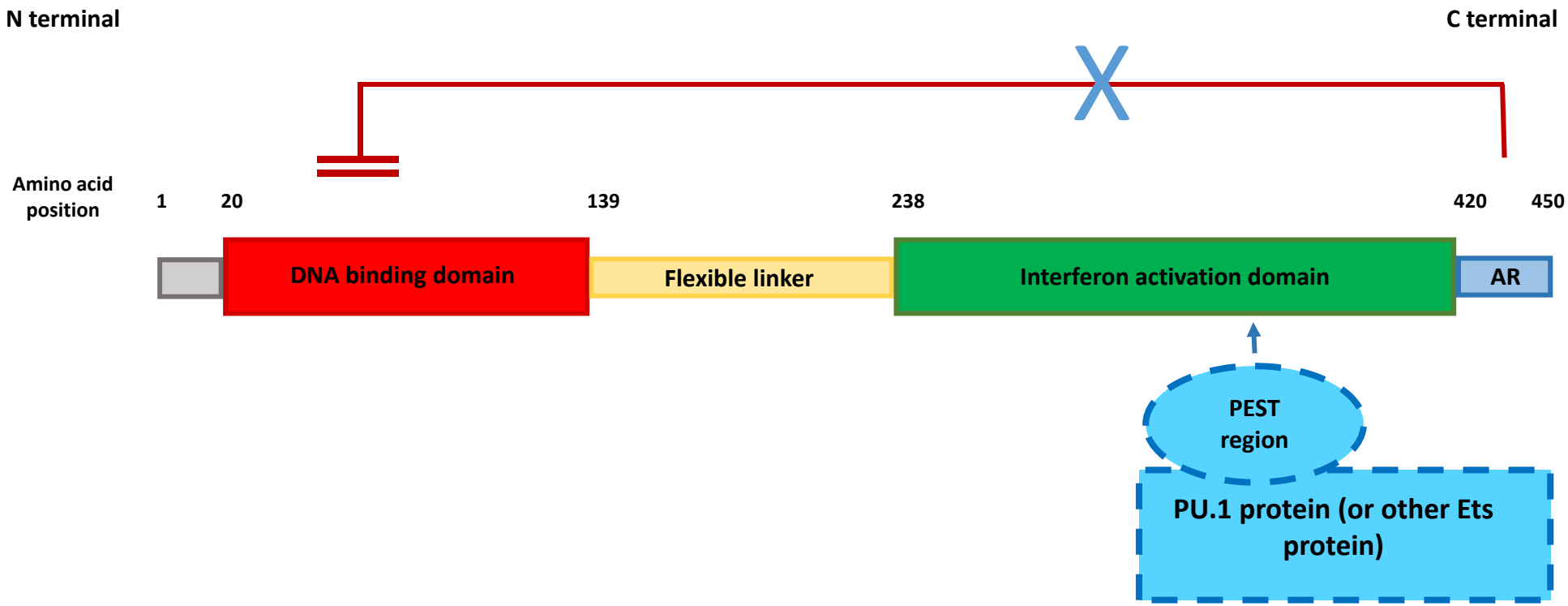

Figure 1.3 IRF4 protein structure

IRF4 is a 450 amino acid protein comprising an N terminal DNA binding domain and a C terminal interferon activation domain (IAD), separated by a flexible linker. (Pongubala *et al.*, 1992; Eisenbeis *et al.*, 1995; Grossman *et al.*, 1996; Brass *et al.*, 1999; Remesh *et al.*, 2015) The IAD is critical for mediating protein-protein interactions. The DNA binding domain shares significant homology with other members of the IRF family courtesy of a tryptophan-repeat sequence (five tryptophans repeated at 10-18 amino acid intervals). (Nguyen *et al.*, 1997) At this region, IRF4 is able to bind to the interferon stimulated response element (ISRE) of target genes. (Nguyen *et al.*, 1997; Mamane *et al.*, 1999) An autoregulatory (AR) domain at the C terminal of the protein contains an autoinhibitory region which physically interacts with the DNA binding domain and maintains the protein in an inhibited state. (Brass *et al.*, 1996) Interaction of the IAD with a binding partner such as PU.1 via the PEST (rich in proline (P), glutamic acid (E), serine (S), threonine (T)) region of PU.1 relieves this autoinhibition and allows IRF4 to bind its target sequence. (Pongubala *et al.*, 1993; Brass *et al.*, 1996) In this way, IRF4 can bind to target composite Ets/ IRF consensus element (EICE) sequences in target genes. The mechanism by which autoinhibiton of the DNA binding domain is relieved when IRF4 binds alone or with other binding partners is as yet unestablished.

when it binds with PU.1. (Brass et al., 1996) IRF4 cannot effectively bind or drive transcriptional activation of target sequences alone, (Brass et al., 1996) but acts synergistically with PU.1 to drive transcription of the IgG kappa light chain enhancer (Eκ3') (Pongubala et al., 1992) and the lambda light chain enhancer (EλB) (Eisenbeis et al., 1995). In addition, IRF4 has been shown to transactivate these same light chain enhancer regions when it binds with an alternative partner protein in place of PU.1: the E box protein, E47, or alternative Ets family member, SPI-B. (Su et al., 1996; Nagulapalli and Atchison, 1998) Again acting with PU.1, IRF4 also cooperatively binds and drives transcription of the CD20 promoter, a protein expressed on the surface of all B cells. (Himmelmann et al., 1997)

In stark contrast, IRF4 represses downstream gene targets in the absence of PU.1. (Brass et al., 1996; Yamagata et al., 1996) Specifically, Brass *et al* demonstrated that IRF4 repressed the activity of an interferon-inducible reporter construct which had been transactivated by family-member, IRF1. (Brass et al., 1996) A truncated mutant IRF4 protein lacking the N terminal DNA binding domain was unable to repress this activity, suggesting that IRF4 represses interferon-inducible genes by competing with IRF1 for the interferon consensus binding sequence.

Thus, IRF4 acts as a dichotomous regulator, transactivating gene targets when it binds in conjunction with PU.1 or an alternative binding partner (such as E47 or SPI-B) but repressing interferon-inducible gene transcription when it acts alone.

1.2.3 Expression of IRF4

When it was first identified, IRF4 expression was initially thought to be restricted to cells of the immune system (Pongubala et al., 1992; Eisenbeis et al., 1995; Matsuyama et al., 1995; Yamagata et al., 1996). More recently however, it has also been identified on a number of other tissues, including melanocytes, cardiac muscle cells and neurones. (Shukla and Lu, 2014)

While the complexity of its role is not yet fully understood, there are several lines of evidence to indicate that IRF4, acting in conjunction with family member IRF8, is clearly critical in the maturation and development of B lymphocytes. IRF4 has an

intriguing, biphasic pattern of expression at differing stages of B cell development: it is expressed on immature pre-B cells (Pongubala et al., 1992; Brass et al., 1996; Lu et al., 2003), but is lost from the proliferating centroblasts of the germinal centre. (Falini et al., 2000) It is then re-expressed on a subpopulation of centrocytes in association with the follicular dendritic meshworks of the GC light zone. (Falini et al., 2000) Notably, IRF4 expression peaks in normal plasma cells. (Brass et al., 1996)

IRF4 is expressed in T lymphocytes as well as B lymphocytes, where it also has important roles in T cell differentiation and function. (Nayar et al., 2014)

1.2.4 IRF4 and B cell maturation

In the early stages of B cell development, IRF4 acts with its close family member, IRF8, in the maturation of large pre-B cells. These cells express an immature pre-B cell receptor (pre-BCR), comprising heavy chain μ protein and surrogate light chains. Using a compound deficient IRF4-/IRF8- mouse model, Lu *et al* demonstrated that IRF4-/8- B cells were blocked at the pre-B cell stage, unable to downregulate the pre-BCR, nor to rearrange the immunoglobulin light chain locus. Signalling via the pre-BCR promotes cell survival and expansion, and thus these mutant cells were trapped in a proliferative pre-B cell state, unable to exit the cell cycle. (Lu et al., 2003) Reconstitution of either IRF4 or IRF8 expression by an inducible vector was sufficient to rescue these cells from the block in maturation. (Ma et al., 2006) Specifically, IRF4 and IRF8 downregulated the pre-BCR by inducing expression of transcription factors Ikaros and Aiolos which in turn suppressed expression of surrogate light chains and thus assembly of the pre-BCR. IRF4 and IRF8 behaved redundantly here, though IRF4 acted more potently than IRF8. (Ma et al., 2008) Exit from the cell cycle by IRF4 or IRF8 reconstitution allowed the pre-B cells to enter the resting small pre-B cell stage thus indicating that IRF4 and 8 have roles in limiting clonal cell expansion at this stage. The cells were then able to rearrange the immunoglobulin light chain locus in preparation for expressing the mature B cell receptor. This was demonstrated by the generation of IgM+ cells by flow cytometry. (Ma et al., 2006)

The precise mechanism of IRF4's involvement in immunoglobulin light chain

rearrangement at the pre-B cell stage was subsequently teased out in a further study. (Johnson et al., 2008) Both reconstitution of IRF4 expression, and attenuation of interleukin-7 (IL-7) signalling were independently able to induce kappa light chain gene rearrangement in mutant IRF4-/IRF8- pre-B cells *in vitro*. In addition, IRF4 expression in IRF4-/8- pre-B cells induced lambda light chain gene recombination, whereas IL-7 attenuation had no effect. IRF4 is known to bind to the Eκ3' kappa light chain enhancer and to the EλB lambda light chain enhancer as a heterodimer with PU.1. (Pongubala et al., 1992; Eisenbeis et al., 1993) (Section 1.2.1) Chromatin immunoprecipitation studies demonstrated that both of the lambda light chain enhancers, and the 3' kappa light chain enhancer, Eκ3', were transcriptionally inactive in IRF4-/8- pre-B cells. IRF4 expression restored transcriptional activation at these sites. In contrast, the intronic kappa light chain enhancer, iEK, was not subject to IRF4-induced activation, but was bound by the transcription factor E2A, and transcriptional activation at this site was restored by attenuation of IL-7 signalling. Thus, IRF4 expression and the attenuation of IL-7 signalling act to induce light chain rearrangement in pre-B cells. Furthermore, the attenuation of IL-7 signalling is achieved indirectly, also through the actions of IRF4. IRF4 induces the expression of a number of genes encoding chemokine receptors and adhesion molecules, including *Cxcr4*, the receptor for chemoattractant cytokine (chemokine), CXCL12 in murine cells. CXCL12 is expressed by a distinct set of bone marrow stromal cells which are spatially separate from stromal cells expressing IL-7. It was demonstrated *in vitro* that IRF4-/IRF8- pre-B cells migrated towards cells expressing CXCL12 when IRF4 expression was restored, removing the cells from a stromal source of IL-7, and thus attenuating local IL-7 signalling. Altogether, IRF4 expression and this indirect attenuation of IL7 signalling were demonstrated to act synergistically to promote production of IgM+ B cells with mature B cell receptors. (Johnson et al., 2008)

1.2.5 IRF4 in the germinal centre

IRF4 also plays a critical role in the development and differentiation of mature B cells after antigen-exposure. It is essential to the development of germinal centres in secondary lymphoid organs, and ultimately to the plasma cell differentiation of B cells after they exit the germinal centre. (Figure 1.4)

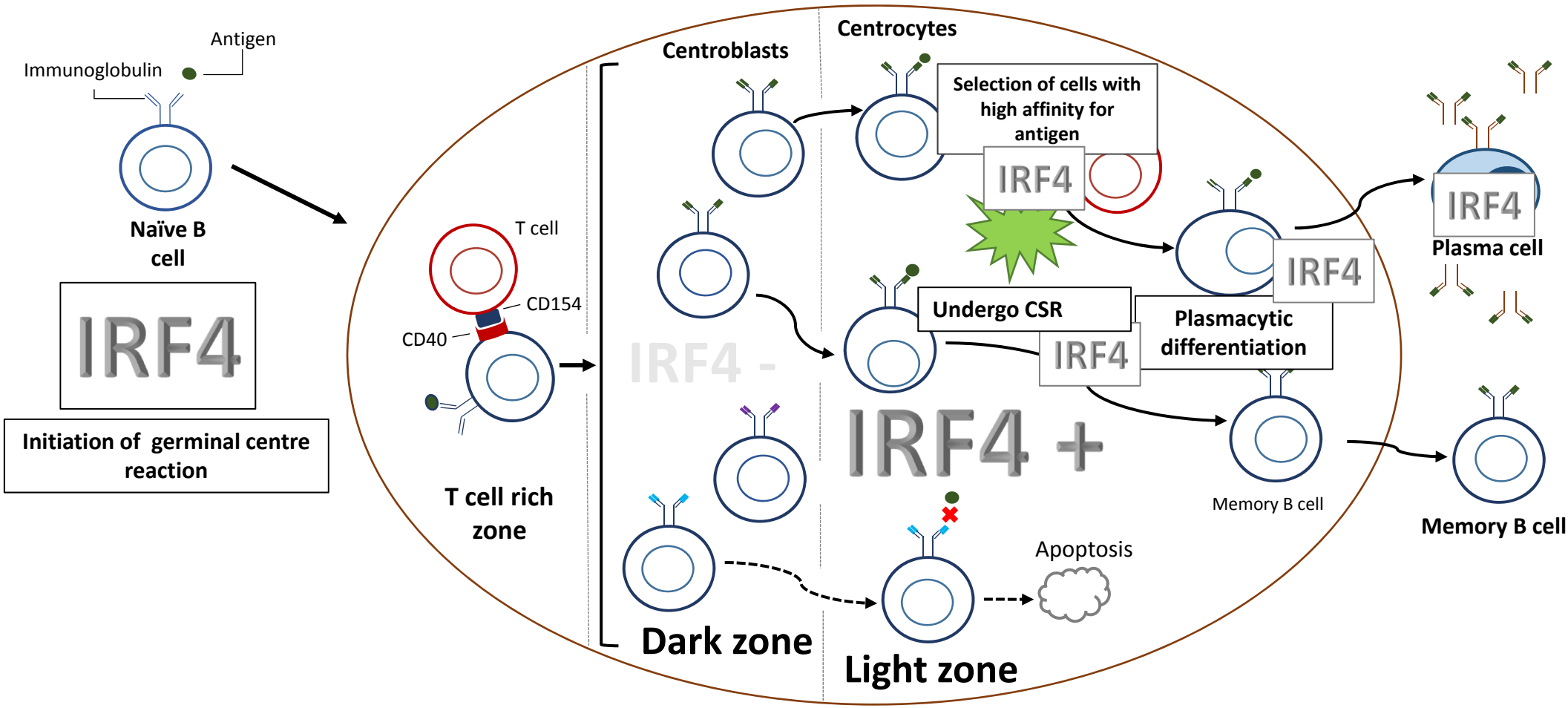

Figure 1.4 IRF4 is essential to the germinal centre reaction
IRF4 is essential to the initiation of the germinal centre reaction and mice who are IRF4 -/- lack germinal centres. IRF4 is not expressed in the germinal centre dark zone but coordinates essential processes in the light zone: class switch recombination (CSR); selection of cells with high affinity for antigen; and plasmacytic differentiation. Plasma cells strongly express IRF4.

The first evidence linking IRF4 with the germinal centre reaction came from a study which showed that Irf4-/- mice display a striking absence of germinal centres and plasma cells. Furthermore, antigen-specific antibody production was absent when the IRF4 deficient mice were immunised. (Mittrucker et al., 1997)

The clearly demarcated expression of IRF4 in the germinal centre gives some clue as to its role. IRF4 expression is restricted to the light zones of the germinal centres, where it is expressed on a subpopulation of centrocytes. In contrast, it is entirely negative in the proliferating centroblast cells of the germinal centre dark zone. (Falini et al., 2000; Tsuboi et al., 2000) Three main processes occur in the GC light zone, and there is strong evidence that IRF4 orchestrates these processes: i) class switch recombination (CSR); ii) the selection of B cells making high affinity antibodies; and iii) differentiation of centrocytes to memory B cells or plasma cells. (Klein and Dalla-Favera, 2008). IRF4 is also strongly expressed on plasma cells. (Brass et al., 1996)

1.2.5.a IRF4 and class switch recombination (CSR)

IRF4 is critical for class switch recombination (CSR). Using an IRF4 deficient mouse model, Klein *et al* demonstrated that IRF4 deficient B cells failed to undergo class switch recombination after *in vitro* CD40 and IL-4 stimulation, as demonstrated by a significant decrease in the production of cells expressing IgG1. (Klein et al., 2006) This was due to a failure to induce AID (activation-induced cytidine deaminase), which is required for CSR. (Muramatsu et al., 2000) Transcription of *Aicda* mRNA (which encodes AID) and AID protein expression were both impaired in *Irf4*-/- B cells. (Klein et al., 2006) IRF4 regulation of *Aicda*/AID expression has been confirmed in a number of other subsequent studies. (Sciammas et al., 2006; Ochiai et al., 2013) In keeping with these findings, Sciammas *et al* also observed a severe defect in the generation of class-switched B cells expressing either IgG1 or IgG3 when splenic B cells from *Irf4* -/- mice were cultured with lipopolysaccharide (LPS) and IL-4. They demonstrated that the defect in CSR in the IRF4 deficient cells was due to a selective impairment in *Aicda* expression, and that the other CSR genes were not impaired. Furthermore, ectopic expression of AID restored CSR in the mutant *Irf4* -/- murine cells, and similarly, reconstitution of IRF4 restored expression of Aicda transcript. (Sciammas et al., 2006)

1.2.5.b IRF4 and plasma cell differentiation

The same authors also went on to show that IRF4 is essential for the terminal differentiation of B cells to plasma cells, after their exit from the germinal centre. Using the *Irf4* -/-mouse model, Sciammas *et al* showed a marked reduction in the generation of Syndecan-1 (CD138, a plasma cell marker)-expressing cells in IRF4 deficient mice (*Irf4* -/-), compared with phenotypically normal heterozygote controls (*Irf4* +/-). *Prdm1* transcription and BLIMP1 expression were also downregulated in *Irf4* -/- mice. BLIMP1 is a transcription factor, encoded by *Prdm1*, and it plays an essential role in the orchestration of plasma cell differentiation, while repressing germinal centre programme genes such as *Aicda* and *Bcl6*. Chromatin immunoprecipitation (ChIP) studies demonstrated that *Prdm1* is a direct gene target of IRF4, and IRF4 positively regulated BLIMP1 expression. Reconstitution of IRF4 expression in the *Irf4* -/- cells was sufficient to restore *Prdm1* expression. However, despite *Prdm1*/BLIMP1 being major regulators of plasma cell differentiation, the upregulation of *Prdm1* expression alone by LPS stimulation in the *Irf4* -/- mice was insufficient to generate cells with a plasma cell phenotype, indicating that the simultaneous expression of IRF4 is also critical. (Klein et al., 2006) Genome wide expression analysis in *Irf4* -/- cells which had been stimulated by lipopolysaccharide (LPS) to engage the B cell receptor in fact revealed that the entire BLIMP1-dependent plasma cell gene expression programme in IRF4 deficient cells, was defective. (Sciammas et al., 2006) Furthermore, forced over-expression of IRF4 in the human GC B cell line, OCI-LY7, repressed *AICDA* and *BCL6* expression and induced the expression of plasma cell proteins, CD138 and BLIMP1. (Klein et al., 2006)

1.2.5.c IRF4 coordinates CSR and plasma cell differentiation

Paradoxically therefore, IRF4 orchestrates two antagonistic processes. It induces the expression of *Aicda* which is essential for class switch recombination (CSR) in the germinal centre, but it also induces *Prdm1* and BLIMP1 which repress *Aicda* and promote plasma cell differentiation and exit from the germinal centre.

Sciammas *et al* subsequently demonstrated that graded expression of IRF4

allows for the coordination of these two opposing processes: low levels of IRF4 expression lead to the induction of *Aicda* and CSR; while a high level of IRF4 leads to downregulation of *Aicda*, induction of *Prdm1* expression and induction of the plasma cell differentiation programme. (Sciammas et al., 2006) In a later study supported by mathematical modelling, they showed that the level of IRF4 expression, and thus the fate of the cell, is determined by the strength of signalling via the BCR. (Sciammas et al., 2011) (Figure 1.5) Murine splenic B cells were cultured *in vitro* with increasing doses of antigens of varying affinity. Cells which had been cultured with a high dose or high affinity antigen expressed higher levels of IRF4. Furthermore, a larger proportion of B cells which expressed plasma cell marker Syndecan-1 by flow cytometry were generated, at the expense of cells which had undergone CSR. However, regardless of antigen dose or affinity, all of the cells were shown to express *Aicda* mRNA initially, with the levels of *Aicda* transcript only decreasing 3 days after antigen-stimulation. Taking these results together, the authors proposed a mechanism of 'kinetic control', in which BCR signalling induces an obligate spell of CSR for all cells, but high affinity or avidity antigen interactions with the BCR curtail CSR through the rapid accumulation of IRF4, downregulation of *Aicda*, and promotion of the plasma cell differentiation programme. (Sciammas et al., 2011) Thus, B cells which express a receptor with a high affinity for the antigen presented to them by the follicular dendritic cells of the germinal centre light zone, are rapidly selected for differentiation to antibody-secreting plasma cells, whilst cells with poor antigen-affinity are retained in the germinal centre for further CSR and somatic hypermutation. In this way, IRF4 has a role in the selection of B cells making high affinity antibodies.

1.2.5.d IRF4 and the initiation of the germinal centre reaction

Ochiai *et al* confirmed in an *in vivo* mouse model that high affinity antigen interactions led to an increased production of high IRF4-expressing plasma cells. Furthermore, they demonstrated that while IRF4 is vital for termination of the germinal centre reaction and the onset of plasma cell differentiation, it is also required at a much earlier stage, for the initial generation of BCL6+ germinal centre cells after antigen exposure. (Ochiai et al., 2013)

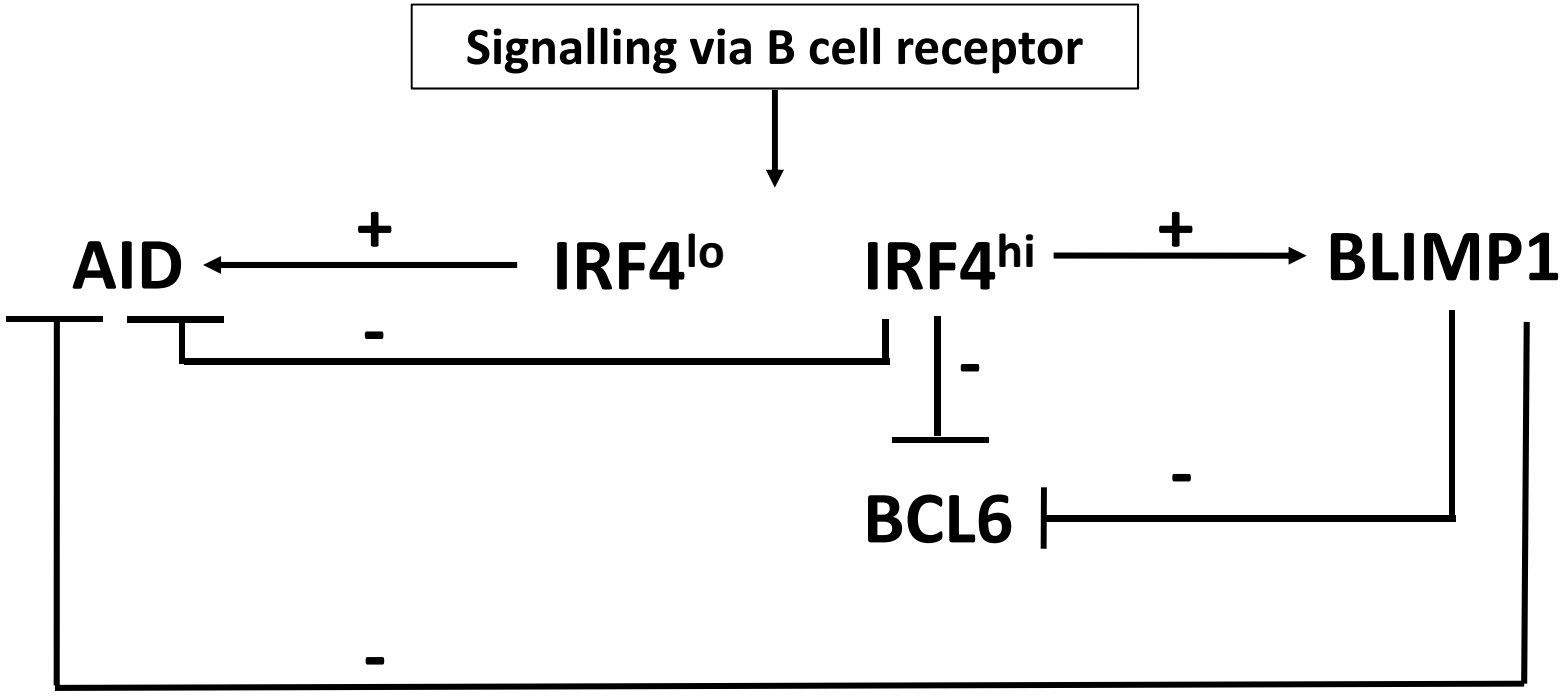

Figure 1.5 Graded expression of IRF4 coordinates class switch recombination (CSR) and plasmacytic differentiation through a model of 'kinetic control'

Low IRF4 expression in mouse studies leads to induction of *Aicda* and AID expression and thus class switch recombination (CSR) in the light zone of the germinal centre. High IRF4 expression in contrast leads to downregulation of Aicda/AID expression and induces *Prdm1* and BLMP1 expression. High IRF4 expression also represses expression of BCL6, a critical regulator of the germinal centre reaction. Thus, high IRF4 expression drives the plasma cell differentiation programme and exit from the germinal centre. The level of IRF4 expression is determined by the strength of signalling via the B cell receptor (BCR). Germinal centre B cells expressing high affinity antibodies thus engage their BCR more readily and receive strong BCR signalling. These cells therefore express high levels of IRF4 and are driven towards the plasma cell differentiation programme and exit from the germinal centre. B cells with low affinity antibodies receive weaker BCR signalling and thus have lower IRF4 expression. These cells are therefore retained in the germinal centre to undergo further rounds of CSR to generate antibodies of higher affinity. (Sciammas *et al.*, 2006; Sciammas *et al.*, 2011)

IRF4 is a direct transcriptional repressor of *BCL6*, (Saito et al., 2007) which is a master regulator of the germinal centre reaction, expressed on proliferating centroblasts and the majority of centrocytes. (Cattoretti et al., 1995) (Klein and Dalla-Favera, 2008) BCL6 and IRF4 expression are mutually exclusive. (Falini et al., 2000) The analysis of B cells from *Irf4* wildtype mice after immunisation with sheep red blood cells revealed two populations of cells: an $IRF4^{hi}BCL6^{lo}$ population representing plasma cells, and an $IRF4^{lo}BCL6^{hi}$ population representing germinal centre B cells. The *Irf4*-/- mice were unable to generate either cell subset, despite engaging appropriately with antigen and helper T cells. The *Irf4* -/- mice also displayed severely compromised transcription of *Bcl6* and *Pou2af1* genes after immunisation. Along with BCL6 and PAX5 proteins, OBF1 which is encoded by *Pou2af1*, regulates germinal centre B cell differentiation. *Bcl6* and *Pou2af1* were shown to require IRF4 expression for their induction, although *Pax5* expression was independent of IRF4. (Ochiai et al., 2013)

In keeping with the model of 'kinetic control', the authors further demonstrated that differing cell fates were determined by different levels of IRF4 expression. They used a tet-inducible *Irf4*-expressing vector in a mouse model, to generate either pulsed or sustained IRF4 expression. Pulsed expression in *Irf4*-/- mice led to the production of BCL6-expressing germinal centre cells which expressed *Aicda*. Meanwhile, sustained IRF4 expression in wildtype *Irf4* +/+ cells led to the increased production of plasma cells at the expense of germinal centre cells. Interestingly, this plasma cell population predominantly secreted only IgM antibody, due to the over-expression of IRF4 and the consequent downregulation of AID and CSR. (Ochiai et al., 2013)

Thus, the induction of IRF4 expression at levels high enough to induce *Prdm1*, also leads to downregulation of BCL6 expression, promoting exit from the germinal centre at the same time as the onset of plasma cell differentiation.

1.2.6 Interaction of IRF4 and IRF8

Intriguingly, while IRF4 and IRF8 act redundantly in the maturation of early pre-B cells, (section 1.2.4) they have opposing effects in mature B cells. (Carotta et al., 2014) Here, IRF8 and PU.1 act together to prevent the premature terminal

differentiation of B cells, suppressing class switch recombination and plasma cell differentiation. They bind in reporter construct studies, to the same promoter element of *Bcl6* as IRF4, and similarly bind to *Prdm1*, but act in a reciprocal manner to IRF4, binding to the same target genes but with opposing transcriptional outcomes. (Carotta et al., 2014)

1.3 CD38

CD38 is a 45kDa single chain type II transmembrane glycoprotein (Malavasi et al., 2011) with a wide tissue distribution including pancreas, smooth muscle cells and brain, as well as haemopoietic cells. (Malavasi et al., 2008) *CD38* gene is located on chromosome 4 and comprises eight exons with the intronic regions making up more than 98% of the gene. Exon 1 is the largest codon region and encodes the N-terminal region, the membrane-spanning region and the first thirty-four amino acids of the extra-cellular region. (Ferrero and Malavasi, 1997)

Intriguingly, CD38 combines functions both as a catalytic ectoenzyme and as a cell surface receptor.

1.3.1 Distribution and function of CD38

Originally defined as a T cell activation molecule, CD38 was first identified in 1980 by the use of monoclonal antibodies.(Reinherz et al., 1980) Monoclonal antibodies (mAbs) have subsequently played a very important role in the determination of the distribution and function of CD38.

One such antibody, A10, was noted to induce activation and proliferation in thymocytes, circulating T lymphocytes, large granular lymphocytes (LGLs) and a number of T lineage acute lymphoblastic leukaemia human lymphocytes (Funaro et al., 1990). Finding that this antibody had agonistic effects on CD38 prompted the idea that there may be a natural ligand for CD38 that the antibody was mimicking.

The observation that CD38 also has roles in selectin-like cell-cell adhesion began the process of discovery of this ligand. Monoclonal IB4 anti-CD38 antibody was noted to inhibit the adhesion of CD38 positive naïve T cells (CD45+RA+) to human umbilical

vein endothelial cells (HUVECs). Similarly, it inhibited the binding of a humanized CD38 positive mouse/human hybrid cell line which expressed only weak integrin protein binding function. IB4 could not inhibit the binding of a number of T-acute lymphoblastic leukaemia (T-ALL) cell lines however, until the experiments were repeated at 4°C in order to impede integrin function. Together, these findings led to the conclusion that CD38 mediates binding in a weak selectin-like fashion. (Dianzani et al., 1994)

These observations ultimately led to the discovery of the natural CD38 ligand. A panel of monoclonal antibodies was raised, by immunising mice with HUVECs, and one of these antibodies effectively blocked CD38 positive cell binding with HUVECs. This antibody, named Moon-1, bound to a 120kDa single chain protein on the HUVEC cell surface, and the tissue wide-distribution of the Moon-1 molecule is consistent with its role as the natural CD38 ligand. (Deaglio et al., 1996) Moon-1 molecule was subsequently identified as CD31. (Deaglio et al., 1998)

1.3.2 CD38 and B cells

While CD38 induces activation signals in T cells, it has pleiotropic effects in B cells, which are strictly linked to their stage of maturation. Bone marrow B cell precursors express CD38 strongly but CD38 has an inhibitory effect on these cells, suppressing lymphopoesis through reduced proliferation and increased apoptosis. (Kumagai et al., 1995) In contrast, CD38 expression is only weak or moderate in circulating peripheral naïve B cells (Kumagai et al., 1995) but is upregulated by ligation of the B cell receptor (Santos-Argumedo et al., 1993) and is then abundantly re-expressed on B cells involved in the germinal centre reaction. In these GC cells, agonistic ligation of CD38 by monoclonal antibody IB4 led to upregulation of anti-apoptotic protein, BCL2, and thus rescued these cells from apoptosis. (Zupo et al., 1994) Thus, CD38 has contrasting effects on B cells at different stages of maturation, inhibiting immature marrow B cells but promoting survival in activated mature germinal centre B cells. It is strongly expressed on terminally differentiated plasma cells.

Signalling via CD38 in B cell progenitors induces a phosphorylation cascade including SYK, LYN and PI3-K. CD38 ligation is also associated with co-localisation of surface immunoglobulin and CD19, with CD38 on the cell surface membrane. (Malavasi et al., 1992; Silvennoinen et al., 1996; Kitanaka et al., 1997) In a murine B cell lymphoma line, IL-2 production by CD38 signalling was in fact shown to be dependent on the presence of an intact BCR. Furthermore, removal of calcium from the system by the addition of EGTA, impeded IL2 production, indicating that calcium mobilisation is also necessary for the functional effects of CD38 signalling. (Lund et al., 1996)

1.3.3 CD38 enzyme function

As well as its role as a receptor signalling molecule, CD38 also has an important role as an ectoenzyme. It has substantial structural homology with the adenosine diphosphate (ADP) ribosyl cyclase of the mollusc Aplysia californica (States et al., 1992) which catalyses the generation of cyclic ADPR (cADPR) from NAD+ through cyclase activity. cADPR is a universal second messenger with the ability to increase intracellular calcium levels, independent of the inositol triphosphate (IP3) pathway, and is thus key in a number of physiological processes. In addition, CD38 uniquely functions as a bidirectional enzyme as it also hydrolyses cADPR to ADPr. (Howard et al., 1993; Takasawa et al., 1993)

Thus CD38 has roles in cell-cell adhesion, cell signalling, and as an ectoenzyme involved in driving intracellular calcium flux and recruiting the B cell receptor for its function.

1.4 Chronic Lymphocytic Leukaemia (CLL)

Chronic lymphocytic leukaemia (CLL) is defined by an accumulation of $>5x10^9$/ml mature CD5 positive (CD5+) clonal B cells, with a characteristic immunophenotype. (Table 1.2) These cells can accumulate in peripheral blood, bone marrow and lymph nodes. (Matutes et al., 1994; Oscier et al., 2012) It is the commonest leukaemia in the Western world, with an age-adjusted incidence rate of 4.2 per 100,000 people. It is typically seen in the older population, and the median age at diagnosis is 72 years. (Howlader N, 2012) CLL, which remains incurable, has a

A

Surface marker	1 point	0 points
Surface Ig	weak	moderate/strong
CD5	positive	negative
CD23	positive	negative
FMC7	negative	positive
CD79b (or CD22)	weak/negative	moderate/strong

B

Binet staging	
A	No anaemia or thrombocytopaenia*; <3 involved nodal areas[$]
B	No anaemia or thrombocytopaenia; ≥3 involved nodal areas
C	Anaemia or thrombocytopaenia[ŧ]

C

Rai staging	Risk group	
0	Low	Lymphocytosis only
I		Lymphadenopathy
II	Intermediate	Hepatomegaly or splenomegaly and lymphocytosis
III/IV	High	Anaemia or thrombocytopaenia[ŧŧ]

Table 1.2 Matute scoring system for CLL diagnosis; Binet and Rai scoring systems for staging disease

A.Matutes scoring system, adapted from Matutes *et al*, 1994.

B. Binet staging system, adapted from Binet *et al*, 1981.

*No anaemia or thrombocytopaenia, defined as haemoglobin ≥10g/dL, platelets ≥100x10^9/l

[$]Nodal areas defined as: cervical, axillary and inguinal lymphoid, hepatomegaly and splenomegaly

[ŧ]Anaemia or thrombocytopaenia, defined as haemoglobin <10g/dL, platelets <100x10^9/l

C. Rai staging system, adaptd from Rai *et al*, 1975.

[ŧŧ]Anaemia or thrombocytopaenia defined as haemoglobin <11g/dL, platelets <100x100^9/l

heterogeneous disease course, and as such, not all patients require treatment at diagnosis.

1.4.1 Monoclonal B cell lymphocytosis

CLL may be preceded by the observation of monoclonal B lymphocytosis in healthy individuals with otherwise normal peripheral blood counts and no evidence of haematological disease. The term 'monoclonal B cell lymphocytosis' (MBL) and accompanying diagnostic criteria were proposed in 2005 by a subcommittee of the International Familial CLL Consortium. A monoclonal B cell lymphocytosis may be detected in the absence of an absolute lymphocytosis and the population prevalence varies depending on the technique used to detect it. Studies combining both light chain assessment for B cell clonality and flow cytometric assessment for B cell phenotype detect MBL in 2-3% of the population, with this number increasing to 5% in adults over the age of 60 years. (Marti et al., 2005). Diagnostic criteria require that the absolute lymphocytosis must be no greater than $5x10^9$/ml, with cell clonality demonstrated by light chain restriction, and a disease-specific phenotype (typically CD5+, CD23+ which corresponds to CLL phenotype, though non-CLL phenotype MBL is also recognised). There must be no other feature of lymphoproliferative disease present, and the monoclonal B cell population must remain stable on repeat testing after at least 3 months (Marti et al., 2005).

Monoclonal B cell lymphocytosis with a B cell count of less than 0.5x109/ml ('low count' MBL) rarely progresses to CLL, while MBL with a count higher than this ('high count MBL') progresses to CLL at a rate of 1-2% per year. Relatives of patients with both familial and sporadic CLL have a higher incidence of MBL than the general population (incidence of about 15% in individuals over 40 years of age from familial CLL pedigrees). (Strati and Shanafelt, 2015)

1.4.2 Staging of CLL

CLL, which remains incurable, has a heterogeneous disease course, and as such, not all patients require treatment at diagnosis. Two well characterised staging systems stratify patients into three and four prognostic groups respectively (Table 1.2B,C) (Rai

et al., 1975; Binet et al., 1981) according to lymphadenopathy, organomegaly and full blood count, and these systems determine median survival in patient groups. They are insensitive however to the differences between individuals particularly within the 'low' and 'intermediate' risk groups, and in an attempt to stratify CLL outcome in more detail, a number of disease-related biological features have subsequently been identified.

1.4.3 Somatic prognostic markers

1.4.3.a *IGHV* mutation

Lack of somatic hypermutation (section 1.1.3) in the variable region of the heavy chain genes (*IGHV*) in CLL cells is significantly associated with poorer outcome. (Hamblin *et al*., 1999) Typically, lack of SHM or 'unmutated' cases are defined as having ≤2% difference from the most similar germline gene. Using this stratification, CLL patients are broadly divided into two equal groups according to whether they have mutated *IGHV* genes (mutated CLL, M-CLL) or unmutated *IGHV* genes (unmutated CLL, U-CLL). Patients with unmutated CLL experience more aggressive disease with a significantly poorer overall survival (OS) (95 months compared to 293 months median OS for mutated CLL cases). (Hamblin et al., 1999) In early stage CLL patients (Binet stage A), *IGHV* status is the strongest predictor of overall survival in univariate analysis, and was one of four significant prognostic markers identified in a multivariate analysis in the same study. (Pepper et al., 2012)

1.4.3.b CD38 expression

Surface expression of CD38 is a well-established poor prognostic marker in CLL. In the seminal paper documenting the impact of CD38 positivity on prognosis in CLL, CD38 positive (CD38+) patients were shown to have a significantly poorer overall survival: 9 years median OS for those with ≥30% cells positive for CD38, whilst median OS was not reached during follow-up for those with <30% cells positive for CD38 surface expression. (Damle et al., 1999) Incidence of CD38 positivity is approximately 70% in phase 3 trials of treatment-naïve CLL patients (Hallek et al., 2010), though the

'cut-off' used to determine CD38 positivity (either 20% or 30% of cells) can vary between studies.

Damle *et al* also noted a highly significant correlation between CD38 positivity and unmutated *IGHV* status which led them to propose that CD38 might be a surrogate marker of unmutated CLL. However, while a number of subsequent studies have gone on to confirm the poor prognosis attributed to CD38+ CLL and the overlap between that and unmutated *IGHV* status, the two prognostic markers do not fully correlate with each other. (Ibrahim et al., 2001; Hamblin et al., 2002; Ghia et al., 2003)

CD38 is not expressed uniformly in the CLL cells of all CD38+ patients. Whilst some patients have a homogenously CD38+ or homogenously CD38 negative (CD38-) CLL cell population as detected by flow cytometry, others have a 'bimodal' population with both CD38+ and CD38- sub-clones of CLL cells present. (Ghia et al., 2003) Furthermore, the expression of CD38 does not remain static throughout the course of disease, and variation in the expression of CD38 in individual patients has been documented. (Hamblin et al., 2002) The clinical significance of this variation within an individual patient is not clear. (Ghia et al., 2004) Specifically, no cases have been documented in which CD38- patients subsequently acquire CD38 positivity, and similarly no CD38+ patients have later become wholly negative.

1.4.3.c ZAP70

While the gene expression profiles of U-CLL and M-CLL largely overlap, the gene encoding the zeta-associated protein of 70kDa (ZAP70) is one of a number of genes that are differentially expressed in the two CLL groups. (Rosenwald et al., 2001) ZAP70 is a receptor-associated protein tyrosine kinase that is expressed by T cells, but not by normal B cells, and rarely by M-CLL cases. It is closely related to IGHV mutational status, with ZAP70 positivity (defined by >20% ZAP70 positive cells by flow cytometry) having a 100% positive predictive value for identifying unmutated CLL cases in a series of 56 patients. Negative predictive value was 88%. (Crespo et al., 2003) The same study demonstrated poorer outcome for patients with ZAP70 positive disease, with more rapid progression and shorter overall survival.

The exact function of ZAP70 in CLL and how it contributes to poorer outcome is not fully understood. However, it does appear to be involved in the amplification of B cell receptor signalling and to an amplification of downstream NFκB signalling. (Chen et al., 2005; Pede et al., 2013)

There is evidence that CD38 and ZAP70 are functionally linked in CLL pathogenesis, and this is discussed further in section.1.4.5.

1.4.3.d Cytogenetics

Cytogenetics make an important contribution to CLL prognostication. Conventional metaphase cytogenetics can be hampered in CLL by the low proliferation rate of CLL cells and therefore fluorescence in situ hybridisation (FISH) is useful in identifying common genetic aberrations.

Döhner *et al* (Dohner et al., 2000) provided pivotal evidence of the effect of genetic aberrations on CLL outcome. Fluorescence in situ hybridisation (FISH) analysis of 325 patients demonstrated the presence of a genetic abnormality in 82% of the patients, with deletion of the long arm of chromosome 13 (del(13q)) being the most common (55% of patients). Nearly a third of the patients had more than one genomic abnormality. Using Cox's proportional hazards regression, a hierarchical model of the prognostic impact of five genetic aberrations was established. (Table 1.3) Deletion of the long arm of chromosome 13 as the sole abnormality was associated with the best prognosis, with median overall survival of over 11 years. In contrast, patients with a deletion of the short arm of chromosome 17 (del(17p)) experienced the worst outcome with a median overall survival of less than three years.

Del(17p) necessarily indicates the loss of the tumour suppressor gene, *TP53*. The *TP53* pathway induces cell death in response to DNA damage and its inactivation is associated with resistance to chemotherapy. Deletion of *TP53* in CLL predicts for poor survival, shorter time to first treatment and absence of response to purine analogues (Dohner et al., 1995), despite advances in treatment and the advent of chemoimmunotherapy (further discussed in section 1.4.6). (Stilgenbauer et al., 2014)

Chromosomal abnormality detected by FiSH	Number of patients (%)	Median survival (months)
del (17p)	23 (7)	32
del (11q)	56 (17)	79
Normal karyotype	57 (18)	111
+ (12q)	47 (14)	114
Del (13q)	117 (36)	133

Table 1.3 Incidence of common acquired cytogenetic abnormalities in CLL and their impact on survival
FISH analysis of 325 patients with CLL revealed a genetic abnormality in 82% of the cases. Cox's proportional hazards regression model was used to construct a hierarchical model of genetic abnormalities, in which each case was assigned to one subgroup only. Patients with del (13q) as their sole genetic abnormality had the longest median overall survival time. In contrast, patients with del (17p) had a significantly shorter median survival of under 3 years. Adapted from Döhner *et al*, 2000.

Deletion of the long arm of chromosome 11 (del(11q)) is detected in approximately 20% of patients (Dohner et al., 2000) and is also associated with a poor outcome. Chromosome 11 is the location of the ataxia telangiectasia mutated (ATM) gene. Approximately half of patients with a del(11q) will also have mutated ATM on the other allele.

1.4.3.e Somatic gene mutations

Over two thousand novel gene mutations have been identified in CLL (Puente et al., 2011; Wang et al., 2011) but only four of these have been demonstrated recurrently at a frequency of over 5% of cases, and shown to influence outcome of disease. These are found in genes: *TP53*, *ATM*, *SF3B1*, *NOTCH1*.

Of these mutations, *TP53* gene mutations have the strongest negative impact on all markers of outcome (response to treatment, overall survival, progression free survival, MRD status), and even in the era of chemoimmunotherapy with current gold standard fludarabine, cyclophosphamide and rituximab (FCR) treatment, patients with *TP53* mutations have an overall survival of less than two years. (Stilgenbauer et al., 2014) Deletion of *TP53* is typically accompanied by a point mutation on the other allele (Dohner et al., 1995) and the mutations are mostly found in the DNA binding domain. (Zenz et al., 2010; Wang et al., 2011) *TP53* mutations are reported in 7-15% of patients (Dicker et al., 2009; Zenz et al., 2010; Gonzalez et al., 2011; Wang et al., 2011; Stilgenbauer et al., 2014) and are frequently, but not exclusively, associated with del(17p) (compound heterozygosity). (Zenz et al., 2010) (Wang et al., 2011) (Dicker et al., 2009) *TP53* mutated patients follow a similar clinical course in terms of chemorefractoriness and poorer overall survival as del(17p) patients, even in the absence of a del(17p). (Dicker et al., 2009; Rossi et al., 2009a; Zenz et al., 2010)

ATM mutations are reported in 12-30% of CLL patients and are significantly associated with *IGHV* unmutated status. Correspondingly, they are associated with poorer outcome, including adverse overall survival. (Stankovic et al., 2002; Austen et al., 2005)

Recurrent mutations in the PEST-coding region of *NOTCH1* have been identified in 4-12% CLL patients (Di Ianni et al., 2009; Puente et al., 2011; Wang et al., 2011; Oscier et al., 2013; Stilgenbauer et al., 2014). The mutations generate a premature stop codon, truncating the terminal protein PEST region and leading to an accumulation of active NOTCH1 isoform in CLL cells (Puente et al., 2011). Furthermore, a non-coding mutation in the 3'UTR of the *NOTCH1* gene has recently been identified which similarly truncates the NOTCH1 protein by removing part of the PEST protein domain. (Puente et al., 2015) CLL cells, but not normal B cells, constitutively express NOTCH1 protein which is important for their survival and for resistance to apoptosis (Rosati et al., 2009). *NOTCH1* mutations are consistently associated with trisomy 12 and with unmutated *IGHV* status. (Wang et al., 2011; Oscier et al., 2013; Stilgenbauer et al., 2014)

While *NOTCH1* and *SF3B1* mutations can both occur in conjunction with a *TP53* mutation, *NOTCH1* and *SF3B1* mutations appear to be almost mutually exclusive, suggesting that they may be involved in distinct pathways driving CLL.

SF3B1 (splicing factor 3b subunit 1) is a major component of the spliceosome complex, which is responsible for the removal of introns from transcribed pre-mRNA. SF3B1 therefore has the potential to affect the transcriptome with functional downstream effects. *SF3B1* mutations are seen in 15-18% CLL patients (Wang et al., 2011; Oscier et al., 2013; Stilgenbauer et al., 2014). They are rarely seen in patients with trisomy 12, in keeping with their mutual exclusivity from *NOTCH1* mutations which are frequently associated with trisomy 12 anomaly. While *SF3B1* mutations have been associated with fludarabine refractoriness (Rossi et al., 2011), these findings were not confirmed in the LRF CLL4 or CLL8 trials (Oscier et al., 2013; Stilgenbauer et al., 2014) where *SF3B1* mutations did not significantly affect overall response to treatment. *SF3B1* mutations were however found to be independent predictors of poorer progression free survival in the CLL4 trial (Oscier et al., 2013) and of overall survival in the CLL8 trial. (Stilgenbauer et al., 2014) The differences between these trials may reflect the differences in treatment administered (chemotherapy versus chemoimmunotherapy). *SF3B1* mutations are significantly associated with del(11q) or

with *ATM* mutations in the absence of del11q (Wang et al., 2011), suggesting an interaction between the *SF3B1* mutation and del(11q) status.

1.4.3.f CD49d

CD49d is an α4 integrin adhesion molecule (also known as very late antigen-4, VLA-4), and its expression in CLL is associated with a poorer outcome. (Zucchetto et al., 2006; Buggins et al., 2011) It is involved in the stromal support of CLL cells and can act via its ligand VCAM-1 (vascular cell adhesion molecule-1) in cell-cell interactions and via fibronectin when it binds to the extracellular matrix. (Rose et al., 2002).

CD49d expression is significantly associated with CD38 positivity in CLL though there is discordance between studies in a proportion of cases. The two factors offer complementary prognostic information. (Zucchetto et al., 2006; Buggins et al., 2011; Zucchetto et al., 2012)

Like ZAP70, CD49d is functionally linked with CD38 in CLL, and this is discussed further in section 1.4.5.

1.4.3.g Telomere length

Telomeres are complex structures comprising nucleotide repeats that cap the ends of chromosomes and protect them from degradation. They have important functions in maintaining genomic stability and integrity and their dysfunction is implicated in the pathogenesis of a number of cancers. (De Lange, 2005) In CLL, short telomeres are significantly associated with a poorer outcome. (Roos et al., 2008; Rossi et al., 2009b; Lin et al., 2014; Strefford et al., 2015)

1.4.4 Aetiology and maintenance of CLL

1.4.4.a CLL cell of origin

The cell of origin of CLL remains a topic of debate. The discovery of the distinct groups of unmutated and mutated CLL suggested that CLL might be two distinct diseases, arising from naïve pre-GC and activated post-GC cells respectively (section 1.1.3). However, all CLL B cells, whether *IGHV* mutated or unmutated, carry surface

markers indicative of B cell activation. (Damle et al., 2002) Specifically, they express CD23, CD25, CD69 and CD71, all consistent with B cell activation, and downregulate CD79b, CD22, CD32, again in keeping with B cell activation. The surface marker signature of the *IGHV* unmutated versus mutated CLL cells however differs in the ratio of CD69:CD71 positive cells observed. Interestingly, CD69 is a surface marker which is expressed within hours of activation, whilst CD71 expression is indicative of a longer interval since activation. Amongst the unmutated CLL cells, a higher proportion of cells express CD69 in comparison to CD71, and the opposite is true of mutated CLL cells, indicating that the unmutated cells are at an earlier stage of activation than the mutated cells. (Damle et al., 2002)

Furthermore, CLL cells express the memory cell surface marker CD27, regardless of their *IGHV* status. (Damle et al., 2002) In addition, an early gene expression profiling study found that CLL cells share a gene expression signature most similar to that of CD27+ memory B cells, rather than transitional CD5+ B cells, or germinal centre cells. The genetic profile of unmutated and mutated CLL largely overlapped, suggesting that they originate from a common precursor cell. (Klein et al., 2001; Rosenwald et al., 2001) However, the study of Klein *et al* did not compare the expression profile of CLL with that of mature CD5+ cells, and a later transcriptome analysis study determined that mature CD5+ B cells are the more likely precursor cell to CLL. This study suggested that unmutated CLL cells derive from mature CD5+ CD27- B cells and that mutated CLL cells derive from a previously unrecognised post GC-centre mutated CD5+CD27+ B cell subset. (Seifert et al., 2012)

1.4.4.b BCR signalling

There is strong evidence that B cell receptor signalling is important in the maintenance and proliferation of CLL cells. In particular, B cell receptor signalling is the most prominent pathway identified by gene expression profiling of CLL cells in the lymph nodes. (Herishanu et al., 2011) This is the case for both unmutated and mutated CLL cases, though the degree of over-expression is greater in the unmutated cases.

Furthermore, Messmer *et al* coined the term ‘stereotypy’ to indicate the

striking restriction in immunoglobulin heavy and light chain gene usage by CLL cells from different patients. (Messmer et al., 2004) Given the degree of variation acquired through V(D)J rearrangement and somatic hypermutation, the chance of two B cell clones expressing the same B cell receptor is incredibly slim. However, up to a third of CLL cases exhibit stereotyped BCRs. Unmutated CLL cases are especially enriched for BCR stereotypy. (Agathangelidis et al., 2012) Patients with stereotyped BCRs have quasi-identical heavy and light chain immunoglobulin gene usage, and the heavy chain complementarity determining region (HCDR) of the immunoglobulin heavy chain is particularly affected. (Agathangelidis et al., 2014) The observation of this strikingly restricted BCR repertoire among some CLL patients also led to the identification of specific 'subsets' of CLL cases, determined by the shared BCR structural components. These subsets share relevant clinical and biological outcomes such as outcome, epigenetic profiling, and genomic aberrations. (Agathangelidis et al., 2014)

B cell receptor stereotypy in CLL provides strong immunogenetic evidence for the importance of the BCR in CLL, and specifically for the idea that selective antigens might activate these restricted receptors, and thus drive the selection and proliferation of CLL cells.

In a search for the antigen involved in this signalling, two intriguing studies have demonstrated that CLL cells can signal autonomously via the B cell receptor. This signalling can occur independently of extrinsic antigens or even of other cells. B cell receptors derived from CLL cells in one of the studies, demonstrated activation and calcium flux in the absence of BCR cross-linking with exogenous ligands, whereas the receptors derived from other lymphoproliferative disorders all required BCR activation. The authors went on to observe that a peptide motif that activated CLL cells in a heavy chain complementarity determining region-3 (HCDR3)-dependent manner was closely homologous to an epitope in the VH domain and that mutation of this domain abolished the autonomous signalling. In the second study, a further peptide motif derived from a closely related area of the variable immunoglobulin region of a single CLL patient was identified, and shown similarly to interact with the B cell receptor of half of the CLL cases tested. Taken together, these data suggest that an intrinsic B cell receptor motif can mediate autonomous BCR signalling via an adjacent B cell receptor

on the same cell. (Duhren-von Minden et al., 2012; Binder et al., 2013)This model is supported by the observation of stereotypy which predominantly affects the HCDR3 region (Agathangelidis et al., 2014), and would suggest that autonomous signalling contributes to maintenance and expansion of the CLL clone.

1.4.4.c Tumour microenvironment

Despite this apparently autonomous drive via the B cell receptor in CLL, there is irrefutable evidence that CLL cells also rely heavily on the support of their microenvironment to survive and prosper. A major piece of experimental evidence that recurrently supports this theory, is the rapid death of *ex vivo* CLL cells in culture. The addition of stromal cells to the culture can rescue the CLL cells from apoptosis. (Lagneaux et al., 1999)

While the progression of CLL was previously thought to be due to an accumulation of mature, quiescent CLL cells slowly dividing in the peripheral blood and retaining a resistance to apoptosis, this model is now at least partially redundant. Heavy water experiments (Messmer et al., 2005) have demonstrated that proliferative activity in the CLL cell population is far greater than previously thought, with a daily 'birth rate' of 1-2% of the entire clone. In addition, gene expression profiling has revealed differences in the genetic signature of CLL cells found in the peripheral blood, bone marrow, and lymph nodes indicating the more activated state of CLL cells found in the lymph nodes compared to marrow or blood. (Herishanu et al., 2011) These studies support a '2-compartment model', in which the cells cycle between two separate tissue compartments, with different rates of cell division and death. (Messmer et al., 2005) In keeping with this model, is the finding of pseudofollicles or 'proliferation centres' within the lymph nodes, and to a lesser extent, the bone marrow, of CLL patients. (Schmid and Isaacson, 1994; Pileri et al., 2000) In these proliferation centres, the expression of anti-apoptotic protein, BCL2, is low (Schmid and Isaacson, 1994) and large CLL cells express proliferation markers such as KI67. (Hillmen, 2011) CLL cells recirculate between the peripheral blood and these proliferation centres, supported by a complex network of microenvironmental stimuli that govern their entry to the proliferation centres, and thus promote the

maintenance and expansion of the CLL population. Cytokine-mediated effects, cell-cell interactions, and cell-extracellular matrix interactions are all relevant to sustaining the CLL cell *in vivo* and promoting its expansion in the proliferation centres.

1.4.4.d Nurse-like cells

Nurse-like cells (NLCs) are one of the cell types that offer a proliferation and survival advantage to CLL cells. Nurse-like cells, which express high levels of CD68, are present in the peripheral blood of CLL patients (Burger et al., 1999), and differentiate spontaneously from CD14+ monocytoid cells into large, round, adherent, fibroblast-like cells when they are cultured in direct contact with CLL cells *in vitro*. (Burger et al., 2000; Tsukada et al., 2002) CLL cells in culture quickly undergo apoptosis, but retain viability in the presence of a layer of nurse-like cells. (Burger et al., 2000) In part, this survival advantage is delivered through the secretion of the chemoattractant cytokines (chemokines) CXCL12 and CXCL13. (Burger et al., 2000; Burkle et al., 2007) Nurse-like cells secrete CXCL12 (also known as stromal cell-derived-growth-factor 1), which binds to its cognate receptor, CXCR4 on CLL cells. CXCL12 appears to offer important pro-survival signals, as the administration of exogenous stromal-derived-growth factor 1 (SDF-1) to CLL cells *in vitro* rescues them from apoptosis. (Burger et al., 2000) In the bone marrow, marrow stromal cells (MSCs) predominantly express CXCL12 in preference to CXCL13, and are able to protect CLL cells *in vitro* from spontaneous and drug-induced apoptosis. (Kurtova et al., 2009) In addition, CXCL12 behaves as a chemoattractant cytokine when expressed by MSCs, as CLL cells migrate spontaneously underneath marrow stromal cells (pseudoemperipolesis) expressing CXCL12, *in vitro*. This migration is disrupted by pre-treatment of the CLL cells with anti-CXCR4 monoclonal antibodies, confirming the occurrence of CXCL12-CXCR4 cross-talk. (Burger et al., 1999) Once CXCR4 has been activated by CXCL12, the CXCR4 receptor is downregulated by receptor endocytosis (Burger et al., 1999) and this is reflected by the downregulation of *CXCR4* gene expression in CLL cells in the proliferative tissue compartment. (Herishanu et al., 2011)

In addition, chemoattractant cytokine, CXCL13 and its cognate receptor, CXCR5, are both overexpressed in CLL. (Burkle et al., 2007) Nurse-like cells found in the

proliferation centres in the secondary lymphoid organs of CLL patients (Tsukada et al., 2002) secrete CXCL13, a chemokine which is normally expressed in the germinal centre to stimulate the migration of mature circulating B cells to the germinal centre for antigen interaction and selection. CLL cells overexpress CXCR5 in comparison to normal B cells, and thus through CXCR5-CXCL13 interaction, circulating CLL cells are homed to the lymph nodes for further activation and proliferation in pseudofollicles. (Burkle et al., 2007) Activation of the CXCR5 receptor leads to subsequent downregulation of the receptor by endocytosis, and to downstream pathway signalling by the mitogen-activated protein kinase (MAPK) pathway. (Davids and Burger, 2012)

Furthermore, the chemokine genes *CCL3* and *CCL4* are highly upregulated in CLL cells after co-culture with nurse-like cells *in vitro*. (Burger et al., 2009). CCL3 and CCL4 are potent T cell attracting chemokines which support CLL cells by the recruitment of accessory T cells and monocytes. Secreted by CLL cells, CCL3 and CCL4 interact respectively with the CCR1 and CCR5 receptors expressed by CD68+ monocytoid nurse-like cells. Gene expression profiling demonstrates that these chemokines are upregulated in CLL cells of the lymph nodes, in comparison to cells of the peripheral blood. (Herishanu et al., 2011) Incubation of the CLL cells with a Syk-inhibitor almost completely abrogated the induction of CCL3 and CCL4 secretion by NLC co-culture, suggesting that the CCL3 and CCL4 production is Syk-dependent and therefore may be dependent on BCR signalling. (Burger et al., 2009)

Thus, nurse-like cells support CLL cells through the secretion of CXCL12 which rescues CLL cells from apoptosis; the secretion of CXCL13 which stimulates the migration of CLL cells from the periphery to the lymph nodes; and by induction of CCL3 and CCL4 which allow CLL cells to recruit other supportive accessory cells to their microenvironment. In addition, NLCs express a number of other pro-survival molecules, including plexin B1 (Deaglio et al., 2005), B-cell activating factor of the tumour necrosis family (BAFF) and a proliferation-inducing ligand (APRIL) (Nishio et al., 2005) thus indicating that they promote CLL cell survival through a number of distinct pathways. Importantly, NLCs also express CD31, the ligand for CD38, and this is discussed in more detail, in section 1.4.5. (Deaglio et al., 2005)

1.4.4.e Homing CLL cells to lymph nodes

Along with CXCL13/CXCR5 interaction, the chemokines CCL19 and CCL21 are important in the homing of CLL cells from the periphery to the lymph nodes. Through their *in vivo* expression on the high endothelial venules (HEVs) and surrounding stromal cells of the lymph nodes, these chemokines attract CLL cells which express the cognate CCR7 receptor, and lead them to migrate across the vascular endothelium to enter the lymph node in an *in vitro* transendothelial migration assay. (Till et al., 2002) CXCL12 was also observed in stimulating this transendothelial migration, but while CCL19 and CCL21 were observed by immunohistochemistry on HEVs of CLL lymph nodes, CXCL12 was not.

VCAM-1 is also expressed by HEV cells and other endothelial cells in CLL lymph nodes. VCAM-1 is the ligand for CD49d (α1 integrin) which is an adhesion molecule essential for leucocyte trafficking. (Rose et al., 2002) CD49d is expressed by CLL cells, and is associated with poor prognosis. The blocking of α1integrin function by antibodies *in vitro* disrupted CLL cell transendothelial migration, indicating that VCAM-1/α1 integrin (CD49d) interaction is also important in the entry of CLL cells in to lymph nodes. (Till et al., 2002)

The expression of α1 integrin/CD49d is also associated with CXCR4 expression in CLL (Majid et al., 2011) which suggests a coordinated role for these molecules in trafficking CLL cells to lymph nodes. Alpha 1 integrin activation and CXCR4 ligation also lead to the upregulation of matrix-metalloproteinase-9 (MMP-9) expression. MMP-9 is an enzyme involved in the degradation of the extracellular matrix, and it is expressed in CLL cells at higher levels than in normal B cells. (Redondo-Munoz et al., 2006; Redondo-Munoz et al., 2008)

Thus, while CXCL12 and CXCL13 chemokines attract CLL cells to the lymph nodes, the expression of CCL19 and CCL21 by endothelial cells allows transendothelial migration into the lymph node acting via the CCR7 receptor expressed by CLL cells. This migration is likely also supported by the interaction of CD49d and VCAM-1, and the consequent upregulation of MMP-9 secretion.

1.4.4.f T cell interactions

Once homed to the lymph node, CLL cell interactions with T cells further promote their survival and activation. Interactions between normal mature B cells via their CD40 receptor, and the CD40 ligand (CD40L, CD154) expressed by T cells, are essential in the induction of antigen presentation and normal B cell responses.

In CLL patients, proliferation centres in the lymph nodes and bone marrow contain numerous T cells (Pizzolo et al., 1983; Schmid and Isaacson, 1994) and the large, proliferating Ki67+ CLL cells co-localise with activated CD4+ T cells. (Patten et al., 2008). The *in vitro* ligation of the CD40 receptor on CLL cells by its ligand CD40L (secreted by activated T cells) induces activation of intracellular signalling pathways in CLL cells, and the upregulation of antiapoptotic proteins including BCL2 (Scielzo et al., 2011) and survivin. (Granziero et al., 2001) Furthermore, the interaction of T and B CLL cells by CD40/CD40L interaction induces transcription of CCL22 *in vitro*, a chemokine which recruits further CD4+ CD40L+ T cells expressing the corresponding CCR4 receptor. (Ghia et al., 2002)

CLL cells purified from the peripheral blood of CLL patients exhibit higher constitutive activity of the NFκB pathway than normal B cells from healthy blood donors. NFκB pathway proteins are key regulators of differentiation and survival in B cells and protect B cells from apoptosis, and this activity is augmented by *in vitro* ligation with an agonistic anti-CD40 antibody. CD40L was a potent inducer of NFκB activity in CLL cells, with the effect especially dramatic when ligation occurred via cell-bound CD154 ligation. There was a dramatic reduction in cell survival when the CD40/CD154 interaction was blocked by antiCD154 antibodies. (Furman et al., 2000)

To underline the importance of T cell interactions with CLL cells, it has been demonstrated that a T cell population is essential for successful engraftment and proliferation of a CLL xenograft in a mouse model. The administration of anti-CD3 or anti-CD4 monoclonal antibodies to eliminate the T cell population, almost completely aborted CLL growth. (Bagnara et al., 2011)

1.4.5 CD38 and CLL aetiology

CD38 is a well-established poor prognostic marker in CLL but there is also strong evidence to suggest that it has a role in CLL pathophysiology. Numerous lines of evidence indicate that it is associated with a more activated, proliferative CLL population, and that it has important roles in interactions with the supportive microenvironment.

CD38 expression is heterogeneous across the different CLL tissue compartments, in a manner that reflects an association with the more active, proliferative CLL compartment. Specifically, it is more highly expressed in the proliferation centres of the lymph nodes in comparison to the bone marrow or peripheral blood. (Ghia et al., 2003) (Jaksic et al., 2004) In addition, CD38 positivity reflects a more biologically active CLL cell, as it predicts for greater proliferative activity (Patten et al., 2008), and positive cells are enriched for the expression of cell activation and proliferation markers, KI67 and ZAP70, compared to CD38- CLL subclones within the same patient. (Damle et al., 2007) CD38+ CLL cells also demonstrate a global increase in tyrosine phosphorylation and an upregulation in their ability to signal via the B cell receptor and mobilise intracellular calcium, after anti-IgM stimulation. (Zupo et al., 1996; Pepper et al., 2006)

The ligand for CD38 was first identified through the observation of adhesion between CD38 expressing cells and the endothelial HUVEC cell line. (Dianzani et al., 1994) This natural ligand, CD31, is found on endothelial cells and also on monocytoid nurse-like cells (Deaglio et al., 1998; Deaglio et al., 2005) and there is evidence that CD38/CD31 interaction has an important role in the support of CD38+ CLL cells. Increased numbers of vasculature structures have been observed in areas of highest CD38+ density, and CD38+ cells appear to localise preferentially with vascular endothelial cells, expressing CD31. (Patten et al., 2008) CD38/CD31 interaction also leads to an increase in proliferative activity in CD38+ CLL cells *in vitro*. The interaction of CD38 with CD31 leads to remodelling of the CLL cell membrane, with a redistribution of CD38 molecules to the area of cell contact, and in addition, the co-localisation of CD19 and the B cell receptor to this region. (Deaglio et al., 2005) This

lateral association of CD38 and CD19 has also been demonstrated in co-capping experiments in normal and non-CLL malignant B cells, which indicated that functional CD19 is required for effective CD38 signalling. (Kitanaka et al., 1997) Interaction of CD38/CD31 in CLL also leads to the upregulation of pro-survival receptor, CD100, which is then able to interact with its corresponding ligand, plexin-B1, expressed by nurse-like cells. (Deaglio et al., 2005)

Genome profiling of CD38+ CLL cells after co-culture with murine fibroblast cells transfected to express CD31, have further confirmed an upregulation of important cell signalling pathways, including those involved in BCR signalling, MAP-K, Toll-like receptor and NOTCH signalling pathways. Furthermore, there is evidence of dysregulation of a number of apoptosis genes, and upregulation of some pathways involved in transendothelial leucocyte migration. (Deaglio et al., 2010)

The finding that CD38 ligation is associated with the upregulation of pathways involved in transendothelial migration is in keeping with the observation of a physical and functional link between CD38 and CD49d. There is evidence of co-localisation of these molecules in co-capping experiments on the CLL cell surface, alongside the β1 integrin subunit, CD29, which forms a heterodimer with CD49d. (Zucchetto *et al*, 2012). A supramolecular complex has subsequently been demonstrated in CLL cells, comprising CD38, CD49d, MMP-9 and CD44. (Redondo-Munoz et al., 2008; Vaisitti et al., 2010; Buggins et al., 2011) and CD38 has been shown to upregulate MMP-9. (Vaisitti et al., 2012) In addition, a more prominent network of VCAM-1+ endothelial and stromal cells is observed by immunohistochemistry (IHC) of lymphoid aggregates in the bone marrow biopsies of CD38+CD49d+ CLL patients. (Zucchetto, 2009) VCAM-1 is the ligand for CD49d, and CD44 is a cell adhesion molecule. Thus, taken together, these findings strongly suggest that CD38 is involved in an important supramolecular membrane complex with the ability to facilitate CLL cell trafficking and transendothelial migration into lymph nodes.

In addition, CD38+CD49d+ CLL cells overexpress the T cell attractant chemokines CCL3 and CCL4, and levels of these chemokines are further increased by CD38 ligation with either agonistic IB4 anti-CD38 antibody, or with CD31 ligation by

CD31 ligand transfected mouse fibroblasts. CD68+ monocytoid cells expressing CCR1 and CCR5, the receptors for CCL3 and CCL4 respectively, are also enriched in the bone marrow of patients with CD38+CD49d+ CLL cells. (Zucchetto et al., 2009)

Finally, there is a clear association between CD38 and ZAP70 positivity in the majority of patients, and these molecules appear to be functionally linked. CD38 signalling requires the presence of ZAP70, and the ligation of CD38 leads to ZAP70 phosphorylation. Furthermore, CLL cells that are positive for both CD38 and ZAP70 demonstrate enhanced migration to CXCL12 than cells that are positive for only one of these markers. (Deaglio et al., 2007)

Thus, CD38 marks an active, proliferative CLL population, with an enhanced migratory potential, and an increase in pathway signalling through its interaction with cells expressing its ligand, CD31. Furthermore, the involvement of CD38 in the supramolecular complex comprising CD49d, MMP and CD44, also indicates its importance in lymph node homing of CLL cells.

1.4.6 CLL Therapy

Typically, laboratory features such as a rapid lymphocyte doubling time, and clinical symptoms including weight loss, night sweats and increasing lymphadenopathy indicate disease progression, and these determine the need to initiate treatment. (Hallek et al., 2008) Traditionally, CLL treatment has comprised cytotoxics such as alkylating agents (chlorambucil, cyclophosphamide) and purine analogues (fludarabine), alone, or in combination chemotherapy regimens. Steroids are used for the treatment of associated autoimmune cytopaenias, or for short term symptom control in multiply treated patients or those unsuitable for chemotherapy agents. Patients who are fit for intensive treatment regimens receive a chemoimmunotherapy combination comprising fludarabine (F), cyclophosphamide (C) and rituximab (R), with the addition of rituximab bringing significant survival benefits compared to FC alone. (Hallek et al., 2010) This is a moderately toxic regimen with significant immunosuppressive side effects, and some older patients or those with significant comorbidities, may not be able to tolerate it. In these groups, chlorambucil has

typically been the treatment of choice, though bendamustine has been shown to be superior and is now recommended for first line use in patients for whom FCR is inappropriate. (Knauf et al., 2012)

The addition of the anti-CD20 monoclonal antibody, rituximab, to fludarabine and cyclophosphamide (FC), in the German CLL8 trial, saw a marked improvement in progression free survival in nearly all patient groups, and improved overall survival for patients with lower stage disease. However, the effect on del(17p) patients was marginal. (Hallek et al., 2010) Most of the risk groups established by the FISH hierarchical model (Dohner et al., 2000) saw a statistically significant improvement in their 3 year progression free survival (PFS) with FCR, though for the del17p patients, this translated to a 3 year PFS of only 18%. (Hallek et al., 2010) While there were marginal improvements in overall survival for patients with the poor prognostic genomic aberration, del(11q), receiving rituximab in combination with FC compared to FC alone (94% versus 83% 3 year overall survival, p=0.036); del(17p) patients saw no advantage with the addition of rituximab, and their outcome remained the worst overall (38%, 3 year survival). There was no significant improvement in PFS for patients with normal karyotype. FCR however did offer an advantage in both PFS and overall survival for patients with unmutated *IGHV* genes. In a multivariate analysis of biological and clinical factors, del(17p) retained the greatest negative impact on progression free survival (hazard ratio, (HR) 7.5, 95% C.I. 4.83-11.61, p=<0.0001).

Treatments for patients with del(17p) or *TP53* mutation have therefore become a high priority for moving CLL therapy forward, as these patients experience very poor outcome despite current gold standard FCR chemoimmunotherapy.

In an attempt to stratify treatment to address the poor outcome of del(17p) patients, an alternative monoclonal antibody, alemtuzumab, which targets CD52 has been used with some success. CD52 is expressed on malignant and non-malignant lymphocytes including CLL cells and its activity does not rely on the activity of the p53 pathway. In the CLL206 trial, a single-arm phase II study of 39 untreated and previously treated patients with *TP53* deletions, the combination of alemtuzumab and high dose methylprednisolone achieved remission rates favourable to those achieved by FCR in

previously untreated del17p patients. However, despite improved responses, relapse rates and overall survival were still poorer than patients without del17p treated with FCR. (Pettitt et al., 2012) Management of patients with *TP53* defects therefore remains a major challenge in the treatment of CLL.

1.4.6.a Novel agents in CLL

Ibrutinib is a potent, irreversible inhibitor of Bruton tyrosine kinase (BTK) which exerts its action by binding to cysteine residue 481, inhibiting phosphorylation of the BTK protein. It is delivered orally in a continuous dosing schedule. (Wiestner, 2013)

BTK is a non-receptor tyrosine kinase of the Tec kinase family, and is a critical mediator of BCR signalling. On BCR activation, BTK is activated by LYN and SYK leading to the activation of phospholipase C, intracellular calcium mobilisation, and the activation of transcription factors necessary for B cell activation. As well as its involvement in antigen-mediated BCR signalling, BTK is also important in the downstream signalling of other surface receptors including chemokines CXCR4 and CXCR5, and integrin adhesion molecules (Ponader et al., 2012). Thus, given the role of BCR signalling in CLL, along with the functions of CXCR4, CXCR5, and integrins in the trafficking of CLL cells to proliferation centres and the avoidance of apoptosis, inhibition of BTK was recognised as a very appealing therapeutic target in CLL.

A phase I dose finding study in 56 patients with mature B cell neoplasms, including 16 with CLL, demonstrated the safety and tolerability of ibrutinib. Eleven of the 16 CLL patients experienced a response. Shrinkage of lymph nodes was accompanied by an increase in peripheral blood lymhpocytosis, in keeping with the disruption of trafficking signals to the lymph node. (Advani et al., 2013)

In a pivotal phase II study, 85 relapsed, refractory CLL patients were treated with ibrutinib. The overall response rate was 71% and notably, this response was not influenced by the presence of del(17p) in a third of the patients with this alteration. Responses were durable with an overall survival of 83% at 26 months and progression free survival of 75%. (Byrd et al., 2013)

In a further phase II study, previously untreated and relapsed, refractory patients with a *TP53* aberration were exclusively selected in order to investigate further the effect of ibrutinib in these chemoimmunotherapy-resistant patients. (Farooqui et al., 2015) Forty-seven of the 51 patients had del(17p) and the remaining 4 had a *TP53* mutation in the absence of del(17p). After 6 months of therapy, a response was seen in 92% of patients, five of whom had achieved a complete remission. Notably, serial FISH analysis of CLL cells carrying the del(17p) aberration was carried out at baseline and after 6 months of treatment, to determine whether ibrutinib was selecting for del(17p) cell subclones for improved survival. There was no difference between the number of patients with a demonstrable increase or decrease in the number of cells carrying del(17p), suggesting that ibrutinib was not selecting for del(17p) subclones. In addition, there was no correlation between an increase in the number of cells harbouring del(17p) and adverse outcome. Notably, the frequency of relapse was greater in the previously treated, relapsed, refractory patient group compared to the previously untreated group (20% versus 9% at 24 months), suggesting that patients with *TP53* aberrations do better with ibrutinib when this agent is used up front as first line therapy. (Farooqui et al., 2015)

This suggestion was further supported by the results of a phase III study using ibrutinib as single agent in three patient cohorts: relapsed/refractory, treatment-naïve patients over the age of 65 years, and previously treated patients. Again, ibrutinib was well tolerated and after three years of follow up, 81% patients continued to take the drug. Treatment-naïve patients experienced better PFS, OS and complete remission (CR) rates than those who had received previous treatment for CLL, again supporting the suggestion that patients do better with ibrutinib when it is used upfront rather than in salvage therapy. While this longer follow up revealed that the presence of del(11q) or del(17p) did adversely affect overall outcome, the progression free survival durations remained favourable to those achieved with FCR in these patient groups. (Byrd et al., 2013; Byrd et al., 2015)

1.4.7 Constitutional genetics in CLL

Of all the haematological malignancies, CLL has the strongest heritable component. A population-based registry study of 9,717 CLL patients showed an increased risk of CLL in first degree relatives of 8.5 fold. (Goldin et al., 2009) However, no consistent biological or clinical differences have been demonstrated between familial and sporadic CLL. (Crowther-Swanepoel et al., 2008; Goldin et al., 2010) Furthermore, despite genome wide studies analysing large numbers of CLL families (Sellick et al., 2007), and other studies investigating families with multiple affected members (Raval et al., 2007; Fuller et al., 2008), no single high risk candidate gene to explain familial CLL has been identified.

Thus, a polygenic model of heritability has been proposed, in which a number of low risk variants, each conferring a modest increase in risk of CLL, contribute overall to the development of CLL in specific individuals. In particular cases, for example in familial CLL, the inheritance of a number of these variants would act in concert to lead to a higher risk of CLL than in the general population. (Speedy et al., 2013)

Genome wide association studies (GWAS) in multiple case control studies have thus far robustly identified 31 single nucleotide polymorphisms (SNPs), which increase the risk of the incidence of CLL. (Table 1.4) (Di Bernardo et al., 2008; Crowther-Swanepoel et al., 2010; Slager et al., 2010; Crowther-Swanepoel et al., 2011; Slager et al., 2011; Slager et al., 2012; Berndt et al., 2013; Slager et al., 2013; Speedy et al., 2014; Sava et al., 2015) All of these are common variants with a minor allele frequency (MAF) of more than 0.1. Individually, they each contribute only a small increase to the risk of developing CLL, with odds ratios ranging from 1.2 to 1.5. However, these studies have low power to detect SNPs which are rare (with a MAF of less than 0.1) or which contribute smaller relative risk (less than 1.3). It is therefore possible that additional common allelic variants which contribute only a very small increase in risk for the development of CLL, or moderately penetrant but rare alleles, have yet to be identified. (Di Bernardo et al., 2013)

SNP	Chromosome	Gene	OR	Reference
rs872071	6p25.3	*IRF4*	1.54	(Di Bernardo *et al.*, 2008)
rs735665	11q24.1	*GRAMD1B*	1.45	
rs7176508	15q21.3		1.4	
rs13397985	2q37.1	*SP140, SP110*	1.4	
rs17483466	2q13	*ACOXL, BCL2L11*	1.4	
rs11083846	19q13.32	*PRKD2, STRN4*	1.4	
rs2456449	8q24.21		1.3	(Crowther-Swanepoel *et al.*, 2010)
rs757978	2q37.3	*FIR*	1.4	
rs305061	16q24.1	*IRF8*	1.2	
rs7169431	15q21.3	*RFX7, NEDD4*	1.4	
rs783540	15q25.2	*CPEB1*	1.2	(Crowther-Swanepoel *et al.*, 2011)
rs674313				(Slager *et al.*, 2011)
rs210142	6p21.33	*BAk1*	1.4	(Slager *et al.*, 2012)
rs1044873	16q24.1	*IRF8*		(Slager *et al.*, 2013)
rs4406737	10q23	*ACTA2, FAS*	1.3	(Berndt *et al.*, 2013)
rs4987855	18q21	*BCL2*	1.5	
rs7944004	11p15.5	*C11orf21*	1.2	
rs898518	4q25	*LEF1*	1.2	
rs3769825	2q33	*CASP10, CASP8*	1.2	
rs1679013	9p21	*CDKN2B-AS1*	1.2	
rs4368253	18q21	*PMAIP1*	1.2	
rs8024033	15q15	*BMF*	1.2	
rs3770745	2p22	*QPCT*	1.2	
rs13401811	2q13	*ACOXL, BCL2L11*	1.4	
rs10936599	3q26.2		1.3	(Speedy *et al.*, 2014)
rs6858698	4q26		1.3	
rs2236256	6q25.2	*IPCEF1*	1.2	
rs17246404	7q31.33	*POT1*	1.2	
rs10069690	5p15.33	*TERT*		
rs2511714	8q22.33			
rs10735079	12q24.13	*OAS*		(Sava *et al.*, 2015)

Table 1.4 Risk alleles for CLL identified in genome wide association studies (GWAS)

Thirty-one common risk alleles for CLL have been identified in GWAS studies, all with a minor allele frequency (MAF) of greater than 0.1. OR indicates odds ratio for the development of CLL.

1.4.7.a *IRF4* carries a common risk allele for CLL incidence

Of the common risk alleles identified in the GWAS studies conducted so far, the SNP associated with the highest increased risk of CLL incidence (rs872071) was identified in the 3'UTR region of *IRF4.* This risk allele is associated with an odds ratio of 1.54 for the development of CLL. (Di Bernardo et al., 2008) (Table 1.4) In fact, homozygote carriers of the risk allele had a 2.7 fold increase in the risk of developing CLL, compared to non-carriers. (Di Bernardo et al., 2008) *IRF4* risk allele status was subsequently determined in 840 patients of the Newcastle CLL Consortium, and those carrying the risk allele were found to have a significantly worse treatment-free survival than non-carriers. (Allan et al., 2010) (Figure 1.6)

Given that IRF4 has a clear role in both the maturation and differentiation of B cells, it is entirely conceivable that it should be involved in the pathophysiology of CLL. In fact, it is already known to be essential in myeloma, another B cell malignancy, (Shaffer et al., 2008) and in rare cases of myeloma the *IRF4* gene is brought under the control of the immunoglobulin heavy chain gene through a translocation, indicating that IRF4 can act as an oncogene. (Iida et al., 1997) IRF4 is also expressed in the majority of diffuse large B cell lymphomas, a proportion of marginal zone lymphomas, Hodgkin lymphoma, and several T cell malignancies. (Tsuboi et al., 2000) The *IRF4* risk allele in CLL, defined by rs872071, is also associated with increased risk of Hodgkin lymphoma. (Broderick et al., 2010)

Furthermore, the risk allele identified in the GWAS study falls within the 3'UTR region of the *IRF4* gene, a region typically associated with translation efficiency and transcript stability, and with susceptibility to regulation by microRNAs. This indicates that the SNP is in a potentially functional region of the *IRF4* gene, and thus may have a functional role in the onset of CLL.

There is already evidence of IRF4 expression in CLL, though attempts to discern a possible role in affecting disease outcome have thus far generated contradictory results. (Chang et al., 2002a; Ito et al., 2002) More recently however, a novel mouse model of CLL has been developed, in which IRF4-/- mice develop CLL with 100%

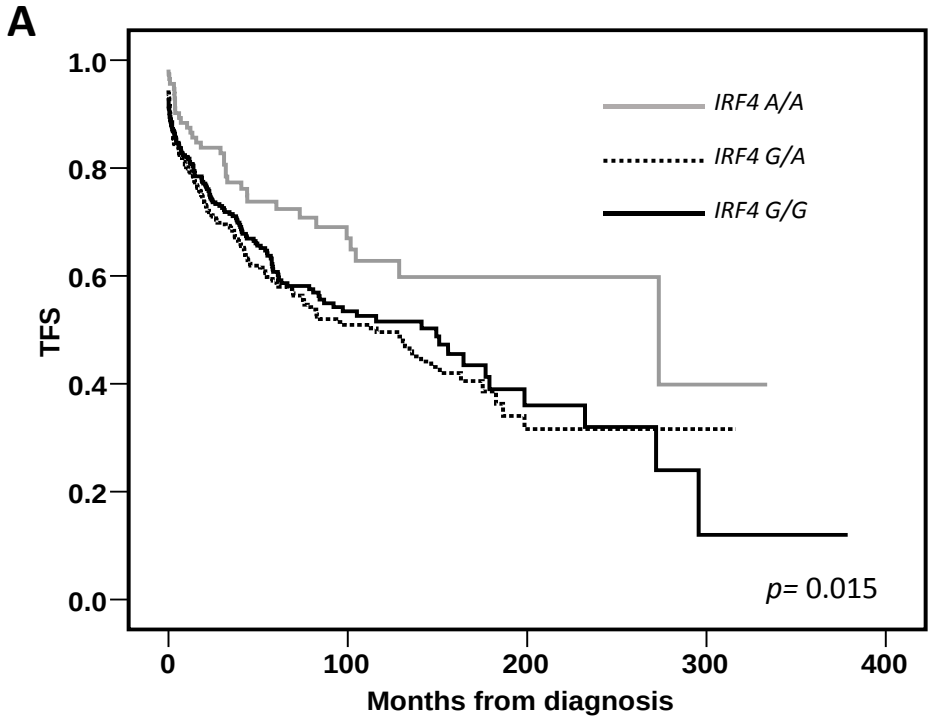

(Allan *et al.*, 2010)

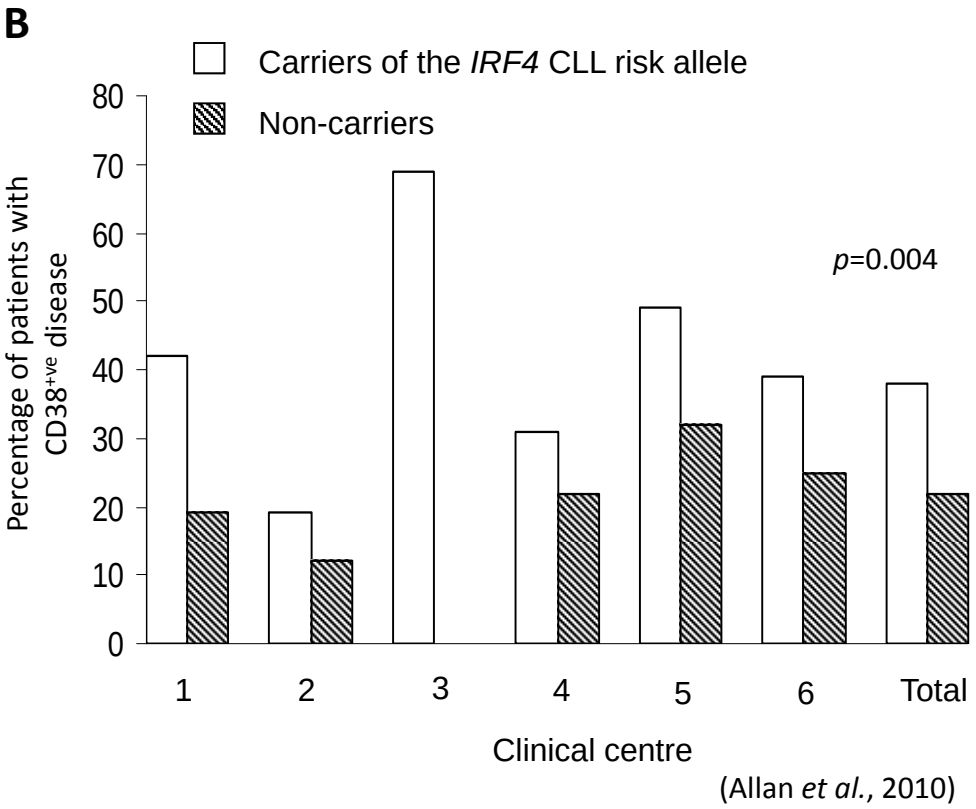

(Allan *et al.*, 2010)

Figure 1.6 rs872071 risk allele in *IRF4*

rs872071, a single nucleotide polymorphism (SNP) in *IRF4*, is a low penetrance, high risk allele for the development of CLL. (Di Bernardo *et al.*, 2008)

A. Furthermore, in an analysis of 840 CLL patients of the Newcastle CLL consortium, both heterozygote and homozygote carriers of the risk allele (A>G) had significantly worse treatment free survival than non-carriers (p=0.015). (Allan *et al.*, 2010)

B. rs872071 is also signficantly associated with CD38 positivity in CLL. (Allan *et al.*, 2010)

penetrance. (Shukla et al., 2013) The GWAS study that identified rs872071 in association with CLL investigated the effect of this SNP on IRF4 expression. *IRF4* mRNA transcript levels were found to be reduced in patients carrying the risk allele (p=0.042), in a dose dependent fashion, though protein expression levels were not investigated. (Di Bernardo et al., 2008) In a separate study, *IRF4* mRNA levels were again reduced in carriers of the rs872071 risk allele, though protein levels were found to be unaffected. (Patz *et al*., 2011) Taken together, these results suggest that low IRF4 expression is important in the development of CLL, and that the risk allele identified in IRF4 may operate to increase CLL risk through a reduction in IRF4 expression. If this were the case, it is conceivable that a lower IRF4 level might disrupt normal B cell development by preventing cell passage from the GC light zone for terminal differentiation to memory B cells and plasma cells, although this model remains to be tested.

1.4.7.b IRF4 risk allele is associated with CD38 positivity

In the same Newcastle study that determined the association of the IRF4 risk allele status with poorer treatment free survival, the CLL risk allele defined by rs872071 was also shown to be associated with CD38 positivity (p=0.004). (Figure 1.6B) (Allan et al., 2010) Initial interrogation of the *CD38* gene also revealed a putative IRF4 binding site, identical to the sequence used to crystallise the IRF4 ternary structure, immediately upstream of the translational start site of *CD38*. (Escalante et al., 2002; Allan et al., 2010)

1.5 Hypothesis

Therefore, given that the IRF4 risk allele is associated with the development of CLL, poor outcome, and CD38 positivity; and given the identification of a potential consensus binding site for IRF4 in the *CD38* gene: the central hypothesis of this project is that IRF4 has a functional role in the regulation of CD38.

1.6 Aims

The overarching aim of this project is to define the genetic and functional relationship between IRF4 and CD38 in CLL. Specifically, the strategies to achieve this aim were as follows:

- To use chromatin immunoprecipitation (ChIP) to investigate binding of IRF4 to *CD38* in a panel of lymphoid cell lines.
- To use RNA interference (RNAi) techniques to establish IRF4 knockdown in a panel of lymphoid cell lines, and to demonstrate the effect of this knockdown on IRF4-*CD38* binding by ChIP.
- To use ChIP targeted against histone methylation marks to investigate the effect of IRF4 knockdown on *CD38* transcriptional activity in lymphoid cell lines.
- To investigate the effect of IRF4 knockdown in lymphoid cell lines, on growth kinetics and sensitivity to cytotoxic agents commonly used in CLL.
- To investigate the effect of IRF4 knockdown on CD38 surface expression in lymphoid cell lines, as determined using flow cytometry.
- To use a CD40L-expressing co-culture system to maintain primary CLL lymphocytes *ex vivo*.
- To investigate evidence of IRF4-*CD38* binding in primary CLL lymphocytes, using ChIP.
- To use ChIP targeted against histone methylation marks to investigate the effect of IRF4 knockdown on *CD38* transcriptional activity in primary CLL lymphocytes.

Chapter 2. **Materials and Methods**

2.1 Chemicals and Reagents

All chemicals and reagents used throughout were of Analar grade. Phosphate buffered saline (PBS) was prepared from PBS tablets (Invitrogen Life Technologies, Paisley, UK) and was autoclaved prior to use. Preparation of reagents for use in specific investigations is described in the relevant sections below.

2.2 Cell Lines

The lymphoblastoid TK6 cell line was a kind gift from Prof. W. Thilly (Massachusetts Institute of Technology, MA, USA). The CD40-ligand expressing mouse fibroblast L-cell line engineered to express the CD40 ligand (CD40L) and parental non-expressor fibroblast line (NTL) were both kind gifts from Professor Chris Pepper (Cardiff University, UK). The CLL cell line MEC-1 and its sister line, MEC-2 were obtained from Leibniz Institute DSMZ-German Collection of Microorganisms and Cell Cultures, (DSMZ, Germany). Specific features of individual cell lines are described in detail in the relevant results chapters.

2.3 General Cell Culture Methods

2.3.1 Routine Cell Culture

All cell media, foetal bovine serum (FBS), and cell media additives including penicillin/streptomycin and L-glutamine, were purchased from Sigma-Aldrich, UK. Tissue culture plastic ware (sterile cell culture flasks and plates) was obtained from Corning Costar® (purchased from VWR International, UK). Cells were incubated at 37°C in a humidified 5% CO2 incubator (Heraeus Equipment Ltd., Essex, UK).

The suspension cell line TK6 and the adherent mouse fibroblast cell lines were all maintained in RF10% media (comprising Roswell Park Memorial Institute, RPMI 1640 medium, supplemented with 10% (v/v) FBS and 50ug/ml penicillin/streptomycin). SU-DHL-6 was maintained as a suspension cell culture in RF20% media (RPMI 1640 medium, supplemented with 20% (v/v) FBS and 50ug/ml penicillin/streptomycin). MEC-1 and MEC-2 cell lines were maintained as suspension cultures in IMDM 10% (Iscove's Modified Dulbecco's Medium, IMDM, supplemented with 10% (v/v) FBS and

Cell line	Optimal density ($x10^6$/ml)	Media
TK6	0.2-1.0	RF10%
SU-DHL-6	0.4-1.0	RF20%
MEC-1 and MEC-2	0.5-2.0	IMDM20% / IMDM 10%
CD40L/NTL fibroblast cells	30-80% confluence	RF10%

Table 2.1 Cell lines

TK6 cell line and CD40L-expressing and parental non-expressor (NTL) fibroblast cell lines were maintained in RF10% media (comprising RPMI 1640 medium, supplemented with 10% (v/v) FBS and 50ug/ml penicillin/streptomycin). SU-DHL-6 was maintained as a suspension cell culture in RF20% media (RPMI 1640 medium, supplemented with 20% (v/v) FBS and 50ug/ml penicillin/streptomycin). MEC-1 and MEC-2 cells were cultured in IMDM 20% (IMDM, supplemented with 20% (v/v) FBS and 50ug/ml penicillin/ streptomycin) for one week after thawing from cryopreserved stocks, and then cultured in IMDM10% thereafter.

50ug/ml penicillin/streptomycin). (Table 2.1). Testing for mycoplasma was performed by E. C. Matheson at 2 monthly intervals using a MycoAlert kit (Lonza Biologics, Slough, UK).

2.3.2 Cell counting and determination of cell density for suspension cell lines

An aliquot of single cell suspension was combined with 0.4% trypan blue (Sigma-Aldrich, UK) in a 1:1 ratio, and 10ul of this was dropped on to a Neubauer haemocytometer (Hawksley, UK) for counting at x50 magnification. A minimum of 100 cells was recorded at each count and used to calculate cell density, measured in cells $x10^6$/ml.

2.3.3 Passage of suspension cell lines

After determining cell density, cells were passaged in order to maintain them in exponential growth phase for experimental use. An appropriate volume of cell suspension and fresh media was transferred to a sterile culture flask in order to achieve the correct cell density for ongoing culture. (Table 2.1)

2.3.4 Passage of adherent mouse fibroblast cell lines

Trypsin-EDTA was used to detach the adherent CD40L and NTL monolayer cells from culture flasks for counting and passage. Specifically, media was first removed from the culture flask by aspiration, and sufficient sterile, warmed PBS was added to cover the cell surface. PBS was then removed by aspiration and 1ml trypsin-EDTA (Sigma-Aldrich, UK) (10% (v/v) in sterile PBS) was added and the culture flask gently tipped to ensure even coverage of the cell layer. Excess trypsin solution was then removed by aspiration and the flask was placed at 37°C for 1-2 minutes. The cells were inspected under the microscope to ensure that they had begun to detach from the flask surface, and the flask was tapped sharply before adding warmed RF10% media to neutralise the trypsin and resuspend the cells. The cells were then either counted (for use in co-culture experiments) or passaged at a ratio of 1 in 4 in fresh, warmed media into a sterile culture flask.

2.3.5 Cryopreservation of cell stocks

After determining the cell density, a sufficient volume of cells containing $5x10^6$ cells (or $7x10^6$ cells for cryopreservation of SU-DHL-6) was centrifuged at 335g for 5 minutes and the supernatant media was discarded. One millilitre of freezing media (10% (v/v) dimethyl sulphoxide (DMSO) in FBS) was then added drop-wise to re-suspend the cell pellet and the suspension was transferred to a sterile polypropylene cryovial (ThermoScientific, UK). Cryovials were placed in a Mr FrostyTM freezing container (ThermoScientific, UK) and transferred to a -80° freezer before being transferred to a liquid nitrogen tank for long term storage.

2.3.6 Resuscitation of frozen cell stocks

Cryopreserved cell pellets were rapidly thawed and then washed twice in 5ml warmed media. At each wash step, the cell suspension was centrifuged at 230g for 5 minutes and all of the supernatant was carefully removed and discarded. The cell pellets were then re-suspended in warmed media in sterile $25cm^3$ culture flasks at optimal cell density. (Table 2.1) The cell lines were all re-suspended into the appropriate media (section 2.3.1), except for MEC-1 and MEC-2 cell lines, which were cultured in IMDM 20% media (IMDM medium, supplemented with 20% (v/v) FBS and 50□g/ml penicillin/ streptomycin) for one week after resuscitation, and then transferred to culture in IMDM 10%.

2.3.7 Preparation of cell pellets

Cell pellets were prepared for use in western immunoblotting and DNA extraction. Cell density was determined, and then sufficient volume of cell suspension to provide $5x10^6$ cells was centrifuged at 525g for 5 minutes and the supernatant discarded. Two washes were then performed in excess PBS with centrifugation at 525g for 5 minutes, and the cell suspension was transferred to a 1.5ml Eppendorf on the second wash. After removing and discarding the second wash supernatant, the cell pellets were transferred to the -80° freezer for future use.

2.3.8 Setting up cell growth curves

After determining cell density with two independent counts of a single cell suspension, cells were then re-suspended in appropriate cell medium to a density of $5x10^4$ cells/ml. Four millilitres of this cell suspension was then added to one well of a sterile 12 well culture plate and kept at 37°/5% CO2. The cells were counted at 24 hour intervals until cell numbers had reached a plateau phase. Cell numbers were then plotted to generate cell growth curves.

2.3.9 Setting up cytotoxic growth inhibition assays

After determining cell density with two independent counts of a single cell suspension, cells were re-suspended in the appropriate cell medium to a density of $5x10^4$ cells/ml. Five millilitres of this cell suspension was added to each well of a sterile 6 well culture plate. Cytotoxic agents were made to a 50mM stock concentration in the appropriate solvent (DMSO or sterile water) prior to first use, and stored appropriately. (Table 2.2) The stock solution was diluted in media to a working concentration, and then added to the wells to achieve the target cytotoxic concentration.

A 'vehicle only' control well was prepared, to which solvent alone was added to match the highest concentration of the solvent in the cytotoxic-treated wells. Cell growth in the vehicle only well was compared to an untreated well at the termination of each experiment, to determine any cell toxicity due to the solvent alone.

The cells were counted after 4-6 days. Percentage cell survival was determined in the vehicle only well, compared to the untreated well. Cell survival in the wells treated with cytotoxic agents was then normalised to the vehicle only well, to account for any cytotoxic effects of the solvent. The data were plotted in growth inhibition curves.

Cytotoxic agent	Molecular weight (g)	Solvent	Stock solution (mM)	Storage conditions
Fludarabine	365.21	DMSO	50	-20°C
Ibrutinib	440.5	DMSO	50	-80°C
Bendamustine	394.72	Sterile water	50	-20°C

Table 2.2 Preparation of cytotoxic agents for growth inhibition assays
Cytotoxic agents were prepared and stored according to suppliers' instructions.

2.4 Western immunoblotting

2.4.1 Cytosol preparation

Cell pellets were prepared from exponentially growing cells. Each cell pellet was re-suspended in 100µl of whole cell extract buffer (62.5M Tris-HCl pH 6.8, 2% (w/v) SDS, 20% (v/v) glycerol) and homogenised using a 21G needle and 1ml syringe to disrupt the cell membranes. The suspension was boiled in a 100°C heating block for 5 minutes and then centrifuged for 10 minutes at 18600G. The supernatant, comprising the cytosolic extract, was transferred to a clean 1.5ml tube and the pellet discarded. Protein concentration of the supernatant was determined by Pierce BCA assay. (Section 2.4.2)

2.4.2 Estimation of protein concentration by Pierce BCA assay

Protein concentration of the cytosol was determined by bicinchoninic (BCA) assay, using a Protein Assay (ThermoScientific) kit. Manufacturers' instructions are briefly summarised as follows. Samples were diluted 1:10 in deionised water, to bring them to within the detection range of the kit (0.2-1.2mg/ml). Ten microliters of each diluted sample was then added in quadruplicate to a 96 well plate. An adequate volume of working reagent (Reagent A and Reagent B in a 50:1 ratio) was prepared, and 190µl was added to each well. The plate was then placed at 37°C for 30 minutes, before being cooled to room temperature and analysed using a BioRad Model 680 Microplate Reader. Protein concentration was estimated from the corrected mean absorbance values, using a standard curve that was constructed using bovine serum albumin (BSA) and assayed simultaneously. A multiplication factor of 10 was applied to the resulting sample values, to account for the 1:10 sample dilution.

2.4.3 SDS polyacrylamide gene electrophoresis (PAGE) and electrophoretic transfer

Sodium dodecyl sulphate polyacrylamide gel electrophoresis (SDS-PAGE) was used to separate proteins from the whole cell extract samples, according to protein size. Once protein concentration had been determined (section 2.4.2), samples were prepared in whole cell extract buffer at a protein concentration of 0.2mg/ml or

1.0mg/ml, depending on the protein to be detected. Bromophenol blue (Sigma-Aldrich,UK) and 2-mercaptoethanol (Sigma-Aldrich,UK) were added to a final concentration of 0.01% (v/v) and 5% (v/v) respectively.

Mini PROTEAN® TGX Precast gels (BioRad, UK) were prepared in a Mini PROTEAN® Tetra Cell electrophoresis chamber (BioRad, UK) in SDS running buffer (41.2mM Tris-HCl pH 6.8, 192 mM glycerol, 0.1% (w/v) SDS). Between 10 and 30µl of each sample was loaded on to the gel (depending on the number of samples to be run and thus the well size), and 5µl of Benchmark Pre-stained Protein Ladder (Invitrogen Life Technologies) was loaded in to one well of each gel. Electrophoresis was performed using a PowerPac basic (BioRad, UK) power pack, with a constant voltage of 180V until the bromophenol blue dye front could be seen to have reached the bottom of the gel (approximately 30-60 minutes).

Proteins were then transferred by electrophoresis, from the gel to Whatman® PVDF 0.2µm membrane (Sigma-Aldrich,UK), sandwiched between pieces of Whatman® 3mm chromatography paper (Sigma-Aldrich,UK) in a Mini TransBlot Cell cassette (BioRad,UK) in transfer buffer (10mM CAPS-NaOH pH 11, 10% (v/v) methanol). Electrophoretic transfer was performed at 100V for 1 hour.

2.4.4 Antibody detection and visualisation of bound proteins

Membranes were incubated in a 5% blocking solution (TBS-Tween [0.01M Tris-HCl pH 7.5, 0.1M NaCl, 0.05% (v/v) Tween-20], 5% (w/v) Marvel milk powder) for at least an hour at room temperature, with constant agitation. They were then incubated in primary antibody diluted to the appropriate concentration (Table 2.3) in 5% blocking buffer at 4°C overnight. The following day, membranes were washed 8 times at 5 minute intervals, in an excess of TBS-Tween, to remove any non-specifically bound primary antibody. They were then incubated for 1 hour with a secondary antibody conjugated to horseradish peroxidase (HRP), diluted in 5% blocking buffer. (Table 2.3) The membranes were then washed again, 8 times at 5 minute intervals in excess TBS-Tween. Detection of bound proteins was performed using Amersham ECL Prime Western Blotting detection reagent, according to manufacturer's instructions.

Protein	Molecular weight (kDa)	Antibody type	Isotype	Supplier	Cat No.	Dilution
Primary antibodies						
IRF4	52	Polyclonal	Goat IgG	Santa Cruz	sc-6059	1: 30 000
PU.1	37	Polyclonal	Rabbit IgG	Santa Cruz	sc-352	1:10 000
ICSBP/ IRF8	52	Polyclonal	Goat IgG	Santa Cruz	sc-6058	1:10 000
Tubulin	50	Monoclonal	Mouse IgG	Sigma-Aldrich	T6074	1: 80 000
Secondary antibodies						
Rabbit Anti-Goat IgG, HRP conjugate	-	Polyclonal	Rabbit IgG	Dako	P-0160	1: 5 000
Goat Anti-Mouse IgG, HRP conjugated	-	Polyclonal	Goat IgG	Dako	P-0447	1:5 000
Goat Anti-Rabbit IgG, HRP conjugated	-	Polyclonal	Goat IgG	Dako	P-0448	1:5 000

Table 2.3 Primary and secondary antibodies used in western immunoblotting
Primary western immunoblotting antibodies were optimised for use at the dilutions indicated.

Chemiluminescence was detected by exposure of the membranes to CareStream Kodak BioMax light film (Sigma-Aldrich,UK) and films were developed using a Mediphot 937 X-Ray Filmprocessor (Colenta Lobortechnik, Austria).

To quantify knockdown of protein in cells with siRNA or shRNA-mediated IRF4 protein knockdown (section 2.5), western immunoblots were assessed by densitometry using FujiFilm Intelligent Dark Box, LAS-3000, Luminescent Image Analyser System and the data were analysed using LAS 3000 Image Reader software. Quantification of knockdown was determined by normalizing the signal detected in knockdown cells to the loading control, and then to a mean of the off target control cell signals.

2.5 Generation of knockdown cell lines deficient in IRF4 using short interfering and short hairpin RNA-mediated gene knockdown

Short interfering and short hairpin RNA (siRNA and shRNA, respectively) techniques were used to target *IRF4* mRNA transcript for degradation prior to translation.

Short interfering RNA is capable of delivering transient protein knockdown only, as the transfected siRNA is not present in daughter cells.

Short hairpin RNA interference can establish more permanent knockdown, as the shRNA-expression cassette is integrated into the host cell genome and passed on to daughter cells. Transduction of cells with shRNA establishes a population of cells with varying levels of transduction efficiency and shRNA integration events. A further step is therefore performed to produce cell clones from a single cell, with uniform protein knockdown.

2.5.1 siRNA constructs, controls and reagents

Short interfering RNA constructs targeted to IRF4 were purchased from Qiagen, UK (FlexiTube siRNA) (Table 2.4) and were used in combination (designated 'Combination siRNA' hereafter). Mission® siRNA Universal Negative Control #1 (Sigma-Aldrich, UK) which is targeted against no known mammalian gene, was used as a

siRNA	Target sequence	Sense strand	Antisense strand	Supplier	Cat No.
Hs_IRF4_1	5’-CCCGACGGGCTCTATGCGAAA-3’	5’-CGACGGGCUCUAUGCGAAATT-3’	5’-UUUCGCAUAGAGCCCGUCGGG-3’	Qiagen	SI00038150
Hs_IRF4_10	5’-CAGGCCGTTTCTCATACTACA-3’	5’-GGCCGUUUCUCAUACUACATT-3’	5’-UGUAGUAUGAGAAACGGCCTG	Qiagen	SI04750326

Table 2.4 siRNA constructs for knockdown of *IRF4*
Two siRNA constructs were used in combination (Combination siRNA) for targeted knockdown of *IRF4* in a panel of lymphoid cell lines.

negative control (referred to as 'off target control' hereafter) for transfection. The siRNA stocks were received as lyophilised stock and were reconstituted on ice in HyClone HyPur Molecular Biology grade water (ThermoScientific, UK) to 20µM concentration. Aliquots were prepared to avoid repeat freeze-thaw cycles, and the aliquots were stored long-term at -20°C.

2.5.2 siRNA transfection

siRNA was delivered to the cells by electroporation. On each occasion, two control cell populations were prepared simultaneously. A mock cell sample underwent electroporation only. A second control cell sample underwent electroporation with the off target control siRNA construct.

Exponentially growing cells were counted and an appropriate volume of cell suspension to achieve sufficient electroporated cells for ongoing experiments was then centrifuged at 230g for 5 minutes. Following removal of the supernatant by aspiration, cells were re-suspended in pre-warmed media at a concentration of $20x10^6$/ml in a 50ml BD FalconTM tube. Five hundred microliters of cell suspension (10^7 cells) was transferred to 4mm electroporation cuvettes (Eurogentec, UK). A mock sample underwent electroporation only at 260V for 10 milliseconds. Either the off target control siRNA construct or Combination siRNA (Table 2.4) were then added to the other cuvettes, to a concentration of 500nM or 1 µM (experiment-dependent). The cuvettes underwent electroporation immediately after addition of the siRNA.

Cells were then re-suspended in pre-warmed media, in one of three sterile labelled culture flasks: electroporation only (mock), off target control, or Combination siRNA, at cell density of $6x10^5$/ml (in the case of TK6 and SU-DHL-6) or $8x10^5$/ml (MEC-1).

Cells were counted and pelleted for western immunoblotting at intervals after electroporation, to determine whether knockdown of IRF4 protein had been achieved. Electroporated cells were also used for preparation of chromatin for use in chromatin immunoprecipitation experiments (section 2.6), for proliferation assays (section 2.3.8) or for cytotoxic inhibition assays (section 2.3.9).

2.5.3 shRNA constructs, controls and reagents

Six different shRNA constructs were purchased from Sigma-Aldrich, UK. These were supplied in a pLKO.1 vector and pre-packaged in Mission® shRNA Lentiviral Transduction Particles. The pLKO.1 vector includes a puromycin-resistance gene. The shRNA constructs were targeted against the 3'UTR or coding domain sequence (CDS) of IRF4 and are referred to by their construct number hereafter. (Table 2.5) Transduction particles containing an empty pLKO.1 vector backbone (Mission® pLKO.1-puro Empty Vector Control Transduction Particles, Sigma-Aldrich, UK) (referred to as 'empty vector control' from hereafter) or a pLKO.1 vector with an shRNA insert targeted against no known mammalian gene (Mission® pLKO.1-puro Non-Mammalian shRNA Control Transduction Particles, Sigma-Aldrich,UK) (referred to as 'off target control' from hereafter) were used as negative controls for transduction. The lentiviral particles were received as frozen stock, aliquoted to avoid repeated freeze-thaw cycles, and stored at -80°C. Viral titres (Tu) were provided by Sigma-Aldrich, UK, for each of the shRNA constructs supplied, and this information was used to calculate the multiplicity of infection (MOI). (section 2.5.6)

Polybrene (hexadimethrine bromide, Sigma-Aldrich, UK) was prepared to a working stock concentration of 2mg/ml in sterile water, passed through a 0.2µm filter (VWR International) to sterilise, and then stored at 4°C.

Puromycin (Sigma-Aldrich, UK) was received as 10mg/ml stock and aliquots were stored at -20°C. Puromycin was added to media to achieve a concentration of 2µg/ml (section 2.5.4).

2.5.4 Assessment of puromycin sensitivity

Puromycin is an antibiotic that acts by inhibiting protein synthesis. It is toxic to many eukaryotic cells, but the pLKO.1 vector confers puromycin-resistance to transduced cells. Puromycin can therefore be used as a selection agent to isolate cells successfully transduced with the pLKO.1 vector, bearing the shRNA construct. A puromycin kill curve was used to establish the sensitivity of the non-transduced cells,

Construct number	shRNA construct sequence	Targeted region of *IRF4*
1	5’-CCGGGCCATTCCTCTATTCAAGAATCTCGAGATTCTTGAATAGAGGAATGGCTTTTT-3’	CDS
2	5’-CCGGTGCGCTTTGAACAAGAGCAATCTCGAGATTGCTCTTGTTCAAAGCGCATTTTT-3’	CDS
3	5’-CCGGCCAGCAGGTTCACAACTACATCTCGAGATGTAGTTGTGAACCTGCTGGTTTTT-3’	CDS
4	5’-CCGGGCTCTTTGACACACAGCAGTTCTCGAGAACTGCTGTGTGTCAAAGAGCTTTTT-3’	CDS
5	5’-CCGGCTTTAGTGAAAGCGTCCAATTCTCGAGAATTGGACGCTTTCACTAAAGTTTTTTG-3’	3’UTR
6	5’-CCGGTTTACTGAAATGCGCTCTTTACTCGAGTAAAGAGCGCATTTCAGTAAATTTTTTG-3’	3’UTR

Table 2.5 Mission® shRNA constructs used to target *IRF4* in a panel of lymphoid cell lines
A panel of shRNA constructs were used to generate cell populations with IRF4 knockdown. CDS: coding DNA sequence.

to puromycin. This was performed in each of the cell lines (TK6, SU-DHL-6, MEC-1) prior to transduction with the lentiviral transduction particles, as follows.

After counting the cells, a cell suspension was prepared in fresh media, at a cell density of $7.5x10^4$/ml. Two millilitres of this suspension was added to each of the wells of a sterile 6 well culture plate. Puromycin was then added to the wells to achieve a range of concentrations from 0-10μg/ml. (Table 2.6) Cells were counted at 24 hours intervals for three days.

By 72 hours, all TK6 and MEC-1 cells exposed to ≥2μg/ml puromycin had died. Puromycin was therefore used at a concentration of 2μg/ml in media in TK6 and MEC-1 cells, 72 hours after transduction with shRNA. (section 2.5.6).

All SU-DHL-6 cells however, including those in the control well exposed to 0μg/ml puromycin, had died. Given that the optimal cell density for SU-DHL-6 in culture is $0.4\text{-}1.0x10^6$/ml, it was supposed that the starting cell density ($7.5x10^4$/ml) might have been insufficient to maintain cell viability. The experiment was therefore repeated in SU-DHL-6 a further twice, using escalating cell densities ranging up to $2x10^5$/ml, until a starting cell density was obtained where consistent cell growth was observed in the control 0μg/ml puromycin well. Sustained cell growth was only observed in the control well once the starting cell density reached $1x10^5$/ml. At this cell density, SU-DHL-6 cells all died at a puromycin concentration of 1μg/ml.

2.5.5 Assessment of hexadimethrine bromide sensitivity

Polybrene (hexadimethrine bromide) enhances transduction efficiency but can be toxic to some cell types. Prior to transduction with lentiviral particles, the sensitivity to polybrene of the cell lines (SU-DHL-6, MEC-1) was therefore established. It had previously been demonstrated that polybrene does not affect the growth of TK6 cells (personal communication, S. Fordham, Newcastle upon Tyne Hospitals, NHS Trust).

After counting, a cell suspension was prepared in fresh media at cell density of $5x10^4$/ml. Five hundred microliters of this suspension was added to two wells of a sterile 24 well culture plate. Two microliters of polybrene working stock was then

Volume of puromycin stock (10mg/ml) added (ul)	Concentration of puromycin achieved in wells (µg/ml)
0	0
0.4	2
0.8	4
1.2	6
1.6	8
2	10

Table 2.6 Establishing the sensitivity of cell lines to puromycin

added to one of the wells, to establish a concentration of 8µg/ml. The other well served as a control well and was untreated. The cell density in both wells was determined at 24 hour intervals for 3 days. The growth and cell density of MEC-1 was unaffected by the presence of 8µg/ml polybrene.

As with the puromycin-sensitivity analysis (section 2.5.4), all of the SU-DHL-6 cells, including those in the control well containing no polybrene, died.

2.5.6 Lentiviral transduction

Cell lines were transduced with the six *IRF4*-targeted shRNA constructs described in section 2.5.3. In addition, cells were transduced with the two control vectors. Cells that were subjected to all the steps of transduction, without the addition of any lentiviral particles, were prepared as a blank control. The cell density of exponentially growing cells was determined, and a cell suspension was then prepared in the appropriate media to provide 9ml of cells at $5x10^4$/ml. One millilitre of this suspension was added to each of nine sterile 15ml BD FalconTM tubes. Four microliters of polybrene working stock solution was added to each of the BD FalconTM tubes, to a final concentration of 8µg/ml.

The appropriate volume of each of the six pre-packaged shRNA constructs targeted against *IRF4* (Table 2.5) was then added individually to each of six tubes, to achieve a multiplicity of infection (MOI) of either 2 or 4, depending on cell line. The MOI refers to the ratio of lentiviral particles to target cells and the volume of shRNA construct required to achieve the target MOI is calculated as follows:

$$Volume\ required = \frac{Total\ no.of\ cells \times required\ MOI}{viral\ titre\ \left(\frac{TU}{ml}\right)1}$$

Equation 2.1 *Determining the volume of shRNA construct required to achieve required MOI*

[1] Viral titre was supplied by manufacturer for each vial of lentiviral particles received.

The appropriate volume of either empty pLKO.1 vector control or non-mammalian shRNA control was added to two of the further FalconTM tubes to achieve the same MOI. Lentiviral particles were not added to the final tube of cells, the blank control. The blank control confirmed the efficacy of puromycin selection of transduced cells.

The BD FalconTM tubes were then centrifuged at 800G for 30 minutes at 32°C, and the supernatant was discarded. The cell pellets were each resuspended in 2ml pre-warmed media and transferred to the wells of sterile 6 well culture plates.

2.5.7 Transfer of transduced cells in to puromycin-containing media

After 72 hours, the contents of each well were carefully pipetted into a fresh 15ml BD FalconTM tube and centrifuged at 335g for 5 minutes to pellet the cells. The supernatant was discarded, and each pellet was then resuspended in 500µl of pre-warmed media with puromycin added at 2µg/ml , in one of the wells of a sterile 12 well plate.

Cells were inspected on a daily basis and cell density was established. Each of the transduced cell populations was expanded in increasing media volumes, in order to achieve sufficient cells for western immunoblotting. Cells were then collected for western immunoblotting analysis (section2.4) to determine IRF4 protein expression in the targeted and control cell populations.

Transduced cells were always maintained in puromycin-containing media thereafter, to avoid competition and outgrowth by non-transduced cells lacking puromycin resistance.

2.5.8 Establishing transduced cell clones with uniform IRF4 protein knockdown

Cell populations with the strongest evidence of IRF4 protein knockdown, as determined by western immunoblotting, were selected for cloning on sloppy agar in order to establish clones with uniform knockdown, derived from a single cell. The off target control population was also cloned. Each of the cell lines was cloned in their

respective standard media (Table 2.1), with puromycin added at 2µg/ml and with the FBS concentration increased to 20% (v/v).

The cell density of the transduced cell populations chosen for cloning was established by counting. A cell suspension (10 -100 cells/ml, depending on cell line) of each of these populations was then prepared in fresh pre-warmed puromycin-containing media. One millilitre of each cell suspension was added to the wells of two sterile 6 well culture plates.

Eight hundred milligrams of sterile SeaKem agarose (Lonza, UK) was dissolved by heating in a sterile 50ml BD FalconTM in 20ml sterile PBS. Four millilitres of this suspension was then added to 36ml of pre-warmed puromycin containing media. One millilitre of this sloppy agar was then added to each of the wells of the 6 well plates. These plates were maintained at 37°C in 5% CO2 for 1-3 weeks, with care taken to avoid any agitation. The plates were inspected intermittently on a weekly basis to look for evidence of macroscopically-visible cell clones.

A limiting dilution method was also used to try to generate shRNA-transduced MEC-1 cell clones with constitutive knockdown. The cell density of the transduced cell populations chosen for cloning was established by counting. A cell suspension (25 cells/ml) was then prepared in fresh pre-warmed puromycin-containing media. Two hundred microliters of this suspension were added to the each of the wells of two sterile 96-well culture plates. These plates were then maintained at 37°C in 5% CO2 for 1-3 weeks and inspected intermittently for evidence of cell clones.

Visible clones were inspected by microscopy to ensure that they represented discrete clones arising from a single cell. Individual clones were then picked from the sloppy agar, using a 200µl pipette tip, and resuspended in 500µl of puromycin-containing media in the wells of a sterile 96 well culture plate. Cell numbers were expanded to achieve sufficient cell numbers for western immunoblotting to determine IRF4 protein knockdown.

Cells with IRF4 protein knockdown were used in flow cytometry analysis of CD38 surface expression, growth curves, and cytotoxicity growth inhibition assays.

2.6 Chromatin immunoprecipitation

Chromatin immunoprecipitation (ChIP) enables the detection of protein-DNA interactions, by using an antibody to the protein of interest to pull the relevant chromatin fragments out of solution, and then amplify the DNA using real time PCR (rtPCR). Protein-DNA interactions are first preserved using a formaldehyde solution for cross-linking. A series of lysis steps then disrupt cell and nuclear membranes, isolating only the nuclear contents for the ChIP. This chromatin is then sheared to smaller fragments using sonication, and then incubated with an antibody to the protein of interest, bound to magnetic beads, before washing away any unbound chromatin fragments. Having extracted DNA from the bound chromatin fragments, real time PCR is used to amplify sequences targeted by predesigned primers.

2.6.1 Immunoprecipitation to optimise antibody for ChIP

A direct immunoprecipitation (IP) was first performed in order to confirm that the polyclonal goat IgG IRF4 antibody (sc-6059, Santa Cruz) (Table 2.7) was appropriate for use in ChIP experiments.

One millilitre of IP lysis solution (50mM TRIS, pH7.5, 150mM NaCl, 1% NP40 detergent, 10mM PMSF plus 1 tablet of SigmaFAST^{TM} protease inhibitor was added to every 10ml of lysis buffer) was added to a pellet of $10x10^6$ cells in a 1.5ml tube, and the pellet was carefully resuspended. The cell pellet was then left on ice for 45 minutes before centrifugation at 16500G for 3 minutes in order to pellet the cellular debris. The supernatant, comprising the cell lysate, was transferred to a fresh 1.5ml tube and the pellet was discarded. Fifty microliters of cell lysate was stored at -20°C for use as a control 'input sample'.

A stock solution of Protein G Sepharose 4 Fast flow beads (GE Healthcare, UK) was prepared by centrifugation at 16500G for 3 minutes. The supernatant was removed and the beads were then washed by resuspension in 700µl IP lysis solution followed by centrifugation at 18600G for 3 minutes. The beads were washed a further three times in IP lysis solution and then resuspended in 700µl IP lysis solution. This stock solution of protein G sepharose (PGS) beads was stored at 4°C.

Protein target	Species and isotype	Supplier	Cat no.
Test ChIP antibodies			
IRF4	Goat IgG	Santa Cruz	sc-6059
Histone 3 trimethyl lysine 9 (H3K9me3)	Rabbit IgG	Abcam	ab8898
Histone 3 trimethyl lysine 4 (H3K4me3)	Rabbit IgG	Diagenode	pAb-003-010
Histone 3 trimethyl lysine 9 (H3K9me3)	Rabbit IgG	Diagenode	pAb-056-050
Control ChIP antibodies			
-	Goat IgG	Santa Cruz	sc-2028
-	Rabbit IgG	Diagenode	#AIP-103110

Table 2.7 Antibodies used in chromatin immunoprecipitation (ChIP)
Histone 3 trimethyl lysine 4 (H3K4me3) represents a marker of transcriptional activation, whereas histone 3 trimethyl lysine 9 (H3K9me3) represents a marker of transcriptional repression.

Twenty microliters of the PGS bead stock solution was added to the cell lysate and placed on a rotating mixer wheel for 2 hours at 4°C. The suspension was then centrifuged for 3 minutes at 16500G and the bead pellet was discarded. This pre-clear step allows the removal of proteins that would bind non-specifically to the PGS beads, prior to the addition of the IP antibody.

The remaining supernatant was divided equally between two fresh 1.5ml tubes. Two micrograms of antibody, either IRF4 or polyclonal goat IgG control antibody (sc-2028, Santa Cruz) was added to each tube, which were then incubated on a rotating wheel at 4°C for at least 8 hours. This step generates protein-antibody complexes.

A further 20µl of PGS stock solution was then added to each Eppendorf, and they were then returned to the rotating wheel at 4°C for a further 2 hours. The tubes were then centrifuged at 16500G for 3 minutes and the supernatant was discarded from both.

The pellets, now comprising PGS bead-antibody-protein complexes, were washed twice to remove any non-specifically bound proteins. Each pellet was re-suspended in 1ml of IP wash#1 (350mM NaCl, 0.1% (v/v) Triton in PBS) and centrifuged at 16500G for 3 minutes and the supernatant discarded. The pellets were then resuspended in 1ml IP wash#2 (0.1% Triton (v/v) in PBS) and again centrifuged, and the supernatant discarded.

In order to denature the bead/antibody/protein complexes, 54µl of SDS sample buffer was added to each of the pellets, and 13µl was added to the thawed input sample. The three 1.5ml tubes were heated to 100°C for 10 minutes and then centrifuged at 16500G for 3 minutes. The supernatants were transferred to three fresh 1.5ml tubes and 3µl each of 2-mercaptoethanol and bromophenol blue were added to each.

Western immunoblotting was then performed on the three samples, IRF4-IP, IgG-IP and input.

2.6.2 Preparation of chromatin for ChIP

TK6, SU-DHL-6, MEC-1 cell lines and primary lymphocytes were used in chromatin immunoprecipitation experiments. A working protocol was developed with thanks to Dr Luke Gaughan (personal communication) and optimised using published literature. (Schmidt et al., 2009)

To prepare chromatin from cell lines, the appropriate volume of cell suspension to provide $50x10^6$ cells was transferred to a clean culture flask.

When primary lymphocytes were being used in ChIP, an initial count of cells was made to determine cell density after harvesting the lymphocytes from the co-culture plates, and then all available primary lymphocytes were harvested, up to $5x10^7$, for use in chromatin preparation.

2.6.2.a Cross-linking chromatin

An 11% formaldehyde solution (50mM Hepes-KOH, 100mM NaCl, 1mM EDTA, 0.5M EGTA, 11% (v/v) formaldehyde) was added to achieve a concentration of 1% in the cell suspension and left at room temperature for 7.5 minutes, to promote DNA-protein cross-linking interactions. Glycine (Sigma,UK) was then added to a final concentration of 0.125M in the cell suspension, to quench the formaldehyde action and prevent non-specific cross-linking, and left at room temperature for 5 minutes.

The cell suspension was then transferred to a 50ml BD FalconTM tube and centrifuged at 930g for 5 minutes at 4°C in a pre-chilled centrifuge. The supernatant was discarded, and the remaining pellet was then washed twice in ice-cold PBS, and centrifuged at 930g for 5 minutes, after each wash.

2.6.2.b Lysis of the cellular and nuclear membranes to isolate nuclear material

Ten millilitres of cold lysis buffer 1 (LB1) (50mM Hepes–KOH, pH 7.5, 140mM NaCl, 1mM EDTA, 10% Glycerol, 0.5% NP-40, 0.25% Triton X-100) was added to the cell pellet and placed on ice on a plate rocker for 10 minutes. The suspension was

centrifuged at 930g for 5 minutes at 4°C and the supernatant removed. The pellet was then resuspended in 10ml lysis buffer 2 (LB2) (10mM Tris–HCL, pH8.0, 200mM NaCl, 1mM EDTA, 0.5mM EGTA) and again placed on a plate rocker, on ice, for 5 minutes. It was centrifuged as before, and the supernatant was very carefully discarded. The pellet was then resuspended in lysis buffer 3 (LB3) (10mM Tris–HCl, pH 8, 100mM NaCl, 1mM EDTA, 0.5mM EGTA, 0.1% Na–Deoxycholate, 0.5% N-laurylsarcosine) and kept on ice, for sonication.

The volume of LB3 used was determined by the number of cells obtained for chromatin preparation. (Section 2.8.2) Where $5x10^7$ cells were used, 1.5ml LB3 was added to the final pellet. However, when primary lymphocytes were used and cell numbers were fewer, 0.5 to 1ml LB3 was added, to achieve an opaque lysate. The lysate was then split into the appropriate number of 1.5ml tubes, with 250ul lysate per 1.5ml tube.

2.6.2.c Sonication of chromatin to generate fragments

Using a Diagenode Bioruptor® (TOSHO DENKI Co. Ltd), samples were sonicated, two at a time, at 4°C to produce chromatin fragments of 200-400 base pairs (bp) in length. Water temperature was maintained throughout using a Diagenode Bioruptor® water cooler (PolyScience, USA). Aliquots of lysate were taken prior to sonication and after different intervals of sonication to demonstrate chromatin fragment length on a DNA gel.

2.6.2.d Determining DNA concentration in chromatin preparation

After sonication, the lysate was centrifuged at 18600G for 10 minutes at 4°C. The supernatant was then transferred to a clean tube and the pellet discarded. DNA concentration in nanograms per microliter was determined using a NanoDrop® ND-1000 spectrophotometer (ThermoScientific, DE, USA).

2.6.2.e Confirmation of chromatin fragment length prior to ChIP

Aliquots of sonicated lysate were electrophoresed on an agarose gel to confirm chromatin fragment length.

A 1% or 1.5% agarose gel was prepared by the addition of 1% or 1.5% (w/v) agarose (Sigma-Aldrich, UK) to Tris-borate-EDTA (TBE) buffer (89mM Tris-HCl pH8, 89mM boric acid, 2mM EDTA). After gentle swirling, the mixture was heated cautiously for 1-2 minutes until the agarose was completely dissolved in solution. GelGreen nucleic acid 10 000x DNA stain (Biotium Inc, UK) was added at 1:1000 concentration in order to visualise the DNA fragments. After pouring the gel into a gel cassette, it was allowed to set for at least one hour before loading the samples. To prepare the samples: cross-linked protein-DNA interactions were first reversed, in order to free up DNA fragments for electrophoresis. The aliquots of sonicated lysate taken at different intervals of sonication were centrifuged at 18600G at 4°C and the pellet discarded. 15µl of each lysate was transferred to a clean 1.5ml tube and 0.5µl of Proteinase K (Qiagen, UK) was added. The samples were then heated to 65°C for 90 minutes before being briefly centrifuged to remove any condensation. Three microliters of Blue/Orange 6x loading dye (Promega, UK) was then added to each tube and the samples were loaded on to a 1-1.5% agarose gel, alongside a QuickLoad® 1kb DNA ladder (New England BioLabs(UK), UK) or a QuickLoad® 100bp DNA ladder (New England BioLabs (UK), UK). The gel was then electrophoresed using a Power 608 power pack (Fisher Scientific, UK) at a constant voltage of 100V for approximately one hour or until the samples had migrated nearly the whole length of the gel. The samples were then visualised using a Gel Doc™ XR (Bio-Rad Laboratories Ltd.).

2.6.3 Manual ChIP procedure

ChIP was performed manually, using histone (H3) and IRF4 antibodies (Table 2.7) on TK6 chromatin. The histone (H3) antibody served as a positive control for establishment of the ChIP protocol. (Section 3.3.1.c)

2.6.3.a Preparation of magnetic beads with ChIP antibody

Prior to being combined with ChIP antibody, Dynabeads® Magnetic Separation Technology magnetic beads (Invitrogen, UK) were prepared by washing in PBS-BSA solution (0.5% (v/v) BSA in PBS). For each ChIP using either IRF4 or histone (H3) antibody, 40µl of Dynabeads® was added to each of two 1.5ml tubes. Five hundred

microlitres of PBS-BSA was added to each Eppendorf, before centrifuging at 210G for 5 minutes. The supernatant was removed and the bead pellets were then resuspended in 500µl PBS-BSA and centrifuged again. After removing the supernatant, each of the two bead pellets were finally resuspended in 700µl PBS-BSA solution.

Either 1µg or 2µg of IRF4 antibody, or 2µg of histone (H3) antibody, was added to one of the tubes, and an equal quantity of species-matched IgG control antibody was added to the second tube. (Table 2.7) The tubes were then incubated at 4°C for 8 hours with constant agitation to allow antibody-bead complexes to form.

2.6.3.b Preparation of sonicated chromatin samples for ChIP, and preparation of the input sample

After chromatin had been prepared (sections 2.6.2.a to section 2.6.2.e), a sufficient volume of DNA/chromatin fragments was prepared to provide two 1.5ml tubes each containing up to 150µg of DNA/chromatin in a total volume of 700µl LB3-Triton (1% (v/v) TritonTM X-100, (Sigma-Aldrich, UK) in LB3 lysis solution). Seventy microliters of this solution was removed to a separate Eppendorf and frozen at -20°C as an input sample.

2.6.3.c Chromatin immunoprecipitation step

Samples (prepared in section 2.6.3.a) containing magnetic bead-antibody complexes were briefly centrifuged and then applied to a DynaMag™-2 Magnet magnetic rack (Invitrogen, UK), and the supernatant was removed and discarded.

The contents of one of the 1.5ml tubes (prepared in section 2.6.3.b) containing 150µg chromatin in LB3-Triton, was then added to the tubes containing magnetic beads bound to the test antibody (IRF4 or histone, H3) and the beads were carefully resuspended. This was repeated to combine the contents of the second sample of chromatin in LB3-Triton with the magnetic beads bound to the species-matched control antibody.

Samples were incubated overnight at 4°C with constant agitation, in order to allow complexes to form between chromatin fragments and the ChIP antibodies,

bound to magnetic beads.

The following day, samples were briefly centrifuged, and then washed 6 times in RIPA buffer (50mM HEPES-KOH, pH 7.5; 500mM LiCl; 1mM EDTA; 1% (v/v) NP-40; 0.7% (w/v) Na deoxycholate), at 4°C. For each wash, 600µl RIPA buffer was added, and samples were then applied to the magnetic rack, and the supernatant removed.

After the final RIPA buffer wash, the beads were re-suspended in 600µl ChIP wash#2 (TRIS-buffered saline). The samples were centrifuged at 850G for 5 minutes at 4°C and then applied to the magnetic rack and the supernatant was removed.

2.6.3.d Elution and cross-link reversal of ChIP and input samples

In order to isolate DNA for rtPCR, the chromatin fragments bound to antibody were eluted from the magnetic beads, and the cross-links within the antibody-chromatin complexes were reversed.

Two hundred microliters of ChIP elution solution (50mM Tris–HCl, pH 8; 10mM EDTA; 1% SDS (w/v)) was added to each of the samples which were then heated to 60°C on a heating block, for 8 hours. Simultaneously, the input sample was thawed, and heated with elution solution in the same way as the ChIP samples. At 5 minute intervals for the first 15 minutes of heating, the beads in the ChIP samples were gently resuspended by pipetting.

The ChIP samples were then briefly centrifuged to remove condensation, and applied to the magnetic rack. The supernatant was transferred to fresh tubes and the unbound beads were discarded.

Two hundred microliters of TRIS-EDTA and 4µl Ambion® proteinase K solution (20mg/ml) (Invitrogen, UK) was added to ChIP and input samples, and then heated to 55°C on a heating block for 1 hour. Proteinase K destroys the antibody-protein complexes, allowing them to be removed from solution, leaving DNA fragments only.

2.6.3.e DNA extraction

DNA extraction was performed using a QIAamp DNA Mini Kit (Qiagen, Crawley, UK) according to the manufacturer's protocol.

2.6.4 Robotic ChIP procedure

Once manual chromatin production and the manual ChIP protocol had been established, the SX-8G IP-Star® Compact Automated System (Diagenode, UK) was used to perform automated ChIP on manually prepared chromatin samples, for improved time efficiency and reproducibility. The Auto ChIP kit (Diagenode, UK) was used, according to manufacturer's instructions.

Automated ChIP was performed using chromatin samples generated from wildtype TK6, MEC-1 and SU-DHL-6 cell lines, and from the same cell lines after electroporation with Combination siRNA targeted against IRF4 or off target siRNA control. Automated ChIP was also performed on primary CLL lymphocytes, before and after co-culture on CD40L or NTL fibroblast co-culture monolayer.

Antibodies used in automated ChIP were targeted to IRF4, H3K4me3 (a histone methylation mark that is indicative of transcriptional activation), or H3K9me3 (a histone methylation mark indicative of transcriptional repression). (Table 2.7).

The product generated by the automated ChIP system was suitable for real time PCR, as described in section2.6.5.

2.6.5 Real time PCR set up

Forward and reverse primer sets to potential binding sites in the *CD38* gene were designed in silico using Invitrogen OligoPerfect™ designer software (see section 1.1for details of primer sets). The lyophilised primers were reconstituted to a 100µM solution in molecular grade water and the forward and reverse primer of each set were combined to generate a working stock solution at 10µM in molecular grade water, and stored at -20°C.

Samples were prepared for real time PCR in sterile 384 well plates, on ice. Each well contained 5µl Platinum® SYBR® Green qPCR SuperMix-UDG (Invitrogen, UK), 0.3µl of 10µM primer pair stock solution and 2µl of extracted DNA. Molecular grade water was added to a total volume of 10µl per sample. For convenience, a mastermix of SYBR® Green and water, with each of the primer pair stock solutions, was prepared, and 8µl was pipetted into each well using a Multipipette® stream. Two microliters of DNA was then added to the appropriate wells. Every sample was repeated in triplicate. Molecular grade water was added in place of DNA to non template control (NTC) wells. The plates were then sealed with a MicroAmp Optical adhesive film lid (Applied Biosystems, UK) and briefly centrifuged before running on a PCR machine (Applied Biosystems 7900HT Sequence Detection System, Applied Biosystems, UK) and analysed using SDS 7900HT Sequence Detection System software.

In order to optimise primer pairs, standard curves were constructed over a 2 log dilution to determine the slope of the curve and the coefficient of determination (R2) of each primer set. The efficiency of the primer sets was then determined using formula 3.1:

$$Efficiency = -1 + 10(-\frac{1}{slope})$$

Equation 2.2 *Formula 3.1*

2.6.6 Analysis of ChIP results

ChIP results were expressed as fold enrichment of chromatin fragments by a ChIP antibody to the target protein (IRF4, H3K9me3, H3K4me3), normalised to the enrichment achieved by an IgG control ChIP antibody. This was performed as follows.

After checking for consistency of triplicate results obtained by rtPCR and excluding outliers, a mean Ct value was recorded for each sample (input sample, target ChIP sample, IgG control ChIP sample). An adjusted Ct value was then calculated for the input sample, to account for the dilution of the input sample compared to the target ChIP and IgG control ChIP samples.

$$Adjusted\ input\ Ct\ value = Input\ Ct\ value - \chi^2$$

Equation 2.3 *Determining the adjusted input Ct value*

This adjustment was performed to allow for the 10 fold dilution (in manual ChIP) or 100 fold dilution (in robotic ChIP) of the input chromatin sample, compared to the chromatin samples that underwent ChIP with a target antibody or IgG control antibody. Every 10 fold reduction of concentration of a sample used in rtPCR will increase the Ct value by 3.2.

Ct values obtained from ChIP samples using a target ChIP antibody, or an IgG control ChIP antibody were then normalised to the adjusted input Ct value and the percentage input value (% input) was finally calculated.

$$\%\ input = 100 \times 2 \wedge (ChIP\ Ct\ value - adjusted\ input\ Ct\ value)$$

Equation 2.4 *Calculating the % input achieved using ChIP antibodies*

The % input obtained with the test ChIP antibody was then normalised to that obtained with the IgG control ChIP antibody, to determine fold enrichment by the test ChIP antibody. Statistically significant binding was determined using a t-Test.

2.7 Flow cytometry

Flow cytometry was used to determine the cell surface expression of CD38 protein in cell lines and primary cells. The expression of CD154 (CD40 ligand, CD40L) by the fibroblast cells used in primary cell co-culture was also confirmed by flow cytometry. Primary lymphocyte proliferation on the co-culture layer was also investigated by flow cytometry using carboxyfluorescein succinimidyl ester (CFSE) labelling (section 2.8.6).

[2] χ equals 3.2 in manual ChIP procedures, and χ equals 6.4 in robotic ChIP procedures

All cells were labelled with antibody following the same method. Specifically, after counting, cells were centrifuged at 335g for 5 minutes and resuspended in PBS-azide buffer (2% [v/v] FBS, 0.1% [w/v] azide, in PBS). They were centrifuged again, and then re-suspended in the buffer at a cell density of $1x10^6$/ml. One hundred and fifty microliters of this suspension was dispensed to each Falcon® 5ml round-bottomed flow cytometry tube (VWR International Ltd, UK). For each test, three flow cytometry tubes were prepared and equal concentrations of the appropriate test antibody (section 2.7.1) or matched isotype control antibody were added to two of the tubes. A third tube of cells was left unlabelled. Cells were then incubated at 4°C in the dark for 1 hour and washed to remove unbound antibody by adding 1ml of PBS-azide buffer to each tube and centrifuging for 5 minutes at 335g. The supernatant was removed by swift inversion of the tubes, and the remaining cells were resuspended in 300ul PBS-azide buffer. They were then analysed using a FACSCalibur (BD Biosciences, UK).

2.7.1 Flow cytometry antibodies

Antibodies for use in flow cytometry were all purchased from BD Biosciences, UK. (Table 2.8)

2.7.2 Determining CD38 expression in cell lines and primary leukaemic lymphocytes

Cell lines TK6, MEC-1, MEC-2, SU-DHL-6, and primary CLL lymphocytes were all assessed by flow cytometry for surface CD38 expression. The optimum antibody concentration required to determine surface CD38 expression on primary cells was first determined. (Figure 2.1)

Exponentially growing cells were counted and $1x10^6$ cells were prepared in PBS-azide buffer as described in section 2.7. Three flow cytometry tubes per cell line were prepared. Forty microliters (0.25µg) CD38 antibody was added to one tube, and 5µl (0.25µg) isotype control antibody was added to a second tube. The third tube acted as an unlabelled control, and no antibody was added. After incubation and washing as described in section 2.7, the cells were analysed on a FACSCalibur.

Protein	Fluorochrome	Antibody species	Clone	Isotype	Cat No.
CD38	PE	Mouse Anti-Human	HIT2	Mouse IgG1, κ	555460
CD154	PE	Mouse Anti-Human	TRAP1	Mouse IgG1, κ	555700
CD5	APC	Mouse Anti-Human	UCHT2	Mouse IgG1, κ	555355
CD19	PerCP	Mouse Anti-Human	4G7	Mouse IgG1, κ	345778
CFSE	CFSE	-	-	-	34554 Invitrogen
Isotype control	PE	Mouse Anti-Human	MOPC-21	Mouse IgG_1, κ	556650

Table 2.8 Antibodies used in flow cytometry

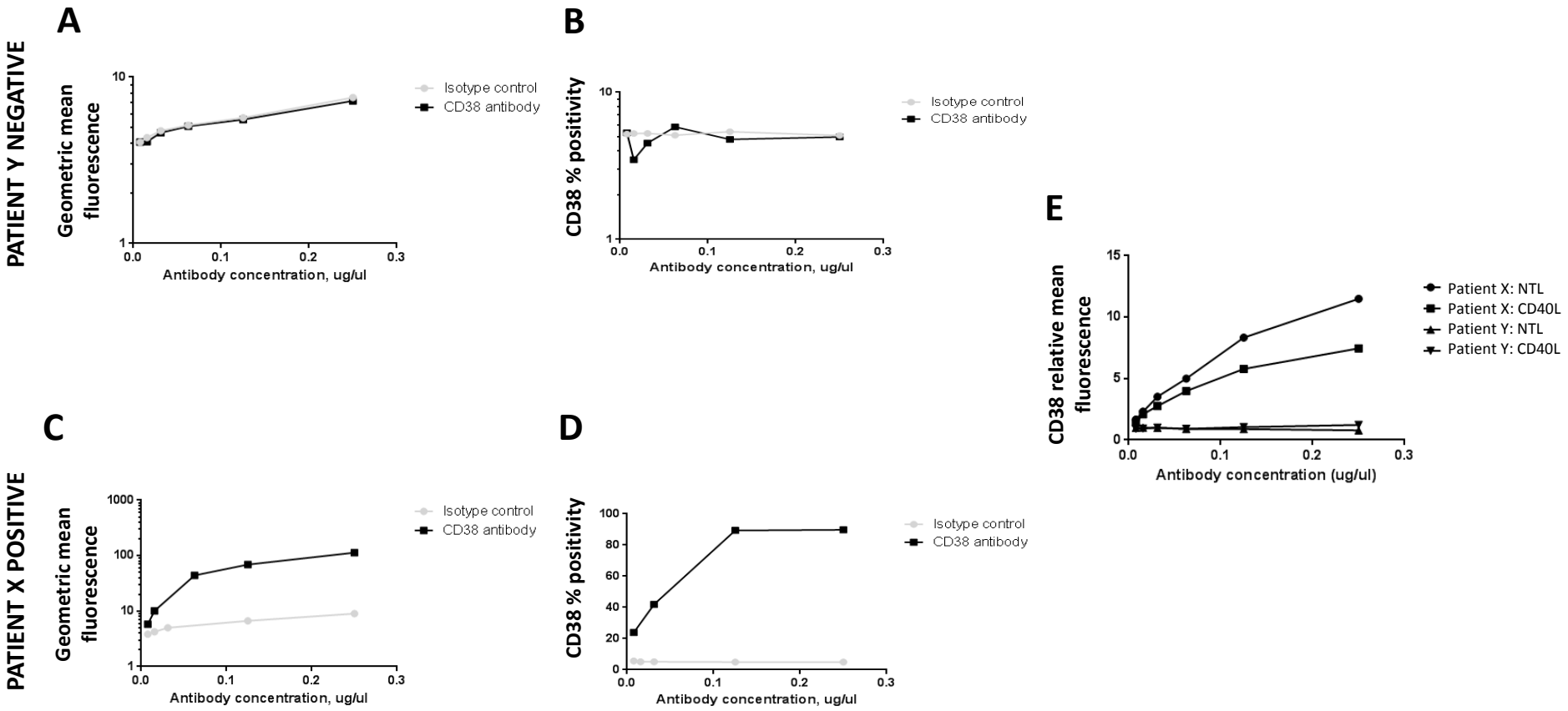

Figure 2.1 Optimising CD38 antibody concentration for use in primary CLL lymphocytes

In order to select the optimal CD38 antibody concentration for use in the investigation of CD38 surface expression in primary CLL lymphocytes, the antibody was titrated at 6 different concentrations (ranging from 0.008µg/µl to 0.25µg/µl). A species-matched isotype control antibody was used at equivalent concentrations. Primary CLL lymphocytes were isolated from two patients, one of whom was known to be CD38 positive (X), and one of whom was CD38 negative (Y). Geometric mean fluorescence intensity and CD38% positivity were analysed.

A and **B.** In patient Y, binding by both antibodies showed a modest increase in geometric mean fluorescence intensity as antibody concentration increased. However, this increased binding occurred in parallel for the two antibodies and there was no evidence of excessive non-specific binding with the CD38 antibody compared to the isotype control antibody, even at the highest concentrations.

C and **D**. In patient X, low concentrations of the CD38 antibody (up to approximately 0.1µg/µl) were insufficient to demonstrate CD38 positivity. In addition, a steep 'shoulder' was observed in (E) in the relative mean fluorescence (RMF) of CD38 positivity in cells from patient X (CD38 positive), using antibody concentrations up to approximately 0.2µg/µl. This steep increase in RMF could lead to large variability in the observed CD38 RMF of samples for very small variabilities in antibody concentration. Antibody concentration of 0.25µg/µl was therefore selected for use.

The geometric mean fluorescence intensity and the relative mean fluorescence (RMF) intensity of CD38 expression were determined using histogram plot statistics obtained from the data using BD CellQuest Pro software. The percentage of cells expressing CD38 was also determined. (**) These parameters were chosen for interpretation of the data, as they correspond with the parameters used in diagnostic clinical work on CLL cells (personal communication, B.Baker, Newcastle upon Tyne Hospitals, NHS Trust).

2.7.3 Determining CD40L expression in co-culture fibroblast monolayer

The expression of CD40 ligand (CD40L, CD154) was determined in the CD40L-expressing fibroblast cells, and its absence confirmed in the non-ligand expressing control (NTL) cells, used for primary cell co-culture. Prior to flow cytometry investigation, these cells were treated with a non-enzymatic Cell Dissociation Solution (Sigma-Aldrich, UK), rather than trypsinisation, to avoid the disruption of cell surface proteins. Culture media was aspirated from one sterile 75cm^3 culture flask each of CD40L cells and NTL cells, and the adherent cell monolayers were washed in an excess of sterile PBS. The PBS was then removed by aspiration, and 5ml of cell dissociation solution was added to each flask. Flasks were left at room temperature for 5-10 minutes until there was evidence of detachment from the flask surface, on inspection by microscopy. Once the cells were in suspension in the dissociation solution, the suspension from each flask was collected in to a 50ml BD FalconTM tube. The cells were centrifuged at 335g for 5 minutes and resuspended in 10ml PBS-azide buffer. The cells were then counted and 1x10^6 cells were prepared for each of CD40L and NTL cell types at 1x10^6/ml in PBS-azide buffer (section 2.7). Three flow cytometry tubes were prepared for each cell type.

Ten microliters of PE conjugated CD154 antibody (Table 2.8) was added to one tube, and 10µl of PE conjugated isotype control was added to a second tube. The third tube of cells was left unlabelled by antibody, as a blank control. Cells were then incubated and washed as described in section 2.7 before being analysed on a FACSCalibur.

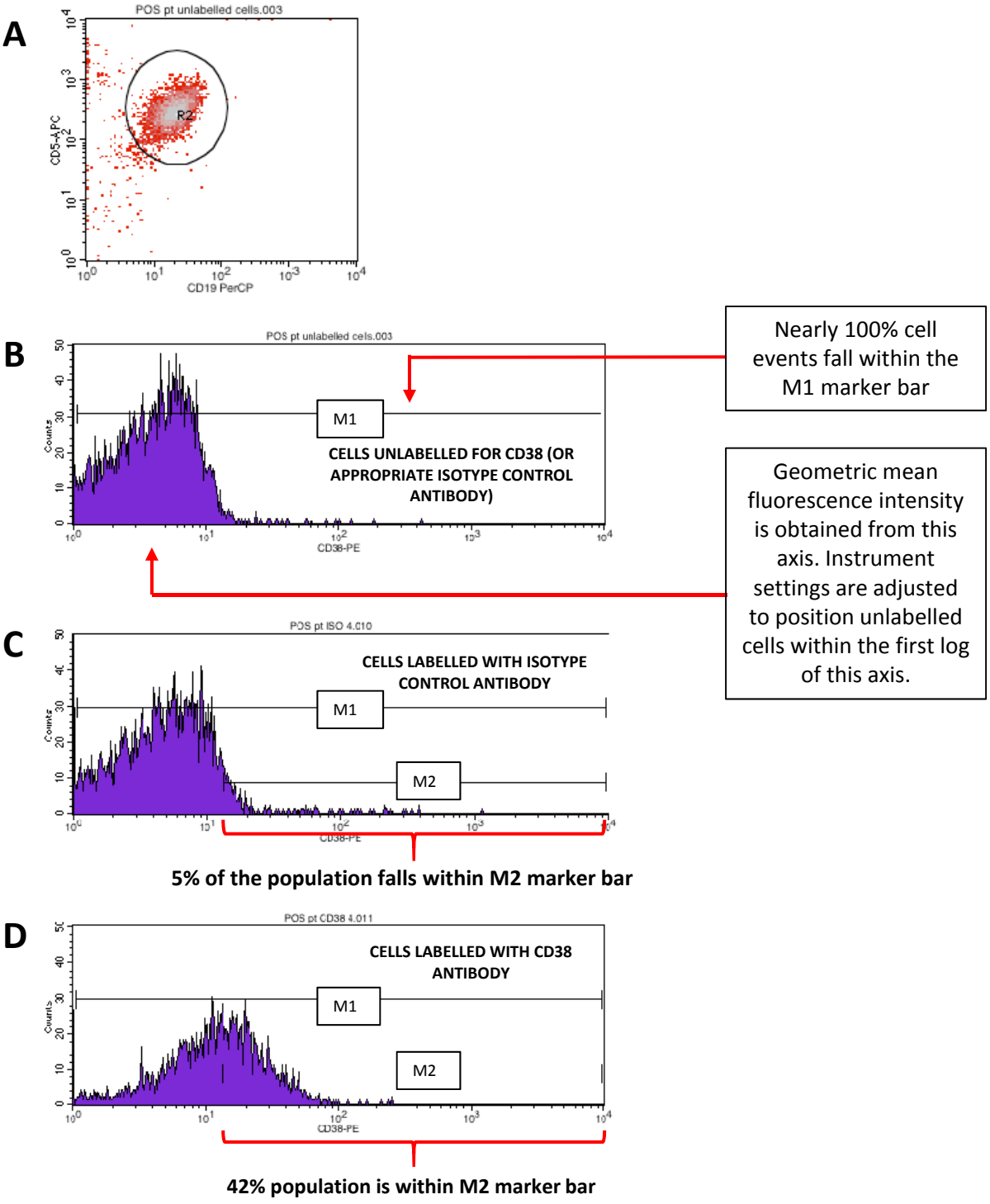

Figure 2.2 Using flow cytometry to assess CD38 expression in primary CLL lymphocytes

A. After gating cells according to forward and side scatter, CLL lymphocytes were selected by gating for a CD5 positive and CD19 positive cell population.

B. This gated population was then inspected in a histogram plot to determine CD38 expression. Instrument settings were adjusted to position the gated population, unlabelled at first for CD38 or isotype matched control antibody, into the first decade of the histogram plot. Nearly 100% of events (cells) are captured within an M1 marker, which allows the determination of the geometric mean and median fluorescence intensity of the cell population.

C. Cells were labelled with isotype control antibody. An M2 marker bar was positioned to capture 5% of this isotype-labelled cell population. This M2 marker bar was then left untouched for analysis of percentage CD38 antibody-labelled cells.

D. CD38 antibody-labelled cells were then analysed. 42% of the cells fall within the M2 marker bar and thus these cells are considered 42% CD38 positive. Geometric mean and median fluorescence data indicating the intensity of the cell population fluorescence can also be obtained from the histogram plot. Relative mean fluorescence was determined by the relative geometric mean fluorescence of the CD38 antibody-labelled cells normalised to the same cell population labelled with isotype control antibody.

2.8 Culture of primary leukaemic lymphocytes

The protocol for co-culture of primary cells was adapted from a method developed by Dr Jack Zhaung, Division of Haematology, School of Cancer Studies, University of Liverpool.

2.8.1 Collection and separation of primary leukaemic lymphocytes from whole blood samples

Whole blood samples were collected from patients attending the CLL clinic at the Freeman Hospital, Newcastle, with consent for research obtained via the Newcastle Haematology Biobank (Research Ethics Committee approval number 07/H0906/109+5). Patients with a total peripheral white cell count of >30x10^9/ml were selected, in order to provide an adequate yield of primary CLL lymphocytes.

Whole blood samples were separated using Lymphoprep™ (StemCell Technologies), a density medium gradient, to obtain the mononuclear cell fraction. Up to 6ml total volume of whole blood, diluted in a 1:1 ratio with sterile PBS, was pipetted carefully on to the top of 3ml Lymphoprep™ in a 15ml BD FalconTM tube. After centrifugation at 1000G for 20 minutes with no break applied in deceleration, the buffy coat layer was removed using a sterile glass Pasteur pipette, and washed twice in sterile PBS, at 300G and then 250G for 10 minutes each. The pellet of mononuclear cells obtained was then re-suspended in 10ml sterile, warmed RF10% media, and an aliquot of this was taken for counting by haemocytometer. Because of the very high primary lymphocyte numbers frequently obtained, the aliquot was diluted 1:100 in PBS before being combined with trypan blue for counting. Once the cell density was determined, cells were then either cryopreserved or used immediately.

2.8.2 Cryopreservation of primary lymphocytes

Primary lymphocytes were cryopreserved for long term storage using the method described in section 2.3.5. Up to 60x10^6 cells were frozen in each sterile cryovial and the storage and subsequent use of primary cells was recorded using the

Achiever sofware (Achiever Medical) compliant with the Human Tissue Authority (HTA).

2.8.3 Preparing fibroblast monolayer for co-culture of leukaemic lymphocytes

CD40L-expressing and the control non-expressor NTL adherent fibroblast cell lines were used concurrently for the co-culture of primary lymphocytes. After trypsinisation and re-suspension in media, the cells were counted. Cell suspensions were then prepared of both CD40L and NTL cells at a cell density of $6x10^5$ cells/ml. The cell suspensions were added to separate, sterile 6 well culture plates, 2ml per well. The plates were then irradiated at 75Gy (dose rate 3.36Gy/min) to mitotically inactivate the cells, and then placed in the incubator for 24 hours before use, to allow the cells to settle and form a confluent monolayer.

2.8.4 Co-culture of primary lymphocytes on fibroblast layer

Both fresh and thawed, cryopreserved primary lymphocytes were used in co-culture, with a preference for fresh cells when available. Primary cell media (RF10% supplemented with recombinant human recombinant interleukin-4 (rhIL-4) (Sigma-Aldrich, UK) at 10ng/ml to promote cell survival) was freshly prepared each time. After determining cell density, cells were re-suspended at $5x10^6$ cells/ml in warmed primary cell media. The fibroblast co-culture plates were inspected at x50 magnification to ensure that cells were confluent, and the fibroblast media was then removed from the wells by aspiration. Two millilitres of primary lymphocyte cell suspension was then added gently to each fibroblast well. Plates were maintained in the incubator and inspected on a daily basis. Media was replaced every 24-48 hours by careful aspiration of existing media from the wells. Aspirated media was centrifuged at 200G to pellet any cells collected with the aspirated media. The pelleted cells were then gently resuspended in fresh media and returned to the wells.

2.8.5 Harvest of leukaemic lymphocytes from co-culture

Primary lymphocytes were harvested from co-culture plates for use in chromatin immunoprecipitation (ChIP), western immunoblotting, and flow cytometry

experiments. Using gentle pipetting, primary lymphocytes were carefully detached from the fibroblast layer in to suspension and collected in a sterile BD Falcon™ tube for subsequent use.

2.8.6 CFSE labelling and measurement to demonstrate proliferation of primary leukaemic lymphocytes

The protocol for CFSE labelling of primary cells was adapted from a method developed by Dr Jack Zhaung, Division of Haematology, School of Cancer Studies, University of Liverpool.

CFSE labelling was used to investigate evidence of proliferation in primary CLL cells grown on co-culture fibroblast monolayers. CFSE is a fluorescent cell-permeable molecule which diffuses via the cell membrane to bind covalently with intracellular amines. The fluorescence is present in daughter cells after the division of labelled cells, and progressively halves with each cell division, allowing cell proliferation to be analysed by flow cytometry.

Cell Trace™ CFSE, for flow cytometry (Invitrogen, UK) was received as frozen stock and was stored at -20°C. The Cell Trace™ CFSE kit comprised ten 50µg vials of CFSE, and a new vial was used for each experiment. Immediately prior to use, 180µl of sterile DMSO was added to a 50µg vial of CFSE to produce a 0.5mM stock solution.

Primary lymphocytes were isolated from peripheral blood and then labelled with CFSE using a protocol. Specifically, after counting, cells were suspended in RF10% medium at a cell density of $3x10^6$/ml. CFSE stock solution was added to the cell suspension at a concentration of 1:1000 and the suspension was incubated at 37°C for 20 minutes. The suspension was then centrifuged at 550g for 5 minutes, and the supernatant discarded. The cells were resuspended in an excess of fresh RF10% medium and again incubated at 37°C for 20 minutes to quench excess undiffused CFSE. They were then centrifuged at 550g for 5 minutes and washed again by resuspension in RF10% medium. Following centrifugation, the supernatant was discarded and the cell pellet was resuspended in primary cell media at $3x10^6$/ml and 1ml of this suspension was added to each well of pre-prepared CD40L and NTL fibroblast plates for co-culture.

One millilitre of the labelled cells were kept back for analysis without co-culture, in order to determine successful CFSE labelling of primary cells, and to provide a baseline for comparison with proliferating cells. These cells, and $3x10^6$ primary cells unlabelled for CFSE, were centrifuged at 335g for 5 minutes and the supernatant was discarded. The cell pellets were each resuspended in 500µl of PBS-azide buffer. One hundred and fifty microliters of the CFSE-labelled cell suspension was added to one flow cytometry tube, and 10µl each of APC conjugated CD5 and PerCP conjugated CD19 antibodies (Table 2.8) were added. Similarly, 150µl of primary cells unlabelled for CFSE were transferred to a flow cytometry tube and labelled with CD5 and CD19 antibodies. The tubes were then incubated on ice in the dark for 1 hour. One millilitre of PBS-azide buffer was added to each tube, and the tubes were then centrifuged at 335g for 5 minutes to wash off unbound antibody. The supernatant was removed by swift inversion of the tubes, and then the cells were resuspended in 300µl PBS-azide buffer for analysis by FACSCalibur.

At 24 hour intervals after CFSE labelling, 1ml of primary cells (containing approximately $3x10^6$ cells) were harvested from both the CD40L and NTL co-culture plates. The cells were centrifuged at 335g for 5 minutes and the supernatant discarded. The resulting cells were resuspended in 500µl PBS-azide buffer, and 150µl of cells was transferred to a flow cytometry tube for labelling with CD5 and CD19 as above. After incubation on ice in the dark for 1 hour, the cells were washed in 1ml PBS-azide buffer and centrifuged at 250G for 5 minutes. The supernatant was removed by swift inversion as before, and the cells were resuspended in 300µl of PBS-azide buffer.

In each case, a viable cell population was gated by forward and side scatter, and then CD5 positive, CD19 positive lymphocytes were gated. This population was analysed for CFSE fluorescence detected in the FITC channel, and the number and fluorescence intensity of cells was determined prior to co-culture and at 24 hour intervals after co-culture.

Chapter 3. **Binding of IRF4 to *CD38***

3.1 Introduction

3.1.1 IRF4 consensus binding site

All members of the IRF family share a conserved N terminal region which comprises the DNA-binding domain, characterised by a conserved tryptophan repeat sequence via which they bind to their target genes. (Mamane et al., 1999)

IRF4 was first identified in the early 1990s as part of a heterodimeric protein complex with the ETS family transcription factor, PU.1. This heterodimer was able to bind sequences within the enhancer elements of genes encoding immunoglobulin κ and λ light chains. (Pongubala et al., 1992; Eisenbeis et al., 1993)

The oligomer used to crystallise the PU.1/IRF4/DNA ternary complex was derived from the λB light chain, and featured a composite ETS/IRF consensus element (EICE), which is represented by 5'-GGAANNGAAA-3' (Escalante et al., 2002). This EICE fuses the PU.1 binding site, 5'-GGAA-3' with the IRF4 binding site which is represented by 5'-AANNGAAA-3'. (Shaffer et al., 2009)

3.1.2 Interrogation of the CD38 upstream flanking sequence and 5'UTR reveals six putative binding sites for IRF4

A consensus IRF4 binding site, 5'-AAGTGAAA-3', was previously identified in the *CD38* 5'UTR, 108bp upstream of the translational start site. (Allan et al., 2010) (Section 1.4.7.b)

The *CD38* 5'UTR and upstream flanking sequence were interrogated for evidence of other putative IRF4 binding sites, denoted by the consensus sequence, 5'-AANNGAAA-3'. A further putative IRF4 DNA binding sequence was identified just 11 bases upstream of the original site, also within the 5'UTR. Further interrogation of the *CD38* upstream flanking sequence revealed another four putative IRF4 binding sites within 3550 bases upstream of the translational start site. (Figure 3.1)

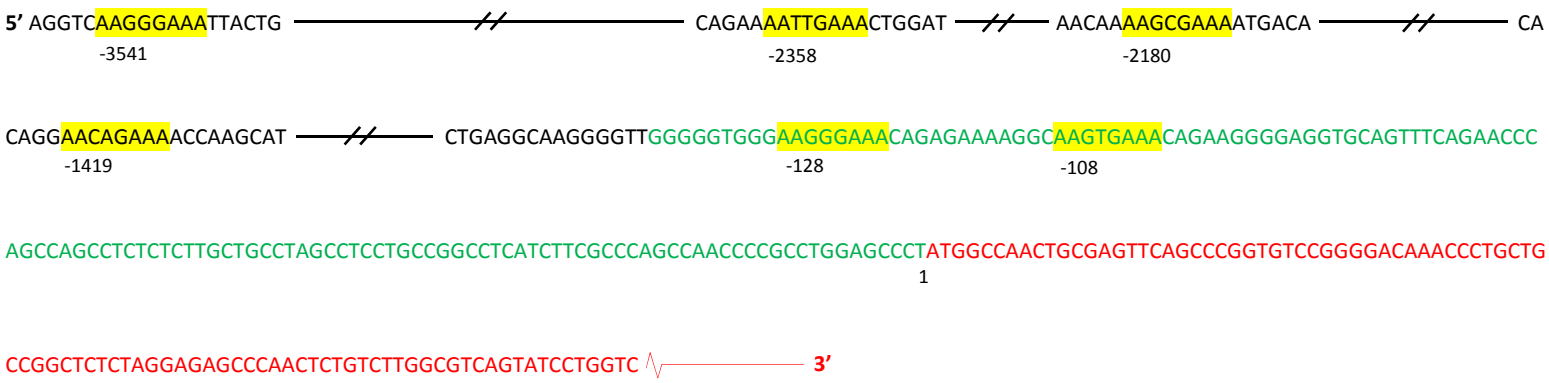

Figure 3.1 Six putative IRF4 binding sites are found in the *CD38* 5'UTR and upstream flanking sequence

Interrogation of the forward strand of the *CD38* 5'UTR and upstream flanking sequence revealed a total of six putative IRF4 binding sites, represented by the sequence 5'AANNGAAA 3'. Two of these fall within the 5'UTR, separated by only 11 base pairs.

The forward strand sequence is displayed and base positions are indicated underneath the sequence. Black text indicates the upstream flanking sequence; green text indicates 5'UTR; red text indicates coding sequence. The 5' base position of each putative binding site is indicated by yellow highlighting and numbered according to the human genome assembly release, Genome Reference Consortium human 38 (GRCh38) as viewed in the ENSEMBL genome browser.

3.1.3 Chromatin immunoprecipitation (ChIP)

Chromatin immunoprecipitation (ChIP) allows the detection of protein-DNA interactions, and was therefore used to investigate evidence of IRF4-*CD38* binding in a panel of cell lines. Briefly, after a formaldehyde cross-linking step to preserve any IRF4-*CD38* binding, chromatin was obtained from the cells in a series of lysis steps, and then sheared to chromatin fragments by sonication. In an immunoprecipitation step, chromatin fragments containing IRF4 protein were pulled out of solution using an antibody directed against IRF4, and the purified DNA sequences generated from this chromatin were amplified using real time PCR (rtPCR). Primer sets to the putative binding sites in the *CD38* gene were used in this PCR step in order specifically to identify evidence of IRF4-*CD38* binding at these sites.

3.2 Aims of chapter 3

Given that there are six perfect consensus binding sites for IRF4 in the *CD38* 5'UTR and further upstream in the flanking sequence, the primary aim of this chapter was to determine whether IRF4 binds to *CD38* using chromatin immunoprecipitation (ChIP).

Specifically, the experimental aims of this chapter were as follows:

- Select a suitable IRF4 antibody for use in ChIP, and demonstrate successful ChIP technique using an appropriate positive control.
- Design primers to target the putative IRF4 binding sites and demonstrate their efficiency prior to ChIP work.
- Use ChIP to investigate binding of IRF4 to *CD38* in a panel of lymphoid cell lines.

3.3 Results

3.3.1 Initial ChIP work in TK6 B-lymphoblastoid cell line

TK6 is a B cell line, derived from the non-malignant spleen of a 5 year old boy with hereditary spherocytosis. (Levy et al., 1968) TK6 was phenotyped using flow cytometry, courtesy of Dr. Andy Rawstron, Haematological Malignancy Diagnostic Service, Leeds Teaching Hospitals NHS Trust. TK6 has a pre-germinal centre phenotype negative for IgG and only weakly expressing CD79b. Furthermore, TK6 cells are positive for surface CD38 expression (Table 3.1), and IRF4 protein (52kDa), as demonstrated by western immunoblotting using whole cell extract. (Figure 3.2) Thus, while TK6 is unlikely to accurately represent the CLL cell of origin, its expression of both CD38 and IRF4 establishes it as a potentially useful model in which to investigate IRF4-*CD38* interaction.

3.3.1.a Immunoprecipitation to identify a functional IRF4 antibody suitable for ChIP

A literature search identified a goat polyclonal IRF4 antibody (Santa Cruz, M17, sc-6059) potentially suitable for use in ChIP. (Kwon et al., 2009; Staudt et al., 2010) Prior to performing ChIP, the IRF4 antibody was used in an immunoprecipitation experiment to confirm its suitability. Specifically, the antibody demonstrated successful enrichment of a TK6 whole cell lysate for IRF4 protein. (Figure 3.3) In contrast, IRF4 protein was not detectable when the lysate was immunoprecipitated with a species-matched control antibody raised against an unrelated protein, demonstrating suitability of the IRF4 antibody for use in ChIP.

Surface marker	Phenotype	% positive cells
CD20	+	67%
CD10	-	2%
CD3	-	1%
CD5	-	0%
IgG	-	0%
IgM	-	14%
IgD	+/-	21%
CD79b	+/-	40%
CD38	+	76%

Table 3.1 TK6 expresses surface CD38
Flow cytometry of TK6 cell line reveals a CD10 negative B cell line which weakly expresses CD79b and is negative for IgG. It expresses CD38. (With thanks to Dr Andy Rawstron.)

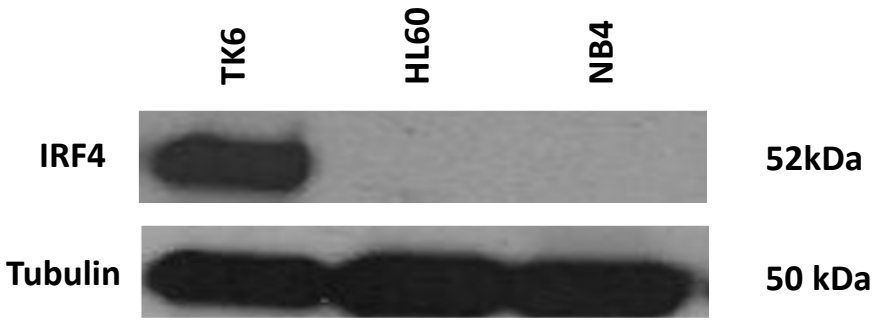

Figure 3.2 TK6 cell line expresses IRF4 protein
Whole cell extracts were prepared from B-lymphoblastoid cell line, TK6, and from the myeloid leukaemia cell lines, HL-60 and NB4. After quantifying the protein concentration obtained from each cell line using Pierce BCA assay, equal quantities of protein per sample were loaded for gel electrophoresis by SDS-PAGE. The proteins were transferred by electrophoresis to PVDF membrane which was blocked in 5% blocking buffer and then probed with primary antibody directed against IRF4. The membrane was then probed with a species-specific secondary antibody conjugated to horseradish peroxidase and treated with a chemiluminescent detection reagent. Proteins were visualised by development of films which had been exposed to the membrane. TK6 cell line expresses IRF4 protein, in contrast to the myeloid HL60 and NB4 cell lines which do not.

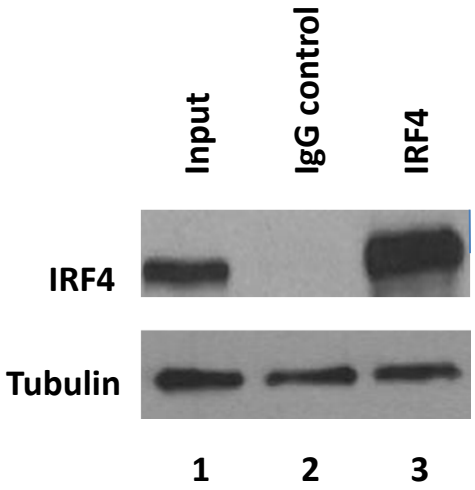

Figure 3.3 A goat polyclonal IRF4 antibody (Santa Cruz, M17, sc-6059) was used in an immunoprecipitation (IP) experiment in TK6 cells, to assess its suitability for ChIP

A whole cell lysate prepared from TK6 cells in exponential growth phase, was incubated with protein-G-sepharose (PGS) beads in a pre-clear step to remove non-specifically binding proteins. The PGS beads were then removed by centrifugation, and the lysate was incubated with equal concentrations of either IRF4 antibody (Santa Cruz, M17, sc-6059) or a species-matched control antibody. Further PGS beads were added in order to bind the antibody-protein complexes, and the remaining lysate comprising unbound proteins, was removed by centrifugation. The immunoprecipitated proteins were then separated from the PGS bead-antibody-protein complexes in a denaturation step and western immunoblotting was performed to detect IRF4 protein. A rabbit-derived IRF4 antibody was used to probe the membrane in the western immunoblot. Using IRF4 antibodies raised in different species (goat and rabbit for the IP and the western immunoblot respectively) avoids interactions between the heavy chains of the two antibodies.

This western immunoblot demonstrated a successful immunoprecipitation of IRF4 protein from the whole cell lysate by the goat IRF4 antibody (lane 3), in contrast with the species-matched control antibody which failed to enrich the lysate for IRF4 (lane 2). The input sample (lane 1) represents whole cell lysate that has not undergone any immunoprecipitation and thus expresses IRF4 protein, but has not been enriched for it.

3.3.1.b Primer design for amplification of IRF4 binding sites in the *CD38* 5'UTR and upstream flanking sequence

Primer sets were designed to amplify the six identified putative IRF4 binding sites in the *CD38* 5'UTR and upstream flanking sequence, and these were designated *CD38* primer sets 1-5. (Table 3.2) Because the two putative IRF4 binding sites within the 5'UTR fall only 11 bases apart, *CD38* primer set 5 was designed to generate a single amplicon, encompassing both putative IRF4 binding sites.

The efficiency of these primer sets was determined during the course of the preliminary ChIP experiment (described in section 3.3.1.c). At the PCR stage, a standard curve of the sample used in the experiment was constructed over a 2-log dilution and the efficiency (slope of the curve) and coefficient of determination (R2) were derived from the PCR results of these standard curves. The amplification plots generated slopes that varied between -2.9 and -3.5, with R2 values not less than 0.98, demonstrating that all 5 primer pairs had an efficiency of at least 93%, calculated using Formula 3.1. (Section2.6.5) (Table 3.3)

CD38 primer sets	Primer sequence	Amplicon length (bp)
Primer set 1	Forward: CCAGCTACTCGGGAGACTGA Reverse: TGCTGGGATGACCCAGTAG	68
Primer set 2	Forward: AAATGGTGCTGGGAAAACTG Reverse: AATCCATCTTGAGTTAATTTTTGAA	48
Primer set 3	Forward: TAGGCATGGGCAAAGATTTC Reverse: TTCGGTGTGCAGAAGTTCCT	65
Primer set 4	Forward: GCTGGAAGCCATTATCCTCA Reverse: CCCTCCCTGTGTTCATTGTT	61
Primer set 5	Forward: GTGTAACCAGCCACGGAACT Reverse: GCTAGGCAGCAAGAGAGAGG	86

Table 3.2 *CD38* 5'UTR and upstream flanking sequence primer sets
Primer sets 1-4 each amplify one of the four putative IRF4 binding sequences within the *CD38* upstream flanking sequence. Primer set 5 generates an amplicon which includes both putative IRF4 binding sites in the *CD38* 5'UTR, as they are only 11 bases apart from each other.

CD38 primer sets	Slope of the standard curve	R^2 value	% efficiency
Primer set #1	-3.3	0.98	100.9
Primer set #2	-2.9	0.99	121.2
Primer set #3	-2.9	0.99	121.2
Primer set #4	-3.3	0.98	100.9
Primer set #5	-3.5	0.99	93.1

Table 3.3 Efficiency of CD38 primer sets 1-5
Using a standard curve with a 2 log dilution, the efficiency of the CD38 primer sets 1-5 was determined. The slope of the standard curve is an indicator of the amplification efficiency, where a slope value of -3.32 indicates 100% efficiency. The R^2 value is the coefficient of determination. All 5 primer pairs had an efficiency of at least 93%, calculated using Formula 3.1. (Section 2.6.5)

3.3.1.c Establishment of ChIP using an antibody to histone as a positive control

In order to demonstrate successful manual ChIP technique, the protocol was initially established using an antibody to histone 3 (H3). H3 is one of the four core histone proteins, abundantly expressed in eukaryotic cells as a major constituent of chromatin, bound to DNA within nucleosomes. Given that it is expressed throughout the genome, H3 serves as an excellent positive control for ChIP experiments.

Chromatin was prepared from exponentially growing TK6 cells, and 125µg chromatin was used in each ChIP. (Table 3.4) Twenty cycles of sonication was used to prepare the chromatin samples, generating fragments of less than 500bp. (Figure 3.4) Chromatin fragment size of between 100-1000bp in length is optimal for successful ChIP studies. (Schmidt et al., 2009), (www.diagenode.com/files/protocols)

Successful ChIP was achieved using the H3 antibody, with enrichment clearly seen at *CD38* upstream flanking sites 1-4 with the histone antibody, compared to the matched control antibody. (Figure 3.5) Although the experiment was performed in duplicate, only one result is available for site 5: the standard curve for *CD38* primer set 5 failed in the duplicate experiment, and so the results from this site were disregarded. This failure of primer set 5 was consistent with it demonstrating the poorest amplification efficiency of the 5 primer sets. (Table 3.3)

A

Sample	Nanodrop of chromatin obtained after lysis steps (ng/ul)	Number of cycles of sonication	Chromatin per ChIP (ug)	Antibody used in ChIP
TK6 #1	541	20	125	Histone (H3) and IgG control (2µg)
TK6 #2	457	20	125	Histone (H3) and IgG control (2µg)

B

Sample	Nanodrop of chromatin obtained after lysis steps (ng/ul)	Number of cycles of sonication	Chromatin per ChIP (ug)	Antibody used in ChIP
TK6 #3	1036	20	150	IRF4 and IgG control (2µg)
TK6 #4	879	20	150	IRF4 and IgG control (1µg)

Table 3.4 Chromatin used in initial ChIP experiments in TK6
A. To establish the experimental protocol, ChIP experiments were carried out in TK6 cells using histone 3 (H3) antibody as a positive control. Sufficient chromatin was obtained to use 125µg in each ChIP.
B. ChIP was then performed in TK6 using IRF4 antibody. 150µg chromatin was used in each ChIP, but the antibody was reduced from 2µg to 1µg in the second experiment, to try to reduce non-specific antibody-protein binding.

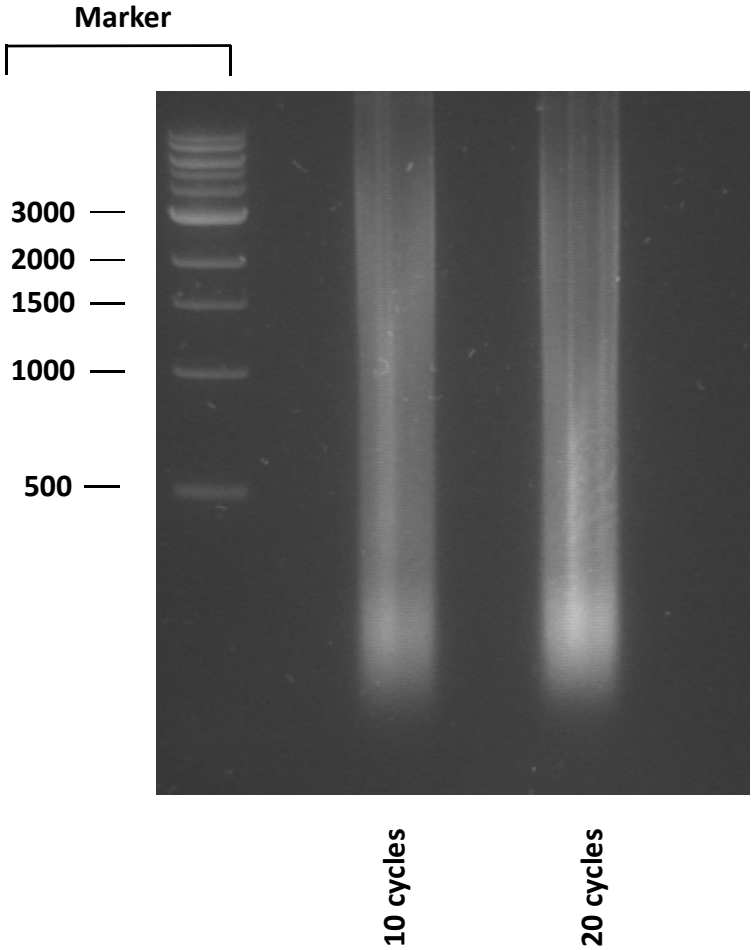

Figure 3.4 Chromatin fragments obtained from TK6 cells for ChIP using antibody to histone 3 (H3)

Denatured samples of sheared chromatin were electrophoresed on a 1.5% agarose gel to determine the size of the fragments after sonication. The marker lane indicates the size of the corresponding DNA fragments, in base pairs.

After 10 or 20 cycles of sonication, a signal is detected. While the signal is blurred, without a discrete band, the most concentrated signal is detected well below the marker indicating 500bp. Chromatin fragment size of 100-1000bp is optimal for successful ChIP experiments.

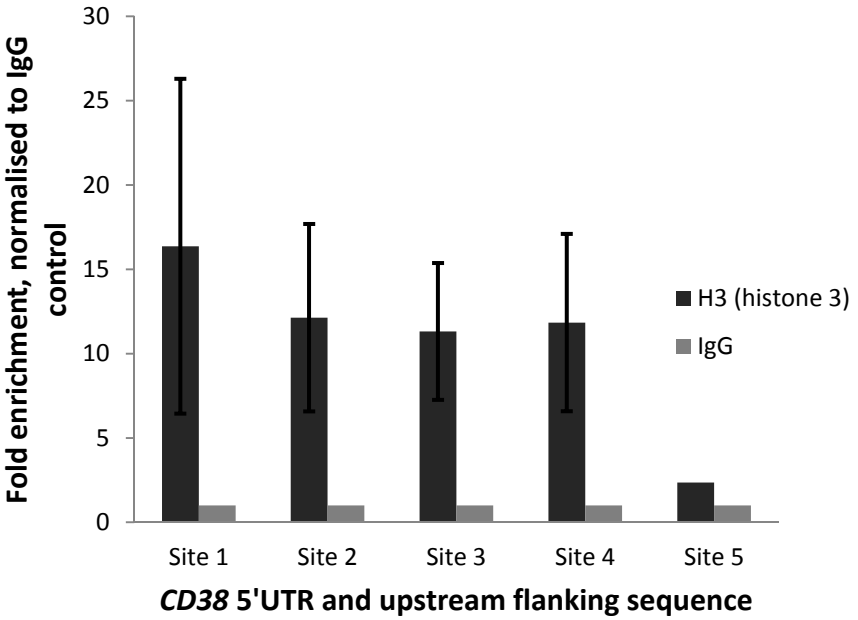

Figure 3.5 Successful establishment of manual ChIP protocol in TK6 cells, using antibody to histone 3 (H3)

ChIP was performed in chromatin prepared from exponentially growing TK6 cells, using histone (H3) antibody as a positive control, in order to confirm successful chromatin preparation and manual ChIP technique.

Primer sets to the four putative IRF4 binding sites in the upstream flanking sequence (sites 1-4) and to the two putative binding sites in the 5'UTR (site 5) were used to amplify DNA fragments purified from the ChIP experiment.

There was clear enrichment of the chromatin using the H3 antibody, compared to that obtained with the species-matched IgG control antibody.

125µg chromatin and 2µg histone (H3) antibody (or control IgG antibody) was used in each ChIP. Data shows the mean values from two replicate experiments, except for site 5 where only one experiment was performed (see section 3..3.1c). Error bars represent standard error of the mean of the two replicates.

3.3.1.d IRF4 does not bind at the *CD38* 5'UTR or upstream flanking sequences in TK6

Having successfully demonstrated chromatin preparation and manual ChIP technique in TK6 cells using the H3 antibody, ChIP experiments were then performed using IRF4 antibody, to look for evidence of IRF4-*CD38* binding. Chromatin was prepared and sheared by 20 cycles of sonication and the chromatin fragment size was evaluated by agarose gel electrophoresis (representative gel shown in Figure 3.6) One hundred and fifty micrograms of chromatin (Table 3.4) was used in duplicate ChIP experiments.

These two independent duplicate experiments provided no evidence for IRF4 binding at sites 1-4 in TK6. (Figure 3.7) In fact, in the first experiment, enrichment of the chromatin with the IgG antibody appeared to be greater than the enrichment achieved with the IRF4 antibody. This was an unexpected result, given that one would expect binding with the control IgG antibody to be, at most, no greater than, or equal to, the binding achieved with the IRF4 antibody. (Figure 3.7A) This was suggestive of excessive non-specific chromatin-antibody binding by the control antibody and for this reason, the antibody concentration of both IRF4 and control IgG antibody was reduced in the repeat experiment from 2µg per ChIP to 1µg. Accordingly, in the repeat experiment, enrichment of the chromatin by the IRF4 antibody exceeded the enrichment the control antibody, but the difference was only marginal and did not indicate significant evidence of IRF4 binding to *CD38*. (Figure 3.7B)

There was some weak evidence of binding to site 5 in the second of the two replicate experiments (Figure 3.7B), suggesting minimal binding of IRF4 to one or both of the IRF4 sites in the 5'UTR captured by this PCR amplicon. However, interrogation of the dissociation curve obtained with primer set 5 suggested issues regarding the specificity of this primer set, as indicated by the presence of a putative non-specific amplicon. (Figure 3.8) As such, and given that primer set 5 displayed the poorest amplification efficiency (Table 3.3), a further three sets of primers were designed to target the two binding sites in the 5'UTR and the results from these experiments are detailed in section 3.3.4.

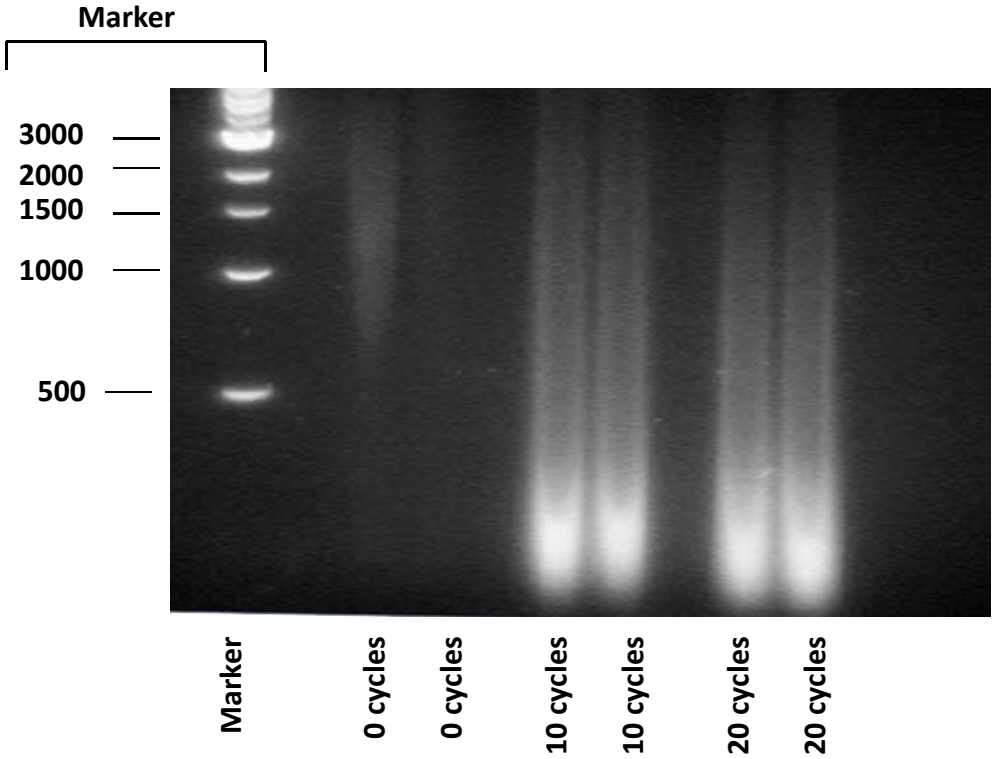

Figure 3.6 Chromatin fragments obtained from TK6 cells for ChIP using IRF4 antibody
Denatured samples of sheared chromatin were electrophoresed on a 1.5% agarose gel to determine the size of the fragments after sonication. The marker lane indicates the size of the corresponding DNA fragments, in base pairs. Chromatin fragments of less than 500bp were obtained after 10 and 20 cycles. Chromatin that had undergone 20 cycles of sonication was used for ChIP.

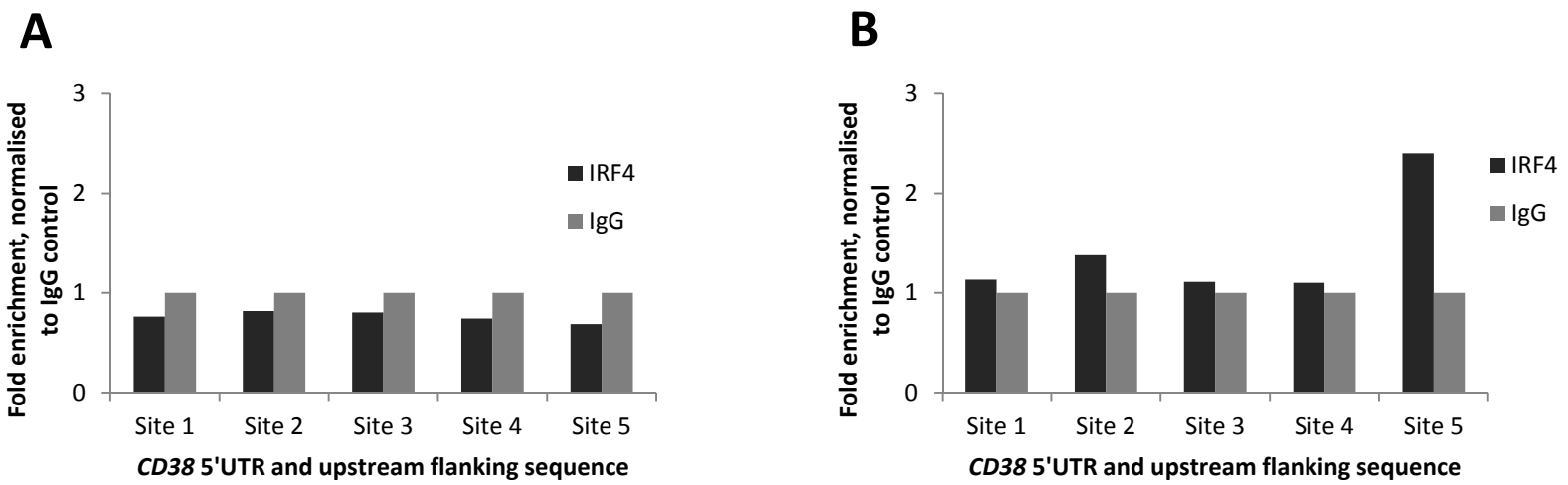

Figure 3.7 ChIP using antibody to IRF4 in TK6 cells

In two independent experiments, ChIP was performed in TK6 cells using IRF4 antibody and a species-matched control IgG antibody. Consistent IRF4-*CD38* binding was not demonstrated at any of the 6 putative binding sites in *CD38* in TK6. 150µg chromatin was used for each ChIP.

A. Enrichment with the IRF4 antibody was not seen at any of the 5 putative IRF4 binding sites in *CD38* in the first experiment. 2µg IRF4 and species-matched control antibody was used. Notably, binding by the IRF4 antibody appeared to be less than that of the control IgG antibody at each of the 5 sites, suggesting excessive non-specific binding by the IgG antibody.

B. In order to reduce non-specific binding with the control antibody, only 1µg of either IRF4 or control antibody was used in the duplicate experiment. No enrichment was seen with the IRF4 antibody at sites 1-4. Approximately two fold enrichment was seen at site 5 in the experiment.

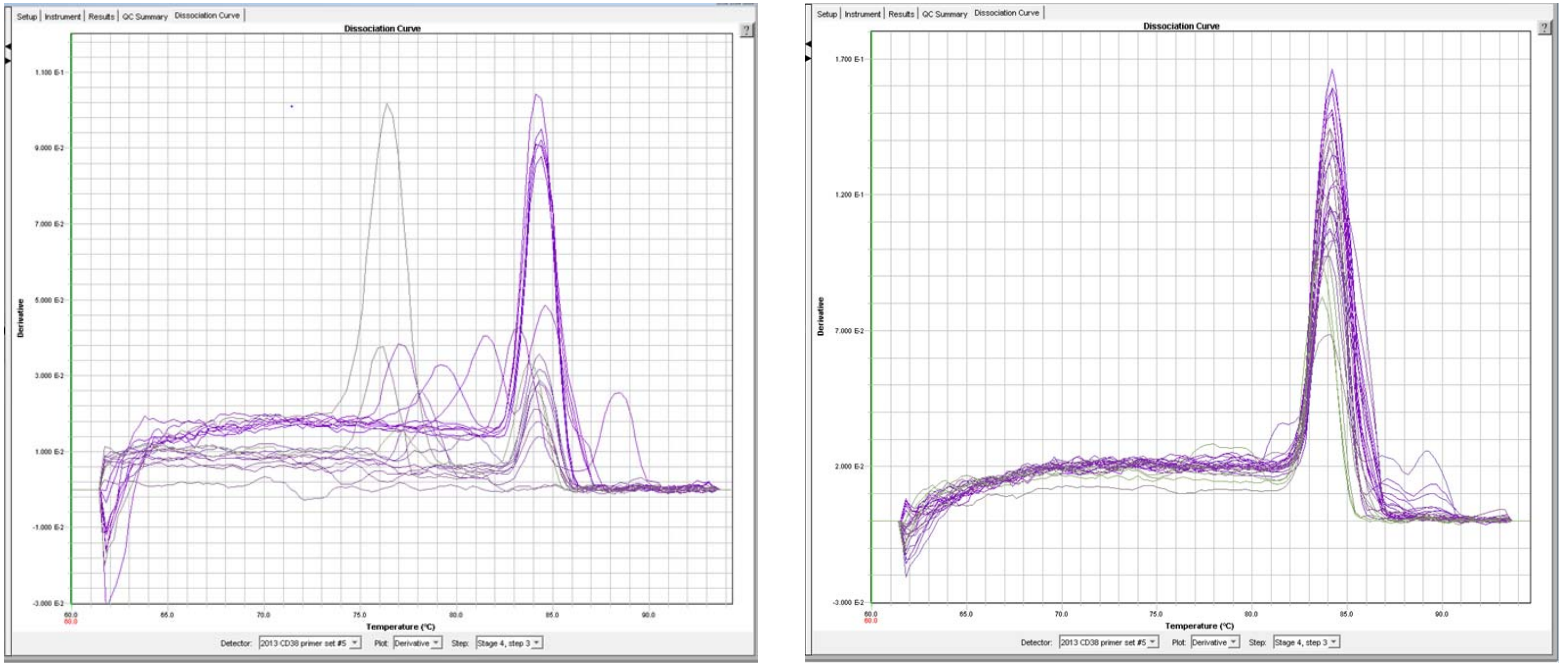

Figure 3.8 Dissociation curves for *CD38* primer set 5

Inspection of the dissociation curves obtained with *CD38* primer set 5 in two separate experiments demonstrated peaks in addition to the main amplicon. In addition, this primer set demonstrated the poorest amplification efficiency. (Table 3.3) Further primer sets to this region were therefore designed and optimised. (Section 3.3.4)

Taken together, these data provide no evidence for IRF4 binding to the upstream flanking region of *CD38* in TK6. It is not possible to draw any firm conclusions regarding IRF4 binding to the 5'UTR of *CD38* in TK6.

3.3.2 Cell lines and expression of IRF4 binding partners

Data suggesting that IRF4 does not bind to *CD38* in the upstream flanking sequence in TK6 led to consideration of the importance of IRF4 binding partners, and their expression in TK6. While TK6 expresses both CD38 and IRF4, the expression of potentially relevant IRF4 binding partners was unknown. PU.1 is the best characterised IRF4 binding partner, though IRF4 can bind with other ETS family transcription factors, such as SPI-B. (Su et al., 1996; Nagulapalli and Atchison, 1998; Shaffer et al., 2009) (Section 1.2.2) IRF4 can also bind with its own family member, IRF8. (Rosenbauer et al., 1999)

The IRF4/PU.1 heterodimer was first demonstrated to bind sequences within the enhancer elements of genes encoding immunoglobulin κ and λ light chains. (Pongubala et al., 1992; Eisenbeis et al., 1993) A DNA sequence 3' to the PU.1 binding site, was identified by methylation studies as the binding site for IRF4. (Pongubala et al., 1992) IRF4 binding to this sequence was confirmed by electrophoretic mobility shift assays (EMSAs) by three groups, which demonstrated that IRF4 requires the consensus DNA sequence 5'-GAAA-3' to be intact in order for binding to occur. (Pongubala et al., 1992; Eisenbeis et al., 1993; Himmelmann et al., 1997) However, while PU.1 could bind independently of IRF4, IRF4 was unable to bind when the upstream PU.1 binding sequence (5'-GGAA-3') was mutated in the light chain enhancers, suggesting that IRF4 was unable to bind to DNA in the absence of a suitable binding partner. (Pongubala et al., 1992; Eisenbeis et al., 1993) In contrast, both ETS and IRF4 consensus sequences were required to be intact in order for binding of either protein to occur at the CD20 promoter site. (Himmelmann et al., 1997) (Figure 3.9)

Figure 3.9 Wildtype oligonucleotide probes used in electrophoretic mobility shift assays (EMSAs) to investigate the DNA binding domains of the PU.1/ IRF4 complex

These oligonucleotide sequences were used by Pongubala *et al* (**A**), Eisenbeis *et al* (**B**) and Himmelmann *et al* (**C**) in EMSAs to determine the binding of the PU.1/IRF4 complex to the 3’ enhancer element of the kappa immunoglobulin light chain (κE3’), the λB domain of the lambda immunoglobulin light chain (EλB), and the *CD20* promoter, respectively. The Ets binding sequence is represented by 5’-GGAA-3’. When the wildtype oligonucleotide sequences were intact, PU.1 and IRF4 were both able to bind the DNA sequences.

Binding was disrupted when mutations were introduced into these oligonucleotides. Mutations in 5’-GAAA-3’ in (**A**) and (**B**) abolished binding of IRF4, though PU.1 was still able to bind independently. However, mutating the ETS binding sequence, 5’-GGAA-3’ in (**A**) and (**B**) disrupted binding of both PU.1 and IRF4, indicating that IRF4 required intact PU.1/DNA binding in order to bind to DNA itself. (Pongubala *et al.*, 1992; Eisenbeis *et al.*, 1993)

In contrast, neither PU.1 nor IRF4 were able to bind when either the 5’-AGAA-3’ or 5’-GAAA-3’ sequences of oligonucleotide (**C**) were mutated, indicating that PU.1 required intact IRF4/DNA binding to be present, in order to bind to the degenerate ETS sequence found in the *CD20* promoter. (Himmelmann *et al.*, 1997)

The oligomer used to crystallise the PU.1/IRF4/DNA ternary complex was derived from the λB light chain, and featured a composite ETS/IRF consensus element (EICE), which is represented by 5'-GGAANNGAAA-3'. (Escalante et al., 2002) This EICE fuses the PU.1 binding site, 5'-GGAA-3' with the IRF4 binding site, 5'-AANNGAAA-3'.

Given that PU.1 is the best characterised IRF4 binding partner, its expression was investigated in TK6. Critically, western immunoblotting revealed that TK6 does not express PU.1. (Figure 3.10A)

The *CD38* 5'UTR and upstream sequence were therefore reviewed for evidence of EICE sites, where IRF4 might be predicted to bind alongside PU.1. Notably, two of the previously identified consensus IRF4 binding sites (at base positions -1419 and -128) (section 3.1.2) were identified as EICE binding sites (Figure 3.11Figure 3.1) represented by 5'-GGAANNGAAA-3'.

If IRF4-driven transcription of *CD38* is mediated via heterodimerisation with PU.1, then TK6 does not represent a good model to explore potential IRF4-*CD38* binding. Rather, an appropriate experimental cell model would express IRF4, CD38, and PU.1, and ideally represent a similar stage of B cell development to the leukaemic CLL lymphocyte.

Data from the Cancer Biomedical Informatics Grid (CaBIG) was therefore used to identify cell lines expressing IRF4, CD38 and PU.1. Cell lines expressing both *IRF4* and *PU.1* transcript at the highest levels were identified (Figure 3.12) and included myeloid leukaemia cell lines (BDCM, Kasumi), lymphoid leukaemia cell lines (REC-1, RCH-ACV, SEM, JM1) and other B cell lines (SU-DHL-6, Toledo, ST486). Of these, cell lines derived from acute myeloid and lymphoid leukaemias were excluded from further consideration. Similarly, the REC-1 cell line, which is of naïve pre-germinal centre phenotype was also excluded, as it was judged too immature and not sufficiently representative of the more mature CLL phenotype. Of the remaining three cell lines, SU-DHL-6 was selected as a suitable experimental model, rather than Toledo (CD10 positive diffuse large B cell lymphoma cell line) or ST 486 (a Burkitt lymphoma cell line), as it was deemed to be the more representative of the mature CLL

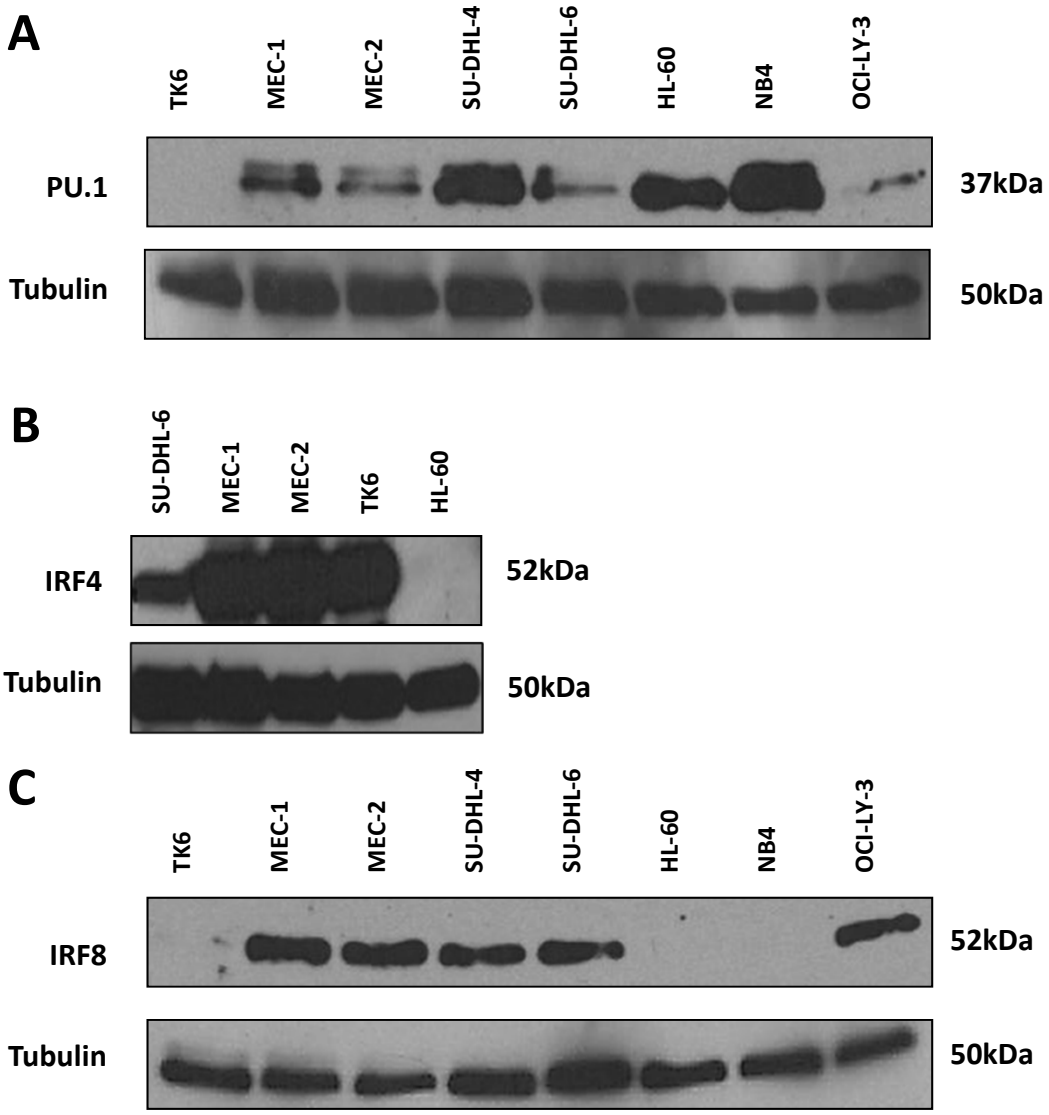

Figure 3.10 Western immunoblots demonstrating the expression of IRF4 and its common binding partners in a panel of cell lines

Whole cell extracts from the cell lines indicated were used for western immunoblotting to investigate the expression of IRF4 and its common binding partners.

A. TK6 cell line does not express PU.1 protein (37kDa), in contrast to MEC-1 and its sister cell line, MEC-2, and B lymphoma cell line, SU-DHL-6. (SU-DHL-4 and OCI-LY-3 are lymphoma cell lines; HL-60 and NB4 are myeloid leukaemia cell lines.)

B. SU-DHL-6, MEC-1 and MEC-2 also express IRF4 protein.

C. MEC-1 and SU-DHL-6 cell lines express IRF8 protein (52kDa). Neither TK6, HL-60 nor NB4, express IRF8.

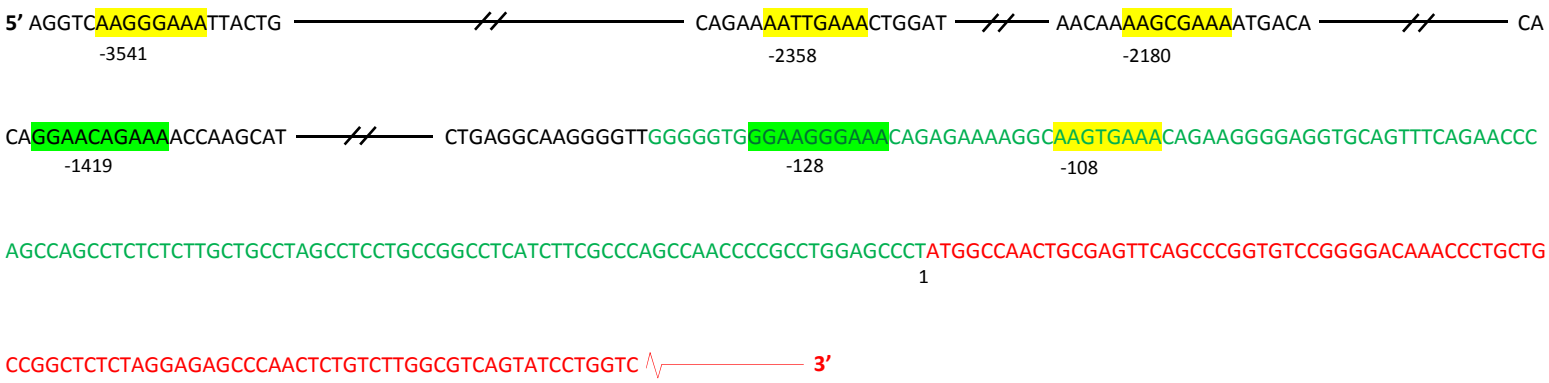

Figure 3.11 Composite Ets/IRF consensus element (EICE) binding sites in *CD38* upstream flanking sequence and 5'UTR

Two of the previously identified putative IRF4 consensus binding sites (represented by 5'-AANNGAAA-3') at base pair positions -1419 and -128, also represent composite Ets/IRF consensus elements (EICE). These are highlighted in bright green

The forward strand sequence is displayed and base positions are indicated underneath the sequence. Black text indicates the upstream flanking sequence; green text indicates 5'UTR; red text indicates coding sequence. The 5' base position of each putative binding site is indicated by yellow highlighting and numbered according to the human genome assembly release, Genome Reference Consortium human 38 (GRCh38) as viewed in the ENSEMBL genome browser.

phenotype, of these three options. SU-DHL-6 is a cell line derived from a germinal centre B cell lymphoma, of small and large cell type. (Epstein et al., 1978) In addition to IRF4 and PU.1, it expresses *CD38* mRNA transcript as indicated by the CaBIG dataset. (Figure 3.12B)

In addition, the MEC-1 cell line was also selected as a suitable experimental model. CLL-derived cell lines are rare. MEC-1 and its sister cell line, MEC-2, are derived from a 61 year old male with CLL in prolymphocytoid transformation. (Stacchini et al., 1999) MEC1 expresses *IRF4* mRNA transcript as indicated by the CaBIG dataset, and also appeared to have modest expression of *CD38* and *PU.1*. (Figure 3.13)

Western immunoblotting was further used to confirm the expression of PU.1 and IRF4 in SU-DHL-6 and MEC-1. (Figure 3.10 A, B) Flow cytometry confirmed that MEC1 and SU-DHL-6 also express surface CD38 though SU-DHL-6 expression is substantially stronger. (Figure 3.14, Table 3.5)

Whilst PU.1 is the best characterised binding partner for IRF4, IRF4 is also known to heterodimerise with other proteins to enable DNA binding. Like PU.1, the SPI-B transcription factor (SPI-B) is another member of the ETS protein family, and is able to recruit IRF4 to the kappa light chain enhancer element in the absence of PU.1. (Su et al., 1996) Attempts to confirm the expression of SPI-B were not successful due to lack of a suitable antibody for western immunoblotting.

In addition, IRF4 can also heterodimerise with IRF8, its most closely related IRF family member, and together they can bind the interferon-stimulated response element (ISRE) which has the consensus binding sequence, 5'-GAAANN-3' in macrophages. (Rosenbauer et al., 1999) IRF4 and IRF8 also bind with a further IRF protein, IRF2, which is ubiquitously expressed (Nguyen et al., 1997), at the same ISRE sequence in lymphocytes. (Rosenbauer et al., 1999) Given that all of the putative IRF4 sites identified in the *CD38* promoter could also represent an ISRE sequence, the expression of IRF8 was also confirmed in MEC-1 and SU-DHL-6. (Figure 3.10C) Interestingly, TK6 cells did not express detectable IRF8 protein.

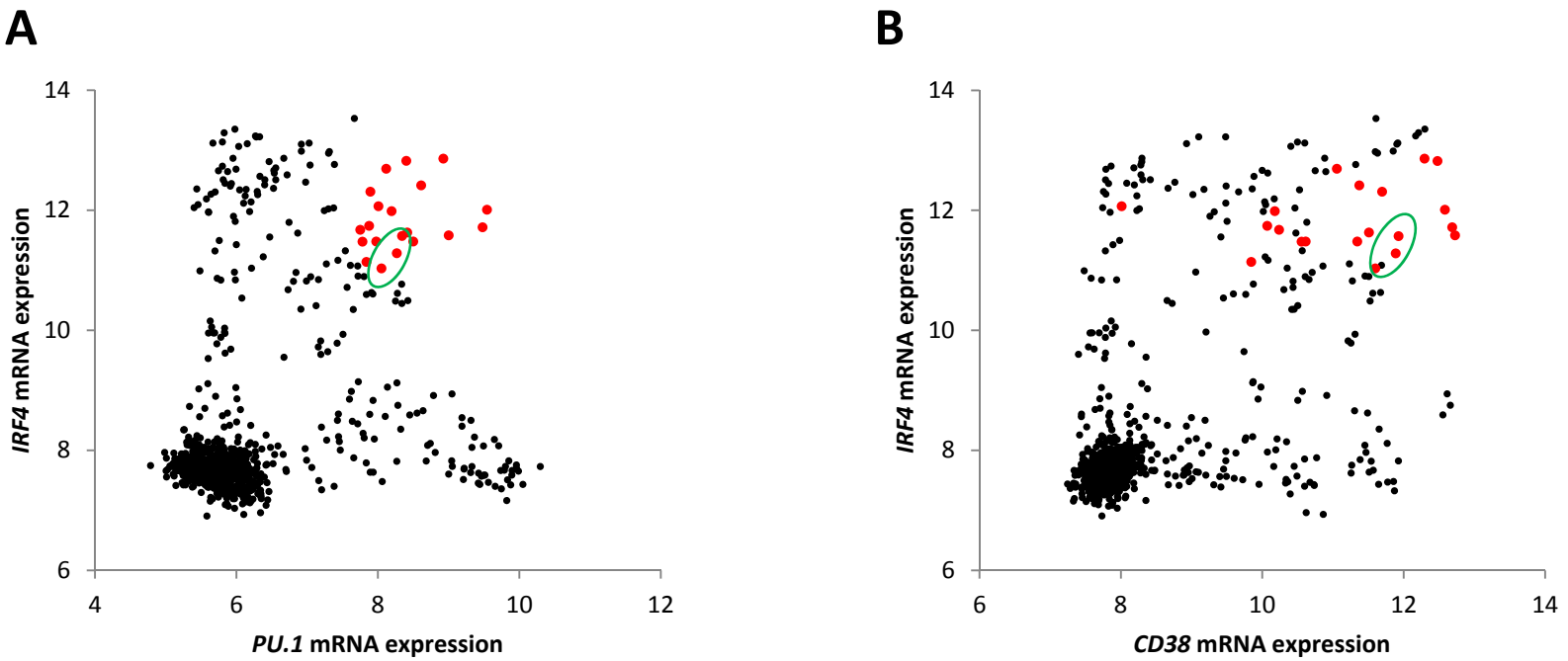

Figure 3.12 Comparison of *IRF4, PU1* and *CD38* mRNA expression by cell lines

A. Data from the Cancer Biomedical Informatics Grid (CaBIG) were used to investigate the levels of *IRF4* and *PU.1* mRNA transcript in hundreds of cell lines. Each data point represents a cell line. Data points that indicated high expression of both *IRF4* and *PU.1* (marked in red) were used to identify the corresponding cell lines.

B. *CD38* mRNA transcript levels in the same cell lines were then plotted. The distribution of *CD38* mRNA expression amongst the cells which have high expression of *IRF4* and *PU.1* (marked in red) can be seen.

Data points corresponding to data from SU-DHL-6 cell line are circled in green.

(Note that each cell line was replicated more than once in the data set, and so is represented by more than one data point.)

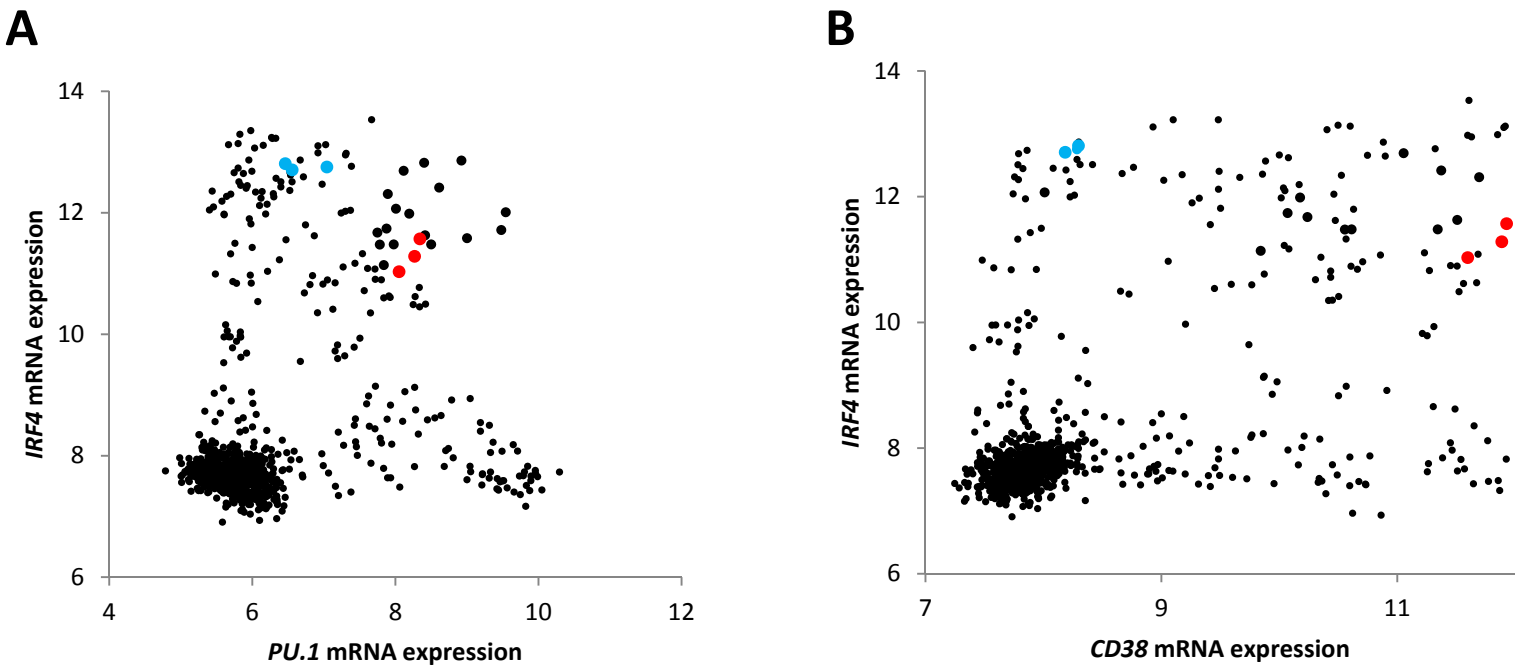

Figure 3.13 *IRF4, PU.1* and *CD38* mRNA expression by MEC-1 cell line

A. MEC-1 (indicated by blue data points) expresses *IRF4* mRNA transcript and appeared to express some *PU.1*, though expression of *PU.1* is less than in SU-DHL-6 (red data points).

B. MEC-1 also appears to weakly express *CD38* mRNA transcript. However, its *CD38* expression is again substantially less than that of SU-DHL-6.

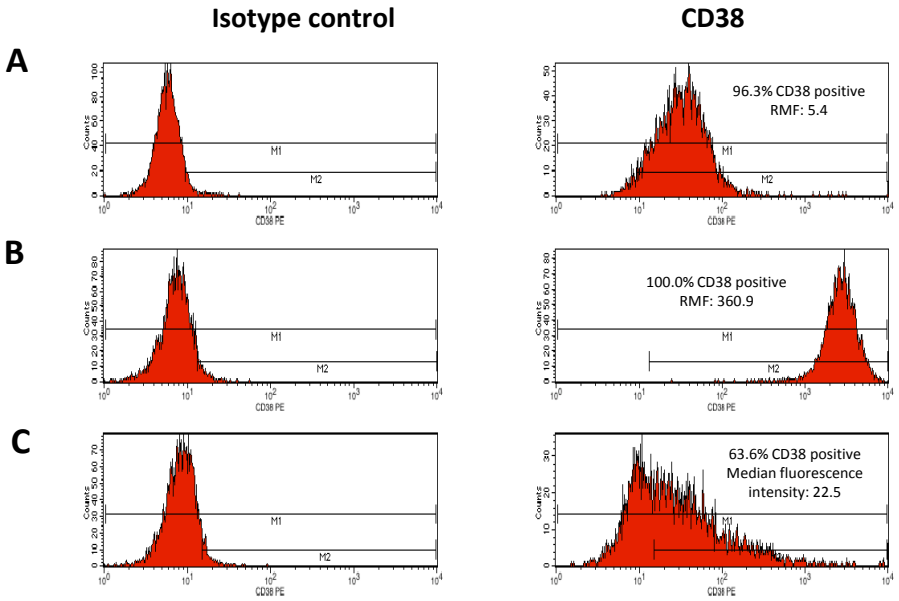

Figure 3.14 Flow cytometry histogram plots: CD38 expression in TK6, SU-DHL-6 and MEC-1 cell lines

Cells were incubated with a PE-conjugated isotype-matched control antibody, or a PE conjugated CD38 antibody. A viable cell population was gated by forward and side scatter and this population was then analysed by a histogram plot (shown here), in which all of the cells were captured within an M1 marker bar. An M2 marker bar was positioned for each of the cell lines to include 5% of cells labelled by the isotype control antibody (panels on the left). Cells labelled by the CD38 antibody which fell within the pre-set M2 marker bar were deemed CD38 positive (panels on the right) and expressed as % positive.

A. TK6 cells B. SU-DHL-6 cells C. MEC-1 cells

Geometric mean fluorescence of cells					
Cell line	**CD38 % positivity**	**Isotype control**	**CD38**	**Relative mean fluorescence (RMF)**	**Median fluorescence CD38**
TK6	96.3	5.8	31.4	5.4	32.2
SU-DHL6	100.0	7.2	2606.0	360.9	2641.7
MEC-1	63.6	8.2	27.8	3.4	22.5

Table 3.5 CD38 expression in TK6, SU-DHL-6 and MEC-1 cell lines

Using the histogram plots (Figure 3.13): the percentage of CD38 positive cells (CD38 % positivity) for each cell line was determined from the percentage of cells falling within the pre-set M2 marker bar after incubation with PE-conjugated CD38 antibody. The geometric mean fluorescence of cells labelled with either isotype or CD38 antibody was obtained from the histogram plots, and used to calculate the relative mean fluorescence (RMF) of the cells labelled with CD38 antibody. It is notable that both the histogram plots (Figure 3.1.3) and the numerical data indicate that SU-DHL-6 cells strongly express CD38. In contrast, MEC-1 cells display much weaker CD38 expression. Furthermore, MEC-1 cell CD38 labelling conforms to a skewed, non-normal distribution (Figure 3.14C): median fluorescence intensity values are therefore indicated for MEC-1.

Subsequent ChIP experiments were therefore performed using a panel of experimental cell models that included MEC-1 and SU-DHL-6. TK6 was also included as a negative control for PU.1 or IRF8 dependent binding.

1.1.1 Genome wide ChIP binding data across the CD38 locus

A 2014 study took a global approach to the investigation of IRF4 gene targets in lymphoma cell lines. (Care *et al*., 2014) ChIP sequencing (ChIP-Seq) was used to determine sites of binding by IRF4 and its associated binding partners, throughout the genome.

Unpublished data were kindly made available from this study by Dr R.M.Tooze (Leeds Institute of Molecular Medicine, University of Leeds), in order that potential IRF4-*CD38* binding sites might be identified. In contrast to the original hypothesis, neither PU.1-dependent nor SPI-B-dependent IRF4 binding was observed in this dataset at the *CD38* 5'UTR or in the upstream flanking sequence. However, IRF4 binding was demonstrated in the *CD38* first intron.

Specifically, ChIP sequencing data revealed a binding peak for IRF4, PU.1 and SPI-B between base positions 15 786 698 and 15 786 876 (hereafter referred to as 'element 1') on the forward strand of *CD38*. (**Error! Reference source not found.**A) A perfect EICE consensus binding site (5'- GGAAGTGAAA-3') was identified within this sequence. (**Error! Reference source not found.**B)

Further downstream, a second binding peak was seen at 'element 2'. (**Error! Reference source not found.**A) This spans the sequence between base position 15 807 819 and position 15 808 048. While there is no EICE site in this sequence, there is evidence of an IRF4 binding site (5'-AACAGAAA-3') on the reverse strand, with the reverse complementary sequence present on the forward strand: 5'-TTTCTGTT-3'. (**Error! Reference source not found.**B) Both element 1 and element 2 fall within the first intron of *CD38*. (**Error! Reference source not found.**)

ChIP-Seq data provided no evidence for binding of IRF4 to the 5'UTR and upstream flanking region in OCI-LY3 and OCI-LY10 lymphoma cells. Although

upstream of the translational start site in *CD38* plays either no role or a limited role in IRF4-mediated transcription of *CD38* in these cell lines.

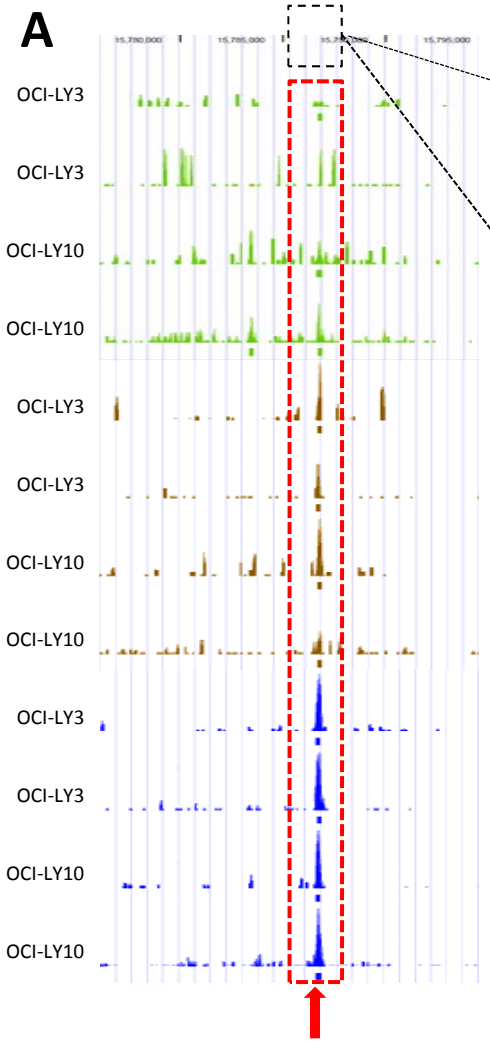

B

5'.....GTTCTAAGAATCTTAGGTGCAGGCGAGGCACGGTGGCTCACACCTGTAATCCCAGCATTTTGGGA
GGCTGACGTGGGTGGATGACGAGGTCAGGGGATTGAGACCATCCTGGCAAACATGGTGAAACCCCGTC
TCTACTAAAAATACAAAAATTAGCCGGGTGTGGTTGCGTGCACCTGTAGTCCCAGCTACTCAGGAGGCT
GAGGCAGGAGAATCGCTTGAACCTGGGAGGCGGAGGTTGCAATGAGCTGAGCTCACGCCACTACACTC
CAGCCTGGGTGACAGAGCAAGACTCTGTCTTAAAAAAAAAAAAATCTCAGGTGCACCTGAGACAGATTGA
ATGT**GGAA**GG**GGAAGTGAAA**CAGGCCTTCCAGGTGTGGGGCCTGGGTGCTGCTATAGTTACAAATGG
GGAAGTGAGACTATAGGTCTCAGTTACCTGT**GGAAGGAA**GGGTAGAGTGGAGTACTTACGCAAATTAG
CTAATTCTGGGAGCTTGGGGTGCTACCAGGGTATCAGGGAGAATACAGCCAG**GGAA**TAGAATCTTCTT
GAAGCAAAGGCTGTTT**GGAA**GCCCCCAGAGTGGATGAAAAGGCTCAGTG**GGAAA**CAACAGATATCAG
GAGAGGGAGAAGAAGATACCTATTTCTATACCTTTTGGCCTTGTGTTTTGCTTCAGACACTGTTCCCAGC
AAGGTCAGT**GGAA**CCCACTGCTCAAAACACACACTTGCTCC....3'

Figure 3.15 Element 1 binding: ChIP sequencing (ChIP seq) data demonstrates binding in *CD38* by IRF4, PU.1 and SPI-B in OCI-LY3 and OCI-LY10 lymphoma cell lines
A. The dotted red box indicates a binding peak detected by ChIP seq in the first intron of *CD38,* in OCI-LY3 and OCI-LY10 lymphoma cell lines. IRF4 and its binding partners, PU.1 and SPIB bind specifically between base positions 15 786 698 and 15 786 876, and this region is designated element 1. IRF4 binding peaks are shown in green; PU.1 binding peaks are shown in brown; SPIB binding peaks are shown in blue. (With thanks to Dr R.M.Tooze, unpublished data.)
B. The element 1 binding site and the surrounding sequence (corresponding to the dotted red box in (A), base positions 15 786 449 to 15 787 099) are shown. A 5'-GGAAGTGAAA-3' EICE binding site is highlighted in red. ETS binding sites, 5'-GGAA-3', are shown in bold.

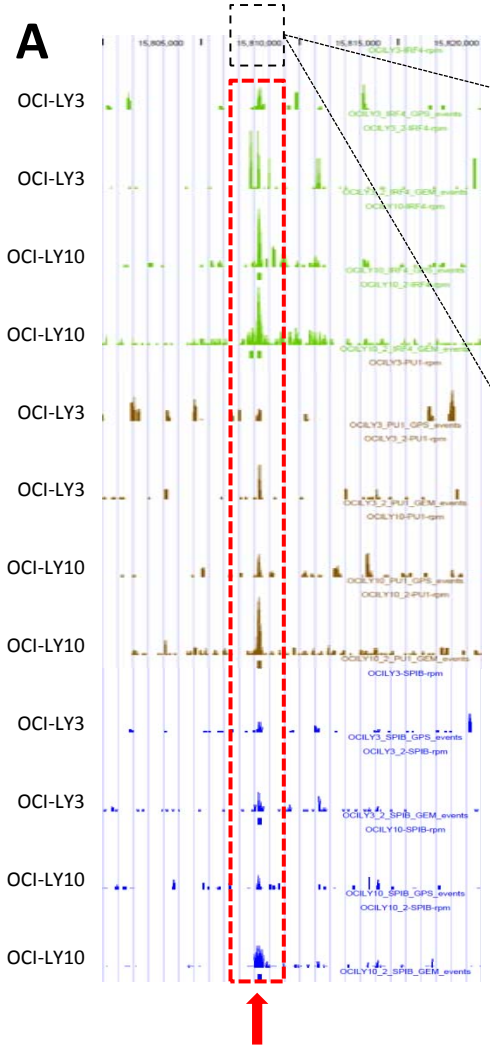

B

5'.....AGTGTAATTACCCTGCAAGATCTGAGTGCTTTTAGGCAAGAGGATTTAGGGGGTGAGAGT
TTTCCTGGAGAGGGACACATTATGAAGGTGATATTGCTTAATTGATGGGGACTTTGAAACATAGT
TGCTCTTTGTGAGAATGGTATAGGTTTAGAGAGAGGTGCTAGCACAGAGCTGTGACACCTGAAG
TAGGCTGACCGCAGACAAATTGGATTTAACCACCAAATATATCTGTGTTTTCATGTCTTCCTGCCC
CGTGCCCTCTTATCTGACTCACTTTACCCCAGCACTGGGGAATAACTGTGCCCTATTCTGGTCCTG
ACCCTTTTGTACCATCTAG**GGAA**ATGAGAACTCCTCTTGGGGTCTCAGATCCTCA**TTTCTGTT**AGA
ACCAATCCTATTCTGTGGGTAGGGCCATGGTTGTAAATTTCCTGTGGGAGGCAGCATTGCTTTGC
AAAAGAACACAGTTTGGCATGTGAGGCAGCTCTGCCACTTGGACAAGGTGATAACGCTTTAGTCT
CTTTATTTCTAAAACAG**GGAA**GATGCTAATACCCCGCCCATGGACTAGTATGAGATTTAAATGGC
AGGTACTTGGCACAGTGGCAGGTGGTGAATGCTCTTTGGTGATCATGACTATCCCTTTCTCCTGGT
AGTGCTGCCTCCTCCCTCTGAGCACCTGGAGTCAATCCACCTTGGGTAGGTCAGAGAAGGCAGAA
GAAAGTGGTGGGAGGTGAACTCGAC**GGAA**TGATGTACAGGGCGATAGGGTGAGTGAGAGGTCT
GGG....3'

Figure 3.16 Element 2 binding: ChIP sequencing data demonstrates binding in *CD38* by IRF4, PU.1 and SPI-B in OCI-LY3 and OCI-LY10 lymphoma cell lines

A. The dotted red box indicates a second binding peak detected by ChIP seq at a region in the first intron of *CD38,* designated element 2. Binding by IRF4, PU.1 and SPI-B occurs between base positions 15 807 819 and 15 808 048. IRF4 binding peaks are shown in green; PU.1 binding peaks are shown in brown; SPIB binding peaks are shown in blue. (With thanks to Dr R.M.Tooze, unpublished data.)

B. The element 2 binding site and the surrounding sequence (corresponding to the dotted red box in (A), base positions 15 807 559 to 15 808 338) are shown. The 5'-TTTCTGTT-3' sequence (highlighted in red) indicates the presence of an IRF4 binding site, 5'-AANNGAAA-3', on the reverse strand. ETS binding sites are shown in bold.

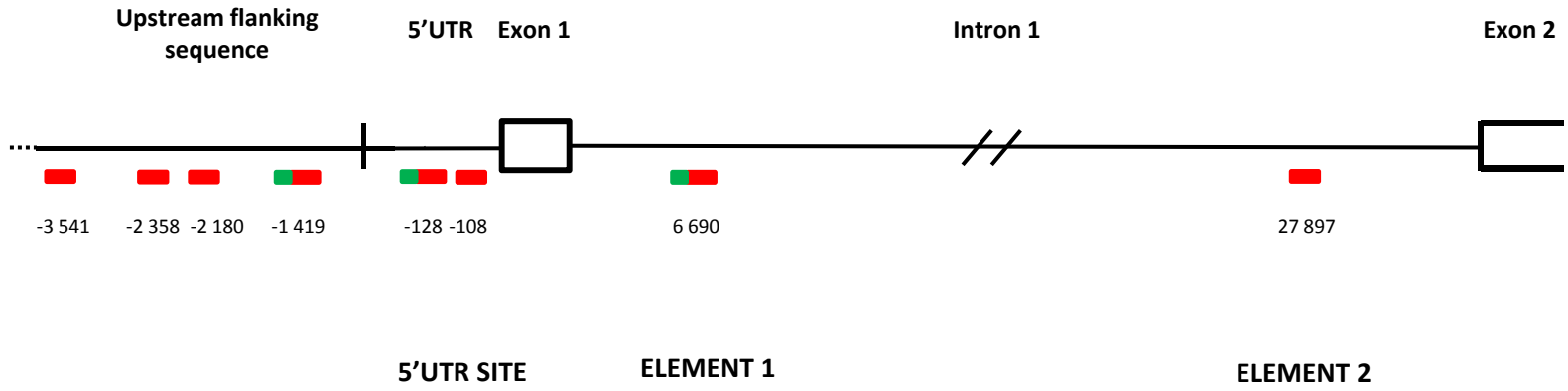

Figure 3.17 *CD38* gene and potential IRF4 binding sites

A diagrammatic representation of *CD38* gene: the upstream flanking sequence, 5'UTR, first exon and intron. IRF4 binding sites (5'-AANNGAAA-3') (represented by a red box) are seen in the upstream flanking sequence, 5'UTR and intron 1. Three of these fuse the IRF4 binding site with an ETS binding site, creating the composite EICE binding sequence (5'-GGAANNGAAA-3') (represented by a green and red box). The base positions of the first nucleotide within *CD38* of each of these binding sites is indicated. The element 1 and element 2 binding sites demonstrated by ChIP sequencing data in OCI-LY3 and OCI-LY10 lymphoma cell lines (section 3.3.3), are indicated.

3.3.4 Investigation by ChIP of IRF4-CD38 intron 1 binding in SU-DHL-6 and MEC-1 cell lines

Following ChIP-Seq evidence of IRF4 binding at two independent sites in intron 1, (section 3.3.3) the focus of the investigation into IRF4-*CD38* interaction was re-directed to element 1 and element 2 in the first intron, using cell lines MEC-1, SU-DHL-6 and TK6. The 5'UTR site also remained a focus of investigation, as it had the potential to act as a negative control for binding, given that the ChIP-Seq data did not demonstrate any IRF4-*CD38* interaction in this region.

Primer sets were designed to target the EICE site in element 1 (hereafter designated element 1 primer sets 1, 2 and 3) and the inverted IRF4 site in element 2 (designated element 2 primer sets 1, 2, 3 and 4). (Table 3.6A) In addition, three new primer sets were designed to target the *CD38* 5'UTR site (designated Primer sets 5A-C) (Table 3.6B) in view of the concerns raised during earlier experiments about the specificity of existing primers targeting this region. (Section 3.3.1.d)

3.3.4.a Validation of primers to elements 1 and 2, and to *CD38* 5'UTR

In order to select the most efficient primers to target the binding sites in element 1 and element 2 of intron 1, standard curves were produced using genomic DNA from TK6 and MEC-1 cell lines, across a 2-log dilution. The primers were used to amplify the DNA in these standard curves in a real time PCR reaction, and the results were used to determine the efficiency of amplification and coefficient of determination using Formula 3.1, as before. (Table 3.7) The dissociation curve was also interrogated for each primer set. One primer set to target each of the two sites was then chosen based on these results, and designated the 'element 1 primer set' and 'element 2 primer set' respectively. (Table 3.7)

Using the same approach, the efficiency of the new *CD38* 5'UTR primer sets was also determined (Table 3.8) and one set was selected for use in subsequent experiments, and designated the '5'UTR primer set'.

A

Primer set	Primer sequence	Amplicon length (bp)
Element 1 primer set 1	Forward: GGTGCACCTGAGACAGATTG Reverse: AGTCTCACTTCCCCATTTGTAA	58
Element 1 primer set 2	Forward: GGTGCACCTGAGACAGATTG Reverse: AGTCTCACTTCCCCATTTGTAAC	57
Element 1 primer set 3	Forward: GGTGCACCTGAGACAGATTG Reverse: AGTCTCACTTCCCCATTTGTAACT	56
Element 2 primer set 1	Forward: TTCTGGTCCTGACCCTTTTG Reverse: TGGCCCTACCCACAGAATAG	64
Element 2 primer set 2	Forward: TTCTGGTCCTGACCCTTTTG Reverse: TTTACAACCATGGCCCTACC	74
Element 2 primer set 3	Forward: GGTCCTGACCCTTTTGTACC Reverse: TGGCCCTACCCACAGAATAG	60
Element 2 primer set 4	Forward: GGTCCTGACCCTTTTGTACC Reverse: TTTACAACCATGGCCCTACC	70

B

CD38 5'UTR primer sets	Primer sequence	Amplicon length (bp)
Primer set 5A	Forward: GTGTAACCAGCCACGGAACT Reverse: GGGTTCTGAAACTGCACCTC	60
Primer set 5B	Forward: GTGTAACCAGCCACGGAACT Reverse: GAAACTGCACCTCCCCTTCT	53
Primer set 5C	Forward: ACTCTGAGGCAAGGGGTTG Reverse: GGGTTCTGAAACTGCACCTC	60

Table 3.6 Primer sets to putative IRF4 binding sites in *CD38* element 1 and element 2

A. *CD38* Intron 1: primer sets were designed to target the EICE site in element 1 and the inverted IRF4 site in element 2.

B. Given that previously designed primer sets to the putative IRF4 and EICE binding sites in the 5'UTR generated a non-specific amplicon and had an amplification efficiency of only 93% (section 3.3.1.d), new primer sets were designed to target the these two putative binding sites in the 5'UTR.

EICE site and inverted site primer sets	Slope of the standard curve	R^2 value	% efficiency
Element 1 primer set 1	-3.15	0.98	107.7
Element 1 primer set 2	-3.25	0.96	103.1
Element 1 primer set 3	-3.05	0.96	112.8
Element 2 primer set 1	-3.40	0.99	96.8
Element 2 primer set 2	-3.45	0.97	94.9
Element 2 primer set 3	-3.29	1.00	101.4
Element 2 primer set 4	-3.23	0.96	104.0

Table 3.7 Efficiency of primer sets to elements 1 and 2 in *CD38* intron 1
Using a standard curve with a 2 log dilution, the amplification efficiency and the coefficient of determination of each of the primer sets was determined. The dissociation curves were also viewed to ensure only one product of amplification was obtained (not shown). One primer set to each element was then selected (boxed in red) and designated 'element 1 primer set', and 'element 2 primer set' respectively.

CD38 5'UTR primer sets	Slope of the standard curve	R^2 value	% efficiency
Primer set 5A	-3.3	0.99	100.9
Primer set 5B	-3.1	0.96	110.2
Primer set 5C	-3.2	0.95	105.4

Table 3.8 Efficiency of new primer sets to *CD38* 5'UTR
Using a standard curve with a 2 log dilution, the amplification efficiency and the coefficient of determination of each of the primer sets was determined. The dissociation curves were also viewed to ensure only one product of amplification was obtained (not shown). One primer set was then selected (boxed in red) and designated '5'UTR primer set'.

3.3.4.b Evidence of IRF4-*CD38* binding in SU-DHL-6 and MEC-1 cells

ChIP experiments were performed using chromatin prepared from exponentially growing SU-DHL-6, MEC-1, and TK6 cell lines. The enrichment of chromatin obtained by ChIP with IRF4 and IgG control antibody was compared at elements 1 and 2, and the 5'UTR site. The experiments were performed in triplicate in each case.

The quantity of chromatin prepared from the SU-DHL-6, MEC-1 and TK6 cell lines was determined by nanodrop. Agarose gel electrophoresis was also performed in SU-DHL-6 and MEC-1 to confirm the size of the sonicated fragments. (Figure 3.18) The chromatin and antibody used in each ChIP in the SU-DHL-6, MEC-1 and TK6 cell lines is detailed in Table 3.9.

Following the generation of satisfactory chromatin, ChIP was performed using the SX-8G IP-Star® Compact Automated ChIP System, which substantially improved time efficiency and reproducibility, compared to the manual ChIP procedure.

Statistically significant IRF4-*CD38* binding occurred at the intron 1 element 1 EICE site (p=0.041), and at the 5'UTR (p=0.019) in SU-DHL-6 cells. (Figure 3.19) Average enrichment of the chromatin by the IRF4 antibody was over 35 fold at the element 1 site. It was rather less, only 6 fold, at the 5'UTR site. No significant binding occurred at the element 2 binding site in SU-DHL-6.

There was no statistically significant binding demonstrated at the element 1 or element 2 sites, in MEC-1 cells. (Figure 3.20) There was a suggestion of binding at the element 1 site, with more than 9 fold average enrichment of the chromatin by IRF4 antibody, over the three experiments. However, using a two-sample t-Test assuming unequal variances, the *p* value generated was non-significant at 0.09. However, there was statistically significant evidence of modest binding at the 5'UTR site with over 3 fold average enrichment of the chromatin by IRF4 antibody. Using a two-sample t-Test assuming unequal variances, the *p* value at this site was 0.039.

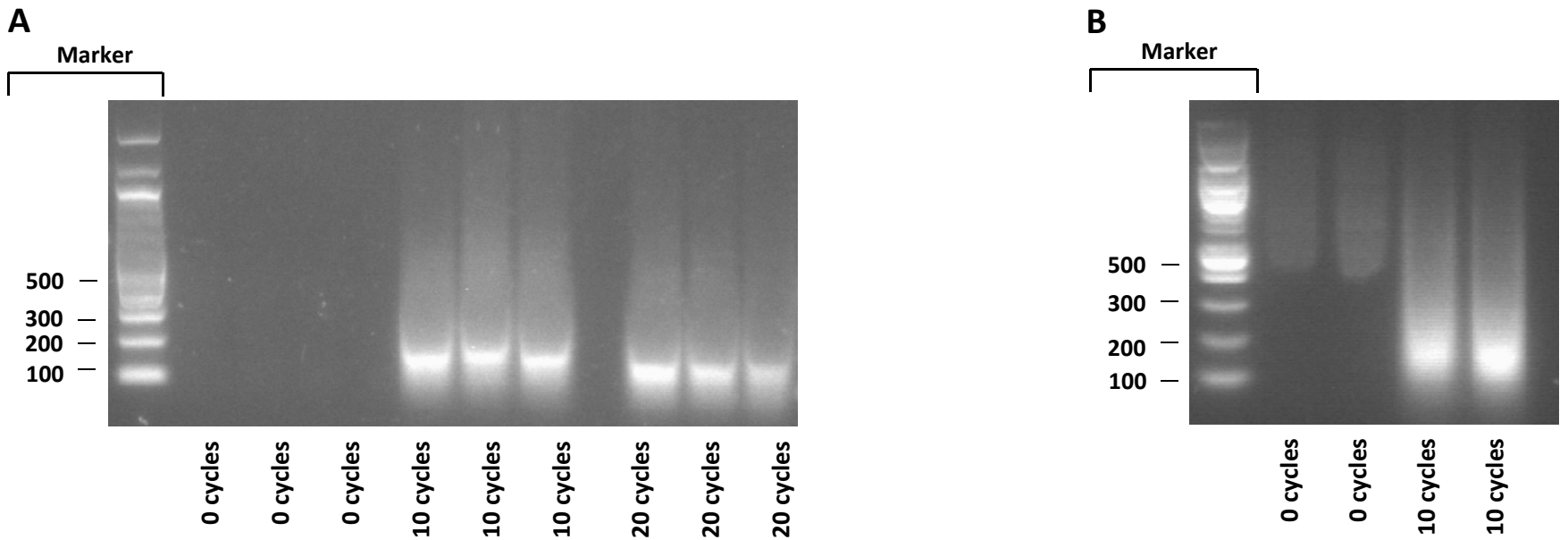

Figure 3.18 SU-DHL-6 and MEC-1 chromatin fragment size after sonication

Chromatin fragments were denatured and then electrophoresed on a 1% agarose gel. Representative gels are shown. Marker band sizes are indicated, in base pairs.

A. SU-DHL-6: A discrete signal is seen after 10 and 20 cycles of sonication. Chromatin which had undergone 20 cycles of sonication was used in the first experiment. In the subsequent two replicate experiments, SU-DHL-6 chromatin underwent only 10 cycles of sonication.

B. MEC-1: Fragments between 100 and 200 base pairs are obtained after 10 cycles of sonication.

A

Sample	Nanodrop (ng/ul)	Number of cycles of sonication	Chromatin per ChIP (ug)	Antibody used in ChIP
SU-DHL-6 #1	528.9	20	50	IRF4 and IgG control (2µg)
SU-DHL-6 #2	578.0	10	50	IRF4 and IgG control (2µg)
SU-DHL-6 #3	557.9	10	50	IRF4 and IgG control (2µg)

B

Sample	Nanodrop (ng/ul)	Number of cycles of sonication	Chromatin per ChIP (ug)	Antibody used in ChIP
MEC-1 #1	593.5	10	50	IRF4 and IgG control (2µg)
MEC-1 #2	626	10	50	IRF4 and IgG control (2µg)
MEC-1 #3	472	10	45	IRF4 and IgG control (2µg)

C

Sample	Nanodrop (ng/ul)	Number of cycles of sonication	Chromatin per ChIP (ug)	Antibody used in ChIP
TK6 #1	727.4	10	50	IRF4 and IgG control (2µg)
TK6 #2	1079.6	10	50	IRF4 and IgG control (2µg)
TK6 #3	846.6	10	50	IRF4 and IgG control (2µg)

Table 3.9 Chromatin used for ChIP in SU-DHL-6, MEC-1 and TK6 cells, with IRF4 antibody

Chromatin was prepared for ChIP from SU-DHL-6 (**A**), MEC-1 (**B**) and TK6 (**C**) cells in exponential growth phase. After sonication, the concentration of chromatin generated was determined by nanodrop. The number of cycles of sonication used in each case is indicated. 50µg chromatin was used for ChIP in all cases except for one MEC-1 cell line ChIP. 2µg IRF4 antibody or species-matched control antibody was used in each ChIP.

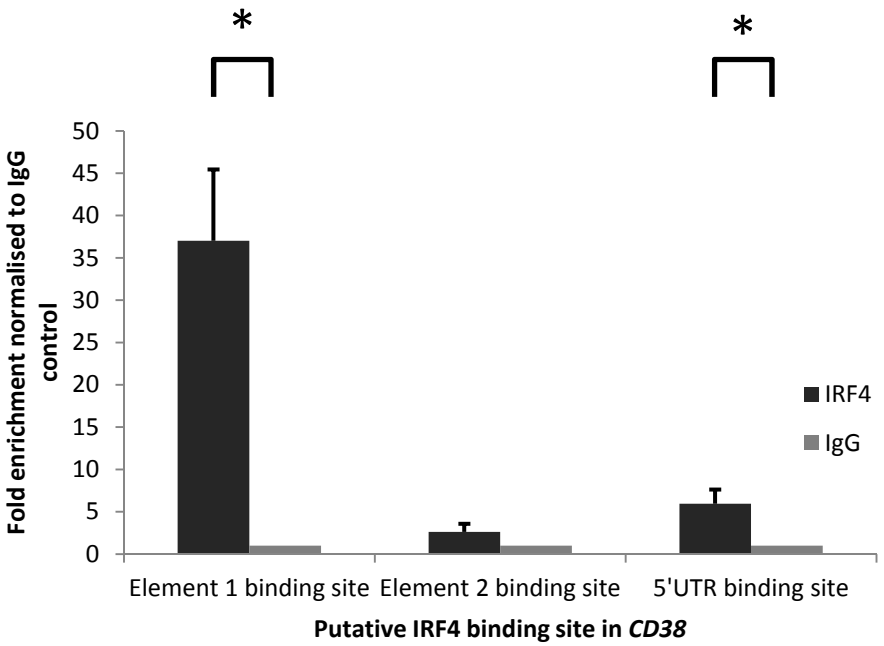

Figure 3.19 ChIP in SU-DHL-6 using IRF4 antibody to determine IRF4-*CD38* binding

Chromatin was manually prepared to the sonication stage from exponentially growing SU-DHL-6. ChIP was then performed using the Diagenode ChIP robot, with either 2µg of goat IRF4 antibody or 2µg of species-matched control antibody. The product of the ChIP then underwent PCR amplification using the three optimised primer sets, targeted to putative binding sites in *CD38* at elements 1 and 2 (in intron 1) and the 5'UTR. Enrichment at these sites by ChIP with IRF4 or control IgG antibody was calculated according to the input sample (chromatin that did not undergo ChIP). Fold enrichment of the chromatin by the IRF4 antibody was then normalised to enrichment by the IgG control antibody. The experiment was performed in triplicate and error bars indicate the standard error of the mean. Asterisks indicate significant two-tailed *p* values, calculated using a two sample t-Test. Significant binding was seen at element 1 (p=0.041) and at the 5'UTR (p=0.019).

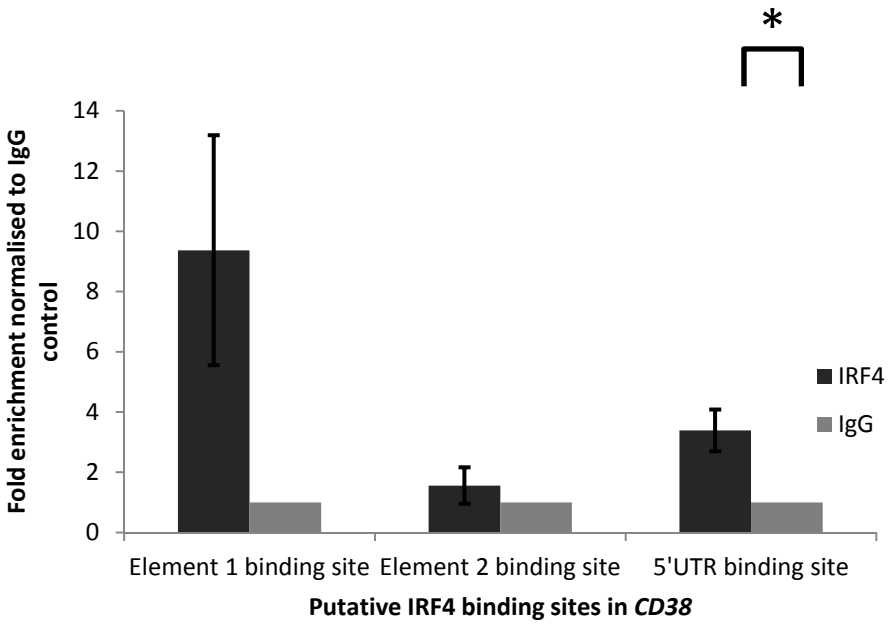

Figure 3.20 ChIP in MEC-1 using IRF4 antibody to determine IRF4-*CD38* binding

Manually prepared chromatin underwent ChIP with either 2µg of IRF4 antibody or 2µg of species-matched control antibody, using the Diagenode ChIP robot. The product of the ChIP was amplified by PCR reaction, using the three optimised primer sets, designed to target *CD38* element 1 and element 2 sites in intron 1, and the putative binding sites in the 5'UTR. The experiment was performed in triplicate and error bars indicate the standard error of the mean. While the data appears to demonstrate binding at the element 1 site, this did not reach statistical significance, using a two sample t-Test (p=0.090). Binding at the 5'UTR site however was statistically significant (p=0.039).

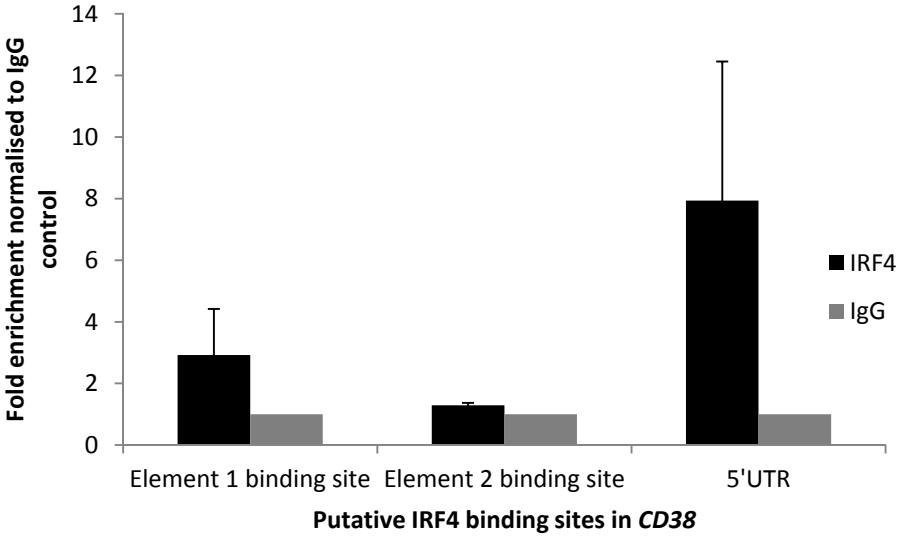

Figure 3.21 ChIP in TK6 using IRF4 antibody to determine IRF4-*CD38* binding

Chromatin was manually prepared to the sonication stage, before undergoing ChIP with either 2µg of IRF4 antibody or 2µg of species-matched control antibody, using the Diagenode ChIP robot. The product of the ChIP was amplified in a PCR reaction using optimised primers designed to target elements 1 and 2 in *CD38* intron 1, and a sequence in the *CD38* 5'UTR. The experiment was performed in triplicate and error bars indicate the standard error of the mean. No statistically significant binding was demonstrated at any of the three sites, using a two sample t-Test. Although there was the suggestion of binding at the 5'UTR site, the *p* value generated was non-significant at 0.26.

In TK6 cells, there was a suggestion of binding with average chromatin enrichment of nearly 8 fold at the 5'UTR site. However, this was not statistically significant (p=0.26) and the median enrichment value was only 4. There was no evidence of binding at the element 1 or element 2 sites in TK6. (Figure 3.21)

3.4 Discussion

3.4.1 IRF4-CD38 binding

Given the identification of a putative IRF4 binding site in *CD38* upstream of the translational start site (Allan et al., 2010), ChIP was used to investigate IRF4-*CD38* binding. The *CD38* sequence was interrogated for additional putative binding sites and a total of six potential IRF4 binding sites were initially identified in the 5'UTR and upstream flanking sequence. However, there was no consistent evidence of IRF4-*CD38* binding at any of these sites in TK6 lymphoblastoid cell line. Critically, TK6 was subsequently demonstrated not to express PU.1 or IRF8: two established IRF4 binding partner proteins.

Further interrogation of the putative binding sites in the 5'UTR and upstream flanking sequence of *CD38* revealed that two of these sites in fact represented EICE binding sites: DNA sequences that fuse the PU.1 binding sequence, 5'-GGAA-3' with the IRF4 binding sequence, 5'AANNGAAA-3'. Additionally, unpublished ChIP sequencing data from lymphoma cell lines OCI-LY3 and OCI-LY10 revealed evidence of IRF4-*CD38* binding at two sites in *CD38* first intron at 'element 1' which represents an EICE site, and at 'element 2' which represents an inverted IRF4 binding site. These global genome-wide data demonstrated no evidence of IRF4-*CD38* binding in the upstream flanking sequence or 5'UTR.

Therefore, given that the *CD38* gene contains EICE sites in the upstream flanking sequence, 5'UTR and first intron, it was appropriate to select cell lines expressing PU.1, a member of the ETS family, in addition to IRF4 and *CD38*. In this regard, while TK6 was an adequate model in the first instance to demonstrate the suitability of the IRF4 antibody and to confirm successful ChIP technique, it was not a suitable model in which to comprehensively explore IRF4-*CD38* interaction. SU-DHL-6 and MEC-1 cell lines were chosen as suitable models in which to investigate IRF4-*CD38* binding. Both of these cell lines express IRF4, CD38, PU.1 and IRF8, though CD38 expression in MEC-1 was demonstrated to be modest.

ChIP experiments performed in SU-DHL-6 clearly demonstrated statistically significant binding at element 1: the EICE site in intron 1 of *CD38*. There was a suggestion of binding at this site in MEC-1 but binding was not statistically significant. In contrast, binding at this site was not seen in TK6. TK6 lacks PU.1 expression in contrast to MEC-1 and SU-DHL-6. It is interesting to note that the binding at this site was clearly more substantial in SU-DHL-6 than in MEC-1. While western immunoblotting (Figure 3.10) did not clearly illustrate differential expression of PU.1 protein in SU-DHL-6 and MEC-1, the CaBIG data (Figure 3.13) suggests that PU.1 transcript levels are higher in SU-DHL-6. Based on these observations, a model could be postulated whereby PU.1 expression drives IRF4 binding at the intron 1 EICE site. As such, with high PU.1 expression seen in SU-DHL-6, PU.1-dependent IRF4 binding occurs readily. Binding occurs, but to a lesser extent when PU.1 expression is a limiting factor, as may be the case in MEC-1. In the absence of PU.1 expression as is observed in TK6 cells, IRF4 binding to the intron 1 EICE site does not occur. As such, the model predicts that IRF4 binding to the intron 1 EICE site is mediated primarily by PU.1.

It is important to mention that PU.1 can be substituted by Ets family member SPI-B in recruiting IRF4 to an EICE site. Significantly, it is not clear whether TK6, SU-DHL-6 and MEC-1 express SPIB protein. Western immunoblotting to demonstrate SPIB expression was unsuccessful as no reliable antibody could be identified. It is entirely possible that SPI-B, not PU.1, is mediating the IRF4 binding at the EICE site in *CD38*.

No significant binding was seen using targeted ChIP at the inverted IRF4 site (element 2) in any of the cell lines. This site represents a consensus IRF4 binding site on the reverse strand, and no EICE site is found in this region. Given this lack of EICE sequence, it is perhaps therefore surprising that binding by PU.1 and SPI-B was apparent by Chip-Seq at this site in OCI-LY3 and OCI-LY10, in addition to IRF4 binding. (Section 3.3.3) Notably however, the peaks detected by ChIP-Seq for PU.1 and SPI-B appeared substantially smaller at element 2, than those detected at the EICE site in element 1. (Figure 3.15Figure 3.16A)

IRF4 can bind the ISRE sequence, 5’-GAAANN-3’ alone (Matsuyama et al., 1995; Yamagata et al., 1996), or with IRF8 in the presence (lymphocytes) or absence

(macrophages) of IRF2. (Rosenbauer et al., 1999) SU-DHL-6 and MEC-1 express IRF8, while TK6 does not. IRF2 is ubiquitously expressed (Nguyen et al., 1997) although its expression was not specifically confirmed in the cell lines used here. The ISRE sequence is present in all of the putative IRF4 binding sites investigated in this chapter, but it is notable that when IRF8, IRF2 and IRF4 were demonstrated to heterodimerise to bind the ISRE in the interferon stimulated gene 15 (ISG15) sequence in lymphocytes (Rosenbauer et al., 1999), the number and spacing of the consensus ISRE sequences was found to be critical. Specifically, three 5'-GAAANN-3' consensus binding sequences immediately adjacent to each other with no interrupting sequence, were associated with the strongest evidence of binding by EMSA. Disruption of any of these three sequences, including the insertion of additional bases between the sequences, interfered substantially with binding. Interference with the middle and 3' of the three ISRE sequences was especially crucial. Further interrogation of the *CD38* intron 1 reveals only one instance of three ISRE consensus sites falling adjacent to each other, but an additional base separates the middle and 3' of the three consensus sites. This sequence is found on the reverse strand, at base positions 15 782 369 to 15 782 386, outside of either element 1 or element 2 sites. At this site, the 5' and middle ISRE consensus sites are immediately adjacent to each other but the 3' sequence is separated by one additional base (5'-CTTTTACTTTTGTCTTTTC-3'). The ChIP sequencing data provided by Dr R. Tooze (section 3.3.3) did not indicate evidence of IRF4 binding at this region and so targeted ChIP for IRF4-*CD38* binding was not specifically investigated here. Lack of binding at this site would be in keeping with the findings of Rosenbauer *et al*, where the introduction of additional bases between the middle and 3' of the three ISRE consensus sites resulted in no binding. Taken altogether, the lack of IRF4-*CD38* binding at the element 2 inverted IRF4 site as determined by the targeted ChIP work presented here, and the lack of binding demonstrated by ChIP sequencing (section 3.3.3) at the latterly identified sequence of three adjacent ISRE sites on the reverse strand, suggest that binding by IRF4 alone, or in conjunction with IRF family members IRF8 or IRF2, is either very weak or absent, at *CD38*.

Statistically significant binding at the 5'UTR site was observed in SU-DHL-6 and MEC-1. In both cases, the degree of binding, as determined by the amount of

chromatin enrichment achieved by the IRF4 antibody, was less at the 5'UTR than at the element 1 site. Average chromatin enrichment at the element 1 site in SU-DHL-6 was 37 fold but only approximately 6 fold at the 5'UTR site. In MEC-1 cells, average chromatin enrichment was 9 fold at the element 1 site compared to only 3 fold at the 5'UTR site. This suggests that IRF4 binding occurs more readily at the element 1 site in intron 1 than in the 5'UTR site in these two cell lines despite the presence of an EICE site at both locations. It may be that other elements of the surrounding DNA sequence at these sites are stimulatory or inhibitory to ETS-IRF4 binding. Of note, an additional ETS binding sequence, 5'-GGAA-3' is seen just 6 bases upstream of the EICE site at element 1, and a further three ETS binding sequences are found within 200 bases downstream of the EICE site. (Figure 3.15B) This is not the case for the EICE site in the 5'UTR: a further ETS binding site is found 28 base pairs upstream of the 5'UTR EICE site but there are no additional ETS sites immediately downstream.

In addition to IRF8 and the ETS family proteins, a number of other potential binding partners for IRF4 also exist. E47, an E box protein, binds the Ig κ 3' enhancer with IRF4, at an E-box protein binding site, 5'-CATCTG-3' immediately 5' of an IRF4 binding site. (Nagulapalli and Atchison, 1998) Whilst E box proteins are expressed in human lymphocytes (de Pooter and Kee, 2010), interrogation of the *CD38* first intronic region, 5'UTR and upstream flanking sequence does not reveal any putative E47-IRF4 binding sites. In fact, no potential E47-IRF4 binding sites were identified in the whole *CD38* gene.

Taken together, these data indicate that IRF4 binding occurs at an EICE site in intron 1 of *CD38* in SU-DHL-6 and MEC-1 cells, but not in TK6 cells. The expression of ETS family member PU.1 in SU-DHL-6 and MEC-1 cells but not in TK6, supports the model that IRF4 binds at this site as a heterodimer with PU.1. In addition, the absence of IRF4-*CD38* binding at element 2 where there is an inverted IRF4 site but no EICE site, is also supportive of the model that IRF4 interacts with *CD38* as a heterodimer with an ETS family binding partner, rather than binding alone. IRF4-*CD38* binding also occurs at a further EICE site in the 5'UTR of the *CD38* gene in SU-DHL-6 and MEC-1 cells, though to a lesser extent than at the element 1 site. It is unknown why the degree of binding should differ between these two EICE sites though it could be speculated that this

reflects differences in the surrounding sequence at these sites in the *CD38* gene. Notably, unpublished ChIP sequencing data (section 3.3.3) showed no evidence of IRF4-*CD38* binding in the OCI-LY3 and OCI-LY10 lymphoma lines at the 5'UTR. There is some suggestion of binding at this site in TK6 but this is not statistically significant and may reflect difficulties in data interpretation due to ChIP inter-assay variability (discussed further in section 3.4.2). The data presented in this chapter do not establish whether the alternative ETS protein SPI-B is involved in binding with IRF4 to *CD38*, as its expression is undetermined in any of the cell lines.

3.4.2 Technical issues in the interpretation of ChIP data

A number of issues in the establishment of ChIP and interpretation of ChIP data were encountered in this chapter.

3.4.2.a Excessive non-specific antibody-chromatin binding

When ChIP was first attempted with the IRF4 antibody in TK6 cells (section 3.3.1d), it was noted that there was an excess of non-specific chromatin-binding by the IgG control antibody, as evidenced by a greater enrichment of the chromatin by the IgG control antibody than by the IRF4 antibody. (Figure 3.7A) Inspection of the PCR data resulting from this first experiment showed that the Ct values generated by amplification of chromatin fragments bound by the IgG control antibody ranged from 24 to 29 across the binding sites. One would expect that the IgG control antibody should bind only at a very low level to chromatin fragments, leading to late amplification of chromatin fragments by PCR and thus a Ct value of 30 or more. In contrast, earlier Ct values less than 30 may indicate an excess of non-specific antibody-chromatin interactions. Excessive non-specific binding may occur because of an excess of antibody, or the use of chromatin fragments of inadequate quality, or a failure to completely disrupt these non-specific interactions due to inadequate washing steps after the immunoprecipitation stage. Reducing the concentration of the antibody from 2µg to 1µg in this case (Figure 3.7B), improved the non-specific control antibody binding somewhat, with Ct values of 29 to 35 generated at the PCR stage from fragments bound by the control antibody in the repeat experiment.

Excessive non-specific antibody-chromatin binding should be avoided as it may lead to uninterpretable or invalid data. Specifically, excessive non-specific binding by the control antibody may lead to an under-estimation of true binding by the antibody of interest (IRF4 in this case) because the IRF4 ChIP data are normalised to a falsely high control ChIP result. Conversely, it may also lead to false positive ChIP results if excessive non-specific binding also occurs with the antibody of interest.

To try to avoid confounding of the data by excessive non-specific binding in ChIP experiments in this and future chapters, careful attention was paid to the Ct values generated by the amplification of chromatin immunoprecipitated by the control antibody. Data were disregarded if there was evidence of greater chromatin enrichment by the control antibody than by the ChIP antibody of interest (suggested by Ct values of less than 30 for the control antibody). Chromatin fragment size was evaluated by gel electrophoresis, because inadequate sonication and larger chromatin fragments are associated with increased non-specific antibody binding. The use of the automated ChIP robot in all subsequent ChIP experiments ensured the adequacy and uniformity of washing steps to disrupt non-specific binding.

3.4.2.b Inter-assay variability within cell lines

Substantial inter-assay variability was observed between some of the replicate experiments within each cell line. This contributed to large variance values between the replicates and thus non-significant *p* values, even when all results in the three replicate experiments indicated substantial IRF4 binding over and above that of the control antibody. For example, IRF4 showed statistically significant binding (p=0.039) at the 5'UTR binding site in MEC-1, but not at the element 1 EICE site (p=0.09). This was despite an average 9.4 fold enrichment by the IRF4 antibody at element 1 compared to only a 3.4 fold enrichment at the 5'UTR site. The fold enrichment values by the IRF4 antibody at the element 1 EICE site ranged from 6.6 to 14.8, contributing to a standard deviation of 4.7. In contrast, the fold enrichment values at the 5'UTR ranged only from 2.5 to 4.2 and thus the standard deviation was only 0.85. Thus, despite the average fold enrichment being clearly greater at the element 1 EICE site,

the variability between the three different replicates delivered substantial variance into the statistical analysis, which hence established a non-significant *p* value.

3.5 Summary of chapter 3

A number of putative IRF4 binding sites were identified in the upstream flanking sequence, 5'UTR and first intronic region of the *CD38* gene. These binding sites include EICE sequences (5'-GGAANNGAAA-3') at which IRF4 could be predicted to bind with an Ets family protein (PU.1 or SPI-B); IRF4 consensus sites (5'-AANNGAAA-3') where IRF4 might bind weakly on its own; and ISRE sites (5'-GAAANN-3') where IRF4 can bind alone or with IRF family member, IRF8.

Unpublished ChIP sequencing data from lymphoma cell lines, demonstrated IRF4 binding in the first intronic region of *CD38*, but not in the 5'UTR or upstream flanking sequence, of OCI-LY3 and OCI-LY10 lymphoma cell lines.

Targeted ChIP demonstrated statistically significant binding of IRF4 at an EICE site in the first intron, in SU-DHL-6, and there was the suggestion of binding at this site in MEC-1 cell line. These cell lines express PU.1 but their SPIB expression status is unknown. Binding at this intronic EICE site is absent in TK6 cell line which expresses neither PU.1 nor IRF8. Taken together, these results suggest that PU.1-dependent binding occurs at this site, though the possible role of SPI-B is unknown.

There is no evidence of binding at an inverted IRF4 site in the first intron of *CD38* in SU-DHL-6, MEC-1 or TK6. SU-DHL-6 and MEC-1 express IRF8. This suggests that there is no role for IRF4 binding alone at this site in these cell lines.

Statistically significant IRF4 binding occurred in SU-DHL-6 and MEC-1 cell lines at the 5'UTR site, which also features an EICE binding sequence, though binding here was less strong than at the EICE site in the first intronic region of *CD38*. This may reflect differences in the surrounding gene sequence at these two sites.

Technical issues in performance of ChIP and interpretation of ChIP data were observed, specifically in the occurrence of excessive non-specific protein-antibody binding and in the observation of prominent inter-assay variability.

Chapter 4. Investigation of the relationship between IRF4 and CD38 using *in vitro* B-cell model systems

4.1 Introduction

Having demonstrated in ChIP experiments that IRF4 binds to *CD38* in SU-DHL-6 and MEC-1 cell lines (section 3.3.4.b), the functional relationship between IRF4 and CD38 was then investigated. Specifically, the effect of IRF4 knockdown on CD38 expression was investigated.

IRF4 protein was targeted for knockdown, in order to determine whether this affected surface CD38 expression, as determined by flow cytometry. Two alternative methods of protein knockdown were adopted, both using RNA interference (RNAi) techniques. (Section 4.1.2)

In addition, ChIP studies were performed to address the effect of RNAi-mediated IRF4 knockdown on IRF4-*CD38* binding, and to look for evidence of an effect on *CD38* transactivation, by performing ChIP with antibodies to histone methylation marks.

4.1.1 The function of IRF4 as a transcription factor

Reporter constructs have been used to determine the functional activity of IRF4 when it binds to its target sequences. IRF4 has the capacity to both transactivate and repress target genes. Specifically, binding the 3' enhancer element of the kappa light chain (κE3') sequence as part of a heterodimer with PU.1, IRF4 was shown to act as a transactivator, and there was a close correlation between binding and transcriptional activity in a downstream CAT (chloramphenicol acetyl-transferase) reporter construct. (Pongubala et al., 1992) IRF4 was unable to transactivate the enhancer on its own. However, there was evidence that IRF4 was not just a silent partner in this functional activity: when the IRF4 binding site was disrupted allowing only PU.1 to bind the light chain sequence alone, transcriptional activity was significantly reduced compared to when IRF4 and PU.1 acted together. IRF4 also leads to transcriptional activation of the κE3' enhancer element, when it binds with E47, an E box protein. (Nagulapalli and Atchison, 1998) The presence of both proteins was required for enhancer activation.

Eisenbeis *et al* similarly demonstrated mutually dependent activation of a CAT reporter construct when IRF4 and PU.1 bound to the B domain of the immunoglobulin lambda light chain enhancer (EλB) sequence. (Eisenbeis et al., 1995). Notably, the IRF4 binding partner affected the degree of transactivation achieved. At the same site in the λB element, co-expression of SPI-B with IRF4 could drive expression of the same CAT reporter gene, but the effect was not as great as when IRF4 bound the site with PU.1. (Su et al., 1996)

IRF4 acts as a transcriptional activator via a transactivation domain at its carboxyl-terminal (C-terminal). (Brass et al., 1996) This was demonstrated by the fusion of full-length or segmented IRF4 protein, to the DNA binding domain of GAL4 protein, in the presence of PU.1. This fusion protein was used to investigate evidence of transcription of a reporter construct, 5xGAL4.E1BCAT, which comprises five GAL4 binding sites and a downstream *CAT* gene. When the fusion protein containing full length IRF4 was used, it stimulated transcription of the reporter construct six fold more than pG4 alone, which expresses only the DNA-binding domain of GAL4. However, the C-terminal IRF4 segment (amino acids 150-450) was twenty fold more active than pG4 alone. In contrast, the amino terminal (N-terminal) segmented IRF4 (amino acids 1-150) was unable to drive transcription. Furthermore, IRF4 was able to transactivate the reporter construct in the presence of a transcriptionally defective PU.1 protein which lacked its own transactivation domain. Taken together, these results indicated that IRF4 contains an activation domain at its C-terminal.

In contrast, however, IRF4 can also repress gene transcription, acting on its own or with family member, IRF8. IRF4 represses transcriptional activation of the interferon inducible gene, ISG15, when it binds to the interferon stimulated response element (ISRE) with IRF8. (Rosenbauer et al., 1999) Furthermore, both IRF8 and IRF4 were shown individually to repress activation of a luciferase vector that contained the ISRE region of the ISG15 gene. When IRF4 and IRF8 were bound as a heterodimer to the response element, luciferase expression was reduced 150 fold, indicating that IRF4 and IRF8 synergistically repressed expression of the ISG15 gene promoter.

In addition, IRF4 negatively regulates IRF-1-induced gene transactivation. IRF-1 is an α/β interferon-inducible factor of the IRF family. IRF1 was shown to bind to the ISRE site within the B domain of the immunoglobulin lambda light chain enhancer after interferon-stimulation, and could also strongly drive transcription of a downstream *CAT* gene in a reporter construct in NIH-3T3 cells. (Brass et al., 1996) Co-expression of the N-terminal of IRF4 protein however blocked this IRF-1-mediated activation, though the C-terminal portion of IRF4 had no effect. Given that the N-terminal of all IRF family members contains the conserved DNA binding region, this suggests that IRF4 interferes with IRF-1-induced gene transactivation by competitive binding at the ISRE. (Brass et al., 1996). Similarly, Yamagata *et al* demonstrated that IRF4 suppressed IRF1-induced transactivation in a luciferase assay. (Yamagata et al., 1996)

In summary therefore, IRF4 acts as a dichotomous regulator. (Table 4.1) It behaves as a mutually dependent transcriptional activator when it binds as a heterodimer with PU.1 or SPI-B, as a result of an activation domain in its C-terminal region. In contrast, it can repress activation of interferon-inducible genes when it binds with close IRF family member, IRF8, or when it works alone to repress IRF1-induced activation of interferon-responsive genes.

4.1.2 RNA interference techniques

RNA interference techniques (RNAi) can be used to establish both transient and constitutive protein knockdown in cell lines. (Figure 4.1) Specifically, electroporation of short interfering RNA (siRNA) can be used to achieve transient knockdown of mRNA transcript leading to a concomitant drop in protein level. By combining with the RNA-induced silencing complex (RISC), the siRNA anti-sense strand is able to bind to the target complementary sequence in mRNA and target it for degradation, thus preventing translation to protein. siRNA achieves only transient protein knockdown in a cell population, because the siRNA is only effective against the mRNA of the transfected cell and is not passed down to daughter cells.

In contrast, short hairpin RNA (shRNA) offers a method for establishing more sustained protein knockdown. shRNA is introduced in to cells in a vector, packaged in

Target gene	Effect on target gene	Binding partner	Reference
3’ enhancer element of the immunoglobulin kappa light chain (IgGκ3’E)	Activation	PU.1	(Pongubala *et al.*, 1992)
3’ enhancer element of the immunoglobulin kappa light chain (IgGκ3’E)	Activation	E47	(Nagulapalli and Atchison, 1998)
B domain of the immunoglobulin lambda light chain enhancer (EλB)	Activation	PU.1	(Eisenbeis *et al.*, 1995)
B domain of the immunoglobulin lambda light chain enhancer (EλB)	Activation	PU.1 or SPI-B	(Su *et al.*, 1996)
CD20 promoter	Activation	PU.1	(Himmelmann *et al.*, 1997)
B domain of the immunoglobulin lambda light chain enhancer (EλB)	Repression	No binding partner; interfered with IRF1-induced activation	(Brass *et al.*, 1996)
Interferon consensus sequence of a luciferase reporter construct	Repression	No binding partner; interfered with IRF1-induced activation	(Yamagata *et al.*, 1996)
ISG15 (an interferon-inducible gene)	Repression	Alone, or with IRF8	(Rosenbauer *et al.*, 1999)
BCL6	Repression	No binding partner identified	(Saito *et al.*, 2007)

Table 4.1 IRF4 acts as a dichotomous regulator of target genes
IRF4 acts as a dichotomous regulator, with the ability to both activate and repress target genes. It carries an activation domain in its C-terminal region. (Brass *et al.*, 1996)

lentiviral particles and delivered via transduction. The vector is then integrated in to the genome of the target cells from where the shRNA is transcribed. The resulting RNA strand is cleaved to short strands which are combined with the RISC in the same way as siRNA. The complementary mRNA sequence is then targeted for degradation. shRNA permits long-term protein knockdown as the shRNA is passed to daughter cells. However, silencing of shRNA expression in the host cell can lead to re-expression of the protein targeted for knockdown.

4.2 Aims of chapter 4

Given that IRF4 binds to *CD38* in the first intronic region and at the 5'UTR in SU-DHL-6 and MEC-1 cells (section 3.3.4b), the aims of Chapter 4 were to investigate the functional effect of IRF4 binding on CD38 expression in these cell lines. In approaching this aim, it was notable that CD38 expression had been demonstrated to be substantially weaker in MEC-1 cells than in SU-DHL-6 cells (section 3.3.2), and thus any effect of targeted IRF4 knockdown in MEC-1 cells might be expected to have only a minimal effect on CD38 expression, compared to SU-DHL-6.

Whilst there was no significant evidence of IRF4-*CD38* binding in TK6 cells (section3.3.4.b), TK6 cells were included alongside SU-DHL-6 and MEC-1, in order to establish the RNAi techniques, and to act as a useful negative control.

Specifically, the experimental aims of this chapter were as follows:

- To use RNA interference techniques to attempt to establish IRF4 knockdown in TK6, MEC-1 and SU-DHL-6 cell lines.
- To analyse the effect of IRF4 knockdown on the expression of CD38 protein, as determined by flow cytometry analysis.
- To demonstrate the effect of IRF4 knockdown on IRF4-*CD38* binding, by ChIP
- To demonstrate the effect of IRF4 knockdown on *CD38* transcriptional activity, as determined by ChIP using histone methylation marks

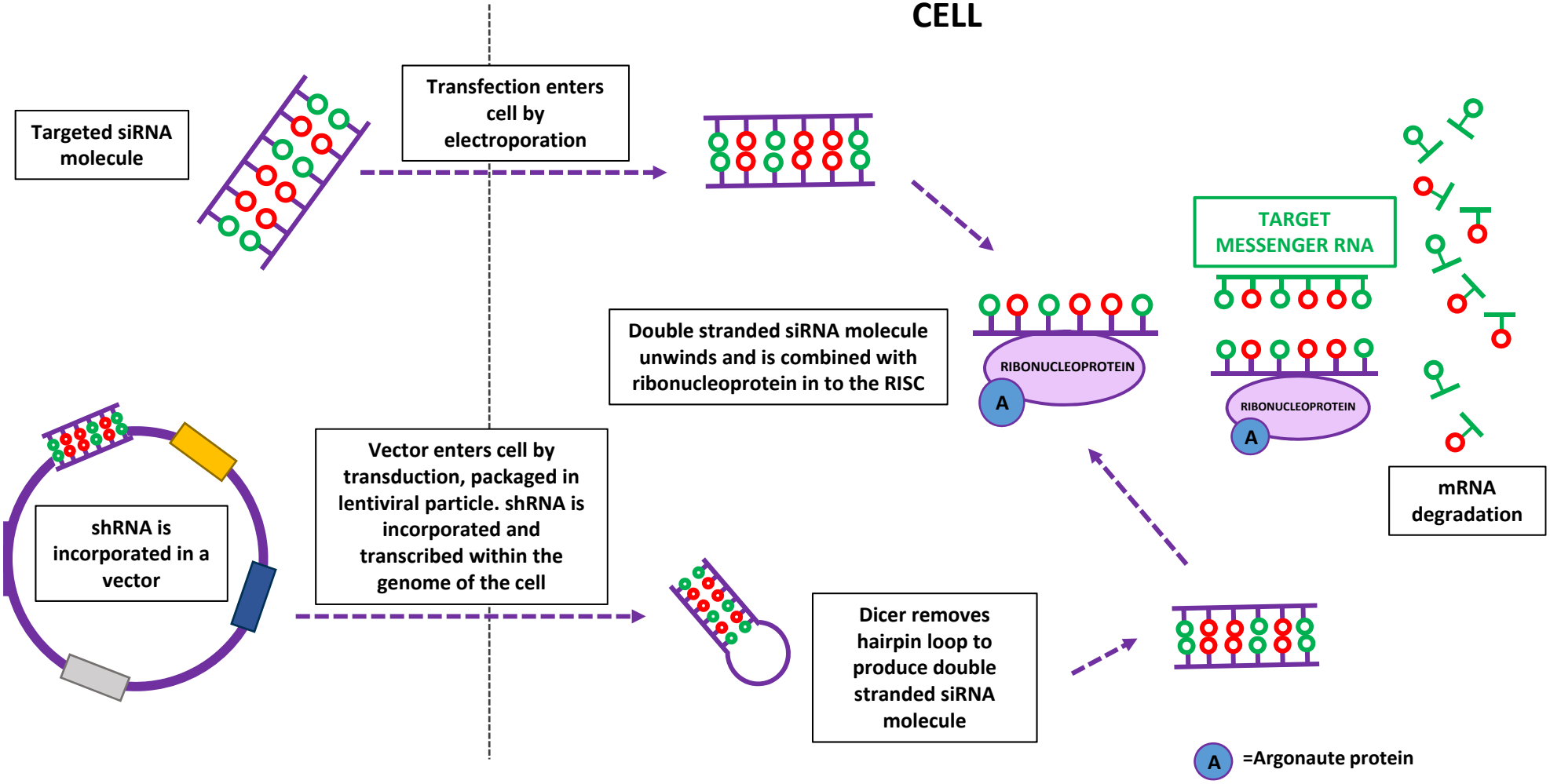

Figure 4.1 Protein knockdown by RNA interference (RNAi) using short interfering (siRNA) and short hairpin (shRNA) constructs

Targeted siRNA or shRNA constructs can be used to target specific mRNA sequences for degradation, leading to reduced protein expression. Double stranded siRNA constructs are transfected into the cell by electroporation. After unwinding, single strand target siRNA construct then combines with ribonucleoprotein in the activated multiprotein RNA-induced silencing complex (RISC). This complex recognises the target mRNA sequence, and the RISC Argonaute protein cleaves the mRNA. shRNA enters the cell packaged within a plasmid vector, in lentiviral particles. The shRNA is incorporated and transcribed within the cell's genome, and thus is passed down to daughter cells producing constitutive protein knockdown. Dicer removes the hairpin loop from the shRNA to produce a double stranded siRNA molecule which separates and combines with RISC to cleave targeted mRNA sequence.

4.3 Results

4.3.1 siRNA-mediated knockdown of IRF4 in TK6 cell line

Knockdown by siRNA was first established in TK6 cells. Naked siRNA was transfected in to the cell lines by electroporation using a combination of two different siRNA molecules (designated "Combination siRNA" hereafter). These siRNAs target regions of the IRF4 transcript within exon 7 and exon 9. (Table 2.4) Using the Combination siRNA at 500nM concentration, knockdown of IRF4 protein was clearly evident on western immunoblotting at 24 hour and 48 hours after a single transfection (Figure 4.2A), compared to control samples which underwent simultaneous transfection with an off target siRNA, or electroporation only. The degree of knockdown was quantified by densitometry normalised to the loading control, and compared to the result obtained with the off-target control. This indicated IRF4 knockdown of nearly 75%, 24 hours after a single electroporation. Expression of IRF4 protein had begun to return to original levels by 72 hours after a single electroporation (data not shown), and this was also the case when cells were subjected to two transfection events, 24 hours apart. (Figure 4.2B) Knockdown was not observed when cells were collected 6 hours after electroporation (data not shown).

In order to determine whether a greater knockdown could be achieved with a higher concentration of siRNA, transfection was repeated using 1μM Combination siRNA in a single transfection. There was no improvement compared to the knockdown achieved with 500nM siRNA concentration (Figure 4.3) which was therefore used in all subsequent experiments.

4.3.1.a Flow cytometry analysis of CD38 expression in TK6 cells with siRNA-mediated transient IRF4 knockdown

In order to determine whether transient knockdown of IRF4 protein was associated with a change in CD38 expression in TK6, the cells were assessed by flow cytometry at time points up to 48 hours after electroporation. CD38 expression was unaffected by transient IRF4 knockdown in TK6 cells, at 6 hours (data not shown), 24 hours and 48 hours after transfection. (Figure 4.4 and Table 4.2)

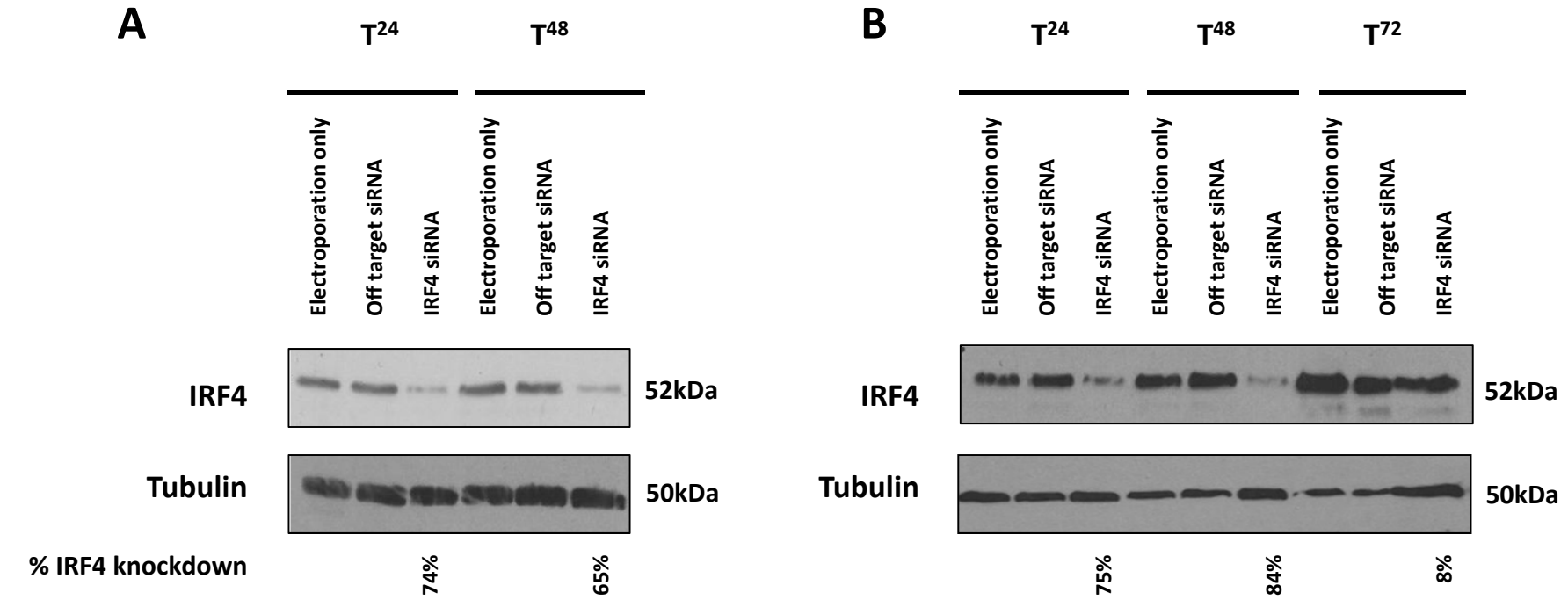

Figure 4.2 IRF4 protein knockdown in TK6 using Combination siRNA

A. After a single electroporation with Combination siRNA targeting the IRF4 transcript, cells were collected at 24 and 48 hours (T^{24} and T^{48}), and the whole cell extracts were analysed by western immunoblotting. Knockdown of IRF4 protein was apparent at both time points, in contrast to the two control samples which underwent electroporation only, or electroporation with an off target siRNA. Nearly 75% IRF4 knockdown was achieved at T^{24}, as demonstrated by densitometry. By T^{48}, IRF4 expression was beginning to return to normal levels (65% knockdown by densitometry).

B. In a separate experiment, cells underwent two electroporations, 24 hours apart, to see if a more durable knockdown could be achieved. 24 hours after the first electroporation, a sample of cells were collected for analysis by western immunoblotting (T^{24}). Consistent with the first experiment, these demonstrated 75% knockdown. The remaining cells were subjected to a second electroporation, and then collected for analysis 24 and 48 hours later (T^{48} and T^{72} time points). Despite this double electroporation, IRF4 protein expression was returning to original levels by 72 hours after the initial siRNA treatment (less than 50% knockdown demonstrated by densitometry).

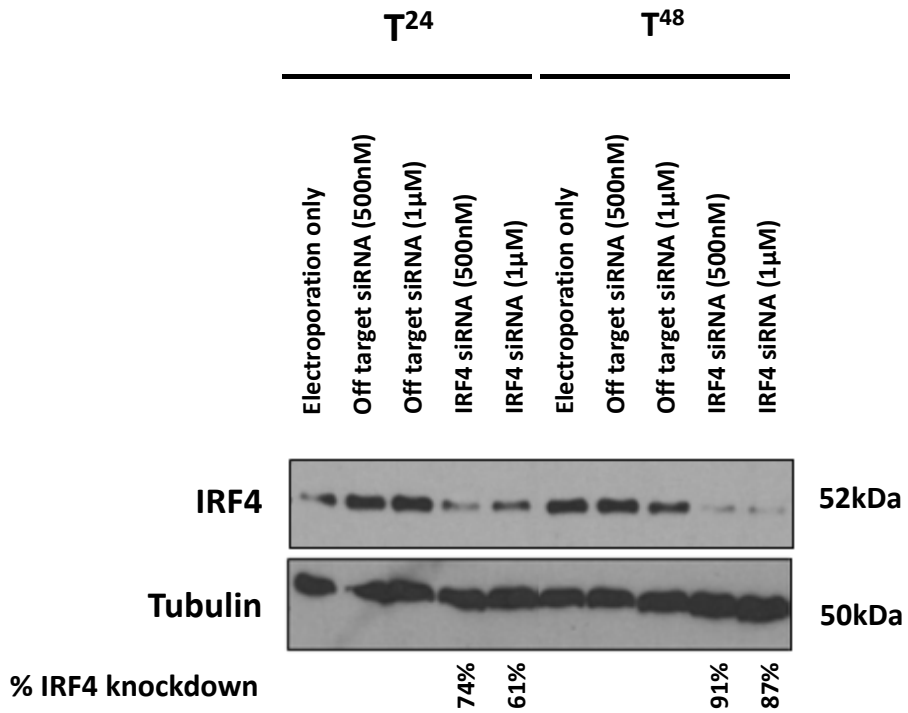

Figure 4.3 Comparing IRF4 knockdown achieved in TK6 cells using 500nM or 1µM concentration Combination siRNA
In order to ensure that the best possible IRF4 protein knockdown was being achieved, transfection with the standard concentration (500nM) of siRNA was compared with the knockdown achieved after transfection with double this concentration (1µM). IRF4 protein expression was determined at 24 and 48 hours post-electroporation and quantified by densitometry. At T^{24}, knockdown of 74% and 61% was achieved with 500nM and 1µM siRNA concentrations respectively. At T^{48}, knockdown was 91% and 87% with the two siRNA concentrations. Standard concentration (500nM) Combination siRNA was therefore used in subsequent experiments.

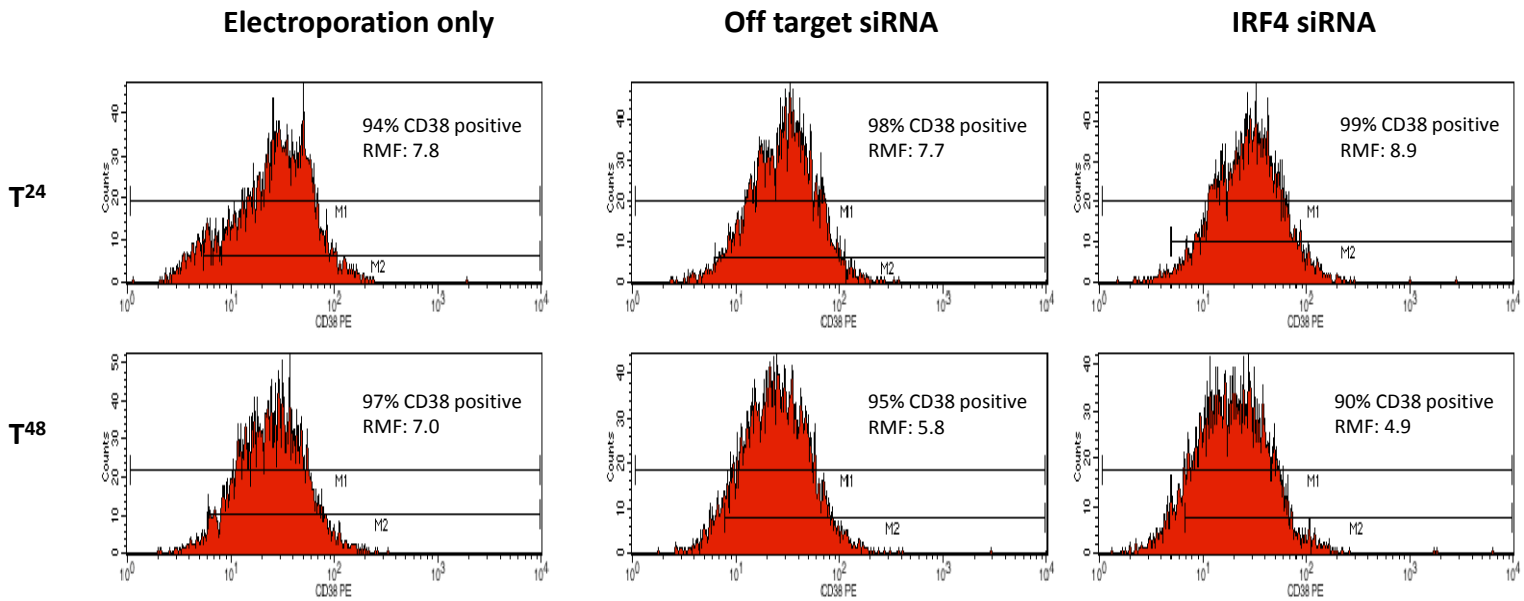

Figure 4.4 CD38 expression in TK6 cells with transient siRNA-mediated IRF4 knockdown

TK6 cells which had been subjected to electroporation only, transfection with an off target control siRNA, or transfection with Combination siRNA targeted against *IRF4* transcript, were analysed by flow cytometry to investigate CD38 surface expression. Cells were incubated with a PE-conjugated CD38 antibody, and the percentage of CD38 positive cells (captured in the M2 marker bar) and the relative mean fluorescence (RMF) of the cells (determined in cells captured in the M1 marker bar) were determined in comparison to isotype-labelled cells (isotype-labelled cell data is not shown). Flow cytometry was performed 6 hours (data not shown), 24 hours (T^{24}) and 48 hours (T^{48}) after a single electroporation. These data did not indicate an effect of siRNA-mediated IRF4 knockdown on CD38 expression in TK6 cells, 24 or 48 hours after electroporation.

Time point	Sample	CD38 % positivity	Geometric mean fluorescence	Relative mean fluorescence (RMF)
T^{6}	Electroporation only	98	46.2	8.6
	Off target siRNA	99	46.9	11.2
	IRF4	99	47.8	9.6
T^{24}	Electroporation only	94	25.4	7.8
	Off target siRNA	98	28.4	7.7
	IRF4	99	26.6	8.9
T^{48}	Electroporation only	97	23.9	7.0
	Off target siRNA	95	23.4	5.8
	IRF4	90	18.8	4.9

Table 4.2 Flow cytometry histogram statistics demonstrating CD38 expression in TK6 cells with transient siRNA-mediated IRF4 knockdown

TK6 cells which had been subjected to electroporation only, transfection with an off target control siRNA, or transfection with Combination siRNA targeted against *IRF4* transcript, were analysed by flow cytometry to investigate CD38 surface expression. Statistics gleaned from the flow cytometry histogram plots of TK6 cells labelled with PE conjugated CD38 antibody (Figure 4.4) are demonstrated, and indicate the percentage CD38 positivity, geometric mean fluorescence and relative mean fluorescence (RMF) of cells. At three time points after transfection, no substantial differences were seen between the CD38 status of cells with siRNA-mediated IRF4 knockdown, compared to those subjected to electroporation only or transfection with an off target siRNA.

4.3.2 siRNA-mediated knockdown of IRF4 in MEC-1 cell line

Using a single electroporation with Combination siRNA targeted against IRF4, IRF4 knockdown was achieved in MEC-1 cells in four independent experiments. (Figure 4.5) Knockdown ranging from 40-67% was demonstrated 24 hours after electroporation, across the four experiments. Notably, there was a considerable degree of inter-experimental variation in the knockdown achieved at 48 and 72 hours after a single electroporation. At T48, knockdown ranging from 45-92% was observed. Similarly, at T72, knockdown ranged from 0-98%. IRF4 expression was beginning to return to original levels by 96 hours in the experiments that included this time point (range of knockdown, 17%-33%).

Cells generated from two of these four knockdown experiments (Figure 4.5A, and replicate, not shown) were used to assess the effect of transient IRF4 knockdown on CD38 expression. (Section 4.3.2.a)

In addition, MEC-1 cells with transient siRNA-induced IRF4 knockdown were also used to investigate the effect of IRF4 knockdown on MEC-1 cell growth, and growth inhibition by therapeutic agents, fludarabine and ibrutinib. (Chapter 5)

4.3.2.a Flow cytometry analysis of CD38 expression in MEC-1 cells with siRNA-mediated transient IRF4 knockdown

CD38 surface expression was determined in MEC-1 cells with transient IRF4 knockdown. The flow cytometry analysis was performed in duplicate, using cells from two independent siRNA experiments. Representative data from cells obtained from one of these flow cytometry experiments is shown, and specifically, the flow cytometry data presented pertain to the siRNA experiment in which the greatest IRF4 knockdown was achieved. IRF4 knockdown of 51% and 92% was achieved at T24 and T48 respectively, in these cells. (Figure 4.5A)

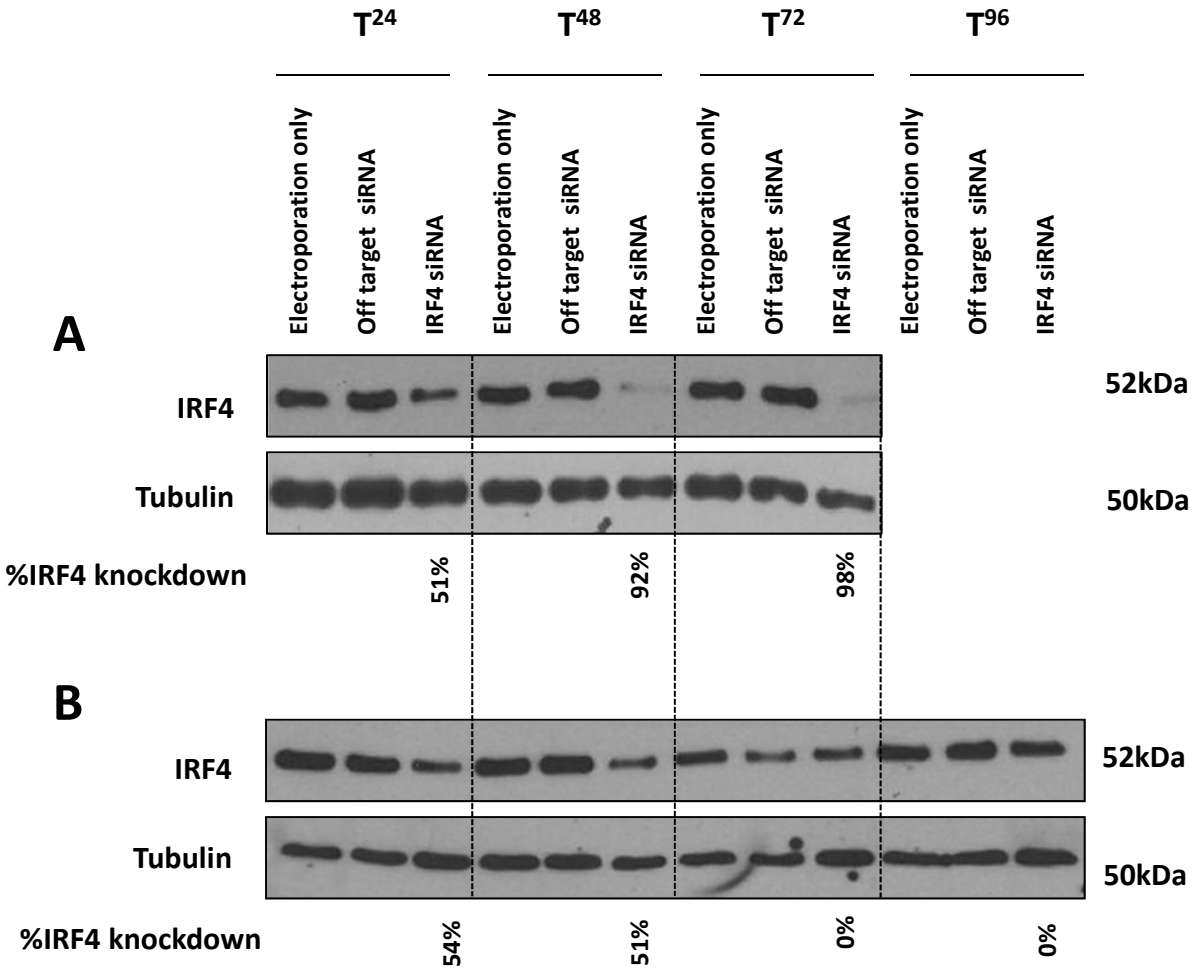

Figure 4.5 IRF4 protein knockdown in MEC-1 using IRF4 Combination siRNA
In 4 independent experiments, MEC-1 cells were transfected with IRF4 Combination siRNA, off target control siRNA, or they underwent electroporation alone. Two representative experiments are shown, indicating the range of knockdown achieved across the 4 replicates.
A. In this example, densitometry demonstrated IRF4 knockdown of 51%, 92% and 98% at T^{24}, T^{48} and T^{72} respectively.
B. In this replicate, densitometry similarly demonstrated 54% knockdown at T^{24}. However, less substantial knockdown was achieved at later time points than in the experiment demonstrated in **A**. At T^{48}, knockdown of only 51% was demonstrated. 0% knockdown was observed at T^{72} in this replicate.

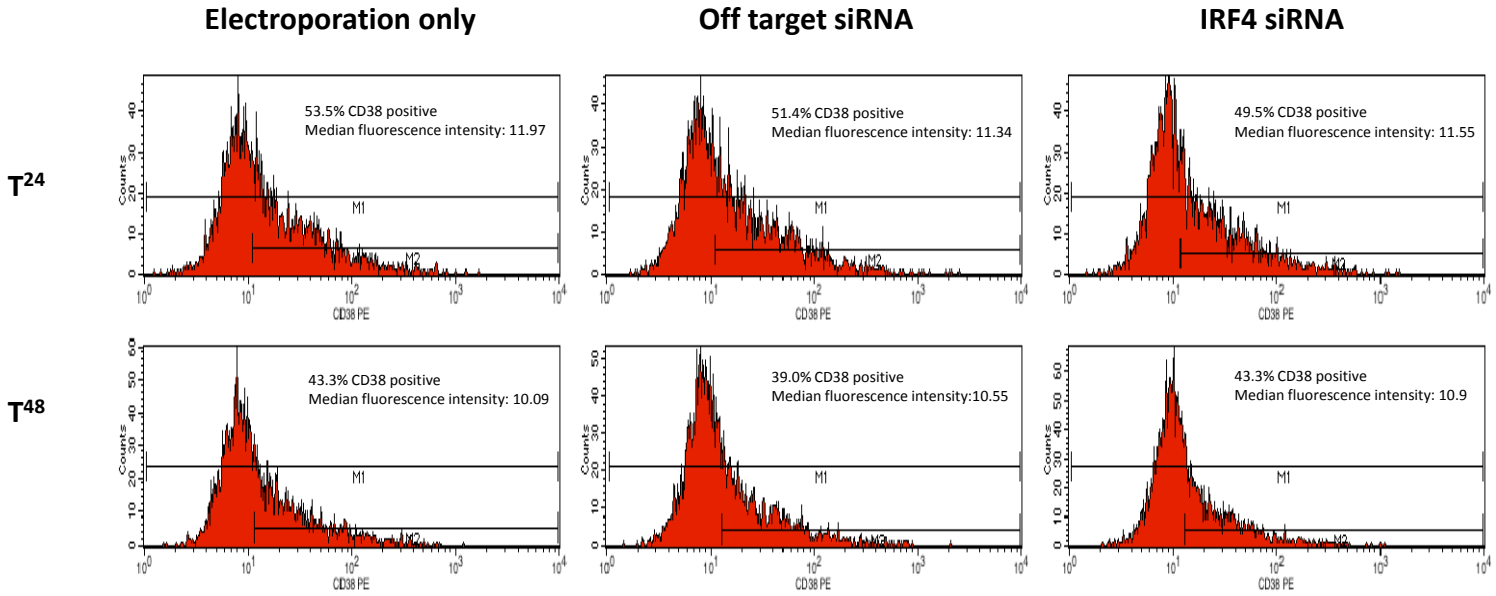

Figure 4.6 CD38 expression in MEC-1 cells with siRNA-mediated transient IRF4 knockdown

MEC-1 cells which had been subjected to electroporation only, transfection with an off target control siRNA, or transfection with Combination siRNA targeted against IRF4 transcript, were analysed by flow cytometry to investigate CD38 surface expression. Cells were incubated with a PE-conjugated CD38 antibody, and the percentage of CD38 positive cells and fluorescence of the cells was determined in comparison to isotype-labelled cells (isotype-labelled cell data is not shown). Cells were analysed at 24 or 48 hours (T^{24} and T^{48}) post-transfection. This experiment was performed using cells from two independent siRNA replicate experiments, and representative data from one of these experiments (Figure 4.5A) is shown. IRF4 knockdown of 51% and 92% at T^{24} and T^{48} had been achieved in the MEC-1 cells, in this experiment (determined by western immunoblotting and densitometry). Histogram plots demonstrated that siRNA-mediated IRF4 knockdown had no effect on CD38 expression at 24 or 48 hours after electroporation. Notably, however, a non-normal distribution is observed in the CD38-labelled MEC-1 cells and the median fluorescence intensity is therefore indicated alongside the CD38 % positivity.

Time point	Sample	CD38 % positivity	Geometric mean fluorescence	Relative mean fluorescence (RMF)	Median fluorescence
T^{24}	Electroporation only	53.51	15.58	2.31	11.97
	Off target siRNA	51.42	15.10	2.28	11.34
	IRF4	49.53	15.28	2.08	11.55
T^{48}	Electroporation only	43.26	13.10	1.88	10.09
	Off target siRNA	39.02	13.51	1.73	10.55
	IRF4	38.95	13.56	1.81	10.94

Table 4.3 Flow cytometry histogram statistics demonstrating CD38 expression in MEC-1 cells with transient siRNA-mediated IRF4 knockdown

MEC-1 cells which had been subjected to electroporation only, transfection with an off target control siRNA, or transfection with Combination siRNA targeted against *IRF4* transcript, were analysed by flow cytometry to investigate CD38 surface expression. Statistics gleaned from histogram plots of MEC-1 cells labelled with PE conjugated CD38 antibody (Figure 4.6) are demonstrated, and indicate the percentage CD38 positivity, geometric mean fluorescence and relative mean fluorescence (RMF) intensity of cells. No significant differences were observed in terms of percentage of CD38 positive cells or relative mean fluorescence of cells with IRF4 knockdown, compared to the two control cell populations, at either time point. Given the non-normal distribution of the MEC-1 cells labelled with CD38 antibody, the median fluorescence intensity is indicated alongside the mean and relative mean fluorescence data.

There was no evidence of any impact on CD38 expression following siRNA-mediated IRF4 knockdown in MEC-1 cells, at either of these time points after electroporation. (Figure 4.6 and Table 4.3) Similarly, CD38 expression remained unchanged 72 hours after electroporation (data not shown).

4.3.3 siRNA-mediated knockdown of IRF4 in DHL6 cell line

IRF4 knockdown was achieved in SU-DHL-6 cells after a single siRNA transfection event. Mean knockdown of 68% (range 42-81%) was seen 24 hours after electroporation in four independent experiments and two representative experiments are shown. (Figure 4.7) Western immunoblotting of cells taken 6 hours after electroporation did not demonstrate evidence of IRF4 knockdown. (Figure 4.7B)

Cells generated in one of these four siRNA experiments were used to assess the effect of transient IRF4 knockdown on CD38 expression in SU-DHL-6 using flow cytometry analysis. (Section 4.3.3.a)

The effect of IRF4 knockdown on SU-DHL-6 growth, and on growth inhibition by fludarabine, was also assessed in the SU-DHL-6 cells generated in these experiments. (Chapter 5)

4.3.3.a Flow cytometry analysis of CD38 expression in SU-DHL-6 cells with siRNA-mediated transient IRF4 knockdown

SU-DHL-6 cells with transient IRF4 knockdown were analysed by flow cytometry to investigate any effect on CD38 surface expression. These cells demonstrated IRF4 knockdown of 42% and 68% at T24 and T48, respectively. There was no effect on the percentage CD38 positivity of cells with IRF4 knockdown, and the geometric mean fluorescence detected remained unchanged. However, there was evidence of a very modest reduction in the CD38 relative mean fluorescence detected in SU-DHL-6 cells with siRNA mediated IRF4 knockdown in comparison to cells transfected with an off target siRNA or exposed to electroporation only. (Figure 4.8 and Table 4.4) This was more apparent at T24, but at T48 the effect was less apparent. Twenty four hours after electroporation, the relative mean fluorescence of CD38 expression on cells with IRF4

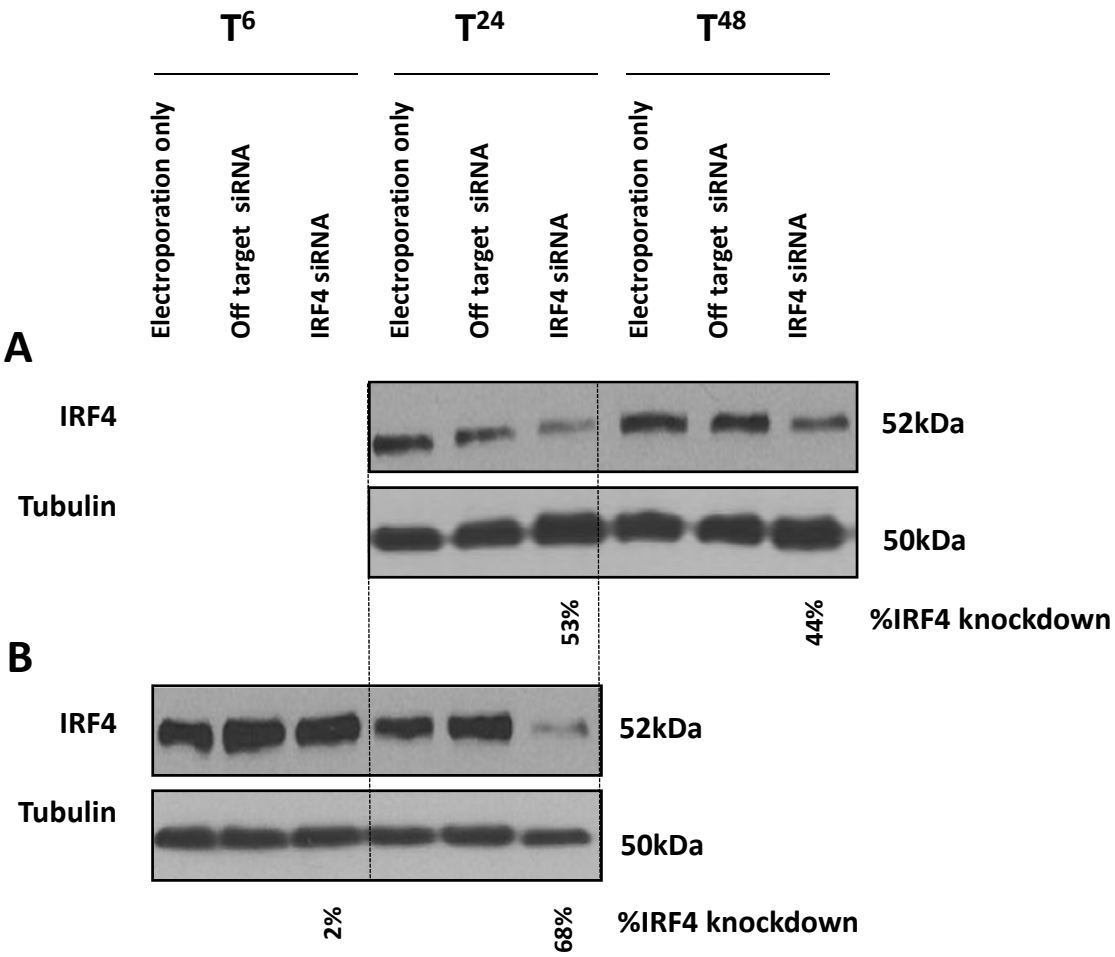

Figure 4.7 Transient siRNA-mediated IRF4 knockdown in SU-DHL-6 cells
SU-DHL-6 cells transfected with Combination siRNA targeted against IRF4, an off target control siRNA, or subjected to electroporation only, were collected at the indicated time points after electroporation and analysed by western immunoblotting. Four independent replicate experiments were performed, and two representative replicates are shown.
A. Knockdown was apparent at T^{24} and modest knockdown remained at T^{48}. Densitometry was used to quantify this, and 53% and 44% knockdown was observed at these time points respectively.
B. In a separate experiment, cells were collected at the earlier time point of 6 hours (T^{6}) to see if any knockdown was apparent at this point. Densitometry confirmed that knockdown was not achieved at this earlier time point. There was again knockdown observed at T^{24} however, of 68%.

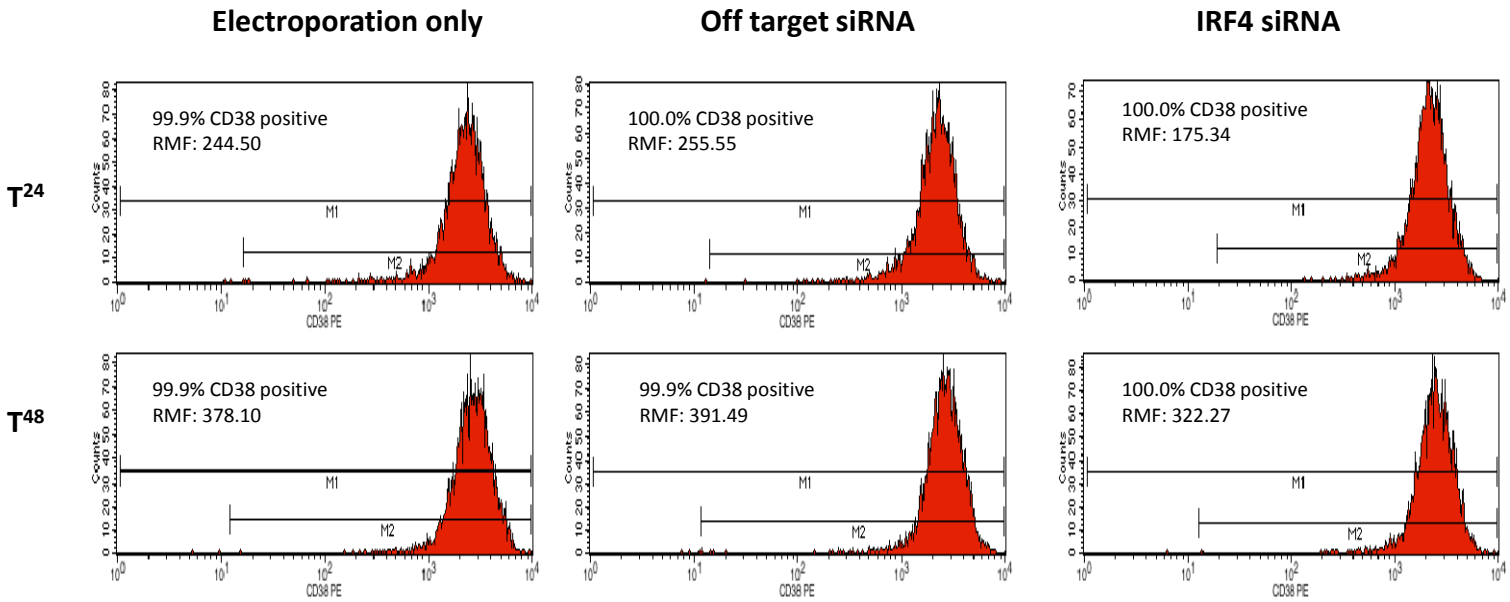

Figure 4.8 CD38 expression in SU-DHL-6 cells with transient siRNA-mediated IRF4 knockdown

SU-DHL-6 cells which had been subjected to electroporation only, transfection with an off target control siRNA, or transfection with Combination siRNA targeted against *IRF4* transcript, were analysed by flow cytometry to investigate CD38 surface expression. Cells were incubated with a PE-conjugated CD38 antibody, and the percentage of CD38 positive cells and relative mean fluorescence (RMF) of the cells were determined in comparison to isotype-labelled cells (isotype-labelled cell data is not shown). Flow cytometry was performed 24 hours (T^{24}) and 48 hours (T^{48}) after electroporation, at which time points, 42% and 68% IRF4 knockdown had been achieved, respectively (determined by western immunoblotting and densitometry). While there is no change in the CD38 percentage positivity of the SU-DHL-6 cells after siRNA-mediated IRF4 knockdown, there is the suggestion of a downregulation of CD38 expression. This was evidenced by a modest reduction in the relative mean fluorescence of CD38 positivity in cells with IRF4 knockdown at both time points.

Time point	Sample	CD38 % positivity	Geometric mean fluorescence	Relative mean fluorescence (RMF)
T^{24}	Electroporation only	99.92	2139.8	244.50
	Off target siRNA	99.96	2086.38	255.55
	IRF4	99.98	2074.16	175.34
T^{48}	Electroporation only	99.92	2552.30	378.10
	Off target siRNA	99.92	2710.95	391.49
	IRF4	99.96	2521.11	322.27

Table 4.4 Flow cytometry histogram statistics demonstrating CD38 expression in SU-DHL-6 cells with transient siRNA-mediated IRF4 knockdown
SU-DHL-6 cells which had been subjected to electroporation only, transfection with an off target control siRNA, or transfection with Combination siRNA targeted against IRF4 transcript, were analysed by flow cytometry to investigate CD38 surface expression. Statistics gleaned from histogram plots of these cells labelled with PE conjugated CD38 antibody (Figure 4.8) are demonstrated, and indicate the percentage CD38 positivity, geometric mean fluorescence and relative mean fluorescence (RMF) intensity of cells. There was no effect on the percentage CD38 positivity of cells with IRF4 knockdown, and the geometric mean fluorescence detected remained unchanged. However, there was evidence of a modest reduction in the CD38 relative mean fluorescence detected in SU-DHL-6 cells with siRNA-mediated IRF4 knockdown in comparison to cells transfected with an off target siRNA or exposed to electroporation only. This was more apparent at T^{24}, but at T^{48} the effect was less apparent. At these two time points, IRF4 knockdown of 42% and 68% respectively had been achieved.

knockdown was 175.34 compared to 244.50 and 255.55 in the electroporation only and off target control siRNA cells, respectively. At T48, relative mean fluorescence of 322.27 was detected in cells with knockdown, compared to 378.10 and 391.49 in the two control cell populations

4.3.4 shRNA-mediated knockdown of IRF4 in TK6 cell line

4.3.4.a TK6 cell populations generated with constitutive IRF4 knockdown, by shRNA transduction

TK6 cells were transduced with viral particles each carrying one of six different shRNA expression constructs (constructs 1-6) targeted against IRF4 transcript (Table 2.5), or with one of two control shRNA constructs (an empty vector and an off-target shRNA construct). A multiplicity of infection (MOI) of two was used. (Section 2.5.6) The shRNA expression vector contained a puromycin-resistance cassette. After expanding the cell populations in puromycin-containing selection media, the cells were analysed by western immunoblotting in order to determine which cell populations showed greatest evidence of IRF4 protein knockdown. (Figure 4.9) A modest reduction in IRF4 protein expression was demonstrated in TK6 cells transduced with shRNA construct 6.

4.3.4.b TK6 cell clones generated with uniform IRF4 knockdown

Transduced cell populations are predicted to be heterogeneous with respect to IRF4 protein knockdown, as there will inevitably be variation in the number of shRNA integration events per cell, and also differences in promoter activity due to the site of genomic integration. In order to generate cells with less variable levels of IRF4 protein knockdown, TK6 cells transduced with shRNA construct 6 were subsequently cloned in soft agar. Western immunoblotting demonstrated successful generation of cell clones with substantial IRF4 knockdown in the cells cloned from the shRNA construct 6 cell population. (Figure 4.10A) As expected, in some cell clones there was virtually no evidence of IRF4 protein knockdown (clone 2), confirming the heterogenous nature of the original transduced cell population. Cells transduced with the off-target shRNA control construct were also simultaneously cloned via this method, and although there

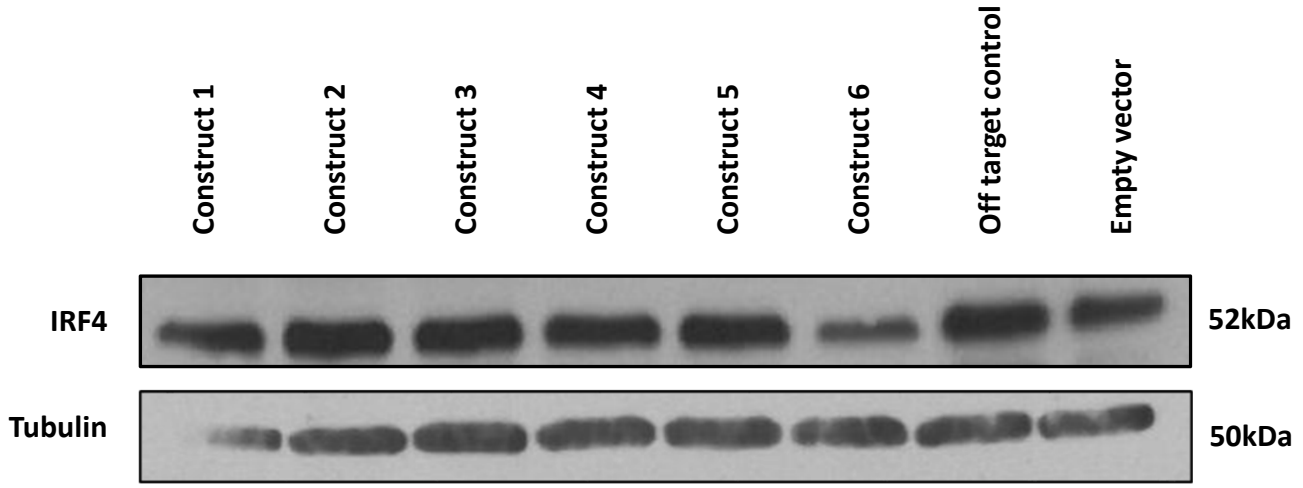

Figure 4.9 TK6 cell populations generated after transduction with shRNA constructs targeted against IRF4
TK6 cells were transduced with six different lentivirally-packaged shRNA constructs targeted against IRF4 transcript (constructs 1-6), or with two control shRNA constructs (an off target shRNA construct and an empty vector) at an MOI (multiplicity of infection) of 2. There was modest evidence of knockdown demonstrated by western immunoblotting in the cell population transduced with shRNA construct 6.

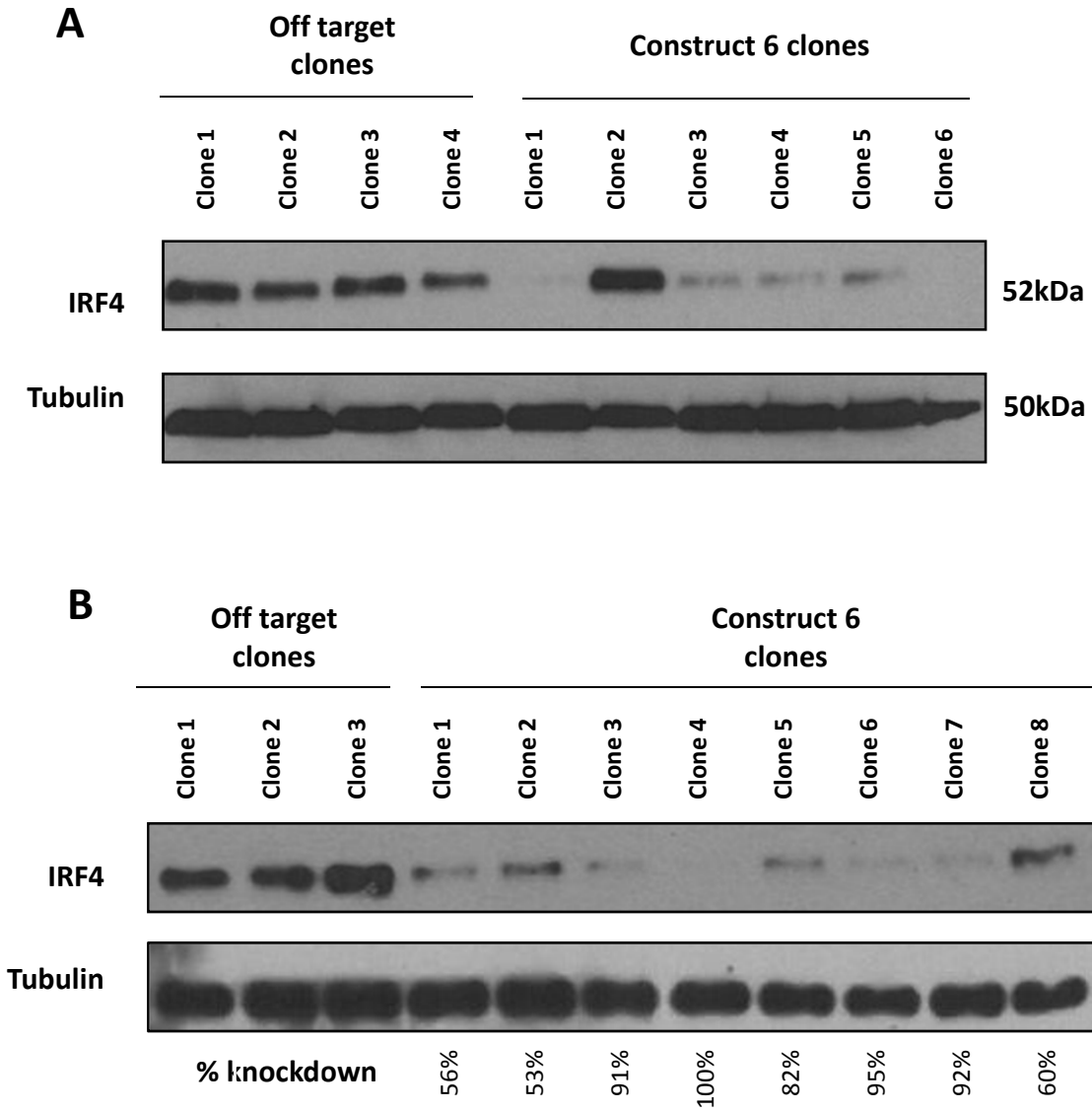

Figure 4.10 TK6 cells cloned from cell populations transduced with off target shRNA or shRNA construct 6, targeted to IRF4

Cell clones were generated on soft agar, from TK6 cell populations transduced with shRNA construct 6, or with off target control shRNA construct. Cell clones were then expanded and cells harvested in order to determine IRF4 expression by western immunoblotting.

A. Four off target control clones all express IRF4 protein strongly. However, all but 1 of the 6 cell clones produced from cells transduced with shRNA construct 6, show evidence of substantial IRF4 protein knockdown.

B. In a replicate experiment, TK6 cells were transduced with construct 6 shRNA or off target control construct, and cell clones were then generated. On this occasion, 9 cell clones with shRNA-induced IRF4 knockdown were generated. IRF4 expression is lowest in construct 6 clones 3,4,6,7 and 9, quantified by densitometry.

was some heterogeneity in IRF4 expression, all resulting off-target clones had relatively high levels of expression compared to the knockdown clones. (Figure 4.10A)

An additional set of cell clones (Figure 4.10B) from a second shRNA transduction procedure were also generated. An MOI of 4 was used in this second transduction experiment, in order to try to achieve even better IRF4 knockdown. Clones 4 and 6 demonstrated greatest evidence of knockdown in this second experiment, and this was quantified as 100 and 95% knockdown, respectively, by densitometry. Densitometry data was generated by normalising signal density of the knockdown clones to the signal obtained with the corresponding loading control, and comparing this to a mean of the off target control signal density. Clones 1 and 2 still retained 50% IRF4 expression.

The clones from this second transduction procedure were expanded and used to determine the effect of constitutive shRNA-mediated IRF4 knockdown on CD38 surface expression. (Section 4.3.4.c)

They were also used to investigate the effect of shRNA-mediated IRF4 knockdown on TK6 cell proliferation, and fludarabine growth inhibition. (Chapter 5)

4.3.4.c CD38 expression by flow cytometry in TK6 cell clones with shRNA-mediated IRF4 knockdown

The TK6 cell clones generated in section 4.3.4.b (Figure 4.10B), were analysed by flow cytometry to determine surface expression of CD38.

There was no evidence of any significant effect of IRF4 protein knockdown on the surface expression of CD38 in TK6 cell clones. (Table 4.5) Specifically, the mean CD38 percentage positivity was 95.1 in IRF4-knockdown clones compared to 97.0 in off-target cell clones (p=0.16; student t-test assuming unequal variance). Likewise, the relative mean fluorescence of IRF4 knockdown clones (7.0, range 5.3-10.9) was not significantly different to that of the off target control cell clones (7.8, range 5.4-10.8) (p=0.54, student t-test assuming unequal variance).

Sample	CD38 % positivity	Geometric mean fluorescence	Relative mean fluorescence (RMF)
OT clone 1	97.8	62.2	7.6
OT clone 2	94.2	42.5	5.4
OT clone 3	99.1	80.5	10.8
All OT clones	97 (±2.07)	61.7 (±15.52)	7.8 (±2.22)
Construct 6 clone 1	94.3	56.8	6.1
Construct 6 clone 2	90.9	84.8	4.6
Construct 6 clone 3	97.6	37.8	10.9
Construct 6 clone 4	94.8	54.9	6.5
Construct 6 clone 5	97.8	67.7	8.1
Construct 6 clone 6	96.5	48.1	6.8
Construct 6 clone 7	92.3	84.8	5.3
Construct 6 clone 8	97.3	35.3	8.3
Construct 6 clone 9	94.4	49.3	6.0
All construct 6 clones	95.1 (±2.29)	57.7 (±17.12)	7.0 (±1.79)

Table 4.5 Flow cytometry histogram statistics demonstrating CD38 expression in TK6 cells with shRNA-induced constitutive IRF4 knockdown

Cell clones derived from cell populations transduced with an off target control shRNA or construct 6 shRNA targeting *IRF4* transcript were analysed by flow cytometry for CD38 surface expression. More than 90% of the cells from all of the clones were positive for CD38. The mean CD38 positivity was 97.0% in the off-target cell clones, and 95.1% in the IRF4 knockdown clones, and this very modest difference was not statistically significant (p=0.16, student t-test assuming unequal variance). No significant difference in the geometric mean fluorescence intensity (GMF) or the relative mean fluorescence (RMF), was seen in any of the construct 6 clones with IRF4 knockdown, compared to the off target control clones. The relative mean fluorescence of the IRF4 knockdown clones was 7.0, in comparison to an RMF of 7.8 in the off-target clones (p=0.54, student t-test assuming unequal variance).

4.3.5 shRNA-mediated knockdown of IRF4 in MEC-1 and SUDHL-6 cell lines

Given the substantial IRF4 knockdown achieved with shRNA construct 6 in TK6 cells, this construct was also used to attempt to achieve constitutive knockdown of IRF4 in MEC-1 and SU-DHL-6 cells. A multiplicity of infection (MOI) of 4 was used.

4.3.5.a MEC-1 shRNA transduction and cell cloning

Modest IRF4 knockdown was seen in MEC-1 cell populations transduced with shRNA construct 6. However, generating MEC-1 cell clones with IRF4 knockdown proved challenging. Two attempts to clone cells from the transduced cell populations on soft agar were unsuccessful and no viable clones were observed. This was performed at a cell density of 10 cells per well in a 12 well plate, suggesting that the cloning efficiency was lower than 0.41% (1 in 240). Cloning by limiting dilution in liquid media in a 96 well plate, using 5 cells per well, was also unsuccessful, suggesting a cloning efficiency of lower than 0.21% (1 in 480). However, cloning was eventually successful when cells were cloned on soft agar at a cell density of 50-100 cells/ml, and this was repeated on two occasions to generate three control vector clones and thirteen construct 6 knockdown clones. An initial assessment of IRF4 protein levels by Western analysis identified considerable inter-clone heterogeneity, including some clones with almost complete knockdown. However, following expansion of the cell clones, protein expression was assessed immediately prior to experimental use in order to confirm maintenance of IRF4 knockdown. IRF4 protein expression had rapidly restored to original levels in all cell clones, making these clones un-useable for subsequent experiments (data not shown.)

4.3.5.b SU-DHL-6 shRNA transduction

An attempt to successfully transduce SU-DHL-6 cells with shRNA to generate cell populations or clones with IRF4 knockdown was unsuccessful. As described previously (sections 2.5.4 and 2.5.5), SU-DHL-6 cells appeared to be highly sensitive both to polybrene (used in the shRNA transduction step, section 2.5.6) and puromycin (used in media for selection of shRNA-transduced cells, section 2.5.7). They were also intolerant of the low cell densities used in the shRNA transduction protocol. No viable

cells were maintained 3 days after transduction, including in the 'blank' control sample (which was treated with polybrene and underwent centrifugation, but was not transduced with an shRNA construct, section 2.5.6).

4.3.6 Effect of siRNA-mediated transient IRF4 knockdown on IRF4-CD38 binding

To further investigate the relationship between IRF4 and *CD38*, ChIP experiments were also performed in MEC-1 and SU-DHL-6 cells, following transient siRNA-mediated IRF4 knockdown. IRF4 has been demonstrated to bind to *CD38* in these two cell lines. (Chapter 3) In addition to ChIP experiments with IRF4 antibody, ChIP was also performed with histone methylation mark antibodies. Specifically, antibodies which bind to trimethylated histone 3 lycine 4 (H3K4me3), and trimethylated histone 3 lycine 9 (H3K9me3) were used as markers for transcriptional activation and repression, respectively.

As described in chapter 3 (section 3.4.2.a), great care was taken in the interpretation and inclusion of ChIP results, in order to avoid any confounding of the data by technical issues. Specifically, attention was paid to evidence of excessive binding by the control antibody. In addition, discrepancies between control antibody binding by chromatin prepared from cells transfected with control siRNA in comparison with chromatin prepared from cells transfected with siRNA targeted against IRF4, were sought, in case this indicated differences in chromatin fragment size and binding capacity.

4.3.6.a ChIP in MEC-1 cells with siRNA-mediated IRF4 knockdown

MEC-1 cells with siRNA-mediated IRF4 knockdown were used to generate chromatin for ChIP with IRF4 and H3K4me3 antibodies, 24 hours and 48 hours after a single siRNA transfection. Cells which had been transfected with either Combination siRNA targeted against *IRF4*, or the off target control siRNA, were investigated simultaneously. The MEC-1 cells which had been transfected with the Combination siRNA showed evidence of moderate IRF4 knockdown by western immunoblotting of 26% and 43%, respectively, at 24 and 48 hours (data not shown).

Twenty four hours after electroporation with control off-target siRNA, ChIP with IRF4 antibody indicated evidence of IRF4 binding at the *CD38* element 1 binding site and 5'UTR binding site. (Figure 4.11A) This was consistent with the findings from previous experiments in wild type MEC-1. (Figure 3.20) In the cells which had been transfected with Combination siRNA targeted against *IRF4*, there was evidence of substantially reduced binding by IRF4 at these two sites. (Figure 4.11A,C)

There was a suggestion of very minimal binding by antibody raised against H3K4me3 to the element 1 and 5'UTR *CD38* regions in the MEC-1 cells transfected with control siRNA construct. Interestingly however, this binding was increased by seventeen fold at the 5'UTR site, in cells with IRF4 knockdown. (Figure 4.11B) H3K4me3 is associated with transcriptional activation of genes. Taken together, these data suggest that IRF4 may be operating as a transcriptional repressor at the 5' UTR site of *CD38* in MEC-1 cells.

Forty eight hours after transfection, there was again evidence of IRF4-*CD38* binding at the element 1 binding site in the control MEC-1 cells, and less binding occurred in cells with siRNA-mediated IRF4 knockdown. (Figure 4.11C) IRF4 binding at the 5'UTR was uninterpretable on this occasion, due to technical issues at this site at the PCR stage of the ChIP procedure. However, the corresponding western immunoblot for this time point confirmed IRF4 knockdown in these cells (data not shown). There was again an increase in binding by H3K4me3 at the 5'UTR *CD38* site in the cells with IRF4 knockdown. (Figure 4.11D)

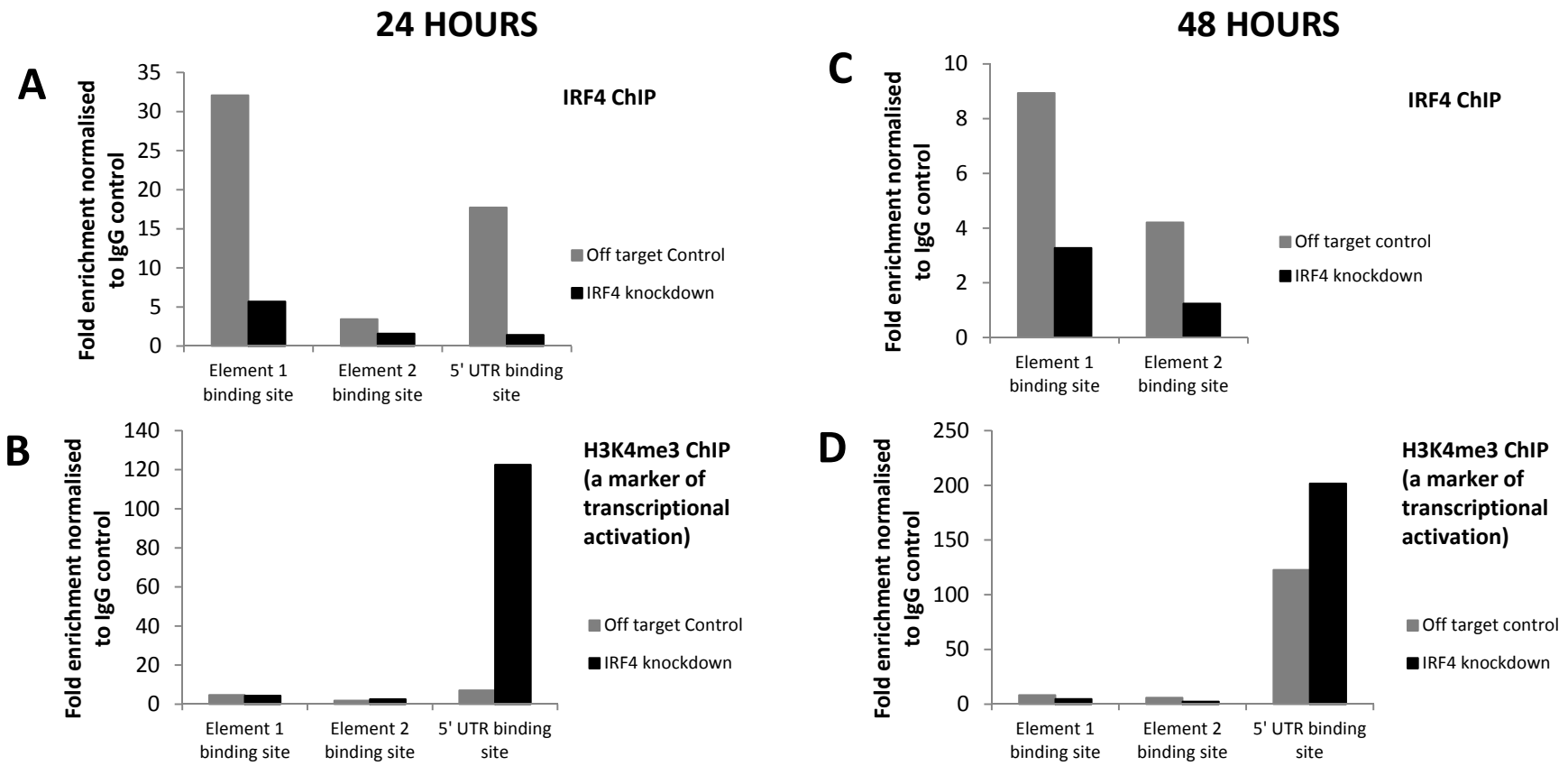

Figure 4.11 ChIP using IRF4 and H3K4me3 antibodies in MEC-1 cells with siRNA-mediated IRF4 knockdown

MEC-1 cells were transfected with either Combination siRNA targeted against *IRF4*, or off target control siRNA. Cells were harvested 24 hours (**A** and **B**) or 48 hours (**C** and **D**) after transfection, and used in ChIP experiments.

A. 24 hours after electroporation, cells transfected with control siRNA demonstrated IRF4-*CD38* binding at the element 1 and 5'UTR binding sites. Less binding occurred at all three sites in cells with transient siRNA-mediated IRF4 knockdown.

B. In the same cells, binding of H3K4me3 at all three sites was negligible in the off target control cells. However, notably, binding at the 5'UTR site was significantly increased in cells with siRNA-mediated IRF4 knockdown. H3K4me3 is associated with transcriptional gene activation.

C. 48 hours after electroporation, evidence of IRF4-*CD38* binding was reduced at element 1 binding site in the MEC-1 cells with IRF4 knockdown. Technical issues rendered binding at the 5'UTR site uninterpretable in this experiment.

D. Notably, binding by H3K4me3 at the 5'UTR site was again significantly increased in cells with siRNA-mediated IRF4 knockdown.

4.3.6.b ChIP in SU-DHL-6 cells with siRNA-mediated IRF4 knockdown

SU-DHL-6 cells with transient IRF4 knockdown were harvested 24 hours after siRNA transfection and used in ChIP experiments with IRF4 antibody and H3K9me3 antibody (indicative of transcriptional gene repression). Data from the 5'UTR site failed due to technical issues, but in cells transfected with off-target control siRNA there was evidence of IRF4 binding at the element 1 binding site (Figure 4.12A), consistent with previous findings in wildtype SU-DHL-6 cells. (Figure 3.19) IRF4-*CD38* binding was substantially reduced in comparison, in the cells with siRNA-mediated IRF4 knockdown. (Figure 4.12A) Binding at the element 1 binding site by H3K9me3 was increased in cells with IRF4 knockdown. (Figure 4.12B) Taken together, these data suggest that IRF4 may be operating as a transcriptional activator of *CD38*, possibly via the element 1 site, in SU-DHL-6 cells.

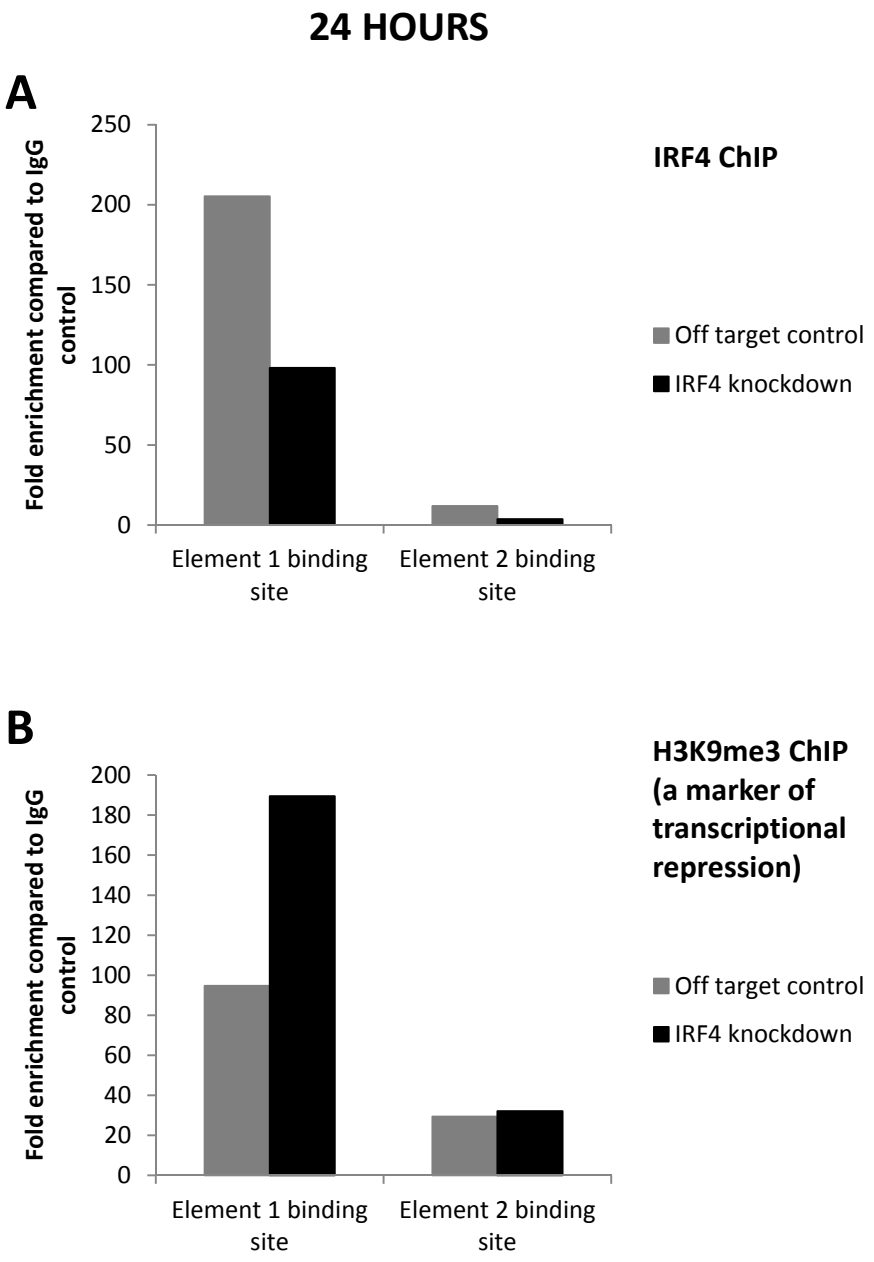

Figure 4.12 ChIP using IRF4 and H3K9me3 antibodies in SU-DHL-6 cells with siRNA-mediated IRF4 knockdown

SU-DHL-6 cells were transfected with either Combination siRNA targeted against *IRF4*, or off target control siRNA. Cells were harvested 24 hours after transfection, and used in ChIP experiments.

A. Cells transfected with off target control siRNA demonstrated IRF4-*CD38* binding at the element 1 binding site. This was substantially reduced in cells with siRNA-mediated IRF4 knockdown. Data from the 5'UTR site failed due to technical issues.

B. In the same cells, binding at the element 1 site by H3K9me3 was seen in cells transfected both with off target control siRNA or Combination siRNA targeted against *IRF4*. However, H3K9me3 binding was substantially greater in cells with siRNA-mediated IRF4 knockdown. H3K9me3 is associated with transcriptional repression.

4.4 Discussion

IRF4 binds at the element 1 and 5'UTR sites in *CD38* gene in MEC-1 and SU-DHL-6 cell lines. (Section 3.3.4b) Given that IRF4 functions as a dichotomous transcription factor with the capacity to either upregulate or downregulate transcription of its target genes, the relationship between these two proteins was further explored to determine whether IRF4 has a role in affecting CD38 expression in these B cell lines.

In order to explore the relationship between IRF4 and CD38, attempts were made to generate cells with transient and constitutive IRF4 protein knockdown using RNA interference techniques. These cells were then used for flow cytometry analysis of CD38 expression, to determine whether reduced expression of IRF4 protein affected the surface expression of CD38. In addition, some of the cells with transient IRF4 knockdown were used in ChIP experiments with antibodies to IRF4 and to histone methylation marks (markers of transcriptional gene activation or repression).

4.4.1 Generating cells with IRF4 knockdown

Cells with transient IRF4 knockdown were successfully generated by siRNA transfection in TK6, MEC-1 and SU-DHL-6 cell lines, using two siRNA constructs in combination. These constructs target exons 7 and 9 of the *IRF4* transcript.

In all three cell lines, IRF4 knockdown was observed by 24 hours after transfection, though there was no evidence of knockdown in either TK6 or SU-DHL-6 when cells were collected only 6 hours after transfection. This indicates IRF4 protein turnover of approximately 12-24 hours. By 72 hours after transfection, IRF4 protein was re-expressed in TK6 cells. In MEC-1 cells, knockdown was still present 72 hours after transfection in the experiments that included this time point, but the knockdown was lost by 96 hours. Knockdown was also consistently seen at 24 hours after transfection in SU-DHL-6 cells but was only variably present 48 hours after transfection. No time points beyond 48 hours were documented in the SU-DHL-6 cells. These data indicate that all three cell lines were able to tolerate a transient loss of IRF4 knockdown, before the protein was subsequently re-expressed. It is presumed that re-

expression of IRF4 protein is mediated via a time-dependent reduction in cytoplasmic siRNA concentration, with concomitantly increasing levels of stable IRF4 transcript.

Short hairpin RNA interference was then used to attempt to generate cell clones with constitutive IRF4 knockdown. This was readily achieved in TK6 cell line using shRNA construct 6 which targets a region in the 3'UTR of IRF4. Several clones with substantial IRF4 knockdown were generated and the IRF4 knockdown remained stable during long-term culture.

In contrast to TK6, generating cell clones with successful IRF4 knockdown in MEC-1 and SU-DHL-6 cell lines proved very difficult. After several attempts, clones were generated from MEC-1 populations transduced with shRNA construct 6, but following short term culture, immunoblotting revealed re-expression of IRF4 in all clones, including those with substantial knockdown. Given that MEC-1, along with SU-DHL-6, expresses IRF8 and PU.1 (Figure 3.10), and has evidence of IRF4-*CD38* binding by ChIP (Figure 3.20), there is the suggestion that IRF4 has a more essential role in maintenance of viability in both of these cell lines than in TK6. Specifically, the experimental data suggests that MEC-1 cells are less tolerant to IRF4 knockdown than TK6. MEC-1 cells were able to tolerate transient siRNA-mediated IRF4 knockdown, but the rapid re-expression of IRF4 in cell clones with shRNA-mediated knockdown, suggests a strong selective pressure for maintenance of IRF4 expression in this cell line.

In addition, attempts to transduce SU-DHL-6 with shRNA were entirely unsuccessful. Whilst it may be tempting to attribute this failure to the cells' perceived inability to tolerate IRF4 knockdown, this is unlikely to be the full explanation, for several reasons. Firstly, SU-DHL-6 cells were able to tolerate transient siRNA-mediated IRF4 knockdown indicating that loss of IRF4 is not an immediately terminal event in SU-DHL-6. In addition, cells transduced with the off-target shRNA construct or empty pLKO.1 vector did not survive, suggesting that the transduction process was fatal to the cells, rather than the knockdown of IRF4. Indeed, the low cell densities, puromycin and polybrene concentrations used in the transduction protocol were not tolerated by SU-DHL-6 (as detailed in sections 2.5.4 and 2.5.5). Successful transduction of SU-DHL-6 with shRNA would require a modification of the protocol, in keeping with these

findings: specifically, cell density at the time of transduction should be increased to 1-2x10^5/ml, with a polybrene concentration no higher than 4μg/ml. A review of the literature indicates that similar modifications have been used previously in SU-DHL-6 to achieve successful shRNA transduction. (Cozma et al., 2007; Ramkumar et al., 2013)

4.4.2 CD38 expression in cells with IRF4 knockdown

Transient siRNA-induced IRF4 knockdown in TK6 and MEC-1 cells had no effect on CD38 expression, as determined by flow cytometry. There was however a suggestion of modest downregulation of CD38 expression in SU-DHL-6 cells, 24 hours after electroporation with siRNA targeted against IRF4. The effect was subtle and CD38 percentage positivity remained unchanged. However, there was evidence of a reduction in the relative mean fluorescence of SU-DHL-6 cells with IRF4 knockdown labelled with CD38 antibody, compared to those labelled with an isotype control.

Given that there is no evidence of statistically significant IRF4-*CD38* binding in TK6, and common IRF4 binding partners (PU.1, IRF8) are absent in this cell line, the absence of an effect of IRF4 knockdown on CD38 expression in TK6 is perhaps unsurprising. Similarly, wildtype MEC-1 cells demonstrate only very modest surface CD38 expression and thus IRF4 knockdown might also not be expected to have a substantial impact on CD38 expression in this cell line.

SU-DHL-6 requires further consideration, however. In particular, given that SU-DHL-6 strongly expresses surface CD38 (Figure 3.14), has evidence of statistically significant IRF4-*CD38* binding (Figure 3.19), and expresses IRF4's common binding partners (Figure 3.10), this would seem a likely cell line in which the effect of IRF4 knockdown on CD38 expression might be observed. There is subtle evidence of a modest effect on CD38 expression in SU-DHL-6 cells with IRF4 knockdown, but it is possible that the experiments demonstrated here were inadequate to reveal this relationship more explicitly. In addition, it is possible that the experiments were also inadequate to reveal a relationship between IRF4 and CD38 in MEC-1, given that IRF4-*CD38* binding does occur in this cell line (Figure 3.20), in spite of the weak surface

CD38 expression. The limits of the experiments presented in this chapter must therefore be considered.

Firstly, transient siRNA-mediated IRF4 knockdown may be insufficient to affect CD38 expression. Data regarding the half-life of CD38 protein *in situ* is currently lacking. If turnover of surface CD38 is substantially longer than 48-72 hours, it is possible that the transient IRF4 knockdown achieved here was of too short a duration to exert a discernible effect on CD38 transcription, and yield a measurable change in surface protein levels. In this regard, future experiments investigating *CD38* mRNA transcript levels in cells with long-term IRF4 protein knockdown may be useful in demonstrating an effect on CD38 which may be apparent before surface protein levels are affected. Successful transduction of MEC-1 and SU-DHL-6 with a targeted shRNA construct to generate a more durable IRF4 knockdown would also be helpful in this regard. This may be achievable with the possible modifications described in SU-DHL-6 transduction. (Section 4.4.1) However, as discussed above, the prevailing evidence suggests that MEC-1 cells are intolerant of long-term IRF4 knockdown, suggesting an essential role for this protein in cell viability.

Secondly, it may be that the necessary threshold for IRF4 knockdown to have a substantial effect on CD38 expression was not reached using siRNA transfection. A maximum knockdown of 68% was achieved at the 48 hour time point in the SU-DHL-6 cells which were analysed by flow cytometry for CD38 expression. The very modest effect on CD38 expression which was observed in these cells may have been more pronounced if a greater degree of knockdown had been achieved. Competition experiments by Ochiai *et al* demonstrated that IRF4 can bind to the EICE motif with PU.1 even when IRF4 is present at low concentration, whereas IRF4 must be present at high concentrations to bind the ISRE (interferon-stimulated response element) on its own. (Ochiai et al., 2013) It may be that inadequate knockdown of IRF4 was achieved by the siRNA experiments in SU-DHL-6 to abrogate the recruitment of IRF4 to the EICE sites at element 1 or the 5'UTR of *CD38*. This would be supported by the observation that IRF4-*CD38* binding, while reduced, was still demonstrated by ChIP at the element 1 EICE site in SU-DHL-6 cells with siRNA-induced IRF4 knockdown. (Figure 4.12)

Furthermore, it is also feasible that different levels of IRF4 knockdown could lead to different effects on *CD38*, in keeping with the model of 'kinetic control' proposed by Sciammas *et al*. (Sciammas et al., 2006) This model was based on the observation that graded expression of IRF4 expression led to opposing (pleiotropic) effects on the downstream gene target, *Aicda*. Again, successfully establishing a number of SU-DHL-6 cell clones with constitutive IRF4 knockdown might inform this issue, particularly as the cell cloning process often generates clones with a range of knockdown. Thus, the CD38 expression of clones with very substantial IRF4 knockdown could be compared with that of clones with only moderate knockdown.

Turning to MEC-1 cells: flow cytometry was performed on cells with a very substantial IRF4 knockdown of 92% at T48. CD38 surface expression was unchanged in these cells, which suggests that very substantial IRF4 knockdown has no significant effect on CD38 expression in this cell line. Notably however, endogenous surface CD38 expression in wildtype MEC-1 cells is substantially lower than that of SU-DHL-6 cells and so this cell line may be inadequate to reveal any subtle changes in CD38 expression.

Thus, there could be several possible explanations for the absence of an effect on CD38 expression in cells with transient IRF4 knockdown. Despite ChIP evidence that IRF4 binds the *CD38* gene in MEC-1 and SU-DHL-6, IRF4 may have no direct effect on the expression of CD38 in these cells, and CD38 expression may be governed by other pathways in which IRF4 plays no role. Alternatively, the IRF4 knockdown achieved may have been inadequate in duration or depth, and thus insufficient to effect any change in CD38 expression. In particular, there was very limited opportunity to test for an effect on CD38 expression in SU-DHL-6 cells, due to the failure to generate any clones with constitutive knockdown.

4.4.3 ChIP in MEC-1 and SU-DHL-6 cells with siRNA-induced IRF4 knockdown

As MEC-1 and SU-DHL-6 clones with constitutive stable IRF4 knockdown were not achieved, ChIP experiments were carried out using cells with transient siRNA-mediated IRF4 knockdown, in an attempt to shed light on any functional IRF4-*CD38*

interaction. Cells generated from siRNA transfection experiments in these cell lines were used to prepare chromatin for ChIP experiments using both IRF4 antibody and antibodies to histone methylation marks. The histone methylation marks were specifically chosen for their association with transcriptional activation and repression of target genes.

These experiments proved challenging, for a number of reasons. Firstly, the number of cells that underwent transfection with siRNA had to be scaled up considerably, in order to generate sufficient chromatin for ChIP. Secondly, in order to compare cells transfected with control siRNA to those transfected with siRNA targeted against IRF4, chromatin had to be generated simultaneously from the two cell populations. This introduced the potential for considerable inter-assay variability as the chromatin generation and fragment size was often not consistent in the two populations. As previously discussed, the size and quality of chromatin fragments is crucial to ChIP results. This potential variability between the fragments obtained from cells transfected with control siRNA and those transfected with siRNA targeted against *IRF4*, thus had the potential to substantially affect non-specific binding and the overall ChIP result. As a consequence, only a limited number of the attempted experiments yielded valid, interpretable data, and are presented here.

ChIP experiments using MEC-1 and SU-DHL-6 were suggestive of different roles for IRF4 in the transcriptional regulation of *CD38*. In MEC-1, there was clear evidence of a reduction in IRF4-*CD38* binding at element 1 and the 5' UTR binding sites, 24 hours after transfection, in cells which had transient IRF4 knockdown. Simultaneously, whilst binding by H3K4me3 was barely affected at the element 1 binding site, binding at the 5' UTR site increased dramatically in cells with IRF4 knockdown. Given that H3K4me3 is associated with transcriptional activation, these data suggest that IRF4 knockdown is associated with increased transcriptional activity at the 5'UTR site of *CD38* in MEC-1. Whilst data for IRF4 binding at the 5'UTR were unavailable in cells collected 48 hours after transfection, there was evidence of a further increase in H3K4me3 binding at this site in MEC-1 cells with IRF4 knockdown, supporting data from the earlier time point. Taken together, these data suggest that IRF4 may act as a negative regulator of *CD38*

transcription in MEC-1 cells, functioning primarily via the 5' UTR and possibly the element 1 site.

In contrast, IRF4 knockdown in SU-DHL-6, was associated with an increase in binding by H3K9me3: a histone methylation mark which is strongly associated with transcriptional repression. These data suggest that IRF4 knockdown in SU-DHL-6 might be associated with repression of transcriptional activity, and that IRF4 thus functions as a transcriptional activator of *CD38* in SU-DHL-6 cells, acting primarily via binding at the element 1 site. Although not conclusive, this observation is consistent with the modest reduction in CD38 relative mean fluorescence demonstrated in SU-DHL-6 cells with transient IRF4 knockdown. Taken together, these data are both supportive of a model in which IRF4 positively regulates CD38 expression in SU-DHL-6 cells.

Whilst these ChIP data are very limited, they are consistent with the model that IRF4 has pleiotropic effects on its downstream targets, and that IRF4-induced transcriptional regulation may differ depending on the cell background, or on the level of IRF4 expression. This is consistent with the strong body of evidence (previously discussed in section 1.2) that demonstrates the pleiotropic effect of IRF4 in B cell maturation and development.

4.5 Summary of chapter 4

IRF4 is a dichotomous regulator which can both activate or repress its target genes. IRF4 acts as a transcriptional activator of target genes when it binds with PU.1 or SPI-B, and activation occurs courtesy of its C terminal activation domain. In contrast, it represses the activation of interferon-inducible genes when it binds with IRF8, or when it binds alone to repress IRF1-induced activation of interferon-responsive genes.

Transient knockdown of IRF4 was achieved in TK6, MEC-1 and SU-DHL-6 cell lines using siRNA. There was no evidence that this knockdown had any effect on CD38 expression in TK6 or MEC-1, though wildtype MEC-1 cells only weakly express CD38. Knockdown of IRF4 in SU-DHL-6 led to a modest reduction in the relative mean fluorescence of CD38 expression, twenty four hours after electroporation with the target siRNA. This suggestion of a positive regulation of CD38 expression by IRF4 was further supported by the ChIP experiment that demonstrated upregulation of H3K9me3 binding at the EICE site of *CD38* element 1, in SU-DHL-6 cells with IRF4 knockdown. H3K9me3 is associated with transcriptional gene repression, and taken together, these data are suggestive of a model in which IRF4 positively regulates CD38 expression in this cell line. The generation of SU-DHL-6 cell clones with constitutive IRF4 knockdown would have been extremely useful in the further interrogation of this model. However, attempts to transduce SU-DHL-6 with shRNA constructs were unsuccessful, though this may be achievable with further modifications to the protocol.

In contrast, transient knockdown of IRF4 in MEC-1 led to an upregulation of H3K4me3 at the 5'UTR of *CD38*, whilst IRF4-*CD38* binding was simultaneously demonstrated by ChIP to be downregulated. H3K4me3 is associated with transcriptional gene activation, and so this finding, which was observed at two separate time points, is suggestive of negative regulation of *CD38* by IRF4 in MEC-1.

Taken together, these contrasting findings in the SU-DHL-6 and MEC-1 cell lines are consistent with previous observations in the literature of the pleiotropic effect of IRF4 on its downstream gene targets.

Chapter 5. Effect of IRF4 knockdown on cell growth, and sensitivity to cytotoxic agents using *in vitro* B cell model systems

5.1 Introduction

5.1.1 IRF4 in B cell malignancies

IRF4 was first suggested as a therapeutic target in haematological malignancy following the observation by Shaffer and colleagues that multiple myeloma is 'addicted' to IRF4. (Shaffer et al., 2008) Specifically, using an RNA-interference-based genetic screen, they demonstrated that inhibition of IRF4 induced death in multiple myeloma cells irrespective of somatic genetic background. The direct downstream target genes of IRF4 in myeloma cell lines were identified by genome wide ChIP techniques, and included *MYC*, a key coordinator of cellular proliferation, which was upregulated in myeloma cells but not in normal plasma cells. Thus, these data identified IRF4 as a potential therapeutic target in multiple myeloma, despite the fact that the locus encoding this key B cell transcription factor is only rarely somatically altered in malignant plasma cells. (Iida et al., 1997)

Subsequent studies have expanded on these initial findings, confirming the dramatic effect of IRF4 knockdown in additional myeloma cell lines. (Zhang et al., 2013) Furthermore, current myeloma therapies including lenalidomide and pomalidomide have been shown to inhibit IRF4 expression, possibly through inhibition of the protease, cereblon, which is a direct target of these immunomodulatory drugs. (Zhu et al., 2013)

A similarly important role for IRF4 has been identified in other B cell malignancies.

IRF4 expression is a hallmark of activated B cell like diffuse large B cell lymphoma (ABC DLBCL) in which it governs a key regulatory survival network through repression of interferon-β expression and upregulation of NF-κB signalling pathways. IRF4 has thus also been identified as a potential therapeutic target in this aggressive lymphoma, and was successfully targeted in ABC DLBCL cell lines, through cereblon-dependent inhibition by lenalidomide. (Yang et al., 2012)

In Hodgkin lymphoma, IRF4 plays a key role in regulating the intrinsic apoptotic pathway, and IRF4 knockdown in Hodgkin lymphoma cell lines induced apoptosis. (Aldinucci et al., 2011) IRF4 is also important in the maintenance of the Hodgkin tumour microenvironment. (Aldinucci et al., 2012)

Finally, IRF4 also has a clear role in T cell malignancies: knockdown of IRF4 is toxic to anaplastic large cell lymphoma cell lines (Weilemann et al., 2015) and translocations involving IRF4 have been identified in peripheral T cell lymphomas. (Feldman et al., 2009)

Given the clear evidence of IRF4 as a potential therapeutic target in other lymphoid malignancies, it remains plausible that targeting IRF4 may prove efficacious in CLL, either as a single agent or in combination with currently deployed anti-leukaemic agents.

5.1.2 Cytotoxic agents currently used for the treatment of CLL

Fludarabine is a purine analogue that interferes with DNA replication. It continues to be used as the standard first line cytotoxic agent in chemo-immunotherapy regimes alongside cyclophosphamide and rituximab, in CLL patients who can tolerate intensive chemotherapy.

However, fludarabine-containing regimes are associated with significant myelosuppressive toxicities (Catovsky et al., 2007; Hallek et al., 2010) and are ineffective for patients with somatic aberrations of *TP53*. (Oscier et al., 2013; Stilgenbauer et al., 2014)

Bendamustine is an alkylating agent which is currently used in patients considered unfit for strongly myelosuppressive fludarabine-containing regimes, particularly older patients. In combination with rituximab, it offers similar progression-free survival and overall survival rates to the intensive FCR regime, in the over 65 year old population, though FCR is still the superior option in younger patients who are fit for intensive therapy. (Eichorst *et al*., 2014) It is also ineffective at overcoming the poorer outcome associated with *TP53* mutation or deletion.

The landscape of CLL therapy is thus rapidly changing with the advent of new inhibitors targeted against critical B cell receptor pathways that do not rely on intact *TP53* signalling pathways.

Ibrutinib is an inhibitor of Bruton's tyrosine kinase (BTK) and is effective in treatment-naïve, previously treated and relapsed/refractory patients, including those with *TP53* aberrations. (Byrd et al., 2015)

5.2 Aims of chapter 5

The aim of this chapter is to investigate whether targeted knockdown of IRF4 affects cell growth, and sensitivity to cytotoxic agents used in the treatment of CLL.

- Specifically, cells with transient siRNA-mediated IRF4 knockdown (TK6, MEC-1, SU-DHL-6) or stable shRNA-mediated IRF4 knockdown (TK6) were used to investigate the effect of IRF4 protein knockdown on cell growth and sensitivity to cytotoxic agents: fludarabine, bendamustine, ibrutinib.

5.3 Results

5.3.1 Effect of siRNA-mediated IRF4 knockdown on cell growth in MEC-1 cells

The growth of MEC-1 cells with siRNA-mediated IRF4 knockdown was assessed. Cells from two independent siRNA experiments were used, and were plated for growth kinetics 24 hours after electroporation. Knockdown of at least 50% was evident by western immunoblotting at 24 hours in both experiments, and this was confirmed by densitometry. In one experiment, IRF4 protein knockdown of over 90% was achieved by 48 and 72 hour time points. (Figure 4.5A)

Transient IRF4 protein knockdown mediated by siRNA transfection in MEC-1 cells did not have any significant effect on proliferation. (Figure 5.1)

5.3.2 Effect of siRNA-mediated IRF4 knockdown on sensitivity to cytotoxic agents in MEC-1 cells

The effect of siRNA-mediated IRF4 knockdown on MEC-1 sensitivity to ibrutinib and fludarabine in growth inhibition assays was assessed over the course of three independent siRNA transfection experiments.

To demonstrate any growth inhibition due to the solvent (DMSO) in which both drugs were delivered, a DMSO-only control was prepared simultaneously, for each growth inhibition assay. Cells with siRNA-mediated IRF4 knockdown were exposed to the highest concentration of DMSO (0.1%) used in the fludarabine and ibrutinib experiments, alongside cells which had been transfected with an off-target control siRNA construct, or subject to electroporation only. Cells were counted in exponential growth phase and compared to cells which were untreated with DMSO. Growth inhibition data from each fludarabine and ibrutinib inhibition experiment were normalised to the DMSO-only data from the same experiment.

DMSO at concentrations 0.03% and 0.1% did not substantially impair cell growth in any of the siRNA treated MEC-1 cells (Figure 5.2) (p= 0.34 and 0.50

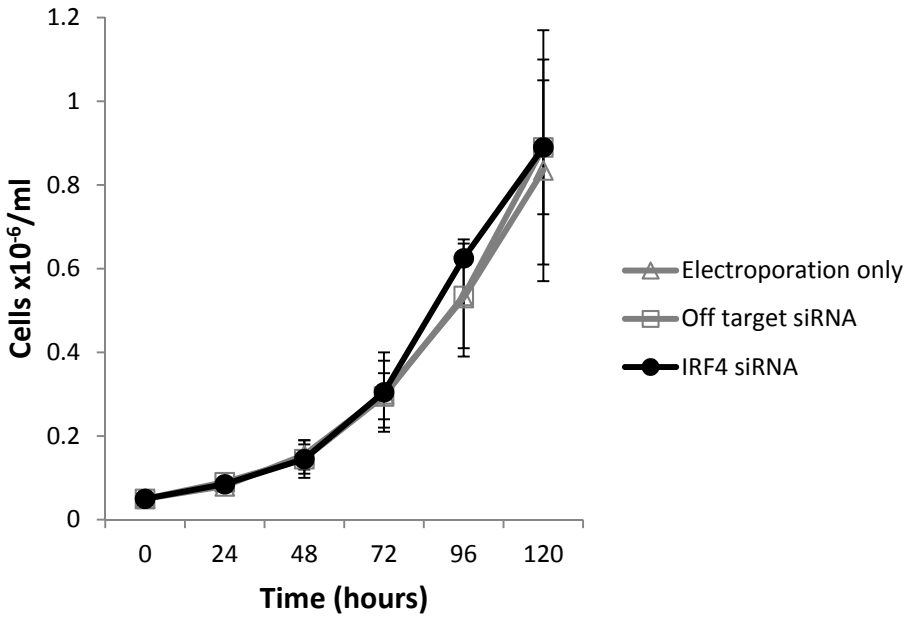

Figure 5.1 Proliferation of MEC-1 cells with transient siRNA-mediated IRF4 knockdown

MEC-1 cells were transfected with Combination siRNA targeted against *IRF4*, an off target control siRNA, or subjected to electroporation only. Analysis by western immunoblotting and densitometry demonstrated knockdown of at least 50%, 24 hours after electroporation, and the cells were plated at this point. Cells were seeded at $5x10^4$/ml in sterile 6 well culture plates, and counted at 24 hour intervals for 5 days. The experiment was repeated in duplicate using cells from two independent siRNA experiments, and IRF4 knockdown of over 90% was achieved in the cells from one of these experiments. Knockdown of IRF4 protein did not affect the proliferation of MEC-1 cells. Error bars represent standard error of the mean.

respectively, by paired t test). There was the suggestion of a hormetic effect in the off-target control cells exposed to 0.1% DMSO (Figure 5.2B) which grew more readily in the presence of DMSO than the untreated cells.

5.3.2.a Fludarabine

In the first growth inhibition experiment, MEC-1 cells with demonstrable siRNA-mediated IRF4 knockdown of 50-100% (Figure 4.5A) were treated with fludarabine in a dose range of 0-15μM. IRF4 knockdown rendered MEC-1 cells less sensitive to growth inhibition by fludarabine at all drug concentrations in this experiment. (Figure 5.3A) However, at the highest dose in this range, 20-30% of all cells survived, and so the dose range was increased to 50μM in two subsequent experiments.

The growth inhibition assay was repeated in duplicate at the higher dose range, in a further two independent siRNA experiments. Fewer than 10% cells survived when they were treated with 50μM fludarabine. IRF4 knockdown did not affect sensitivity to fludarabine at any dose. (Figure 5.3B) However, the IRF4 knockdown achieved in these two higher dose fludarabine inhibition assays (western immunoblotting data not shown) was less prominent than in those used in the low-dose fludarabine experiment. Specifically, maximal IRF4 knockdown was between 50-70% in these high-dose experiments compared to nearly 100% in the low-dose experiment. These data suggest that loss of IRF4 protein sensitises MEC-1 cells to the inhibitory effects of fludarabine, but that potentiation of growth inhibition by fludarabine may require a relatively high level of IRF4 knockdown.

5.3.2.b Ibrutinib

IRF4 knockdown had no effect on the growth kinetics of MEC-1 cells in the presence of ibrutinib, at a concentration range of 0-50μM. (Figure 5.4) At 50μM ibrutinib concentration, fewer than 1% of the cells survived. The cells used in these experiments had evidence of modest IRF4 knockdown (55-60%) by western immunoblotting (data not shown). As such, the possibility of potentiation of ibrutinib-induced growth inhibition in MEC-1 cells with high levels of IRF4 knockdown (up to 100% knockdown), similar to that seen with fludarabine (5.3.2.a), cannot be excluded.

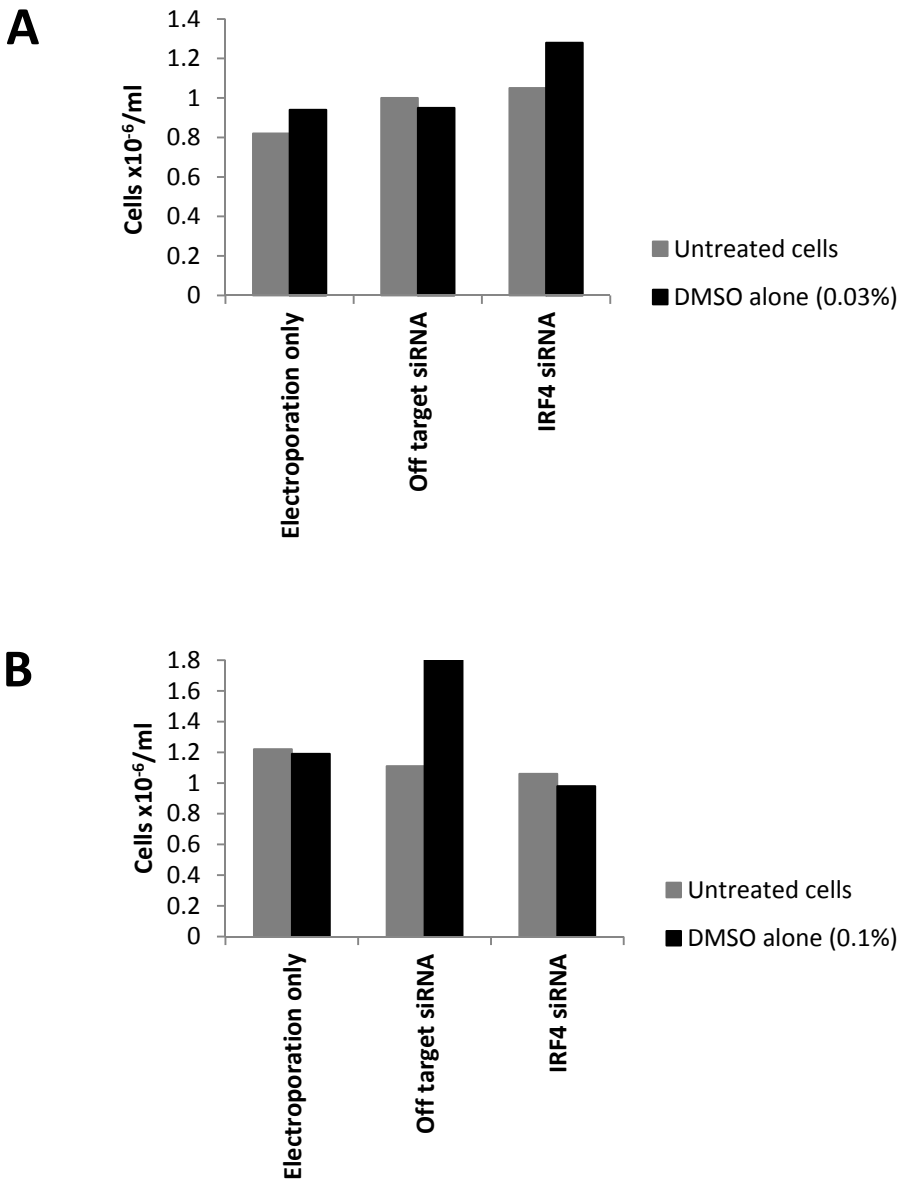

Figure 5.2 Effect of DMSO on siRNA treated MEC-1 cells

In order to determine the cytotoxic effect of DMSO which was used as a diluent for ibrutinib and fludarabine in growth inhibition studies, MEC-1 cells were exposed to DMSO alone, at the highest concentration of DMSO used in the drug-treated wells. MEC-1 cells which had been subjected to electroporation only, transfection with an off target siRNA or transfection with Combination siRNA targeted against *IRF4*, were seeded at $5x10^4$/ml in sterile 6 well culture plates, and exposed to DMSO at a concentration of 0.03% (**A**) or 0.1% (**B**). One representative experiment is shown in both cases.

A. There was no evidence of substantial cytotoxicity in any of the cells exposed to 0.03% DMSO compared to the untreated cells (p = 0.34).

B. The higher concentration of DMSO (0.1%) also did not negatively impact on cell growth (p =0.50). The cells transfected with an off target siRNA appeared to grow more readily in the presence of DMSO in this experiment.

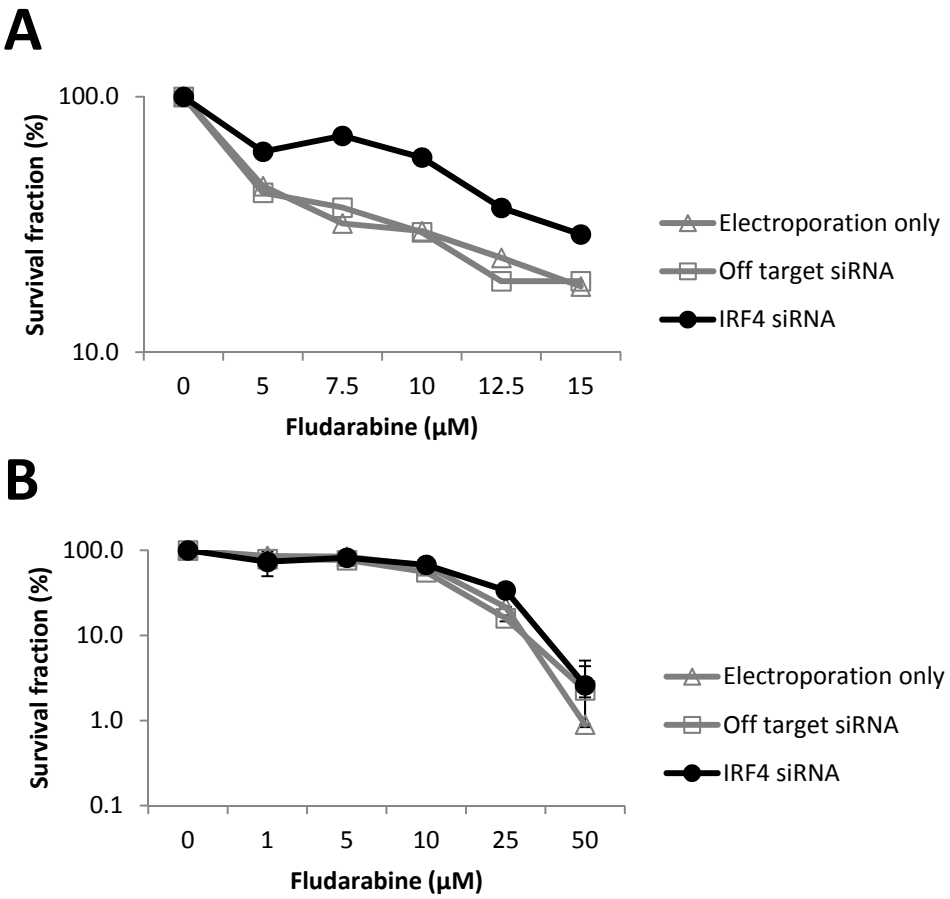

Figure 5.3 Fludarabine cytotoxicity in MEC-1 cells with siRNA-mediated IRF4 knockdown

MEC-1 cells which had been subjected to electroporation only, transfection with an off target siRNA or transfection with Combination siRNA targeted against *IRF4*, were seeded at $5x10^4$/ml in sterile 6 well culture plates, and treated with fludarabine. Cells were then counted in exponential growth phase, and a percentage of surviving cells at each drug dose was calculated in comparison to the survival of cells treated with DMSO vehicle only.

A. Cells with demonstrable IRF4 knockdown of 50-100% were treated with fludarabine in a dose range 0-15μM. At all doses, there was evidence of reduced drug-sensitivity in the cells with IRF4 knockdown.

B. Given that 15μM fludarabine did not achieve more than 85% cell killing, cells from two independent siRNA experiments were then treated with fludarabine at higher doses, ranging up to 50μM. There was no evidence of differential drug sensitivity in the IRF4 knockdown cells at these doses. Error bars represent standard error of the mean for the two experiments. However, the maximum IRF4 knockdown achieved with siRNA transfection in the cells used in these experiments with higher dose fludarabine (up to 50μM) was less (50-70%) than that achieved in the cells used in the first fludarabine experiment.

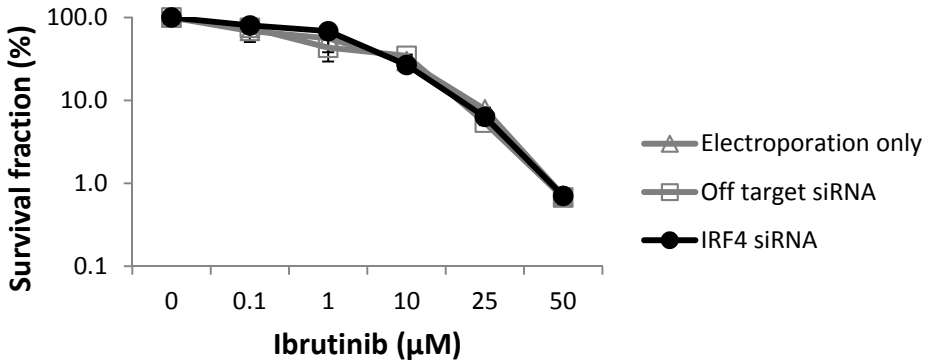

Figure 5.4 Ibrutinib cytotoxicity in MEC-1 cell line with transient IRF4 knockdown

MEC-1 cells which had been subjected to electroporation only, transfection with an off target siRNA or transfection with Combination siRNA targeted against *IRF4*, were seeded at $5x10^4$/ml in sterile 6 well culture plates, 24 hours after electroporation, and treated with ibrutinib at a dose range of 0-50µM. Cells were counted in exponential growth phase and normalised to growth inhibition in cells treated with DMSO only. The experiment was repeated in duplicate, using cells from two independent siRNA experiments with maximal IRF4 knockdown of 55-60%, demonstrated by western immunoblotting and densitometry. There was no apparent effect on drug sensitivity in cells with IRF4 knockdown. Error bars represent standard error of the mean for the two experiments.

5.3.3 Effect of siRNA-mediated IRF4 knockdown on cell growth in SU-DHL-6 cells

The effect of siRNA-mediated IRF4 knockdown on SU-DHL-6 cell proliferation was investigated in three independent experiments. The growth curves were prepared 6 hours after electroporation (in contrast to the MEC-1 cell growth curves, section 5.3.1) due to some early western immunoblotting data which was initially suggestive of knockdown prior to the 24 hour time point in this cell background (data not shown).

In contrast to MEC-1, SU-DHL-6 cells with siRNA-mediated IRF4 knockdown proliferated more slowly than cells transfected with an off-target control siRNA or with cells subjected to electroporation only (Figure 5.5), and this was statistically significant (p=0.032 and 0.037, respectively) by two way ANOVA. Critically, siRNA-mediated IRF4 knockdown in SU-DHL-6 was relatively high, with a mean knockdown of nearly 70% compared to off-target control cells.

5.3.4 Effect of siRNA-mediated IRF4 knockdown on sensitivity to cytotoxic agents in SU-DHL-6 cells

The effect of siRNA-mediated IRF4 knockdown on SU-DHL-6 sensitivity to fludarabine was assessed over the course of two independent siRNA transfection experiments.

The toxicity of DMSO alone in SU-DHL-6 was assessed alongside each growth inhibition assay, as described previously. SU-DHL-6 cell growth was not impaired by DMSO alone when cells were treated with the highest concentration (0.1%) of DMSO achieved in the fludarabine-containing wells. (Figure 5.6) Conversely, there is the suggestion of a degree of hormesis in siRNA-treated cells, as the cells transfected with both the off-target control siRNA or Combination siRNA targeted against *IRF4*, appeared to grow more readily in the presence of DMSO (1%). However, none of these differences were statistically significant (p=0.07 by paired t test).

5.3.4.a Fludarabine

SU-DHL-6 cells with demonstrable IRF4 knockdown were treated with fludarabine six hours after electroporation, at a dose range of 0-50μM. Fewer than 1%

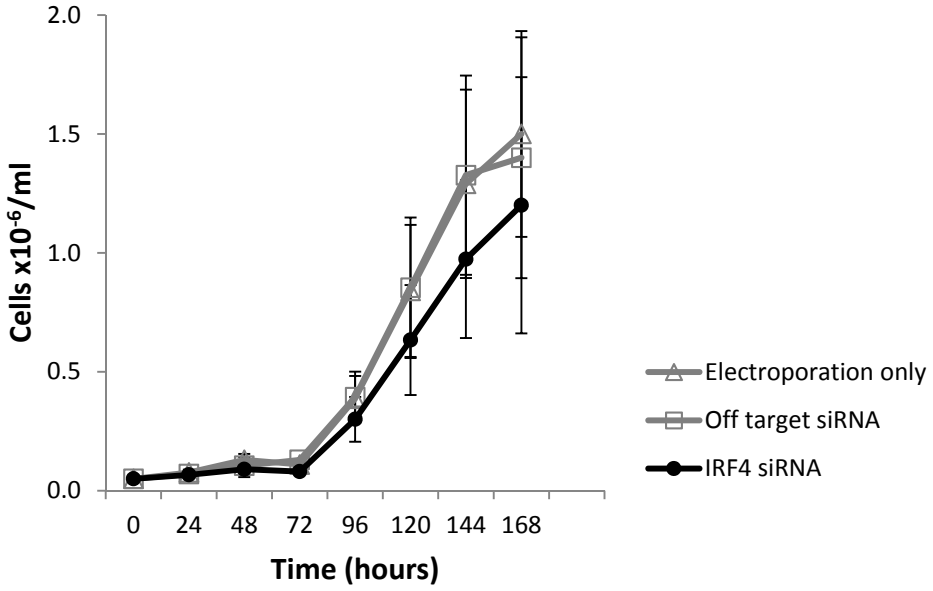

Figure 5.5 Proliferation of SU-DHL-6 cells with transient IRF4 knockdown

Six hours after transfection with Combination siRNA targeted against *IRF4*, transfection with an off target control siRNA, or electroporation only, cells were seeded at $5x10^4$/ml in sterile 6 well culture plates and counted at 24 hour intervals. The experiment was repeated in triplicate. The SU-DHL-6 cells with siRNA-mediated IRF4 knockdown grew significantly more slowly than those subjected to electroporation only or to transfection with an off target control siRNA (*p* value =0.037 and 0.032 respectively, by two way ANOVA). Mean knockdown of nearly 70% in the three independent siRNA experiments, was demonstrated by western immunoblotting and densitometry, 24 hours after electroporation. Error bars represent the standard error of the mean.

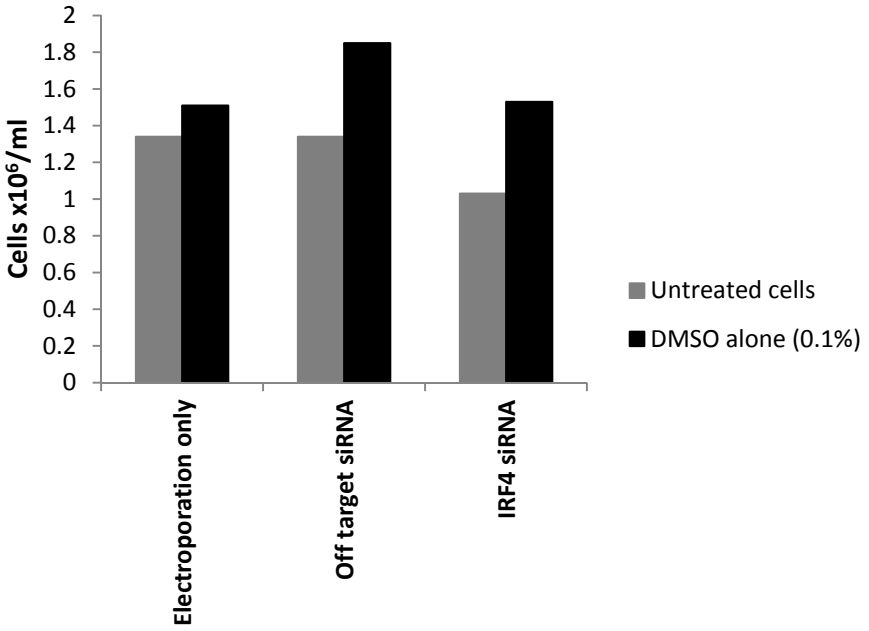

Figure 5.6 Effect of DMSO on siRNA-treated SU-DHL-6 cells
In order to determine the cytotoxic effect of DMSO which was used as a diluent for fludarabine in growth inhibition studies, SU-DHL-6 cells were exposed to DMSO alone, at the highest concentration of DMSO used in the drug-treated wells. SU-DHL-6 cells which had been subjected to electroporation only, transfection with an off target control siRNA or transfection with Combination siRNA targeted against *IRF4*, were seeded at $5x10^4$/ml in sterile 6 well culture plates, and exposed to DMSO at a concentration of 0.1%. The growth of these DMSO-exposed cells was compared to untreated cells. DMSO did not significantly affect cell growth (p=0.07) and there was some evidence of it having a hormetic effect in the cells transfected with siRNA, which appeared to grow more readily in the presence of DMSO. One representative experiment is shown.

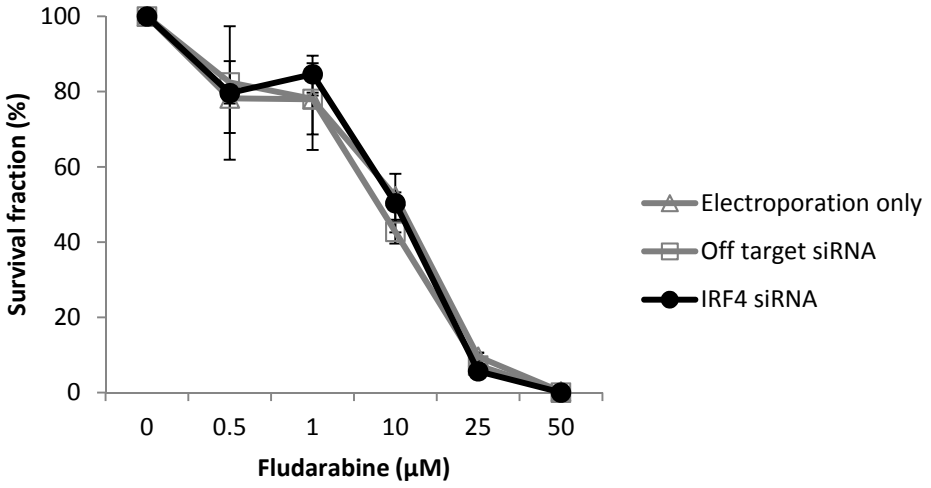

Figure 5.7 Fludarabine cytotoxicity in SU-DHL-6 cells with siRNA-mediated IRF4 knockdown

Six hours after electroporation, SU-DHL-6 cells which had been subjected to electroporation only, transfection with an off target siRNA or transfection with Combination siRNA targeted against IRF4 protein, were seeded at $5x10^4$/ml in sterile culture plates and treated with fludarabine at a dose range of 0-50µM. The cells were counted in exponential growth phase, and the cell counts were normalised to cells that had simultaneously been exposed to DMSO only. The experiment was repeated in two independent replicates with demonstrable IRF4 knockdown of between 65 and over 80%, 24 hours after electroporation. IRF4 knockdown had no effect on the cells' sensitivity to fludarabine. Error bars represent the standard error of the mean.

cells survived at the highest fludarabine dose. IRF4 knockdown did not affect the sensitivity of the cells to fludarabine. (Figure 5.7) In these two independent experiments, IRF4 knockdown was substantial and ranged from 68% to 81%, 24 hours post-electroporation.

5.3.5 Effect of shRNA-mediated constitutive IRF4 knockdown on cell growth in TK6 cells

The effect of constitutive shRNA-mediated IRF4 knockdown on TK6 growth kinetics was assessed.

Nine TK6 cell clones with demonstrable IRF4 knockdown generated from cells transduced with an shRNA construct directed against IRF4 were compared with three control cell clones, generated from cells transduced with an off target control shRNA. The knockdown in the targeted clones ranged from 50-100% as determined by densitometry. (Figure 4.10B) IRF4 knockdown led to significantly slower cell growth in the TK6 cells. (Figure 5.8) This approached statistical significance by two way ANOVA test in the first experiment (p=0.06) and achieved significance in the second (p=0.04).

5.3.6 Effect of shRNA-mediated constitutive IRF4 knockdown on sensitivity to cytotoxic agents in TK6 B cells

TK6 cells with shRNA-mediated IRF4 knockdown were treated with fludarabine and bendamustine in independent growth inhibition assays.

Fludarabine was delivered to the cells in DMSO solvent; bendamustine was delivered in sterile water.

In order to determine the cytotoxicity of DMSO, cells were treated with DMSO alongside each of the two independent fludarabine growth inhibition assays. Cells were exposed to the highest concentration of DMSO used in the fludarabine-treated wells (0.1% and 0.15% in the two experiments) and growth of the DMSO-treated cells was then compared to growth of the untreated cells. At both concentrations, DMSO had a modest adverse impact on TK6 cell growth. (Figure 5.9) This was the case

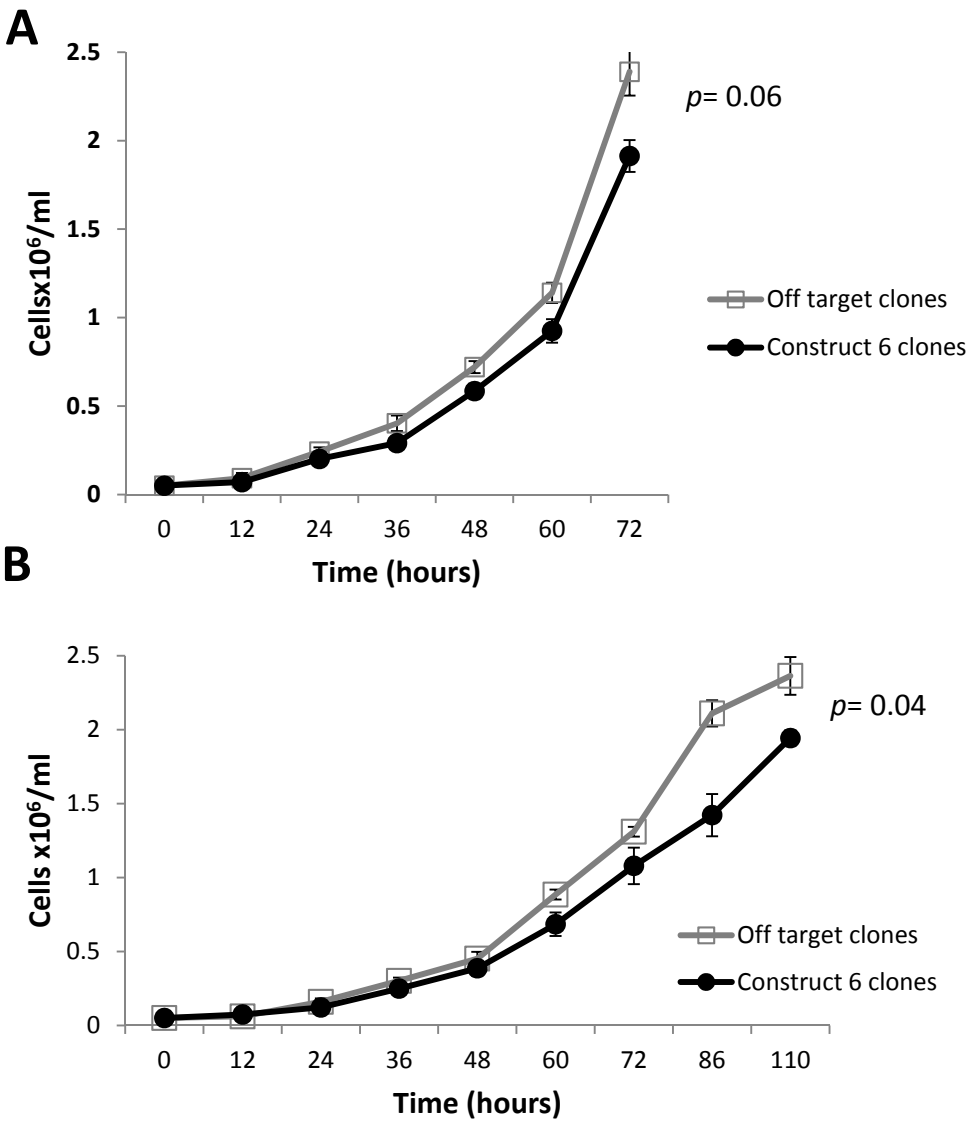

Figure 5.8 Proliferation of TK6 cell clones with shRNA-mediated constitutive IRF4 knockdown

Nine cell clones were generated from TK6 cells which had been transduced with shRNA construct 6 targeted against *IRF4*, and three cell clones were generated from cells transduced with an off target control shRNA. The IRF4 knockdown achieved in the target clones ranged from 50-100%. In two independent experiments (**A** and **B**), cells were seeded at $5x10^4$/ml in sterile 6 well culture plates, and counted at 24 hour intervals. In both cases, proliferation in cell clones with IRF4 knockdown was slowed compared to those without IRF4 knockdown. This approached, and reached statistical significance by two way ANOVA with *p* values of 0.06 and 0.04 respectively. Error bars represent standard error of the mean.

both for the nine cell clones with shRNA-induced IRF4 knockdown and for the three control cell clones.

Growth inhibition data from cells treated with fludarabine were normalised to the DMSO-only data from the same experiment.

Bendamustine was delivered in sterile water and the highest concentration of water achieved in drug-treated wells was 0.2%.

5.3.6.a Fludarabine

The nine TK6 IRF4 knockdown clones and three TK6 off-target control cell clones were each treated with fludarabine at a dose range of 0-10μM. (Figure 5.10A) At doses up to 1μM, there was no difference in the inhibition of growth of the knockdown or control cell clones. At 10μM however, there was evidence that the cell clones with IRF4 knockdown were more sensitive to fludarabine cytotoxicity than the control clones (p=0.007).

In light of the suggestion that fludarabine-induced growth inhibition may be dependent on high levels of IRF4 knockdown, the knockdown clones were separated according to the IRF4 expression as determined by western immunoblotting. (Figure 4.10B) Knockdown clones 4 and 6 demonstrate the lowest expression of IRF4 by western immunoblotting (100% and 95.5% knockdown determined by densitometry compared to the off target control clones); clones 1 and 2 are the highest IRF4 expressors of the knockdown clones (56.3% and 53.0% knockdown, respectively, compared to off-target control clones). While the effect is subtle, there is evidence that the lowest IRF4 expressing clones were more sensitive to fludarabine at 10μM concentration (Figure 5.10B) compared to the highest IRF4 expressing clones (Figure Figure 5.10C).

In order to further explore the relationship between sensitivity to fludarabine and IRF4 knockdown an additional independent experiment was performed using a single high IRF4 expressing clone (clone 4) and a single low expressing clone (clone 2). Furthermore, the fludarabine dose range was increased to include three doses greater

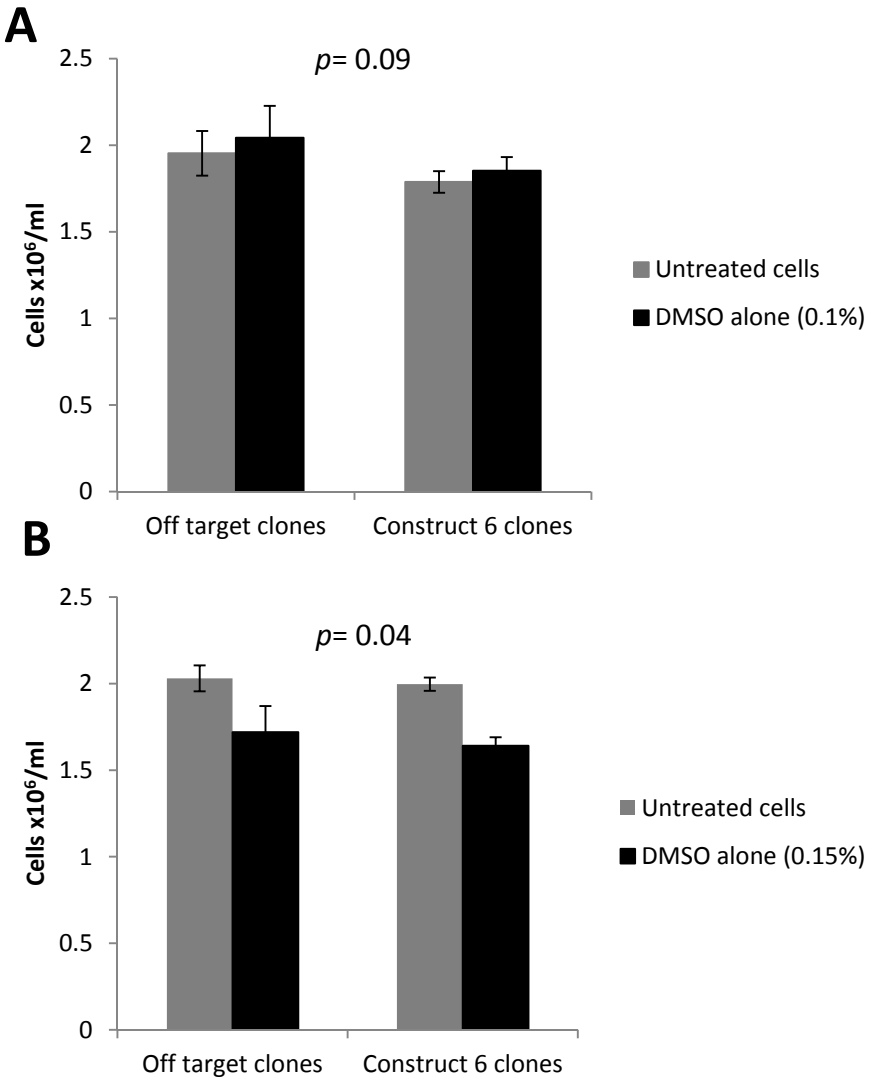

Figure 5.9 Effect of DMSO on TK6 cells with shRNA-mediated constitutive IRF4 knockdown

TK6 cells with shRNA-mediated IRF4 knockdown were treated with fludarabine in growth inhibition assays. In order to determine any cytotoxicity of the DMSO vehicle in which fludarabine was delivered, cells were treated separately with DMSO alone, at the highest concentration of DMSO achieved in the drug-treated wells. Nine cell clones transduced with shRNA Construct 6 targeted against *IRF4*, and three cell clones transduced with an off-target control shRNA construct, were each seeded at $5x10^4$/ml in sterile culture plates and treated with DMSO at 0.1% (**A**) or 0.15% (**B**). Cells were counted in exponential growth phase, and compared to cells untreated with DMSO. Error bars represent the standard error of the mean. Cell growth in cells exposed to DMSO, was modestly impaired, at both DMSO concentrations. This reached statistical significance when DMSO was at 0.15% concentration. Both knockdown and control cell clones were affected.

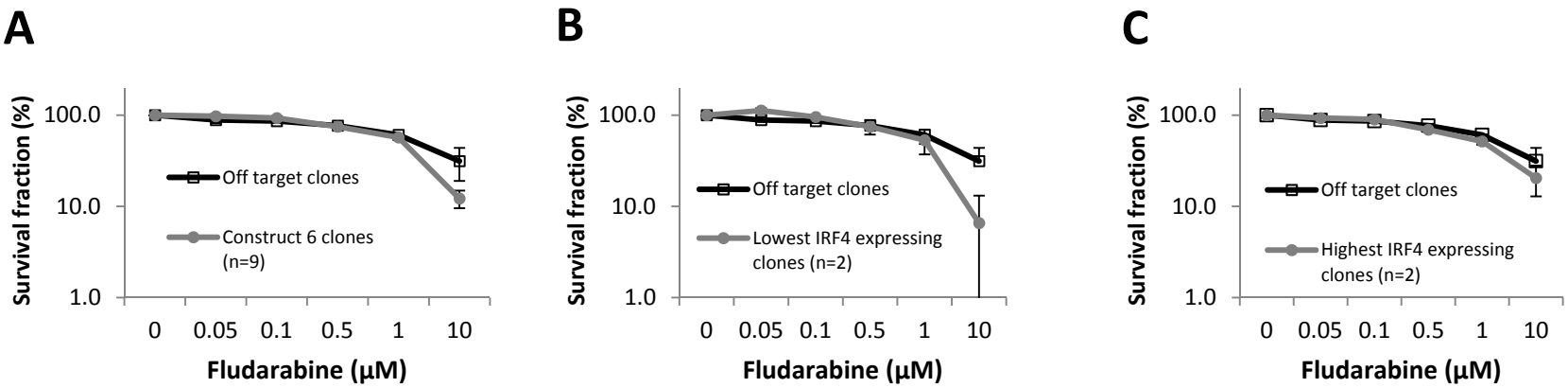

Figure 5.10 Growth inhibition with fludarabine (0-10µM) in TK6 cell clones with shRNA-mediated constitutive IRF4 knockdown

TK6 cell clones generated from cells transduced with an off target shRNA construct or with construct 6 shRNA targeted against *IRF4*, were seeded at $5x10^4$/ml in sterile 6 well plates and treated with fludarabine at the doses indicated. Cells were counted in exponential growth phase, and growth was normalised to cells which had been treated with DMSO alone (the vehicle in which fludarabine was delivered). Error bars represent the standard error of the mean.

A. No significant difference in growth inhibition was seen between three off target clones and nine clones with IRF4 knockdown, when they were treated with fludarabine doses up to 1µM. There was however, differential killing at the highest dose of 10µM where IRF4 knockdown clones were more sensitive to the drug than the control clones (p=0.007).

B. Given the evidence of differential killing at 10µM fludarabine, the two knockdown clones with the lowest expression of IRF4 by immunoblotting and densitometry (clones 4 and 6) were compared separately to the three off target clones. There is the suggestion of a further increase in sensitivity to fludarabine at 10µM in these two clones.

C. This effect is lost when the two knockdown clones with the highest expression of IRF4 by densitometry (clones 1 and 2) are compared to the three off target clones.

than 1μM. (Figure 5.11) Consistent with a dependency on low IRF4 expression, there was strong evidence of differential killing at high fludarabine doses (10 and 15μM) in clone 4 (the lowest IRF4 expressor), which was less apparent in clone 2 (a high IRF4-expressing clone). Indeed, at the highest dose of fludarabine (15 μM), the relative growth fraction of clone 4, with low IRF4 expression, was almost 3 logs lower than the control clone. These data demonstrate that IRF4 knockdown sensitises TK6 cells to the growth inhibitory effects of fludarabine, but that this phenotype is dependent on high level IRF4 knockdown.

5.3.6.b Bendamustine

Stable IRF4 knockdown had no effect on sensitivity to bendamustine in TK6 cells. (Figure 5.12) There was no evidence of an effect of IRF4 knockdown on growth inhibition at any doses and the level of IRF4 knockdown did not affect this.

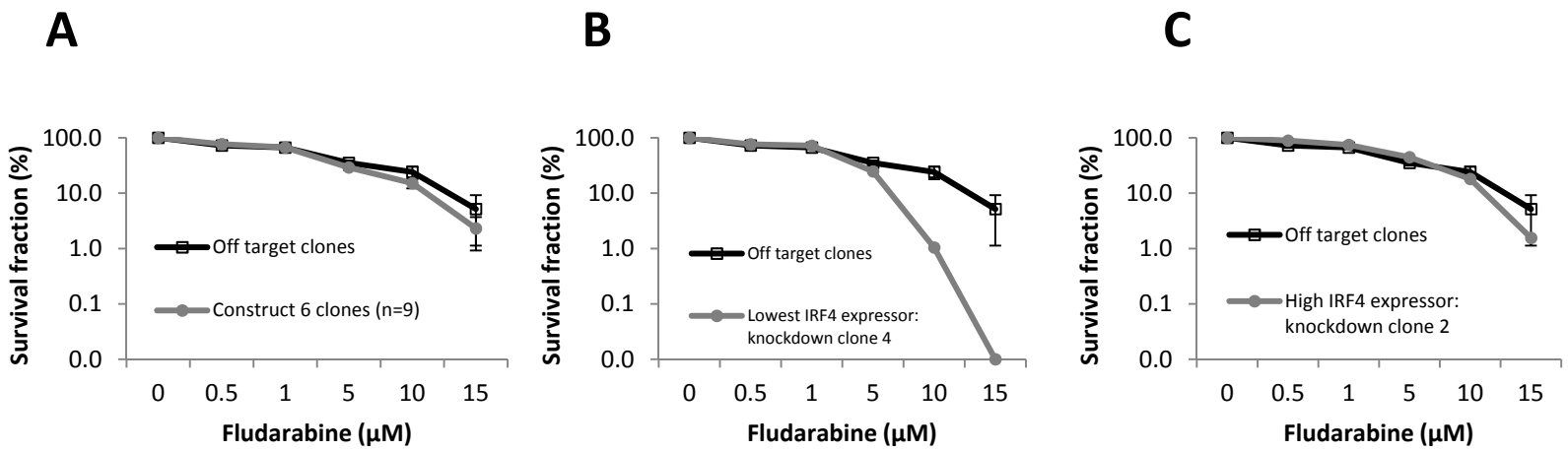

Figure 5.11 Growth inhibition with fludarabine (0-15µM) in TK6 cell clones with shRNA-mediated constitutive IRF4 knockdown

Three control TK6 cell clones generated from cells transduced with an off target shRNA construct and nine TK6 cell clones with constitutive IRF4 knockdown, generated from cells transduced with construct 6 shRNA targeted against *IRF4*, were seeded at $5x10^4$/ml in sterile 6 well plates and treated with fludarabine at the doses indicated. Cells were counted in exponential growth phase, and growth was normalised to cells which had been treated with DMSO alone (the vehicle in which fludarabine was delivered). Error bars represent the standard error of the mean.

A. Taken altogether, there was very little evidence in this experiment that IRF4 knockdown in the nine knockdown clones affected TK6 cell sensitivity to fludarabine at doses up to 15µM.

B. However, when the fludarabine-sensitivity of the lowest IRF4-expressing knockdown clones (clones 4) was compared directly to the three control clones, there was evidence of increased cytotoxicity in the clone with IRF4 knockdown at doses of 10 and 15µM.

C. In contrast, this increased sensitivty to fludarabine was much less apparent in the knockdown clones with highest IRF4 expression (clone 2).

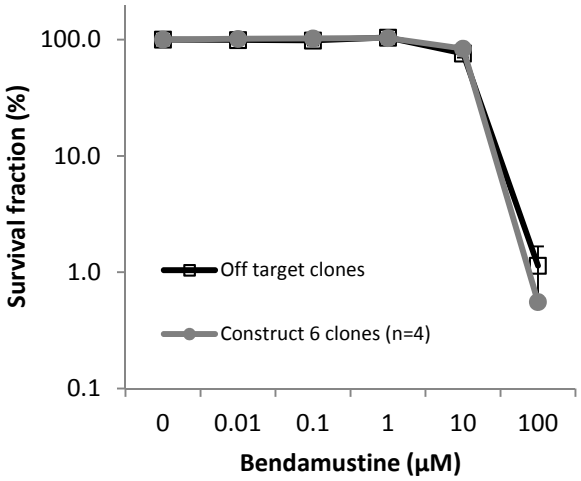

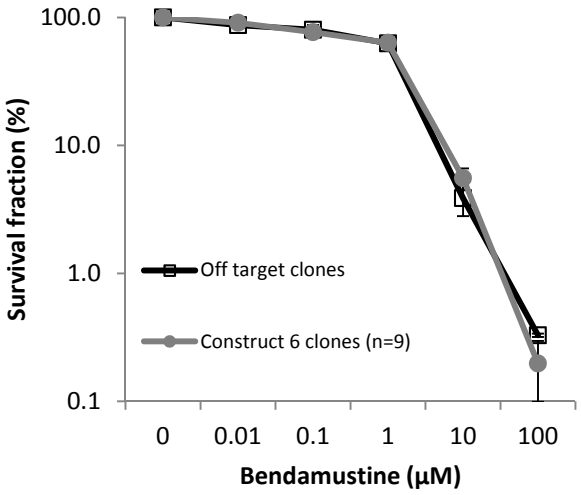

Figure 5.12 Bendamustine cytotoxicity in TK6 cells with stable shRNA-mediated IRF4 knockdown

TK6 cell clones with shRNA mediated IRF4 knockdown, and TK6 cell clones generated from cells transduced with an off target shRNA construct, were seeded at $5x10^4$/ml in a sterile 6 well plate and treated with bendamustine at the doses indicated. Cells were simultaneously treated with sterile water (the vehicle in which bendamustine was delivered) alone, and growth inhibition in bendamustine-treated cells was normalised to the the vehicle-only wells. Error bars represent standard error of the mean.

A. In an initial experiment, four knockdown clones (the two highest IRF4 expressors and the two lowest IRF4 expressors) were compared with the three control clones. There was no evidence of an effect of IRF4 knockdown on bendamustine sensitivity.

B. The experiment was repeated using all nine knockdown clones in comparison with the three control clones. Again, IRF4 knockdown did not affect TK6 cell sensitivity to bendamustine.

5.4 Discussion

The effect of IRF4 knockdown on growth kinetics and sensitivity to cytotoxic agents in TK6 was investigated using shRNA-mediated constitutive knockdown in stable cell clones. However, as discussed in chapter 4, the generation of MEC-1 and SU-DHL-6 cell clones with persistent, constitutive shRNA-mediated IRF4 knockdown was not achievable (section 4.3), and so cell growth and sensitivity to cytotoxic agents in these cell lines was investigated using only cells with transient siRNA-mediated IRF4 knockdown.

The generation of cell clones with stable, persistent shRNA-mediated IRF4 knockdown would have been preferable. Indeed, variability in the degree of siRNA-mediated knockdown often made interpretation of experimental data challenging. However, by using a combination of both approaches it was possible to discern some of the effects of IRF4 knockdown on growth kinetics and sensitivity to cytotoxic agents in these three B cell lines.

5.4.1 IRF4 knockdown and growth kinetics in B cells

Transient IRF4 knockdown had no effect on cell growth in MEC-1 cell line. In contrast, transient loss of IRF4 significantly impaired growth in SU-DHL-6 cells. Similarly, constitutive shRNA-mediated IRF4 knockdown impaired growth in TK6 cells. These findings are suggestive of a functional role for IRF4 in the maintenance of SU-DHL-6 and TK6 proliferation but not in MEC-1. The observation that MEC-1 and SU-DHL-6 express common IRF4 binding partners (IRF8 and PU.1) but TK6 does not (Figure 3.10), suggests that the role played by IRF4 in promoting proliferation in TK6 is independent of IRF8 and PU.1. It is also notable that IRF4 knockdown caused a slowing of growth (cytostatic) but not an overall depletion of cell numbers (cytotoxic), as was observed in a panel of myeloma cell lines through non-apoptotic cell death when IRF4 was knocked down by RNA interference techniques. (Shaffer et al., 2008) In the same study, the survival of the majority of a panel of lymphoma cell lines was unaffected by IRF4 knockdown. (Shaffer et al., 2008) In contrast, cell growth in Hodgkin lymphoma cell lines has also been shown to be impaired by IRF4 knockdown. (Aldinucci et al.,

2011) Thus, it appears that the effects of targeting IRF4 on growth kinetics and survival are not uniform, and are highly cell line dependent.

A further study has teased apart the effect of IRF4 knockdown in lymphoma cell lines, in more detail. This study demonstrated that IRF4 knockdown impairs growth in diffuse large B cell lymphoma lines of activated B cell type (ABC DLBCL), but not in diffuse large B cell lines of germinal centre type (GC DLBCL). Interestingly, IRF4 knockdown of only 50-60% was sufficient to demonstrate these effects in the ABC lymphoma lines. (Yang, 2012) It is perhaps surprising therefore, that SU-DHL-6 proliferation was observed here to be impaired by IRF4 knockdown, given that it is thought to be a lymphoma cell line of germinal centre origin. (Table 5.1)

Cell line sensitivity to IRF4 knockdown may relate to the stage of cell differentiation and to inherent differences in IRF4-mediated transcriptional programming. Consistent with this hypothesis, genome wide expression analysis has revealed that the programme of genes targeted by IRF4 in non-malignant B cells varies according to the stage of cell differentiation. For example, genes involved in cell proliferation are targeted by IRF4 in activated B cells but not in plasma cells. (Shaffer et al., 2008)

The data from this thesis demonstrate IRF4 dependency in an immature pre-GC B cell (TK6) and also a more mature B cell of GC origin (SU-DHL-6). The work by Shaffer and colleagues demonstrated IRF4 dependency in mature activated B cells and in post-GC malignant myeloma cells. (Shaffer et al., 2008) However, the data presented in this thesis suggest that MEC-1, a line derived from a CLL patient and expressing mature B cell markers (CD19, CD20, CD21, CD22) is not dependent on IRF4 expression for proliferation. This was despite IRF4 knockdown of at least 50% being achieved in the two independent siRNA experiments in MEC-1 in which growth kinetics were assessed, and knockdown of over 90% in one of them. Taken altogether, these data suggest that broad classification in terms of malignant cell of origin and germinal centre status does not predict IRF4 dependency. (Table 5.1)

Cell line/ tumour type	Origin of cell	Evidence for effect of IRF4 on growth	Reference
SU-DHL-6	GC origin, mature B cell	Growth impaired by IRF4 knockdown	Figure 5.5
TK6	Immature pre-GC centre, lymphoblastoid B cell	Growth impaired by IRF4 knockdown	Figure 5.8
MEC-1	Post GC, mature B cell, expressing surface immunoglobulin and CD22	Cell growth unaffected by IRF4 knockdown	Figure 5.1
Activated B cells	Mature circulating B cells, stimulated by IgM	IRF4 target genes include *MYC*, important for growth and proliferation	(Shaffer *et al.*, 2008)
Plasma cells	Post GC mature B cells	IRF4 does not target genes such as *MYC*	(Shaffer *et al.*, 2008)
Hodgkin lymphoma cell lines*	GC B cells	Growth impaired by IRF4 knockdown	(Aldinucci et al., 2011)
Myeloma cell lines$	Post GC mature B cells	Growth impaired by IRF4 knockdown	(Shaffer et al., 2008; Yang *et al.*, 2012)
Germinal centre lymphoma cell lines**	GC cell type	Cell growth unaffected by IRF4 knockdown	(Shaffer et al., 2008; Yang *et al.*, 2012)
Activated B cell lymphoma cell lines†	Activated B cell type	Growth impaired by IRF4 knockdown	(Shaffer *et al.*, 2008; Yang *et al.*, 2012)

Table 5.1 Effect of IRF4 on proliferation of a range of B cell lines
*Hodgkin lymphoma cell lines included: KM-H2, HDLM-2, L-428
$Myeloma cell lines included: ANBL6, UTMC2, L363, JIM3, LP1, EJM, KMS12, OCI-My5, SKMM1, H929
**Germinal centre lymphoma cell lines included: BJAB, OCI-Ly19, OCI-Ly7, Ramos, HT
† Activated B cell lymphoma cell lines included: TMD8, OCI-Ly10, U2932, HBL1, HLY1
GC: germinal centre

5.4.2 IRF4 knockdown and sensitivity to anti-leukemic chemotherapy

Transient IRF4 knockdown did not have any effect on the sensitivity of SU-DHL-6 cells to fludarabine-induced growth inhibition in two independent experiments. There were however suggestions of a possible effect of IRF4 knockdown in MEC-1 and TK6 cell lines, and some evidence that these effects might be governed by the threshold of IRF4 knockdown achieved.

In an initial experiment in MEC-1 cells with transient IRF4 knockdown, there appeared to be a suggestion of increased sensitivity to fludarabine, but this was not reproduced in two replicate experiments. Notably, however, the siRNA-mediated IRF4 knockdown achieved in the cells used in the initial fludarabine assay was far greater than that achieved in the cells used in the subsequent experiments.

In addition, TK6 cell clones with the greatest constitutive IRF4 knockdown achieved by shRNA transduction showed strong evidence of increased sensitivity to fludarabine-induced growth inhibition, at doses of 10 and 15µM, while the cell clones with only modest IRF4 knockdown were insensitive to fludarabine-induced inhibition.

Taken together, these data suggest that IRF4 knockdown potentiates fludarabine–induced growth inhibition in TK6 and MEC-1 cells, but only if IRF4 expression is reduced to a critical threshold. In addition, the failure to generate clones with constitutive IRF4 knockdown from MEC-1 and SU-DHL-6 cell lines may have limited the ability to detect an effect of IRF4 knockdown on growth or cytotoxic sensitivity in these cell lines, as transient IRF4 knockdown may be insufficient to bring about functional effects on downstream pathways governing cell proliferation and cell death.

It is possible that targeting IRF4 therapeutically could be used to potentiate the anti-leukaemic activity of fludarabine. However, these observations would need to be reproduced with a small molecule inhibitor, which may not render the same effect as phenotypic loss of expression. Moreover, if potentiation is dependent on complete or almost complete loss of IRF4 function, this may be difficult to achieve therapeutically with a small molecule inhibitor, limiting the potential efficacy of such an approach.

Ibrutinib cytotoxicity was investigated in MEC-1 cells only. The effect of ibrutinib was not potentiated by IRF4 knockdown, although the knockdown achieved in the two independent siRNA experiments in which ibrutinib was tested was relatively modest (55-60%). Further examination of ibrutinib sensitivity in TK6 and SU-DHL-6 cell lines with IRF4 knockdown would be particularly interesting, specifically in light of published observations that synthetic lethality is achieved in ABC DLBCL cell lines, by the co-administration of lenalidomide and ibrutinib. (Yang, 2012) Lenalidomide disrupts a central regulatory hub, governed by IRF4, which represses interferon-β expression and augments pro-survival NFκB signalling in ABC DLBCL cells. Simultaneously, ibrutinib interrupts the oncogenic signalling via the B cell receptor, and thus interrupts the induction of IRF4 expression by NFκB signalling. (Yang, 2012) Given that, like ABC DLBCL, SU-DHL-6 and TK6 cell lines display impaired proliferation in the setting of IRF4 knockdown, it would be interesting to see if, similarly, IRF4 knockdown potentiates ibrutinib-induced cytotoxicity in these cell lines.

5.5 Summary of chapter 5

Using *in vitro* investigation of immortalised B cell lines, the effect of IRF4 knockdown on cell proliferation and sensitivity to cytotoxic agents used in CLL was investigated in this chapter. The data presented here are consistent with published literature, indicating that IRF4 knockdown inhibits cellular proliferation in some B cell lines, but not others. The effect of IRF4 knockdown on cell growth cannot be easily predicted by the stage of germinal centre maturation. SU-DHL-6 and TK6 cell lines display impaired growth when they are subjected to IRF4 knockdown, but MEC-1 cell line appears to be unaffected.

Likewise, potentiation of fludarabine-induced growth-inhibition is also cell line dependent, and critically, may be dependent on the degree of IRF4 knockdown achieved. TK6 and MEC-1 displayed increased sensitivity to fludarabine when a substantial degree of knockdown was achieved. However, even substantial IRF4 knockdown did not affect the sensitivity of SU-DHL-6 cells to fludarabine. Benadmustine and ibrutinib cytotoxicity were not affected by IRF4 knockdown in any of the cell lines, in the limited experiments performed here.

Chapter 6. The role of IRF4 as a regulator of *CD38* in primary CLL lymphocytes cultured *ex vivo*

6.1 Introduction

Given that the IRF4 SNP, rs872071, is strongly associated with the risk of CLL, and also significantly associated with CD38 positivity in CLL patients, this chapter sought to investigate whether there was evidence of a functional link between the expression of IRF4 and CD38 in primary CLL cells.

Despite their long half-life *in vivo*, primary CLL lymphocytes are notoriously difficult to maintain *ex vivo* and die rapidly when cultured in media, with at least a fifth of cells dying in the first 30 hours. (Collins et al., 1989) This reflects the importance of the tumour microenvironment to the survival and proliferation of CLL cells. *In vitro* co-culture models have been designed to recreate some of the signals delivered by the tumour microenvironment to facilitate primary CLL cell maintenance and proliferation *ex vivo*. A review of three different co-culture systems, utilising mouse fibroblast monolayers transfected with either human CD40 ligand or CD31, and a human microvascular endothelial cell line, HMEC-1, compared the phenotype and proliferative signals induced in CLL cells. (Hamilton et al., 2012) All three systems markedly enhanced CLL survival *ex vivo*, and CD40L-expressing fibroblast co-culture (CD40L monolayer) led to the greatest promotion of CLL cell proliferation. (Hamilton et al., 2012)

6.2 Aims of chapter 6

Having demonstrated that IRF4 binds to the *CD38* EICE binding site in SU-DHL6 cells, and to the 5'UTR in SU-DHL-6 and MEC-1 cells (section 3.3.4.b), evidence for IRF4-*CD38* binding in primary leukaemic cells was investigated.

Specifically, the aims of Chapter 6 were as follows:

- To use a CD40L-expressing co-culture system to maintain primary CLL cells *ex vivo*.
- To determine IRF4 expression by western immunoblotting and CD38 expression by flow cytometry, in primary CLL lymphocytes before and after co-culture.

- To use ChIP to determine whether IRF4 binds to *CD38* in primary CLL cells
- To use ChIP to determine whether co-culture of primary CLL lymphocytes on CD40L monolayer affects IRF4-*CD38* binding
- To demonstrate the effect of CD40L monolayer co-culture on *CD38* transcriptional activity in primary CLL lymphocytes, as determined by ChIP using histone methylation marks.

6.3 Results

6.3.1 Primary CLL lymphocytes express IRF4

Details of the patients from whom CLL samples were obtained, and the experiments in which the cells were used in this chapter, are shown in Table 6.1. Data from a total 18 patients are presented here.

IRF4 protein expression was determined by western immunoblotting in *ex vivo* primary CLL lymphocytes obtained from 11 patients, prior to co-culture. (Figure 6.1) There was evidence of marked heterogeneity in the degree of IRF4 expression between these patients, with 9 out of 11 patient samples positive for IRF4 expression. Of these, 3 patients had strong IRF4 expression (IRF4+ strong) (patients 1, 4 and 8), a further 3 patients had moderate expression (IRF4+ moderate) (patients 3, 6 and 7), and 3 patients had only weak IRF4 expression (IRF4+ weak) (patients 5, 9 and 10).

6.3.2 Primary CLL lymphocytes co-culture on a CD40L monolayer

6.3.2.a Primary CLL lymphocytes demonstrate upregulation of IRF4 protein expression on CD40L co-culture

Co-culture of primary CLL cells on a CD40L-expressing fibroblast monolayer (CD40L monolayer) led to an upregulation of IRF4 expression in the primary cells, in comparison to CLL cells simultaneously co-cultured on a control non-expressor monolayer (NTL monolayer). (Figure 6.2) This was demonstrated by western immunoblotting and was consistently observed in CLL cells from five different patients (patients 12-16). IRF4 expression was consistently upregulated in cells cultured on the CD40L monolayer within 24 hours of the co-culture, and in two patients (patients 15 and 16) IRF4 upregulation on the CD40L monolayer persisted for up to 14 days relative to those cultured on the control NTL monolayer (data not shown).

Both the CD40L and NTL fibroblast co-culture cells were separately analysed by western immunoblotting to confirm that they do not express IRF4 (data not shown), thus ensuring that any potential contamination from fibroblast cells did not affect the IRF4 expression results of the harvested CLL cells.

Patient	Prognostic information	
1	del(11q), del(13q) CD38+	Immunoblotting: IRF4 expression
2	CD38-	Immunoblotting: IRF4 expression CFSE labelling
3	CD38+	Immunoblotting: IRF4 expression ChIP studies
4	CD38-	Immunoblotting: IRF4 expression ChIP studies
5	CD38-	Immunoblotting: IRF4 expression ChIP studies
6	CD38-	Immunoblotting: IRF4 expression ChIP studies
7	CD38-	Immunoblotting: IRF4 expression ChIP studies
8	del(17p) CD38-	Immunoblotting: IRF4 expression CFSE labelling
9	CD38-	Immunoblotting: IRF4 expression ChIP studies
10	CD38-	Immunoblotting: IRF4 expression
11	del(11q) CD38+	Immunoblotting: IRF4 expression
12		Upregulation of IRF4 on CD40L monolayer co-culture
13		Upregulation of IRF4 on CD40L monolayer co-culture
14		Upregulation of IRF4 on CD40L monolayer co-culture
15	Normal karyotype	Upregulation of IRF4 on CD40L monolayer co-culture
16	CD38+	Upregulation of IRF4 on CD40L monolayer co-culture
17	CD38-	Flow cytometry to determine CD38 expression
18	CD38+	Flow cytometry to determine CD38 expression

Table 6.1 Patient characteristics
Blood enriched for primary CLL lymphocytes was obtained from 18 patients by separation from whole blood by density medium gradient centrifugation. The samples were then used in a number of investigations: western immunoblotting to determine IRF4 expression; CFSE labelling and flow cytometry to determine evidence of proliferation after CD40L monolayer co-culture; flow cytometry to determine CD38 expression; ChIP studies to determine IRF4-*CD38* binding, and binding by histone methylation marks to *CD38*. The experiments in which each sample was used are indicated.

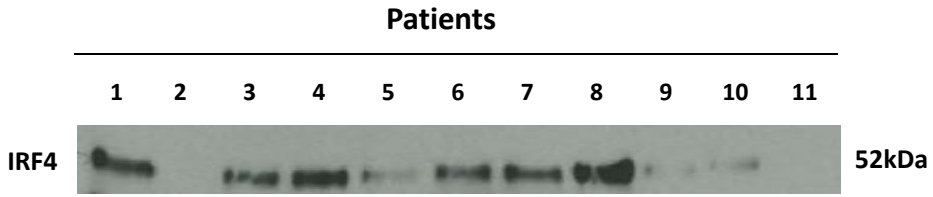

Figure 6.1 IRF4 expression by western immunoblotting in primary lymphocytes from 11 CLL patients
Primary CLL lymphocytes were obtained from 11 patients and whole cell extracts were prepared prior to co-culture. After quantifying the protein concentration obtained from each sample using Pierce BCA assay, equal quantities of protein per sample were loaded for gel electrophoresis by SDS-PAGE. IRF4 expression was heterogeneous. Two of the patients (patients 2 and 11) did not express IRF4. Three patients (patients 5, 9 and 10) had weak expression. Expression was moderate in 3 patients (patients 3, 6 and 7) and strong in the remaining 3 patients (patients 1,4 and 8).

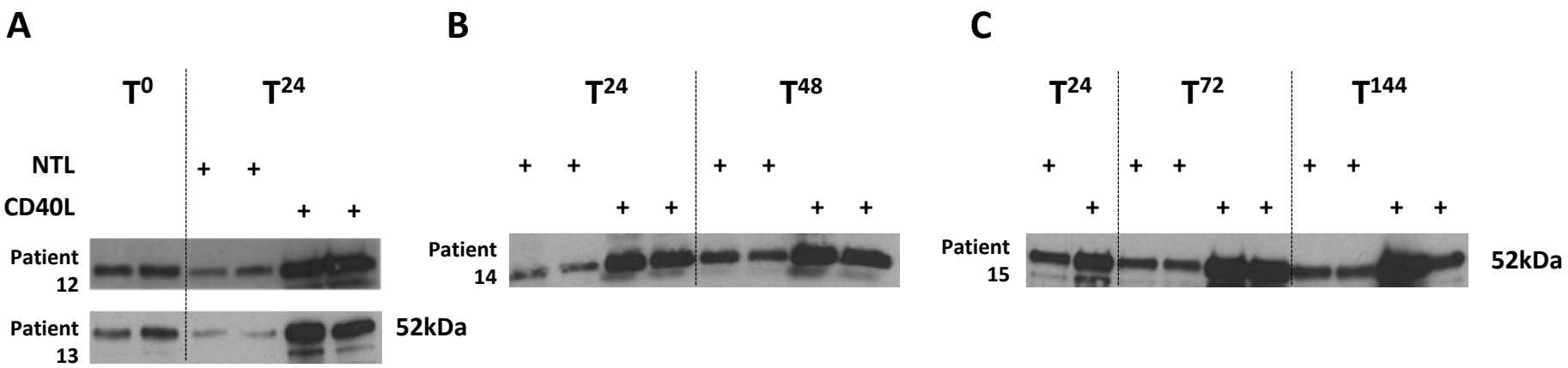

Figure 6.2 IRF4 expression in primary CLL lymphocytes after culture on CD40L-expressing fibroblast monolayer

Primary CLL cells separated from peripheral blood on a density medium gradient were cultured on a CD40L-expressing mouse fibroblast monolayer (CD40L), or simultaneously on a control non-expressor fibroblast layer (NTL). CLL cells were then harvested at the time points indicated and cellular proteins were extracted for western immunoblotting to determine the level of IRF4 protein expression. Whole cell extract protein content was quantified by BCA assay and equal quantities of protein were loaded for each protein electrophoresis. IRF4 expression in primary CLL lymphocytes after CD40L co-culture was investigated in 5 patients. IRF4 expression was consistently upregulated in all of these 5, and representative western immunoblots of cells from 4 patients are demonstrated here.

A. CLL cells from two patients, (12 and 13) both expressed IRF4 at T^0 prior to co-culture. After 24 hours on co-culture, IRF4 expression was substantially greater in the CLL cells that had been cultured on the CD40L-expressing monolayer, compared to those cultured on the control NTL monolayer.

B. Similarly, CLL cells from patient 14 expressed more IRF4 protein at time points T^{24} and T^{48} when they were cultured on CD40L monolayer.

C. Cells from patient 15 were cultured on the CD40L or control NTL monolayer for up to 6 days. IRF4 expression continued to be greater in the cells cultured on the CD40L layer, compared to those cultured on the control NTL layer.

6.3.2.b Primary CLL lymphocyte proliferation on CD40L monolayer

Evidence of CLL lymphocyte proliferation on the CD40L monolayer was demonstrated in cells from two patients (patients 2 and 8). Primary CLL lymphocytes were obtained from whole blood by separation of the mononuclear cell layer by density medium gradient centrifugation, and the mononuclear cells were then immediately labelled with carboxyfluorescein succinimidyl ester (CFSE) prior to co-culture. CFSE is a fluorescent cell-permeable dye that binds to cytoplasmic amines. It remains bound in the cytoplasm in daughter cells after cell division, and its fluorescence intensity thus progressively halves with each cell division. Evidence of cell division can therefore be monitored by flow cytometry. Cells were labelled with CFSE and then co-cultured on either the CD40L monolayer or on the control NTL monolayer.

Measurement of CFSE by flow cytometry provided evidence of proliferation in the CLL cells from both of these patients after culture on the CD40L monolayer. (Figure 6.3) Proliferation is demonstrated by the development of smaller peaks with lower CFSE fluorescence per cell indicating cell proliferation, developing from day 9 (patient 2) and day 5 (patient 8). On the NTL monolayer, there was a modest but progressive loss of CFSE signal due to leaching of CFSE from the membrane, (Lyons, 1999) but no evidence of a loss in peak height concomitant with proliferation.

Attempts were made to demonstrate evidence of proliferation in the primary CLL lymphocytes of a further two patients, but there was no evidence of proliferation demonstrable by CFSE fluorescence in either of these experiments (data not shown). Notably, however, the cells in both of these cases had been previously cryopreserved. Furthermore, an attempt to replicate the CFSE experiment in patient 8, using cryopreserved cells was also unsuccessful (data not shown). While these numbers are small, these data suggest that proliferation is not demonstrable by CFSE staining in primary CLL cells that have been previously cryopreserved.

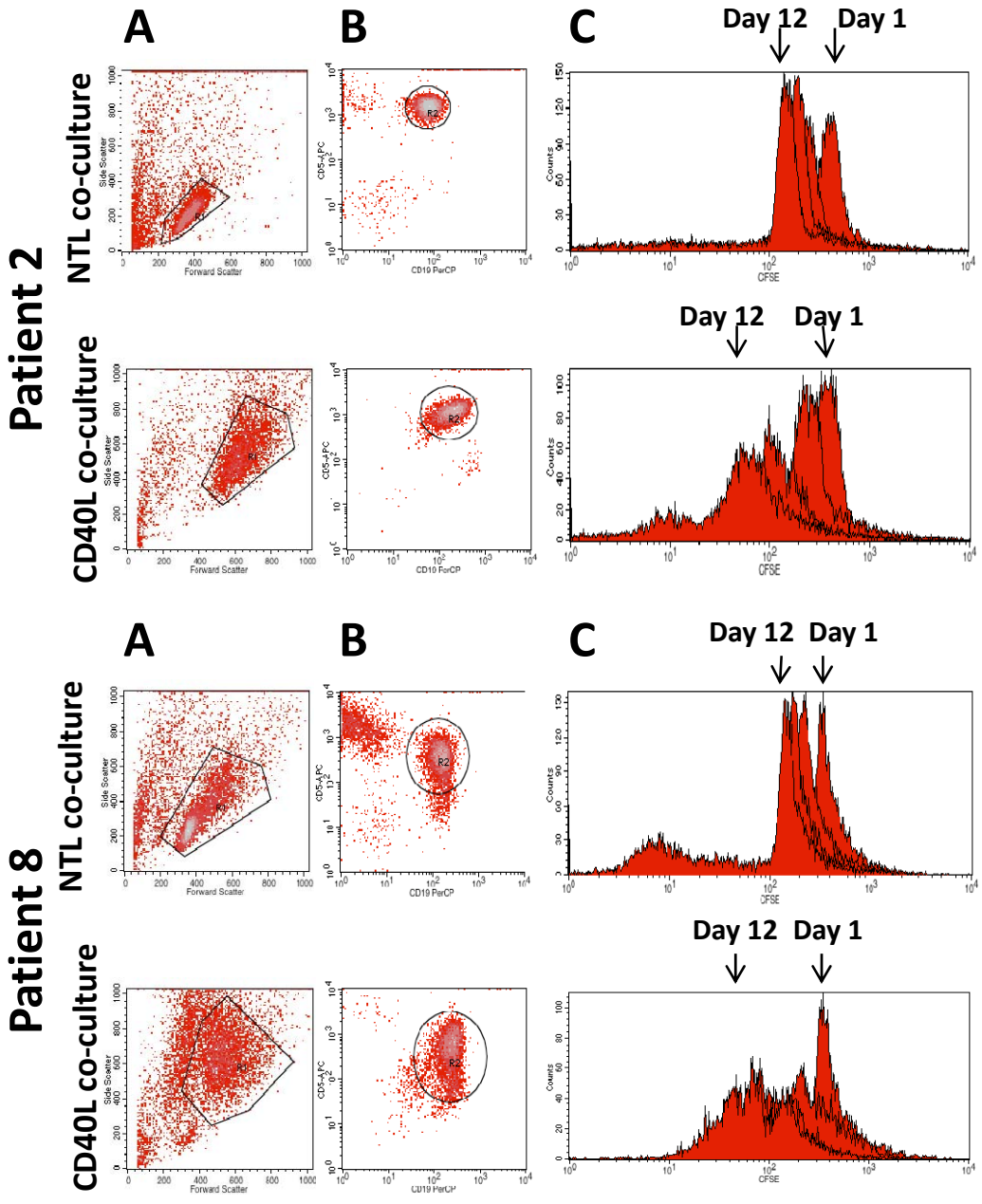

Figure 6.3 Proliferation of CLL lymphocytes cultured on CD40L monolayer
Primary CLL lymphocytes from two patients (patients 2 and 8) were labelled with carboxyfluorescein succinimidyl ester (CFSE). The cells were then cultured on a CD40L monolayer or on an NTL monolayer. Cells were collected at days 1, 5, 9 and 12 and analysed by flow cytometry. Representative dot plots demonstrating cell size and complexity (**A**), and CD5/ CD19 positivity (**B**) are indicated from day 12 for all cells. Overlay histograms demonstrating CFSE expression at days 1,5,9 and 12 (from right to left) for all cells are shown (**C**). Forward and side scatter measurements indicated an increase in the size and complexity of CLL cells cultured on the CD40L monolayer compared to those cultured on the NTL monolayer (**A**). Cells from both patients demonstrated only a modest reduction in CFSE fluorescence intensity from days 1 to 12 with a constant number of cells seen per peak, when cultured on the NTL monolayer (**C**). However, cells cultured on the CD40L monolayer demonstrated a clear reduction in CFSE intensity coupled with a reduction in the cell numbers in each peak. This is in keeping with proliferation of cells cultured on the CD40L monolayer.

6.3.2.c CD38 expression in primary CLL lymphocytes co-cultured on CD40L monolayer

CD38 surface expression was investigated by flow cytometry in primary CLL lymphocytes that had been co-cultured on the CD40L monolayer. Optimal antibody concentration was first selected for use as discussed previously. (Section 2.7.2) CLL cells from two patients, 17 and 18, who had been selected for their contrasting CD38 expression, were analysed by flow cytometry prior to co-culture. This confirmed that patient 18 was CD38+ (90% CD38 positive) and that patient 17 was CD38- (5% CD38 positivity). (Table 6.2) After 24 hours of co-culture, the cells were harvested from the NTL and CD40L monolayers, and re-analysed by flow cytometry. This revealed evidence of a very modest increase in CD38 expression in the cells co-cultured on the CD40L monolayer, as determined by geometric mean fluorescence intensity and CD38 percentage positivity. However, the relative mean fluorescence (RMF) was unchanged. (Table 6.2) Given that the RMF is normalised to the geometric mean fluorescence intensity of the isotype-labelled cells, these findings suggest that no substantial overall change in CD38 expression occurred. Indeed, an overall increase in antibody binding may have occurred secondary to co-culture on the CD40L monolayer. In contrast, after CD40L monolayer co-culture, there appeared to be a modest reduction in CD38 surface expression in cells from patient 18, compared to cells cultured on the NTL monolayer. This was particularly evident in the RMF data which demonstrated a reduction from 12.53 (at baseline) to 7.46 after 24 hours of CD40L co-culture. CD38 positivity as determined by RMF appeared stable after 24 hours of NTL monolayer co-culture in these cells (11.5). (Table 6.2) Furthermore, inspection of the histogram plots presenting cells from patient 18 after 24 hours of co-culture, demonstrated the possible development of a bimodal cell population in cells cultured on the CD40L monolayer. (Figure 6.4) While these data are considered in isolation, they are suggestive of an effect by the CD40L monolayer co-culture, on CD38 expression in the CD38 positive cells from patient 18.

			CD38 % positivity	Geometric mean fluorescence	Relative mean fluorescence (RMF)
Patient 17	**Prior to co-culture**		4.97	7.19	0.95
	T^{24} on co-culture	**NTL co-culture**	1.01	5.73	0.78
		CD40L co-culture	14.61	10.23	1.22
Patient 18	**Prior to co-culture**		89.83	112.98	12.53
	T^{24} on co-culture	**NTL co-culture**	77.79	89.51	11.5
		CD40L co-culture	70.37	81.38	7.46

Table 6.2 CD38 expression in primary CLL lymphocytes after co-culture on CD40L monolayer

Primary lymphocytes from two CLL patients: patient 17 (known to be CD38-) and patient 18 (known to be CD38+) were cultured on the NTL monolayer or CD40L monolayer for 24 hours and then analysed by flow cytometry to investigate any early effect on CD38 surface expression. Prior to co-culture, CD38 negativity was confirmed in patient 17 (4.97% CD38 positivity) and patient 18 was confirmed to be 89.83% CD38+. After 24 hours on the co-culture monolayers, there appeared to be a modest increase in CD38% positivity and geometric mean fluorescence in patient 17 cells that had been cultured on the CD40L monolayer. However, the relative mean fluorescence (RMF), which also takes into account the geometric mean fluorescence intensity of the isotype-control labelled cells appeared unchanged. In contrast there did appear to be a modest reduction in CD38% positivity and geometric mean fluorescence in patient 18 cells after co-culture on the CD40L monolayer. This reduction was also seen in the RMF.

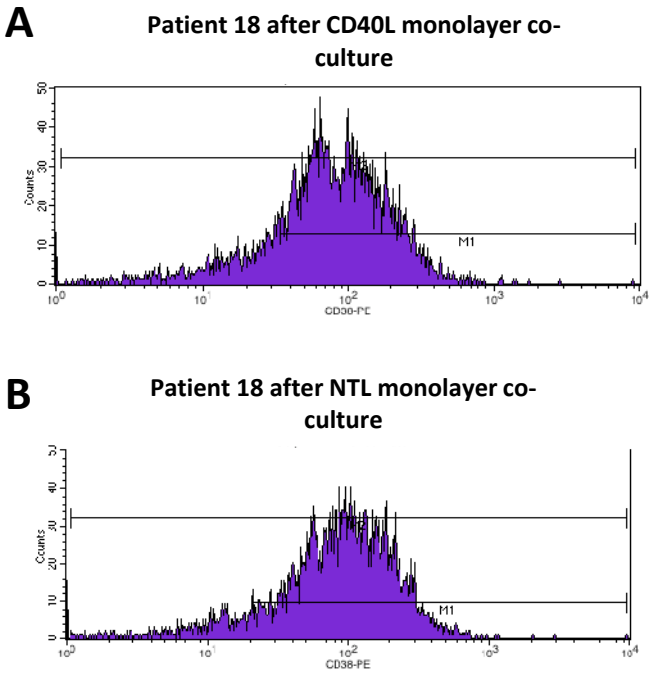

Figure 6.4 CD38 expression in primary CLL lymphocytes from a CD38+ CLL patient, after co-culture on a CD40L monolayer

Primary CLL lymphocytes from patient 18 (CD38+) were co-cultured on the NTL and CD40L monolayers for 24 hours and then analysed by flow cytometry to investigate CD38 expression. It was noted that the histogram plots revealed the suspicion of a bimodal cell population in the cells that had been co-cultured on the CD40L monolayer. **(A)** Cells that had been co-cultured on the NTL monolayer retained a normal distribution. **(B)**

6.3.3 ChIP using primary leukaemic lymphocytes

Having demonstrated IRF4-*CD38* binding in cell lines (Chapter 3), attempts were made to investigate IRF4-*CD38* binding by ChIP in fresh *ex vivo* primary CLL lymphocytes. Binding at the three previously identified putative binding sites in *CD38*: namely the element 1 EICE site and element 2 inverted IRF4 site (located in the first intronic region of *CD38*), were investigated alongside the site in the 5'UTR region of *CD38*.

Firstly, evidence of IRF4-*CD38* binding was sought in *ex vivo* CLL lymphocytes, immediately after their separation from whole blood and prior to any *in vitro* co-culture. Secondly, ChIP was performed on primary cells that had been cultured on either a CD40L monolayer or a control NTL monolayer. Chromatin was prepared manually and ChIP was performed using the SX-8G IP-Star® Compact Automated ChIP System.

Typically, less chromatin was used in the ChIPs performed in primary cells (chromatin per ChIP ranged from 10µg to 45µg) compared to the ChIPs that had been performed using chromatin prepared from cell lines. The amount of chromatin that could be used in the primary CLL ChIPs was dependent on the number of available cells after co-culture, and therefore the amount of chromatin that could be generated.

6.3.3.a IRF4-*CD38* binding in primary *ex vivo* CLL lymphocytes prior to co-culture

CLL cells obtained from one patient, patient 6 (IRF4 moderate +, CD38-) were used in a ChIP experiment, prior to any co-culture. Cells were obtained by density medium gradient centrifugation from whole blood, and chromatin was then manually prepared. Samples of sonicated chromatin were electrophoresed on a 1% agarose gel to determine fragment size, and this demonstrated adequate sonication with fragments of 100-200bp length after 10 cycles of sonication. (Figure 6.5A) There was very little evidence of IRF4-*CD38* binding at the three putative binding sites, with only a 2-fold enrichment by IRF4 antibody compared to control antibody, observed at the element 1 EICE and element 2 inverted IRF4 site. (Figure 6.5B)

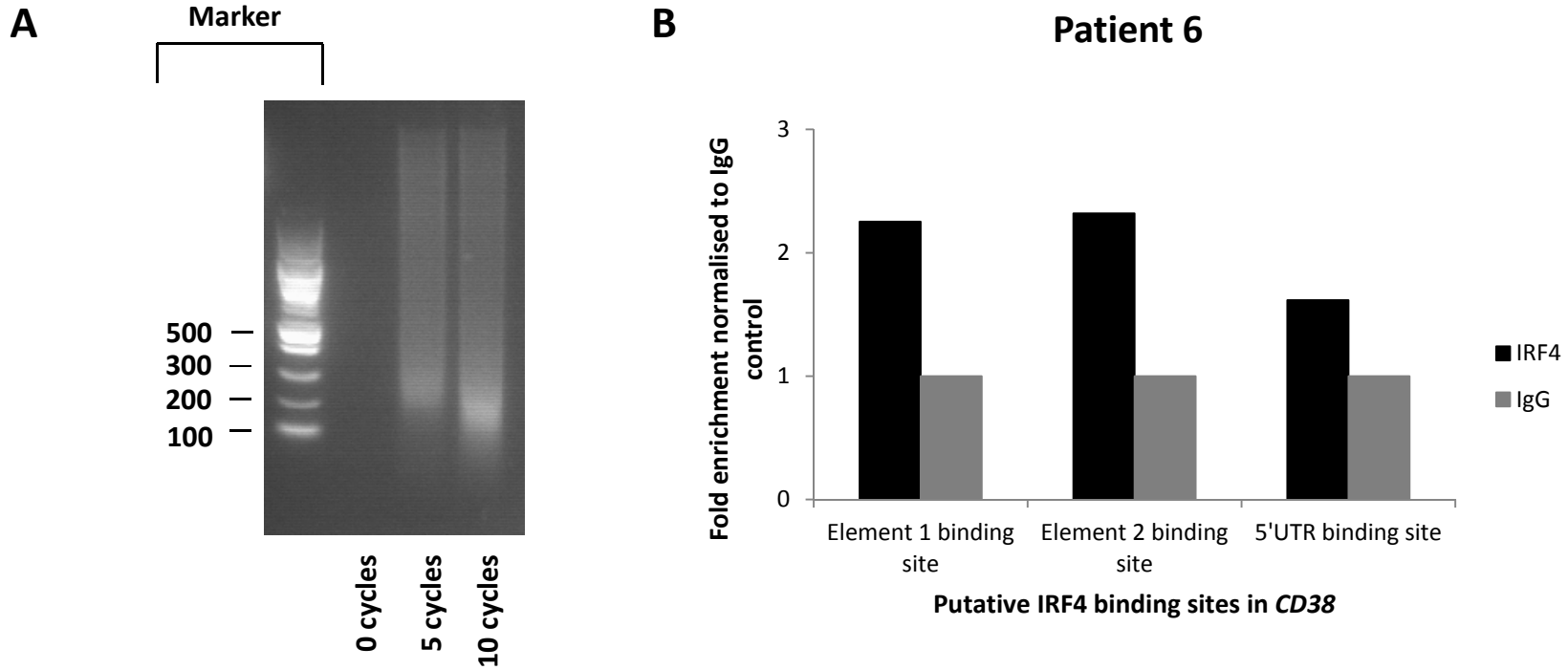

Figure 6.5 IRF4-*CD38* binding in primary CLL cells: patient 6

The mononuclear cell fraction, containing CLL lymphocytes, was separated from peripheral blood of patient 6 by density medium gradient centrifugation. After formaldehyde cross-linking, chromatin was manually prepared from the cells by lysis and then sonicated, to produce chromatin fragments for ChIP.

A. Chromatin fragments were electrophoresed on a 1% agarose gel to determine fragment size after 0, 5 and 10 cycles of sonication. After 10 cycles of sonication, fragments of between 100-200 base pairs were obtained, and these were used in ChIP. Marker band sizes are indicated, in base pairs.

B. There was very little evidence of IRF4-*CD38* binding either at the element 1 or element 2 binding sites in intron 1 of *CD38*, or at the 5'UTR site. Only a 2 fold enrichment of binding at the element 1 and 2 sites was observed, compared to that detected by a species-matched IgG control antibody.

These data therefore suggest very little evidence of IRF4-*CD38* binding in primary *ex vivo* CLL lymphocytes from this patient. Patient 6 is negative for surface CD38 expression (6% CD38 positivity).

6.3.3.b Investigation of IRF4-*CD38* binding in primary *ex vivo* CLL lymphocytes after CD40L monolayer co-culture

A specific aim of this chapter was to look for evidence of IRF4-*CD38* binding in cells that were co-cultured on the CD40L monolayer, which is associated with upregulation of IRF4 expression (Figure 6.2), compared to IRF4-*CD38* binding in cells cultured on the NTL monolayer. However, it became quickly apparent that this direct comparison would be technically challenging, specifically because of difficulties in generating chromatin of consistent quantity and quality from cells cultured on the two different monolayers.

Firstly, in the majority of cases, the chromatin yield post-sonication, as quantified by nanodrop estimation of DNA content, was consistently higher for cells that had been co-cultured on the CD40L monolayer than for cells from the same patient cultured on the NTL monolayer. (Table 6.3) In some cases, there was a 5 fold difference in the chromatin yield generated from cells cultured on the two different monolayers. To allow for this, the amount of chromatin used in each ChIP comparing NTL monolayer-cultured cells with CD40L monolayer-cultured cells was normalised. However, in some cases, there was simply inadequate chromatin generated from NTL monolayer-cultured cells for ChIP analysis.

In addition, there were clear differences in the size of chromatin fragments obtained from cells cultured on the CD40L monolayers compared to those cultured on the NTL monolayers, as determined by electrophoresis of the fragments on an agarose gel. Chromatin fragment size of between 100-1000bp in length is optimal for successful ChIP studies. (Schmidt et al., 2009) The aim was to generate chromatin fragments of equal sizes, from the CLL lymphocytes harvested from the two different co-culture conditions. However, this was very difficult to achieve and in several cases, there were prominent differences in the size of the fragments (data not shown).

DNA yield by nanodrop (ng/µl) after sonication			
Patient sample	**NTL monolayer co-culture**	**CD40L monolayer co-culture**	**Amount of chromatin used per ChIP (µg)**
3	262	452	25
4	47	274	27
5	103	536	45
6	382	557	25
7	104	541	45
9	324	478	25

Table 6.3 DNA yield from chromatin fragments after sonication: a comparison of DNA yield from primary CLL cells cultured on CD40L monolayer with cells cultured on NTL monolayer

Primary CLL lymphocytes were harvested after co-culture on CD40L monolayer or NTL monolayer. After formaldehyde cross-linking, cells were lysed to isolate chromatin and the lysate was then sonicated to produce chromatin fragments for ChIP. In the majority of cases (6 of 8), the DNA yield determined by nanopdrop was substantially greater for cells collected from the CD40L monolayer than for cells collected from the NTL monolayer. In some cases, the yield was up to 5 fold greater for CD40L monolayer-cultured cells.

Taken together, these issues with chromatin yield and chromatin fragment size, made it very difficult to make a valid comparison of IRF4-*CD38* binding in CD40L monolayer-cultured cells and NTL monolayer-cultured cells. The chromatin yield from CD40L monolayer-cultured cells was consistently better, and suitable chromatin fragment size was also more easily achieved in these cells. For these reasons therefore, ChIP results from CD40L monolayer-cultured cells are considered independent of paired results from NTL co-cultured cells, unless otherwise indicated.

6.3.3.c IRF4-*CD38* binding in primary *ex vivo* CLL lymphocytes after CD40L co-culture

Primary CLL lymphocytes from three patients (patients 7, 5 and 4) were used in ChIP experiments, after they had been co-cultured on a CD40L monolayer. The lymphocytes were harvested after three days of co-culture, and chromatin was then manually prepared. Agarose gel electrophoresis confirmed that appropriate chromatin fragment size, between 100-300 base pairs, had been obtained after sonication in all three cases. (Figure 6.6)

There was considerable variation in the degree of IRF4-*CD38* binding demonstrated by ChIP, in the three cases. There was very little evidence of IRF4-*CD38* binding in patient 7 (IRF+ moderate, CD38-), with only 2-fold enrichment seen at each of the three putative binding sites, with the IRF4 antibody. (Figure 6.7A) In contrast, there was much stronger evidence for IRF4-*CD38* binding in patients 5 (IRF4+ weak, CD38-) and 4 (IRF4+ strong, CD38-). Specifically, greater than 7-fold enrichment of chromatin by the IRF4 antibody compared to the control antibody was observed at the element 1 binding site and the 5' UTR site in patient 5. (Figure 6.7B) Furthermore, there was strong evidence of IRF4-*CD38* binding at all three sites in patient 4. Over 10-fold enrichment was seen at the element 2 inverted IRF4 and 5' UTR sites in patient 4, and enrichment at the element 1 EICE site was nearly 45 fold. (Figure 6.7C)

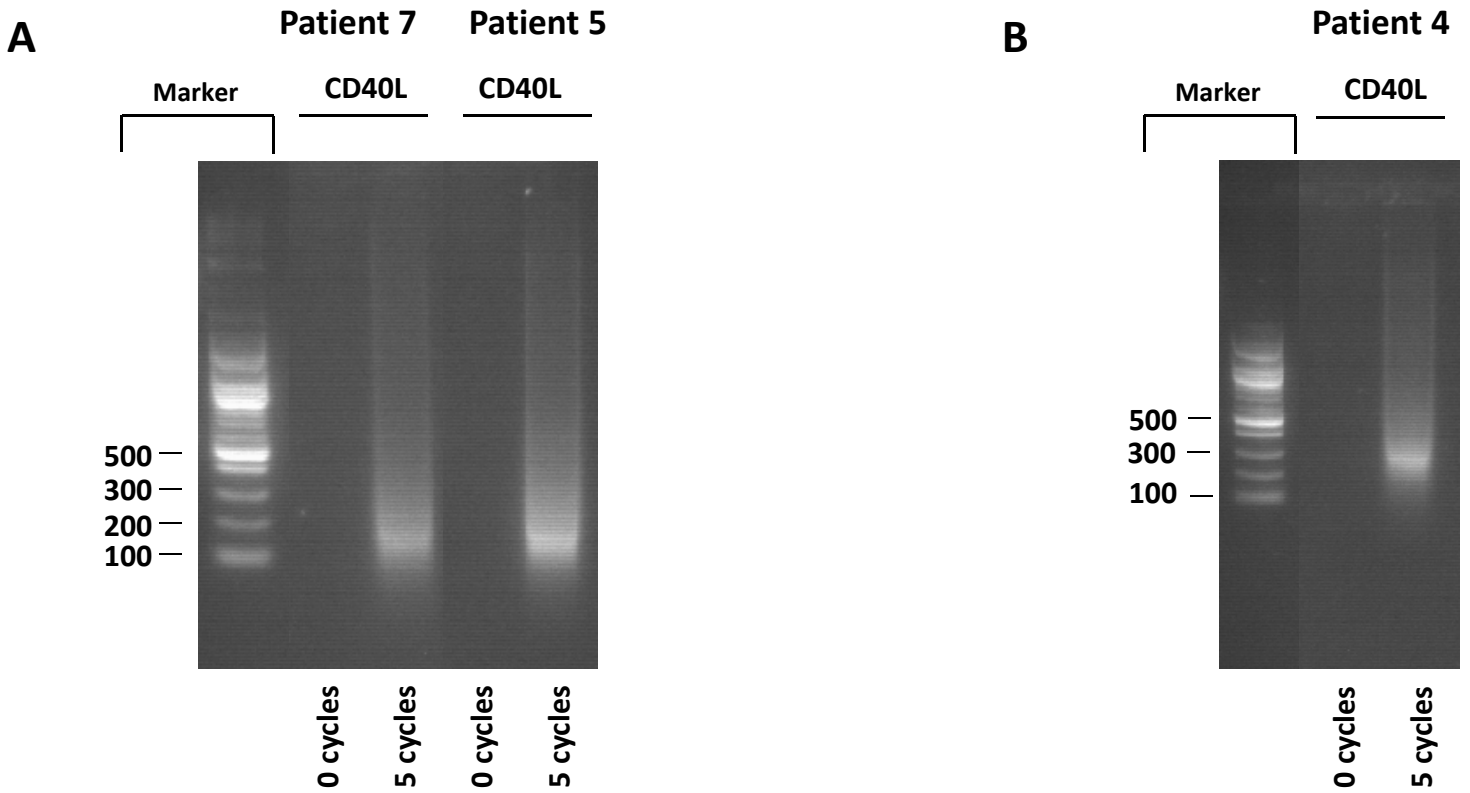

Figure 6.6 Agarose gel electrophoresis of chromatin fragments obtained from primary CLL lymphocytes from 3 patients, after CD40L monolayer co-culture

Primary CLL lymphocytes from 3 patients: patient 7 and 5 (**A**) and patient 4 (**B**) were co-cultured on a CD40L monolayer for three days. After harvesting the cells, chromatin was manually prepared. Sonicated chromatin fragments were then electrophoresed on a 1% agarose gel to determine fragment size. Appropriate fragment size for ChIP, of between 100 and 300 base pairs, was demonstrated in all 3 cases.

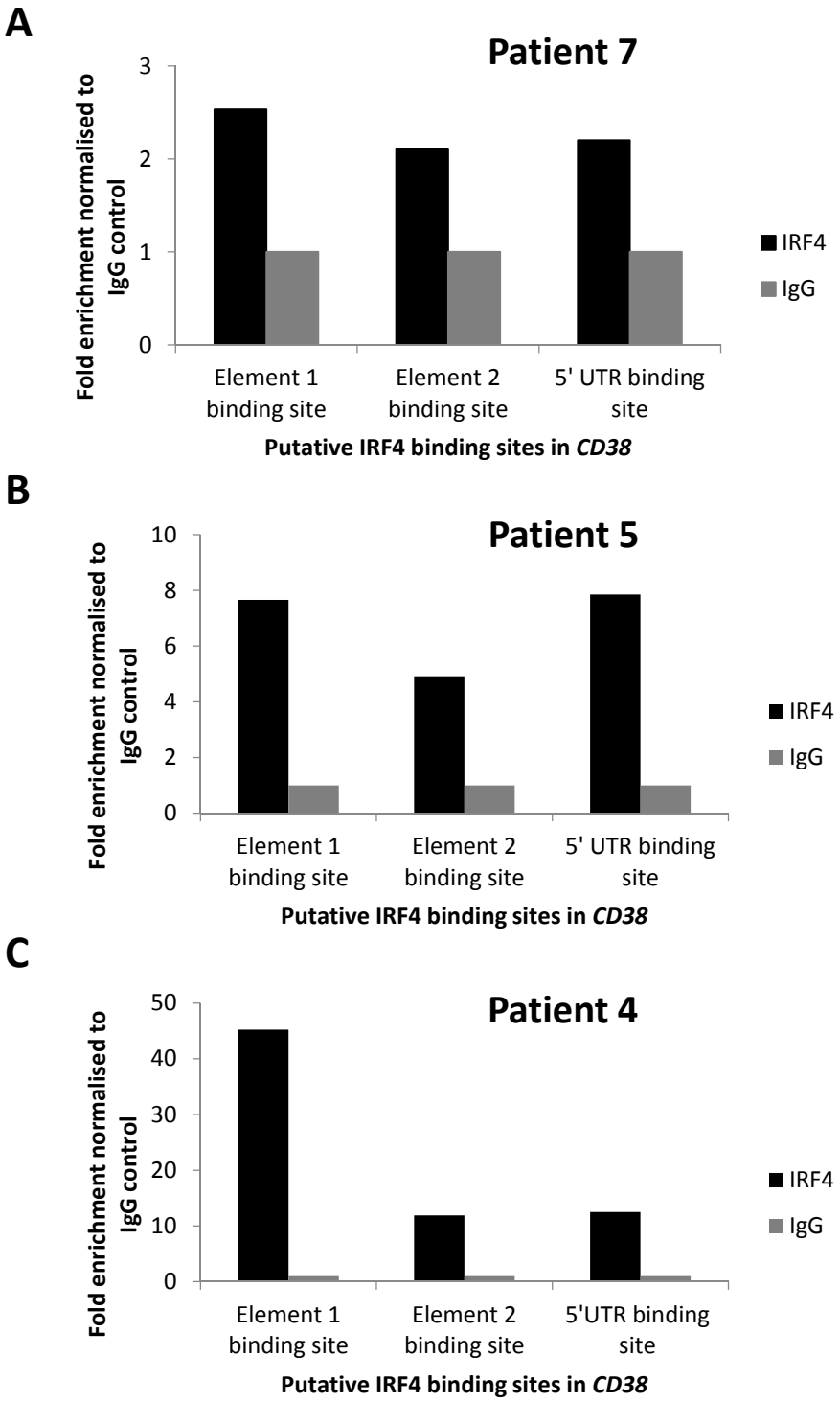

Figure 6.7 IRF4-*CD38* binding in primary CLL lymphocytes from 3 patients after co-culture on CD40L monolayer

Primary CLL lymphocytes from three patients were co-cultured on a CD40L monolayer for 3 days. Chromatin was then prepared from these cells, and used to determine IRF4-*CD38* binding by ChIP, at putative IRF4 binding sites in *CD38.*

A. There was very little evidence of IRF4-*CD38* binding in patient 7.

B. There was some evidence of IRF4 binding in patient 5 with 7-fold enrichment of binding by IRF4 antibody at the element 1 EICE binding site and at the 5'UTR binding site.

C. There was substantial evidence of IRF4-*CD38* binding in patient 4 with 45-fold enrichment of binding by IRF4 antibody at the element 1 EICE site.

These limited data indicate a variation in IRF4-*CD38* binding between three different patient samples, after co-culture on the CD40L monolayer, but the pattern of enhanced binding to *CD38* is independent of IRF4 expression. Notably, all of the patients investigated here had at least weak IRF4 expression by western immunoblotting, and all three patients were negative for surface CD38 expression.

6.3.3.d *CD38* binding by histone methylation marks after CD40L monolayer co-culture

ChIP was also performed using antibodies to histone methylation marks, as previously described in cell lines with siRNA mediated IRF4 knockdown. (Section 4.3) ChIP using histone methylation marks was performed in primary CLL lymphocytes from two patients: patients 3 (IRF4+ moderate, CD38+ strong) and 9 (IRF4+ weak, CD38-), in order to investigate transcriptional activation of *CD38* at the putative IRF4 binding sites before and after co-culture on the CD40L monolayer. Specifically, antibodies raised against trimethylated histone 3 lycine 4 (H3K4me3), and trimethylated histone 3 lycine 9 (H3K9me3) were used. H3K4me3 and H3K9me3 histone marks are associated with transcriptional activation and repression, respectively.

Firstly, ChIP using an antibody to H3K9me3 (repressive histone mark) was performed simultaneously with IRF4 ChIP in cells from patient 3. In this case, results are presented from both NTL monolayer-cultured and CD40L monolayer-cultured cells. Primary CLL lymphocytes from patient 3 were cultured on the NTL or CD40L monolayers for 3 days before being harvested for ChIP. Chromatin was prepared and the fragments obtained after sonication were electrophoresed on an agarose gel to confirm fragment size. (Figure 6.8A) Chromatin fragments of approximately equal and appropriate size for ChIP (between 100-300 base pairs), were obtained from cells cultured on the NTL monolayer as well as from cells co-cultured on the CD40L monolayer. Sufficient chromatin was also generated from both cell populations for ChIP. It was therefore possible to perform ChIP to investigate IRF4-*CD38* binding, in primary cells from this patient that had been exposed to NTL monolayer co-culture as well as in those exposed to the CD40L monolayer co-culture. There was limited evidence of IRF4-*CD38* binding at any of the investigated elements in *CD38*, regardless

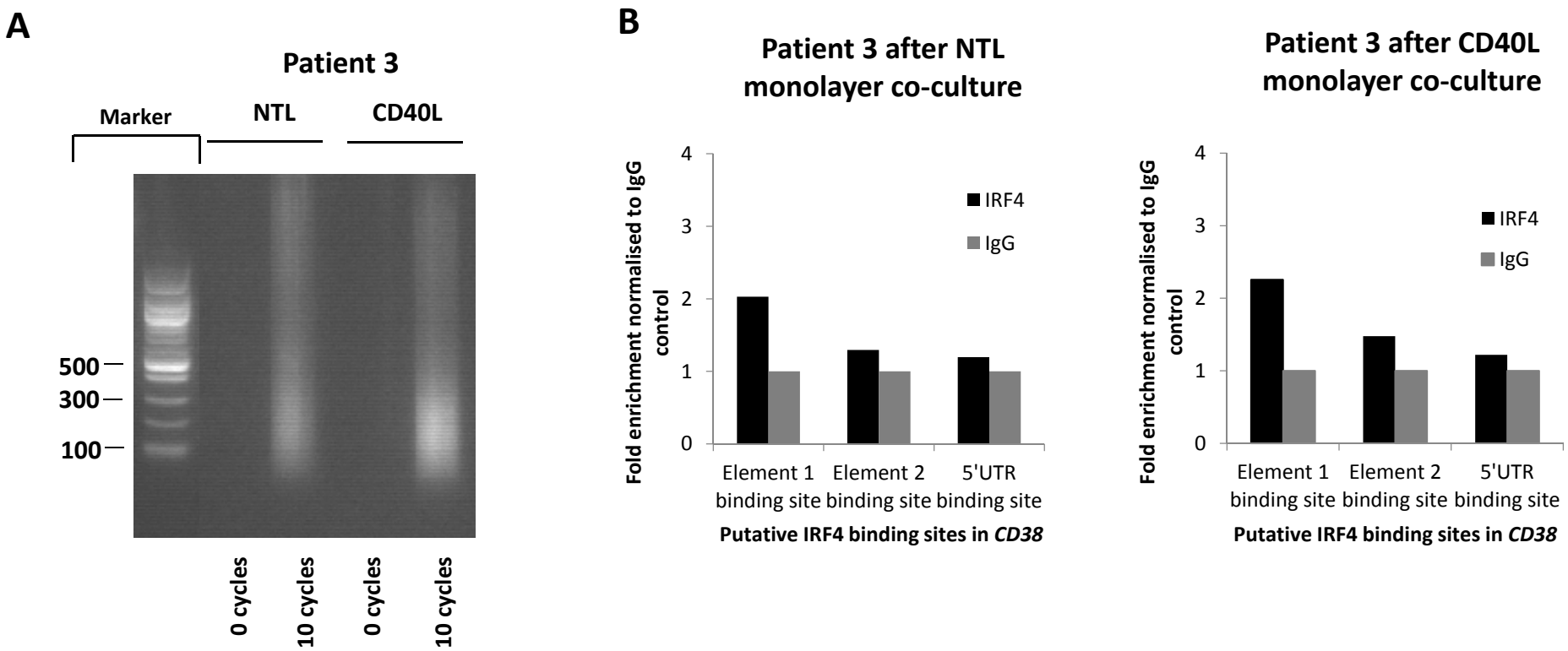

Figure 6.8 ChIP investigating IRF4-*CD38* binding in primary CLL lymphocytes from patient 3 after co culture on NTL or CD40L monolayers
Primary CLL lymphocytes from patient 3 were co-cultured on CD40L or NTL monolayers simultaneously for 4 days. Cells were then harvested and chromatin was manually prepared.
A. After sonication, chromatin fragments were electrophoresed on a 1% agarose gel. This demonstrated that appropriate chromatin fragments lengths had been obtained after 10 cycles of sonication, from cells cultured in both co-culture conditions. In addition, sufficient chromatin was available from cells from both co-culture conditions. ChIP was therefore performed on chromatin from both cell populations (NTL and CD40L monolayer co-culture), to determine evidence of IRF4-*CD38* binding. Size of marker bands is indicated in base pairs.
B. There was very little evidence of IRF4-*CD38* binding in primary CLL lymphocytes from this patient, after NTL monolayer co-culture or after CD40L monolayer co-culture.

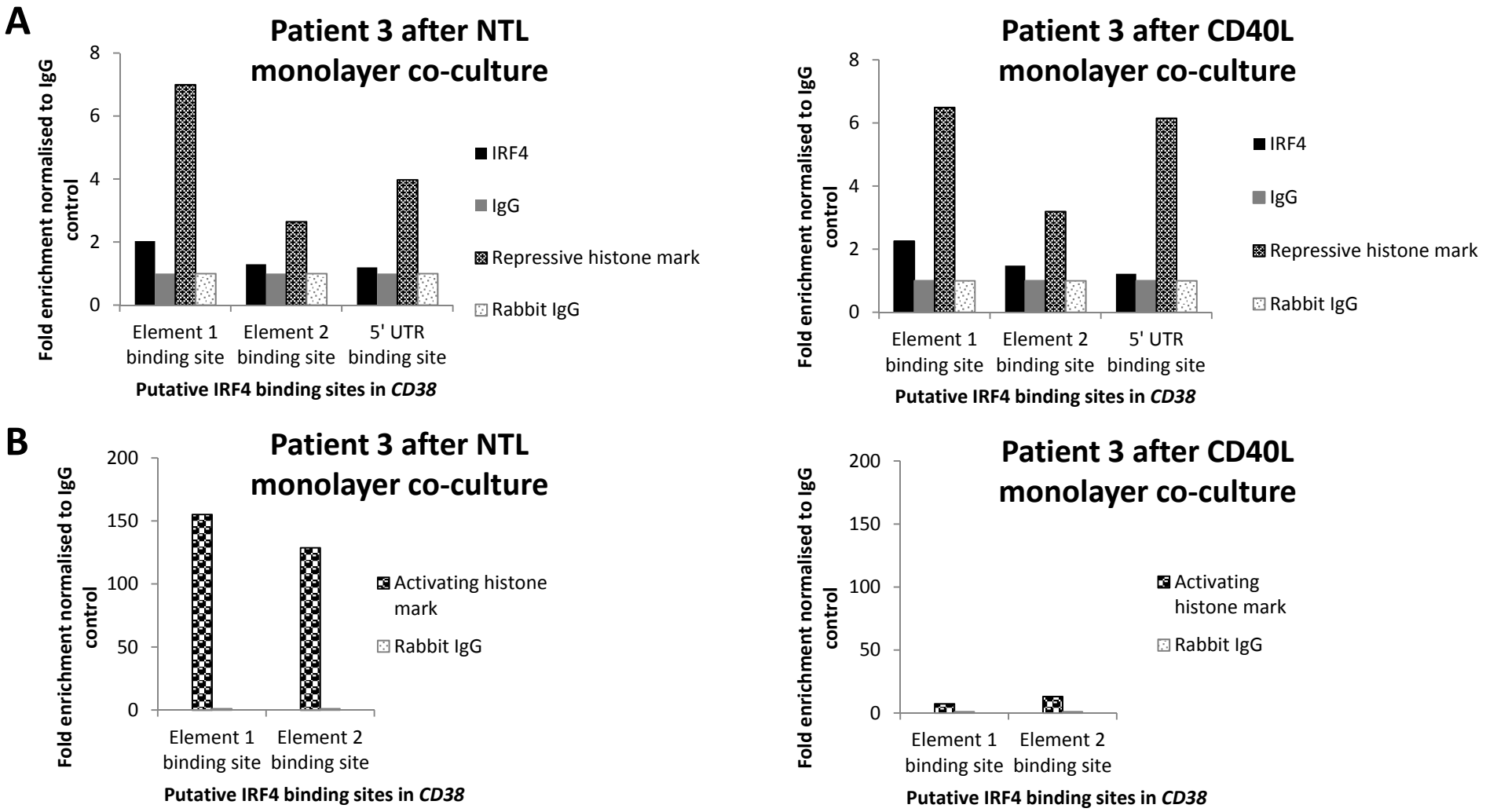

Figure 6.9 ChIP in patient 3 investigating binding by IRF4, H3K9me3 (repressive histone mark) and H3K4me3 (activating histone mark) antibody in *CD38*
A. Minimal IRF4-*CD38* binding was observed after both NTL and CD40L monolayer co-culture. Some binding by H3K9me3 repressive histone mark was apparent, but this did not vary substantially between cells co-cultured on NTL monolayer and those cultured on CD40L monolayer.
B. Subsequently, a ChIP using H3K4me3 activating histone mark antibody was performed. This showed a substantial downregulation in antibody binding in cells that had been co-cultured on the CD40L monolayer compared to those cultured on the NTL monolayer.

of whether cells had been cultured on the NTL or CD40L monolayer. (Figure 6.8B). Simultaneously, alongside the ChIP using IRF4 antibody, ChIP was also performed in cells from patient 3, using H3K9me3 antibody, which is indicative of transcriptional repression. (Figure 6.9A) There was some evidence of modest binding by the H3K9me3 antibody at the element 1 EICE site and at the 5'UTR site, after co-culture on both the NTL and CD40L-expressing cells. The degree of binding did not appear to be affected by the two different co-culture environments.

Given that an adequate quantity of chromatin remained available, a further ChIP was also performed using chromatin from patient 3, using the H3K4me3 antibody to look for evidence of transcriptional activation at the putative IRF4 binding sites in *CD38*. Notably, there was evidence of very substantial binding by H3K4me3 at the element 1 and element 2 binding sites (155 and 128 fold respectively) in cells cultured on the NTL layer. Binding by the H3K4me3 activating histone mark antibody was however substantially less at element 1 and element 2 binding sites in cells that had been cultured on the CD40L layer (7 and 13 fold binding observed, respectively). (Figure 6.9B) No result was available for binding at the 5' UTR site due to a technical error with the control IgG sample.

Finally, ChIP using an antibody to H3K9me3 (repressive histone mark) was performed in a further patient, patient 9. In this case, the chromatin prepared from cells co-cultured on the NTL monolayer was of insufficient quality to generate valid, interpretable results, and so data from the CD40L monolayer-cultured cells are presented only. Sonication of chromatin produced from cells cultured on the CD40L monolayer produced fragments that were 100-200bp in length. (Figure 6.10A) In cells that had been cultured on the CD40L co-culture layer, there was evidence of very substantial binding by the H3K9me3 antibody at the element 1 site, element 2 site and 5' UTR of *CD38* (70-fold, 50-fold and 90-fold, respectively). (Figure 6.10B) There was insufficient chromatin available to perform valid ChIP experiments in this case using the H3K4me3 (activating histone mark) or IRF4 antibodies. While the ChIP data in patient 9 apply only to CD40L-cultured cells, with no paired NTL-cultured cell data for comparison, they do appear to be supportive of the ChIP data from patient 3.

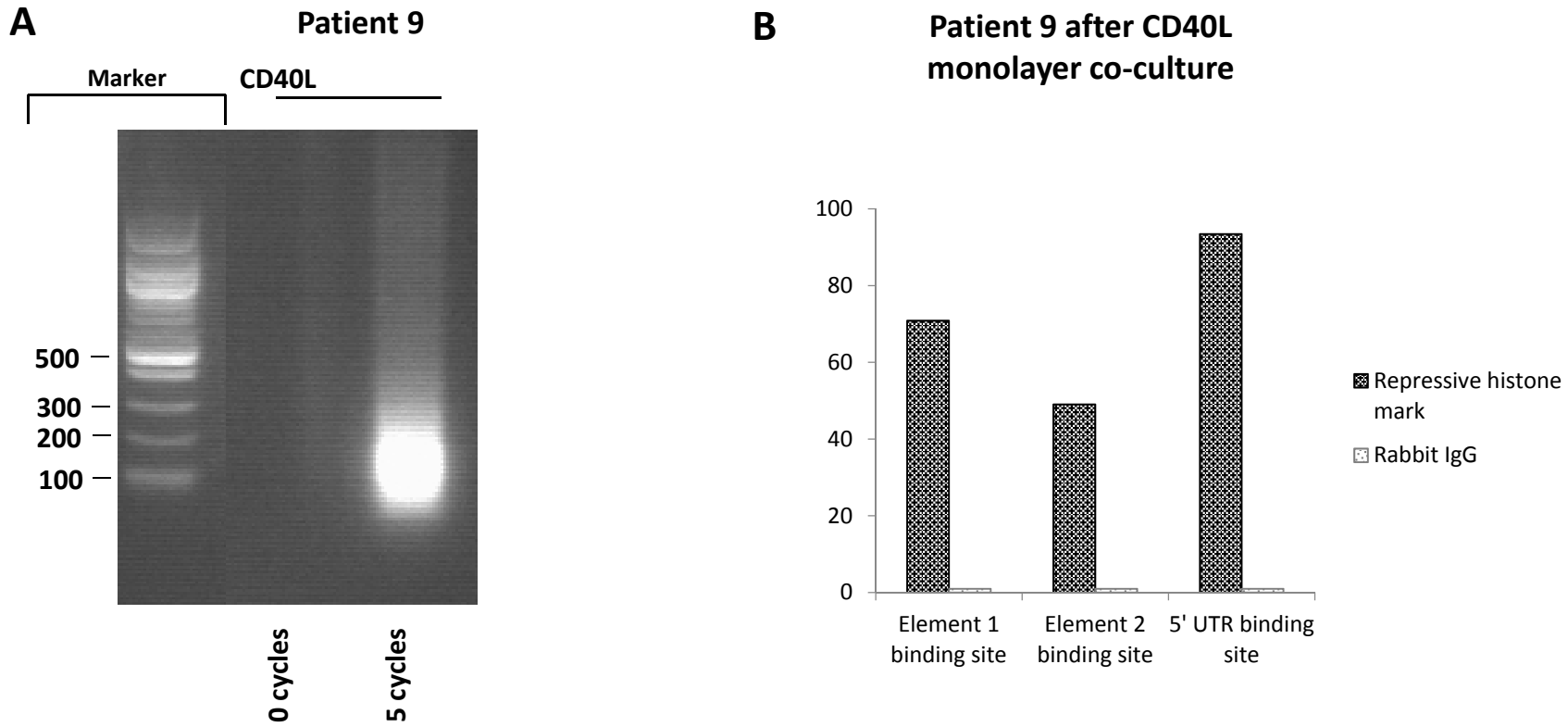

Figure 6.10 ChIP using antibody to H3K9me3 (repressive histone mark) in primary CLL lymphocytes from patient 9 after co-culture on CD40L monolayer

A. Chromatin was prepared from cells from patient 9 after 3 days of co-culture on CD40L monolayer. Electrophoresis of sonicated chromatin fragments on a 1.5% agarose gel demonstrated that fragments of 100-200 base pairs had been generated after 5 cycles of sonication.

B. ChIP using an antibody to H3K9me3 (a histone mark indicative of transcriptional repression) demonstrated evidence of substantial binding at all three putative IRF4 binding sites in *CD38*.

Specifically, the data from both patients are suggestive of reduced transcriptional activation at the three binding elements in *CD38* after co-culture with CD40L monolayer.

6.4 Discussion

In vivo interactions between CLL lymphocytes and CD40L-expressing T cells in the lymph node microenvironment support CLL cell activation and survival (Furman et al., 2000; Granziero et al., 2001; Ghia et al., 2002; Scielzo et al., 2011) and the CD40L co-culture monolayer has been established as one of a number of useful *in vitro* models that can be used to partially recapitulate this part of the microenvironment for the investigation of CLL. (Hamilton et al., 2012) The main aim of this chapter was to investigate evidence of IRF4-*CD38* binding in primary CLL lymphocytes, and to investigate whether this was affected by CD40L co-culture. However, technical difficulties in establishing reproducible, valid ChIP data in primary lymphocytes made this very challenging.

6.4.1 Technical issues in primary CLL lymphocyte ChIP

As previously discussed, the chromatin used in a ChIP assay is of prime importance in obtaining valid, interpretable results. In order to make a valid comparison of IRF4-*CD38* binding in primary CLL lymphocytes exposed to the two different co-culture conditions, it was essential to generate chromatin of equivalent quality and concentration from the two different cell populations. However, this proved very difficult to achieve. CLL cells cultured on the CD40L monolayer typically yielded more chromatin than cells cultured on the NTL monolayer. This may have been for a number of reasons. Firstly, the CD40L monolayer stimulates CLL cell proliferation (Hamilton et al., 2012) (Figure 6.3) such that more cells were available for chromatin generation after co-culture. Even when cells from the two co-culture conditions were counted prior to harvesting from the co-culture plates, the differences in cell density from the two conditions seemed insufficient to explain such large differences in chromatin yield. The differences in chromatin yield may therefore have also reflected intrinsic differences in the cells from the two co-culture conditions. Specifically, cells

may be less robust after NTL monolayer co-culture than CD40L monolayer culture and thus less able to withstand the rigors of the lysis procedure required for chromatin preparation. This would be consistent with the observation that frequently only a small pellet remained after each centrifugation step in the generation of chromatin from NTL monolayer-cultured cells. In addition, by increasing the proliferative index of the cells by CD40L monolayer culture, the proportion of cells in S and G2/M phase of the cell cycle may have been increased at the time the cells were harvested, thus increasing the amount of chromatin available for extraction per cell.

Furthermore, frequent discrepancies in chromatin fragment size generated from cells from the two different culture conditions also made valid comparisons of CD40L monolayer and NTL monolayer-cultured cells impossible in some cases. These discrepancies were likely responsible for the observation of higher than expected IgG control antibody-binding in some cases. As discussed earlier (section 3.4.2) one would expect that the control antibody should bind to chromatin fragments less than or equally to the antibody of interest. However, it was observed during ChIP of some of the primary samples that chromatin binding by the control antibody was greater than binding of chromatin to the antibody of interest (IRF4 antibody or a histone methylation antibody). As previously discussed, excessive non-specific antibody binding interferes with the validity of results, and ChIP data generated in the setting of excessive control antibody binding was not considered valid and is not presented here.

Thus, given these issues with obtaining paired samples of chromatin of sufficient quality and quantity from NTL monolayer-cultured and CD40L monolayer-cultured cells, valid ChIP data was available only from CD40L-co-cultured cells in a limited number of cases.

Nevertheless, despite these technical issues, some conclusions can be drawn from the data presented, and these are discussed further in section 6.4.5.

6.4.2 IRF4 expression in primary CLL lymphocytes before and after CD40L monolayer co-culture

CD40L monolayer co-culture led to an upregulation of IRF4 expression, as demonstrated by western immunoblotting, in CLL lymphocytes from five different patients. These findings were in keeping with previous observations that IRF4 expression is regulated by pathways known to drive lymphoid activation, including engagement of the CD40 receptor by CD40L. (Pernis, 2002) IRF4 expression was upregulated within 24 hours of co-culture, and persisted for up to 14 days in the two cases in which this time point was investigated. Given that CD40L is involved in the maintenance and survival of CLL lymphocytes *in vivo*, these findings would strongly suggest that IRF4 expression is upregulated in CLL cells in the T cell-rich lymph node microenvironment.

Furthermore, 9 out of 11 patients presented here were positive for IRF4 expression prior to co-culture. These findings are in keeping with previous studies which have demonstrated IRF4 expression in CLL. (Falini et al., 2000; Tsuboi et al., 2000; Chang et al., 2002b) However, these are very interesting observations, given the increasing body of evidence that suggests an association between CLL risk and low, or even absent, IRF4 expression, as discussed in section 6.4.3.

6.4.3 IRF4 expression in CLL

Having identified rs872071, the SNP in the 3'UTR region of IRF4, as a risk allele for CLL, Di Bernardo *et al* went on to demonstrate a relationship between rs872071 genotype and *IRF4* mRNA expression. The presence of the risk allele was associated with significantly lower IRF4 expression in Epstein-Barr virus (EBV)-transformed lymphocytes, in an allele dose-dependent fashion. (Di Bernardo et al., 2008) Furthermore, absent IRF4 expression in the bone marrow of CLL patients has been demonstrated to be significantly associated with poorer overall survival. (Chang et al., 2002b)

More recently, a novel CLL mouse model has been developed, in which IRF4 deficient Vh11 knock-in mice (IRF4-/- Vh11) develop CLL with 100% penetrance.

(Shukla et al., 2013) This model was developed using a Vh11 knock-in allele in order to expand the murine B1 cell population. B1 cells are CD5+ B cells which usually comprise only a small B cell subset in the mature mouse and they have been identified as the murine CLL cell of origin. (Hardy, 2006; Chiorazzi and Ferrarini, 2011) Shukla *et al* hypothesised that low IRF4 expression might lead to development of CLL but had not observed it in their other studies of B cell development. (Lu, 2008) They used a knock-in mouse expressing Vh11, an immunoglobulin heavy chain family member that is found uniquely in B1 cells, to expand the B1 cell population. IRF4 deficient mice (IRF4 -/-) expressing this knock-in allele went on to develop CLL with 100% penetrance. (Shukla et al., 2013)

Taken together, the novel CLL mouse model proposed by Shukla *et al*, and the association of low *IRF4* mRNA expression in lymphocytes carrying the IRF4 rs872071 risk allele, indicate that low IRF4 expression predisposes to the development of CLL. Fascinatingly, the IRF4 deficient mouse model also develops a broad spectrum of clinically relevant lymphoproliferative disease, including monoclonal B cell lymphocytosis, indolent CLL and aggressive CLL. (Shukla et al., 2013)

Despite these findings, a proportion of *ex vivo* CLL cells from lymph nodes, bone marrow and peripheral blood (Falini et al., 2000; Tsuboi et al., 2000; Chang et al., 2002a) (Figure 6.1) have been demonstrated to express IRF4. This is strongly suggestive of the pleiotropic nature of IRF4, with differential expression contributing to different stages of the disease. It may be that absent or low IRF4 expression is necessary to drive the initial development of CLL, while the maintenance of CLL is associated with IRF4 at varying levels. Measurement of IRF4 expression in B cells isolated from the same patient at different stages of disease development would inform on the likely divergent roles of IRF4 in both the initiation and progression of disease.

6.4.4 CD38 expression in primary CLL lymphocytes after CD40L co-culture

The flow cytometry data presented here in primary CLL lymphocytes after CD40L co-culture is extremely limited. While there was a suggestion of CD38

downregulation in cells from a CD38+ patient after co-culture, this would be in contrast to data presented by Hamilton *et al* (2012), who demonstrated a statistically significant upregulation of CD38 surface expression in cells from 35 CLL patients after CD40L monolayer co-culture. (Hamilton et al., 2012) Analysis of additional patient samples is required to further explore the relationship between IRF4 and CD38 expression following CD40L co-culture.

6.4.5 ChIP in primary CLL lymphocytes

While the ChIP data are limited, due to the technical difficulties discussed in section 6.4.1, it is still possible to draw some conclusions from the data presented here.

Evidence for IRF4-*CD38* binding varied widely between the four patients in which this was assessed (patients 7, 5, 4 and 3). Binding was virtually absent in two of the four patients (patients 7 and 3) and only moderate in patient 5, but there was evidence of very substantial IRF4-*CD38* binding in patient 4. CD40L co-culture did not affect the degree of binding observed in patient 3, where results from paired NTL and CD40L monolayer-cultured cells were available. No clear association was observed, between the level of IRF4 protein expression prior to co-culture, and the IRF4-*CD38* binding observed. Similarly, only one CD38+ patient was assessed for IRF4-*CD38* binding, and so no conclusions can be drawn as to the association of CD38 positivity with the degree of binding. Notably however, strong IRF4-*CD38* binding occurred in patient 4 who was negative for CD38 expression, suggesting that IRF4-*CD38* binding can occur in the absence of substantial CD38 surface expression.

Significant IRF4-*CD38* binding in the cell lines, SU-DHL-6 and MEC-1, was restricted to the element 1 EICE site and the 5'UTR site in *CD38*, with no binding seen at element 2. There was some modest evidence of binding at element 2 in patients 5 and 4, but predominantly, the EICE element appeared to be the main site of binding in these primary CLL cells, in keeping with the cell line data.

Despite no clear patterns of IRF4-*CD38* binding in these four patients, the histone methylation mark ChIP data, while very limited, did suggest some interesting

and consistent findings. Specifically, NTL and CD40L monolayer co-culture of primary cells from patient 3 were both associated with only modest binding by the H3K9me3 antibody which binds to a histone mark associated with transcriptional repression. However, binding by an antibody to the activating histone mark H3K4me3 was very strongly downregulated at the element 1 EICE and element 2 inverted IRF4 site in cells cultured on the CD40L monolayer, compared to those cultured on the control NTL monolayer. This is suggestive of a downregulation of transcriptional activity at these two putative IRF4 binding elements in *CD38* after CD40L co-culture.

Furthermore, ChIP using an antibody to H3K9me3 (repressive histone mark) in primary cells from patient 9 after CD40L co-culture, showed very substantial binding at all three putative IRF4-*CD38* binding sites, again suggesting transcriptional repression at these sites after CD40L co-culture. While there were no paired data from NTL monolayer-cultured cells for comparison in this case, the strength of the H3K9me3 antibody binding observed after CD40L co-culture was very substantial, consistent with the results derived from patient 3.

Taken together, the ChIP data in primary cells suggest that IRF4-*CD38* binding is observed in leukaemic lymphocytes from some CLL patients, but is not consistently seen in all patients. Furthermore, the limited data do not suggest that it is consistently affected by CD40L co-culture of primary CLL cells. However, there is the suggestion of transcriptional repression at the IRF4 binding sites in *CD38* gene after CD40L co-culture.

6.5 Summary

Expression of IRF4 in primary CLL lymphocytes is variable between patients, and ranges from absent to strong expression. The published literature indicates that absent or low IRF4 expression is required for the initiation of CLL. Taken together, these findings suggest possible IRF4 pleiotropy in the initiation and maintenance of CLL. Furthermore, in all of the patients investigated here, IRF4 expression was upregulated after CD40L monolayer co-culture. This would suggest that IRF4 expression in CLL cells

may be upregulated in the lymph node microenvironment where CD40L-expressing T cells support the CLL population.

There is evidence of IRF4-*CD38* binding in the primary CLL lymphocytes from some patients, though no clear data suggesting an effect of CD40L monolayer co-culture on this binding was obtained. However, ChIP using antibodies to histone methylation marks suggested repression of transcriptional activation at the three putative IRF4 binding sites in *CD38*, after CD40L co-culture. While published data have demonstrated consistent CD38 upregulation in CLL cells after CD40L co-culture, the histone methylation ChIP data presented here suggest that IRF4-driven transcription of *CD38* is not responsible for this upregulation.

Chapter 7. **Concluding Discussion**

7.1 Discussion

Transcription factor IRF4 is a critical regulator of B cell maturation and differentiation. Essential to the development of B cells with a mature B cell receptor, IRF4 also governs the vital B cell differentiation processes of activated B cells within the germinal centre. (Lu, 2008) IRF4 behaves pleiotropically, and a model of 'kinetic control' has been proposed, to describe the coordination of antagonistic germinal centre processes by graded expression of IRF4. (Sciammas et al., 2011) In this way, graded expression of IRF4 promotes class switch recombination and the selection of B cells producing high affinity antibodies within the germinal centre, while sustained IRF4 expression is necessary for B cell exit from the germinal centre and plasmacytic differentiation. IRF4 is expressed in a number of lymphoproliferative malignancies and is essential to the survival of myeloma cells. (Shaffer et al., 2008)

A genome wide association study identified rs872071, a common single nucleotide polymorphism (SNP) in the 3'UTR of *IRF4*, as defining a low penetrance risk allele for the development of chronic lymphocytic leukaemia (CLL). (Di Bernardo et al., 2008) This risk allele is associated with lower expression of *IRF4* mRNA (Di Bernardo et al., 2008), and with poorer outcome in CLL. (Allan et al., 2010) Furthermore, rs872071 is associated with CD38 expression, (Allan et al., 2010) which is a well-established poor prognostic marker in CLL with a role in the pathophysiology of the disease. CD38 expression is associated with an active, proliferative CLL cell population. It enhances the migratory potential of CLL cells, promotes cell-cell signalling, and is involved in the homing of CLL cells to the supportive lymph node microenvironment in combination with CD49d, CD44 and matrix metalloproteinase-9 (MMP-9) in a macromolecular complex. (Buggins et al., 2011)

The identification of putative binding sites for IRF4 in the 5'UTR of *CD38* led to the hypothesis that IRF4 regulates the transcription of *CD38* in CLL lymphocytes.

Building on unpublished data regarding IRF4-*CD38* binding in lymphoma cell lines which was kindly made available by Dr R. Tooze (Leeds Institute of Molecular Medicine, University of Leeds), this study has demonstrated evidence of statistically

significant IRF4-*CD38* binding in two lymphoid cell lines, SU-DHL-6 and MEC-1, at binding sites in the first intron and 5'UTR of the *CD38* gene. Both of these binding sites represent a composite Ets/IRF consensus element (EICE) binding site, represented by 5'-GGAANNGAAA-3', where IRF4 binds as part of a heterodimer with an Ets protein family member, such as PU.1 or SPI-B. (Shaffer et al., 2009) SU-DHL-6 and MEC-1, both mature lymphoid cell lines, express PU.1 by western immunoblotting. In contrast, there was no evidence of IRF4-*CD38* binding in lymphoblastoid cell line, TK6, which does not express PU.1. Furthermore, there was no evidence of IRF4-*CD38* binding at a second putative binding site in the first intron, which was represented by an IRF4 binding site, 5'-AANNGAAA-3' on the reverse strand. Given that this could also represent an interferon stimulated response element (ISRE), 5'-GAAANN-3', where IRF4 can bind alone, these data are altogether suggestive of Ets protein-dependent IRF4 binding at EICE sites in *CD38* in SU-DHL-6 and MEC-1, but of no binding by IRF4 in isolation.

ChIP studies in primary CLL lymphocytes were limited by technical challenges in the preparation of adequate quality chromatin. However, there was evidence of IRF4-*CD38* binding in some, but not all, of the primary CLL lymphocyte samples tested. Similarly to the cell line results, binding occurred primarily at the EICE sites in the first intron and in the 5'UTR and there was very little evidence for binding at the ISRE site on the reverse strand in the first intron. This was therefore again suggestive of Ets protein-dependent EICE binding in the primary CLL lymphocytes. While no data is presented here regarding PU.1 expression in CLL lymphocytes, published data indicates that PU.1 expression in CLL is relatively low. (Mankai et al., 2008) SPI-B is an alternative Ets protein family member that has also been demonstrated to bind with IRF4 at EICE sites. (Su et al., 1996; Nagulapalli and Atchison, 1998) As no reliable western immunoblotting antibody could be identified, SPI-B protein expression could not be determined in either cell lines or in primary CLL lymphocytes. However, a gene expression analysis of CLL has previously demonstrated abundant *SPI-B* mRNA expression in CLL lymphocytes. (Stratowa et al., 2001) It is therefore possible that SPI-B, rather than PU.1, is the binding partner for IRF4 at the EICE sites observed in primary CLL.

Taken together, the evidence indicates that IRF4 binds to the *CD38* locus. Furthermore, it is clear that the expression of key binding partners, PU.1 and SPI-B for example, can impact on the pattern and location of binding. Regardless of binding partner, *CD38* can be identified as a physical binding target for IRF4 in both B cell lines and primary leukaemic lymphocytes. Whether this results in any significant effect on CD38 expression in CLL lymphocytes was the subject of further experiments.

IRF4 acts as a dichotomous regulator of transcription, with the capacity to either transactivate (Pongubala et al., 1992; Eisenbeis et al., 1995; Su et al., 1996; Himmelmann et al., 1997; Nagulapalli and Atchison, 1998) or to repress (Brass et al., 1996; Yamagata et al., 1996; Rosenbauer et al., 1999; Saito et al., 2007) downstream gene targets. *CD38* has been identified as a target gene for IRF4 in a gene expression analysis in myeloma cell lines. (Shaffer et al., 2008) While direct binding was not investigated in this study by ChIP, there was evidence that *CD38* expression was downregulated by IRF4 knockdown, suggesting that IRF4 is a positive regulator of *CD38* in myeloma cell lines. (Shaffer et al., 2008)

Having demonstrated IRF4-*CD38* binding in SU-DHL-6 and MEC-1, ChIP studies were performed to investigate evidence of transcriptional activity at the IRF4-*CD38* binding site in these cell lines, in the setting of RNAi-mediated IRF4 knockdown. These data were limited by difficulties in establishing constitutive IRF4 knockdown. While TK6 cell line tolerated constitutive shRNA-mediated knockdown, IRF4 was rapidly re-expressed in MEC-1 cells that had been transduced with shRNA targeted against IRF4. This is strongly suggestive of a selective pressure for maintenance of IRF4 expression in MEC-1 cells. Furthermore, the shRNA protocol could not be successfully established in SU-DHL-6 cells. Despite the observation that transient siRNA-mediated IRF4 knockdown in SU-DHL-6 significantly impaired cell growth, there was insufficient evidence to suggest that an inability to tolerate constitutive IRF4 knockdown was responsible for the failure to establish shRNA-mediated knockdown in this cell line. ChIP studies investigating transcriptional activity at the IRF4-*CD38* binding sites in MEC-1 and SU-DHL-6 were therefore performed in cells with siRNA-mediated knockdown. Interestingly, these investigations were suggestive of contrasting results in the two cell lines.

Specifically, ChIP studies using a histone methylation mark indicative of transcriptional repression, suggested that IRF4 knockdown was associated with repression of transcriptional activity at the EICE site in *CD38* intron 1 in SU-DHL-6. This would indicate positive regulation of *CD38* by IRF4 in this cell line. This model was supported by some limited flow cytometry data which hinted at a reduction in surface CD38 expression in SU-DHL-6 cells with IRF4 knockdown. These findings are in keeping with the published data that indicate that IRF4 acts as a transcriptional activator when it binds with PU.1 or another Ets family protein.

In contrast, IRF4 knockdown in MEC-1 was associated with an increase in transcriptional activation at the EICE site at the 5'UTR of *CD38*, suggestive of negative regulation of *CD38* by IRF4. No changes in transcriptional activation were observed at the EICE site in intron 1 in MEC-1.

Furthermore, the limited ChIP data in primary CLL lymphocytes indicated a substantial downregulation of transcriptional activation at both the intron 1 EICE site and at the ISRE site on the reverse strand, in *CD38* intron 1. Given the pleiotropic nature of IRF4 in its effects on B cells at different stages of maturation and differentiation, it is interesting to note the similarities and contrasts between the two cell lines and the primary CLL cells. Useful CLL-derived cell lines are rare. MEC-1 is derived from a patient with CLL, while SU-DHL-6 is a cell line derived from a germinal centre B cell lymphoma. The data presented here are suggestive of positive regulation of *CD38* by IRF4 in SU-DHL-6, but are suggestive of negative regulation in both primary CLL lymphocytes and in a CLL-derived cell line, MEC-1. While the findings presented here are not conclusive given the limited number of data replicates, they would be in keeping with previous observations that IRF4 exerts different effects on target B cells depending on the stage of their path through the germinal centre.

When these data are considered in the setting of the published literature regarding the role of IRF4 in CLL, a potential model for IRF4 regulation of *CD38* in CLL is identified. An intriguing mouse model of CLL has been developed, and clearly demonstrates that low or absent IRF4 predisposes to the development of CLL. (Shukla et al., 2013) Furthermore, the GWAS study that identified rs872071 as tagging a risk

allele for CLL, also demonstrated reduced expression of *IRF4* mRNA in EBV-transformed lymphocytes in an allele dose-dependent fashion. (Di Bernardo et al., 2008) CD38 positivity in CLL is associated with rs872071, and with a poorer prognosis. (Allan et al., 2010) Taken together with the data presented in this thesis, these findings are suggestive of a model in which reduced expression of IRF4 is associated with CD38 positivity through negative transcriptional regulation of *CD38* by IRF4.

There are a number of caveats to this model. Firstly, IRF4 is predicted to behave as an activator of gene transcription when it binds to an EICE site with an Ets family member, whereas it represses gene transcription when it binds alone or with another IRF family member. Given that the evidence for binding both in primary CLL lymphocytes and in MEC-1 appears to be at EICE sites rather than at the ISRE site where IRF4 might bind in isolation, one would expect evidence of transcriptional activation here.

Furthermore, the IRF4 deficient mouse model pertains specifically to the initiation and early progression of CLL and may not inform on the role of IRF4 once leukaemia has developed, or in the setting of more advanced progressive disease. Similarly, rs872071 is associated with the risk of developing CLL (Di Bernardo et al., 2008), and with poorer outcomes early on in disease, as evidenced by a significant association with shorter time from diagnosis to first treatment, but with no significant impact on OS. (Allan et al., 2010) Thus, low or absent IRF4 expression may strongly predispose to the initiation of CLL, but the role of IRF4 expression at different stages of disease course is not established. As such, it remains plausible that low IRF4 may not be essential to maintenance of the leukaemic clone once it is fully transformed. Indeed, the heterogenous nature of IRF4 expression in primary CLL lymphocytes shown here suggests that if IRF4 is a key player in the maintenance of the leukaemic clone, then its role may be context or patient specific, and dependent on other signalling components or somatic genetic abnormalities.

Thirdly, published data indicate that primary CLL lymphocytes co-cultured on CD40L-monolayer demonstrate increased expression of surface CD38. (Hamilton et al., 2012) The CD40L monolayer co-culture is also associated with an increased expression

of IRF4 protein in primary CLL lymphocytes, in keeping with IRF4 upregulation by CD40 ligation. (Pernis, 2002) Taken together, these findings do not conform to the proposed model of negative regulation of *CD38* by IRF4 in CLL. However, it is necessary to consider that the proposed model is limited in scope, focusing primarily on the linear signal transduction from IRF4 to *CD38*. In reality, the prevailing evidence suggests a complex signalling network involving numerous other transcription factors and cytokines. Thus, the upregulation of CD38 expression in CLL cells after CD40L monolayer co-culture may be driven by a number of factors, and IRF4 may make a relatively minor contribution to this, again depending on context or somatic genetic abnormalities. Shukla *et al* did not measure the CD38 status of the CLL cells derived from their IRF4 deficient mouse model (personal communication, R. Lu, Department of Genetics, Cell Biology, and Anatomy, University of Nebraska Medical Centre, Omaha) though further work by this group is likely to greatly inform the targets of IRF4 in CLL.

7.2 Further work

Investigation of the relationship between IRF4 and CD38 in this project was carried out primarily in cell line models. Useful CLL cell line models are lacking, and MEC-1 demonstrates only weak CD38 expression. Thus, the ability to demonstrate a functional interaction between IRF4 and CD38 in this CLL cell line model was potentially very limited. Furthermore, the relevance of cell line models to the protein-protein interactions in primary cells is questionable. It would be better advised to focus on expanding this work further in primary CLL cells, as initiated in this project.

In addition, demonstration of all of the key binding partners of IRF4 in the cell lines used here, and in primary CLL cells, is essential. Specifically, the expression of SPI-B was not determined in this project in cell lines or primary cells, due to failure to identify a reliable western immunoblotting antibody. Thus, the possible Ets protein binding partner of IRF4 at the EICE sites in *CD38* is unclear. It is even possible that the IRF4 binding partner at the *CD38* binding sites differs, between cell lines and primary CLL cells. Targeted RNAi-mediated knockdown of these Ets proteins, PU.1 and SPI-B, in the cell line models would be helpful in determining any effect on IRF4-*CD38* binding, and thus could offer confirmation as to the likely IRF4 binding partner at these sites.

IRF4 knockdown was observed to impair cell growth in TK6 and SU-DHL-6 cells. It also made them more susceptible to treatment with the nucleoside analogue, fludarabine. Cell cycle analysis could be used to determine whether the effect of IRF4 knockdown on these cell lines is cytotoxic or cytostatic. Given these findings in cell lines, this preliminary evidence suggests that IRF4 knockdown increases sensitivity to fludarabine and thus targeting of IRF4 may be a useful therapeutic strategy. However, in order to take this forward, further work on fludarabine cytotoxicity in cells with targeted IRF4 knockdown would be essential, in both cell line models and ideally in primary CLL cell lines.

References

Advani RH, Buggy JJ, Sharman JP, Smith SM, Boyd TE, Grant B, et al. (2013) 'Bruton tyrosine kinase inhibitor ibrutinib (PCI-32765) has significant activity in patients with relapsed/refractory B-cell malignancies'. *J Clin Oncol,* **31** (1): 88-94.

Agathangelidis A, Darzentas N, Hadzidimitriou A, Brochet X, Murray F, Yan XJ, et al. (2012) 'Stereotyped B-cell receptors in one-third of chronic lymphocytic leukemia: a molecular classification with implications for targeted therapies'. *Blood,* **119** (19): 4467-75.

Agathangelidis A, Vardi A, Baliakas P and Stamatopoulos K. (2014) 'Stereotyped B-cell receptors in chronic lymphocytic leukemia'. *Leuk Lymphoma,* **55** (10): 2252-61.

Aldinucci D, Celegato M, Borghese C, Colombatti A and Carbone A. (2011) 'IRF4 silencing inhibits Hodgkin lymphoma cell proliferation, survival and CCL5 secretion'. *Br J Haematol,* **152** (2): 182-90.

Aldinucci D, Gloghini A, Pinto A, Colombatti A and Carbone A. (2012) 'The role of CD40/CD40L and interferon regulatory factor 4 in Hodgkin lymphoma microenvironment'. *Leuk Lymphoma,* **53** (2): 195-201.

Allan JM, Sunter NJ, Bailey JR, Pettitt AR, Harris RJ, Pepper C, et al. (2010) 'Variant IRF4/MUM1 associates with CD38 status and treatment-free survival in chronic lymphocytic leukaemia'. *Leukemia,* **24** (4): 877-81.

Austen B, Powell JE, Alvi A, Edwards I, Hooper L, Starczynski J, et al. (2005) 'Mutations in the ATM gene lead to impaired overall and treatment-free survival that is independent of IGVH mutation status in patients with B-CLL'. *Blood,* **106** (9): 3175-82.

Bagnara D, Kaufman MS, Calissano C, Marsilio S, Patten PE, Simone R, et al. (2011) 'A novel adoptive transfer model of chronic lymphocytic leukemia suggests a key role for T lymphocytes in the disease'. *Blood,* **117** (20): 5463-72.

Berndt SI, Skibola CF, Joseph V, Camp NJ, Nieters A, Wang Z, et al. (2013) 'Genome-wide association study identifies multiple risk loci for chronic lymphocytic leukemia'. *Nat Genet,* **45** (8): 868-76.

Binder M, Muller F, Frick M, Wehr C, Simon F, Leistler B, et al. (2013) 'CLL B-cell receptors can recognize themselves: alternative epitopes and structural clues for autostimulatory mechanisms in CLL'. *Blood,* **121** (1): 239-41.

Binet JL, Auquier A, Dighiero G, Chastang C, Piguet H, Goasguen J, et al. (1981) 'A new prognostic classification of chronic lymphocytic leukemia derived from a multivariate survival analysis'. *Cancer,* **48** (1): 198-206.

Brass AL, Kehrli E, Eisenbeis CF, Storb U and Singh H. (1996) 'Pip, a lymphoid-restricted IRF, contains a regulatory domain that is important for autoinhibition and ternary complex formation with the Ets factor PU.1'. *Genes Dev,* **10** (18): 2335-47.

Brass AL, Zhu AQ and Singh H. (1999) 'Assembly requirements of PU.1-Pip (IRF-4) activator complexes: inhibiting function in vivo using fused dimers'. *EMBO J,* **18** (4): 977-91.

Broderick P, Cunningham D, Vijayakrishnan J, Cooke R, Ashworth A, Swerdlow A, et al. (2010) 'IRF4 polymorphism rs872071 and risk of Hodgkin lymphoma'. *Br J Haematol,* **148** (3): 413-5.

Buggins AGS, Levi A, Gohil S, Fishlock K, Patten PEM, Calle Y, et al. (2011) 'Evidence for a macromolecular complex in poor prognosis CLL that contains CD38, CD49d, CD44 and MMP-9'. *Br J Haematol,* **154** (2): 216-22.

Burger JA, Burger M and Kipps TJ. (1999) 'Chronic lymphocytic leukemia B cells express functional CXCR4 chemokine receptors that mediate spontaneous migration beneath bone marrow stromal cells'. *Blood,* **94** (11): 3658-67.

Burger JA, Tsukada N, Burger M, Zvaifler NJ, Dell'Aquila M and Kipps TJ. (2000) 'Blood-derived nurse-like cells protect chronic lymphocytic leukemia B cells from spontaneous apoptosis through stromal cell-derived factor-1'. *Blood,* **96** (8): 2655-63.

Burger JA, Quiroga MP, Hartmann E, Burkle A, Wierda WG, Keating MJ, et al. (2009) 'High-level expression of the T-cell chemokines CCL3 and CCL4 by chronic lymphocytic leukemia B cells in nurselike cell cocultures and after BCR stimulation'. *Blood,* **113** (13): 3050-8.

Burkle A, Niedermeier M, Schmitt-Graff A, Wierda WG, Keating MJ and Burger JA. (2007) 'Overexpression of the CXCR5 chemokine receptor, and its ligand, CXCL13 in B-cell chronic lymphocytic leukemia'. *Blood,* **110** (9): 3316-25.

Byrd JC, Furman RR, Coutre SE, Flinn IW, Burger JA, Blum KA, et al. (2013) 'Targeting BTK with ibrutinib in relapsed chronic lymphocytic leukemia'. *N Engl J Med,* **369** (1): 32-42.

Byrd JC, Furman RR, Coutre SE, Burger JA, Blum KA, Coleman M, et al. (2015) 'Three-year follow-up of treatment-naive and previously treated patients with CLL and SLL receiving single-agent ibrutinib'. *Blood,* **125** (16): 2497-506.

Carotta S, Willis SN, Hasbold J, Inouye M, Pang SH, Emslie D, et al. (2014) 'The transcription factors IRF8 and PU.1 negatively regulate plasma cell differentiation'. *J Exp Med,* **211** (11): 2169-81.

Carsetti R. (2000) 'The development of B cells in the bone marrow is controlled by the balance between cell-autonomous mechanisms and signals from the microenvironment'. *J Exp Med,* **191** (1): 5-8.

Catovsky D, Richards S, Matutes E, Oscier D, Dyer MJ, Bezares RF, et al. (2007) 'Assessment of fludarabine plus cyclophosphamide for patients with chronic lymphocytic leukaemia (the LRF CLL4 Trial): a randomised controlled trial'. *Lancet,* **370** (9583): 230-9.

Cattoretti G, Chang CC, Cechova K, Zhang J, Ye BH, Falini B, et al. (1995) 'BCL-6 protein is expressed in germinal-center B cells'. *Blood,* **86** (1): 45-53.

Chang C-C, Lorek J, Sabath DE, Li Y, Chitambar CR, Logan B, et al. (2002a) 'Expression of MUM1/IRF4 correlates with clinical outcome in patients with B-cell chronic lymphocytic leukemia'. *Blood,* **100** (13): 4671-5.

Chang CC, Lorek J, Sabath DE, Li Y, Chitambar CR, Logan B, et al. (2002b) 'Expression of MUM1/IRF4 correlates with clinical outcome in patients with B-cell chronic lymphocytic leukemia'. *Blood,* **100** (13): 4671-5.

Chen L, Apgar J, Huynh L, Dicker F, Giago-McGahan T, Rassenti L, et al. (2005) 'ZAP-70 directly enhances IgM signaling in chronic lymphocytic leukemia'. *Blood,* **105** (5): 2036-41.

Chiorazzi N and Ferrarini M. (2011) 'Cellular origin(s) of chronic lymphocytic leukemia: cautionary notes and additional considerations and possibilities'. *Blood,* **117** (6): 1781-91.

Collins RJ, Verschuer LA, Harmon BV, Prentice RL, Pope JH and Kerr JF. (1989) 'Spontaneous programmed death (apoptosis) of B-chronic lymphocytic leukaemia cells following their culture in vitro'. *Br J Haematol,* **71** (3): 343-50.

Cozma D, Yu D, Hodawadekar S, Azvolinsky A, Grande S, Tobias JW, et al. (2007) 'B cell activator PAX5 promotes lymphomagenesis through stimulation of B cell receptor signaling'. *J Clin Invest,* **117** (9): 2602-10.

Crespo M, Bosch F, Villamor N, Bellosillo B, Colomer D, Rozman M, et al. (2003) 'ZAP-70 expression as a surrogate for immunoglobulin-variable-region mutations in chronic lymphocytic leukemia'. *N Engl J Med,* **348** (18): 1764-75.

Crowther-Swanepoel D, Wild R, Sellick G, Dyer MJ, Mauro FR, Cuthbert RJ, et al. (2008) 'Insight into the pathogenesis of chronic lymphocytic leukemia (CLL) through analysis of IgVH gene usage and mutation status in familial CLL'. *Blood,* **111** (12): 5691-3.

Crowther-Swanepoel D, Broderick P, Di Bernardo MC, Dobbins SE, Torres M, Mansouri M, et al. (2010) 'Common variants at 2q37.3, 8q24.21, 15q21.3 and 16q24.1 influence chronic lymphocytic leukemia risk'. *Nat Genet,* **42** (2): 132-6.

Crowther-Swanepoel D, Di Bernardo MC, Jamroziak K, Karabon L, Frydecka I, Deaglio S, et al. (2011) 'Common genetic variation at 15q25.2 impacts on chronic lymphocytic leukaemia risk'. *Br J Haematol,* **154** (2): 229-33.

Damle RN, Wasil T, Fais F, Ghiotto F, Valetto A, Allen SL, et al. (1999) 'Ig V gene mutation status and CD38 expression as novel prognostic indicators in chronic lymphocytic leukemia'. *Blood,* **94** (6): 1840-7.

Damle RN, Ghiotto F, Valetto A, Albesiano E, Fais F, Yan XJ, et al. (2002) 'B-cell chronic lymphocytic leukemia cells express a surface membrane phenotype of activated, antigen-experienced B lymphocytes'. *Blood,* **99** (11): 4087-93.

Damle RN, Temburni S, Calissano C, Yancopoulos S, Banapour T, Sison C, et al. (2007) 'CD38 expression labels an activated subset within chronic lymphocytic leukemia clones enriched in proliferating B cells'. *Blood,* **110** (9): 3352-9.

Davids MS and Burger JA. (2012) 'Cell Trafficking in Chronic Lymphocytic Leukemia'. *Open J Hematol,* **3** (S1):

De Lange T. (2005) 'Telomere-related genome instability in cancer'. *Cold Spring Harb Symp Quant Biol,* **70** 197-204.

de Pooter RF and Kee BL. (2010) 'E proteins and the regulation of early lymphocyte development'. *Immunol Rev,* **238** (1): 93-109.

Deaglio S, Dianzani U, Horenstein AL, Fernandez JE, van Kooten C, Bragardo M, et al. (1996) 'Human CD38 ligand. A 120-KDA protein predominantly expressed on endothelial cells'. *J Immunol,* **156** (2): 727-34.

Deaglio S, Morra M, Mallone R, Ausiello CM, Prager E, Garbarino G, et al. (1998) 'Human CD38 (ADP-ribosyl cyclase) is a counter-receptor of CD31, an Ig superfamily member'. *J Immunol,* **160** (1): 395-402.

Deaglio S, Vaisitti T, Bergui L, Bonello L, Horenstein AL, Tamagnone L, et al. (2005) 'CD38 and CD100 lead a network of surface receptors relaying positive signals for B-CLL growth and survival'. *Blood,* **105** (8): 3042-50.

Deaglio S, Vaisitti T, Aydin S, Bergui L, D'Arena G, Bonello L, et al. (2007) 'CD38 and ZAP-70 are functionally linked and mark CLL cells with high migratory potential'. *Blood,* **110** (12): 4012-21.

Deaglio S, Aydin S, Grand MM, Vaisitti T, Bergui L, D'Arena G, et al. (2010) 'CD38/CD31 interactions activate genetic pathways leading to proliferation and migration in chronic lymphocytic leukemia cells'. *Molecular Medicine,* **16** (3-4): 87-91.

Di Bernardo MC, Crowther-Swanepoel D, Broderick P, Webb E, Sellick G, Wild R, et al. (2008) 'A genome-wide association study identifies six susceptibility loci for chronic lymphocytic leukemia'. *Nat Genet,* **40** (10): 1204-10.

Di Bernardo MC, Broderick P, Catovsky D and Houlston RS. (2013) 'Common genetic variation contributes significantly to the risk of developing chronic lymphocytic leukemia'. *Haematologica,* **98** (3): e23-4.

Di Ianni M, Baldoni S, Rosati E, Ciurnelli R, Cavalli L, Martelli MF, et al. (2009) 'A new genetic lesion in B-CLL: a NOTCH1 PEST domain mutation'. *Br J Haematol,* **146** (6): 689-91.

Dianzani U, Funaro A, DiFranco D, Garbarino G, Bragardo M, Redoglia V, et al. (1994) 'Interaction between endothelium and CD4+CD45RA+ lymphocytes. Role of the human CD38 molecule'. *J Immunol,* **153** (3): 952-9.

Dicker F, Herholz H, Schnittger S, Nakao A, Patten N, Wu L, et al. (2009) 'The detection of TP53 mutations in chronic lymphocytic leukemia independently predicts rapid disease progression and is highly correlated with a complex aberrant karyotype'. *Leukemia,* **23** (1): 117-24.

Dohner H, Fischer K, Bentz M, Hansen K, Benner A, Cabot G, et al. (1995) 'p53 gene deletion predicts for poor survival and non-response to therapy with purine analogs in chronic B-cell leukemias'. *Blood,* **85** (6): 1580-9.

Dohner H, Stilgenbauer S, Benner A, Leupolt E, Krober A, Bullinger L, et al. (2000) 'Genomic aberrations and survival in chronic lymphocytic leukemia'. *N Engl J Med,* **343** (26): 1910-6.

Duhren-von Minden M, Ubelhart R, Schneider D, Wossning T, Bach MP, Buchner M, et al. (2012) 'Chronic lymphocytic leukaemia is driven by antigen-independent cell-autonomous signalling'. *Nature,* **489** (7415): 309-12.

Eisenbeis CF, Singh H and Storb U. (1993) 'PU.1 is a component of a multiprotein complex which binds an essential site in the murine immunoglobulin lambda 2-4 enhancer'. *Mol Cell Biol,* **13** (10): 6452-61.

Eisenbeis CF, Singh H and Storb U. (1995) 'Pip, a novel IRF family member, is a lymphoid-specific, PU.1-dependent transcriptional activator'. *Genes Dev,* **9** (11): 1377-87.

Epstein AL, Levy R, Kim H, Henle W, Henle G and Kaplan HS. (1978) 'Biology of the human malignant lymphomas. IV. Functional characterization of ten diffuse histiocytic lymphoma cell lines'. *Cancer,* **42** (5): 2379-91.

Escalante CR, Brass AL, Pongubala JM, Shatova E, Shen L, Singh H, et al. (2002) 'Crystal structure of PU.1/IRF-4/DNA ternary complex'. *Mol Cell,* **10** (5): 1097-105.

Falini B, Fizzotti M, Pucciarini A, Bigerna B, Marafioti T, Gambacorta M, et al. (2000) 'A monoclonal antibody (MUM1p) detects expression of the MUM1/IRF4 protein in a subset of germinal center B cells, plasma cells, and activated T cells'. *Blood,* **95** (6): 2084-92.

Farooqui MZ, Valdez J, Martyr S, Aue G, Saba N, Niemann CU, et al. (2015) 'Ibrutinib for previously untreated and relapsed or refractory chronic lymphocytic leukaemia with TP53 aberrations: a phase 2, single-arm trial'. *Lancet Oncol,* **16** (2): 169-76.

Feldman AL, Law M, Remstein ED, Macon WR, Erickson LA, Grogg KL, et al. (2009) 'Recurrent translocations involving the IRF4 oncogene locus in peripheral T-cell lymphomas'. *Leukemia,* **23** (3): 574-80.

Ferrero E and Malavasi F. (1997) 'Human CD38, a leukocyte receptor and ectoenzyme, is a member of a novel eukaryotic gene family of nicotinamide adenine dinucleotide+-converting enzymes: extensive structural homology with the genes for murine bone marrow stromal cell antigen 1 and aplysian ADP-ribosyl cyclase'. *J Immunol,* **159** (8): 3858-65.

Fuller SJ, Papaemmanuil E, McKinnon L, Webb E, Sellick GS, Dao-Ung LP, et al. (2008) 'Analysis of a large multi-generational family provides insight into the genetics of chronic lymphocytic leukemia'. *Br J Haematol,* **142** (2): 238-45.

Funaro A, Spagnoli GC, Ausiello CM, Alessio M, Roggero S, Delia D, et al. (1990) 'Involvement of the multilineage CD38 molecule in a unique pathway of cell activation and proliferation'. *J Immunol,* **145** (8): 2390-6.

Furman RR, Asgary Z, Mascarenhas JO, Liou HC and Schattner EJ. (2000) 'Modulation of NF-kappa B activity and apoptosis in chronic lymphocytic leukemia B cells'. *J Immunol,* **164** (4): 2200-6.

Ghia P, Strola G, Granziero L, Geuna M, Guida G, Sallusto F, et al. (2002) 'Chronic lymphocytic leukemia B cells are endowed with the capacity to attract CD4+, CD40L+ T cells by producing CCL22'. *Eur J Immunol,* **32** (5): 1403-13.

Ghia P, Guida G, Stella S, Gottardi D, Geuna M, Strola G, et al. (2003) 'The pattern of CD38 expression defines a distinct subset of chronic lymphocytic leukemia (CLL) patients at risk of disease progression'. *Blood,* **101** (4): 1262-9.

Ghia P, Guida G, Scielzo C, Geuna M and Caligaris-Cappio F. (2004) 'CD38 modifications in chronic lymphocytic leukemia: are they relevant?'. *Leukemia,* **18** (10): 1733-5.

Goldin LR, Bjorkholm M, Kristinsson SY, Turesson I and Landgren O. (2009) 'Elevated risk of chronic lymphocytic leukemia and other indolent non-Hodgkin's lymphomas among relatives of patients with chronic lymphocytic leukemia'. *Haematologica,* **94** (5): 647-53.

Goldin LR, Slager SL and Caporaso NE. (2010) 'Familial chronic lymphocytic leukemia'. *Curr Opin Hematol,* **17** (4): 350-5.

Gonzalez D, Martinez P, Wade R, Hockley S, Oscier D, Matutes E, et al. (2011) 'Mutational status of the TP53 gene as a predictor of response and survival in patients with chronic lymphocytic leukemia: results from the LRF CLL4 trial'. *J Clin Oncol,* **29** (16): 2223-9.

Granziero L, Ghia P, Circosta P, Gottardi D, Strola G, Geuna M, et al. (2001) 'Survivin is expressed on CD40 stimulation and interfaces proliferation and apoptosis in B-cell chronic lymphocytic leukemia'. *Blood,* **97** (9): 2777-83.

Grossman A, Mittrucker HW, Nicholl J, Suzuki A, Chung S, Antonio L, et al. (1996) 'Cloning of human lymphocyte-specific interferon regulatory factor (hLSIRF/hIRF4) and mapping of the gene to 6p23-p25'. *Genomics,* **37** (2): 229-33.

Hallek M, Cheson BD, Catovsky D, Caligaris-Cappio F, Dighiero G, Dohner H, et al. (2008) 'Guidelines for the diagnosis and treatment of chronic lymphocytic leukemia: a

report from the International Workshop on Chronic Lymphocytic Leukemia updating the National Cancer Institute-Working Group 1996 guidelines'. *Blood,* **111** (12): 5446-56.

Hallek M, Fischer K, Fingerle-Rowson G, Fink AM, Busch R, Mayer J, et al. (2010) 'Addition of rituximab to fludarabine and cyclophosphamide in patients with chronic lymphocytic leukaemia: a randomised, open-label, phase 3 trial'. *Lancet,* **376** (9747): 1164-74.

Hamblin TJ, Davis Z, Gardiner A, Oscier DG and Stevenson FK. (1999) 'Unmutated Ig V(H) genes are associated with a more aggressive form of chronic lymphocytic leukemia'. *Blood,* **94** (6): 1848-54.

Hamblin TJ, Orchard JA, Ibbotson RE, Davis Z, Thomas PW, Stevenson FK, et al. (2002) 'CD38 expression and immunoglobulin variable region mutations are independent prognostic variables in chronic lymphocytic leukemia, but CD38 expression may vary during the course of the disease'. *Blood,* **99** (3): 1023-9.

Hamilton E, Pearce L, Morgan L, Robinson S, Ware V, Brennan P, et al. (2012) 'Mimicking the tumour microenvironment: three different co-culture systems induce a similar phenotype but distinct proliferative signals in primary chronic lymphocytic leukaemia cells'. *Br J Haematol,* **158** (5): 589-99.

Hardy RR. (2006) 'B-1 B cells: development, selection, natural autoantibody and leukemia'. *Curr Opin Immunol,* **18** (5): 547-55.

Herishanu Y, Perez-Galan P, Liu D, Biancotto A, Pittaluga S, Vire B, et al. (2011) 'The lymph node microenvironment promotes B-cell receptor signaling, NF-kappaB activation, and tumor proliferation in chronic lymphocytic leukemia'. *Blood,* **117** (2): 563-74.

Hillmen P. (2011) 'Using the Biology of Chronic Lymphocytioc Leukaemia to Choose Treatment'. *American Society of Haematology Education Book,* **1** 104-09.

Himmelmann A, Riva A, Wilson GL, Lucas BP, Thevenin C and Kehrl JH. (1997) 'PU.1/Pip and basic helix loop helix zipper transcription factors interact with binding sites in

the CD20 promoter to help confer lineage- and stage-specific expression of CD20 in B lymphocytes'. *Blood,* **90** (10): 3984-95.

Howard M, Grimaldi JC, Bazan JF, Lund FE, Santos-Argumedo L, Parkhouse RM, et al. (1993) 'Formation and hydrolysis of cyclic ADP-ribose catalyzed by lymphocyte antigen CD38'. *Science,* **262** (5136): 1056-9.

Howlader N NA, Krapcho M, Neyman N, Aminou R, Altekruse SF, Kosary CL, Ruhl J, Tatalovich Z, Cho H, Mariotto A, Eisner MP, Lewis DR, Chen HS, Feuer EJ, Cronin KA (eds). (2012) *SEER Cancer Statistics Review, 1975-2009 (Vintage 2009 Populations), National Cancer Institute.* Available at: (Accessed:

Ibrahim S, Keating M, Do KA, O'Brien S, Huh YO, Jilani I, et al. (2001) 'CD38 expression as an important prognostic factor in B-cell chronic lymphocytic leukemia'. *Blood,* **98** (1): 181-6.

Iida S, Rao PH, Butler M, Corradini P, Boccadoro M, Klein B, et al. (1997) 'Deregulation of MUM1/IRF4 by chromosomal translocation in multiple myeloma'. *Nat Genet,* **17** (2): 226-30.

Ito M, Iida S, Inagaki H, Tsuboi K, Komatsu H, Yamaguchi M, et al. (2002) 'MUM1/IRF4 expression is an unfavorable prognostic factor in B-cell chronic lymphocytic leukemia (CLL)/small lymphocytic lymphoma (SLL)'. *Japanese Journal of Cancer Research,* **93** (6): 685-94.

Jaksic O, Paro MMK, Kardum Skelin I, Kusec R, Pejsa V and Jaksic B. (2004) 'CD38 on B-cell chronic lymphocytic leukemia cells has higher expression in lymph nodes than in peripheral blood or bone marrow'. *Blood,* **103** (5): 1968-9.

Johnson K, Hashimshony T, Sawai CM, Pongubala JM, Skok JA, Aifantis I, et al. (2008) 'Regulation of immunoglobulin light-chain recombination by the transcription factor IRF-4 and the attenuation of interleukin-7 signaling'. *Immunity,* **28** (3): 335-45.

Kitanaka A, Ito C, Coustan-Smith E and Campana D. (1997) 'CD38 ligation in human B cell progenitors triggers tyrosine phosphorylation of CD19 and association of CD19 with lyn and phosphatidylinositol 3-kinase'. *J Immunol,* **159** (1): 184-92.

Klein U, Tu Y, Stolovitzky GA, Mattioli M, Cattoretti G, Husson H, et al. (2001) 'Gene expression profiling of B cell chronic lymphocytic leukemia reveals a homogeneous phenotype related to memory B cells'. *J Exp Med,* **194** (11): 1625-38.

Klein U, Casola S, Cattoretti G, Shen Q, Lia M, Mo T, et al. (2006) 'Transcription factor IRF4 controls plasma cell differentiation and class-switch recombination'. *Nat Immunol,* **7** (7): 773-82.

Klein U and Dalla-Favera R. (2008) 'Germinal centres: role in B-cell physiology and malignancy'. *Nat Rev Immunol,* **8** (1): 22-33.

Knauf WU, Lissitchkov T, Aldaoud A, Liberati AM, Loscertales J, Herbrecht R, et al. (2012) 'Bendamustine compared with chlorambucil in previously untreated patients with chronic lymphocytic leukaemia: updated results of a randomized phase III trial'. *Br J Haematol,* **159** (1): 67-77.

Kumagai M, Coustan-Smith E, Murray DJ, Silvennoinen O, Murti KG, Evans WE, et al. (1995) 'Ligation of CD38 suppresses human B lymphopoiesis'. *J Exp Med,* **181** (3): 1101-10.

Kurtova AV, Balakrishnan K, Chen R, Ding W, Schnabl S, Quiroga MP, et al. (2009) 'Diverse marrow stromal cells protect CLL cells from spontaneous and drug-induced apoptosis: development of a reliable and reproducible system to assess stromal cell adhesion-mediated drug resistance'. *Blood,* **114** (20): 4441-50.

Kwon H, Thierry-Mieg D, Thierry-Mieg J, Kim HP, Oh J, Tunyaplin C, et al. (2009) 'Analysis of interleukin-21-induced Prdm1 gene regulation reveals functional cooperation of STAT3 and IRF4 transcription factors'. *Immunity,* **31** (6): 941-52.

Lagneaux L, Delforge A, De Bruyn C, Bernier M and Bron D. (1999) 'Adhesion to bone marrow stroma inhibits apoptosis of chronic lymphocytic leukemia cells'. *Leuk Lymphoma,* **35** (5-6): 445-53.

Levy JA, Virolainen M and Defendi V. (1968) 'Human lymphoblastoid lines from lymph node and spleen'. *Cancer,* **22** (3): 517-24.

Lin TT, Norris K, Heppel NH, Pratt G, Allan JM, Allsup DJ, et al. (2014) 'Telomere dysfunction accurately predicts clinical outcome in chronic lymphocytic

leukaemia, even in patients with early stage disease'. *Br J Haematol,* **167** (2): 214-23.

Lu R, Medina KL, Lancki DW and Singh H. (2003) 'IRF-4,8 orchestrate the pre-B-to-B transition in lymphocyte development'. *Genes Dev,* **17** (14): 1703-8.

Lu R. (2008) 'Interferon regulatory factor 4 and 8 in B-cell development'. *Trends Immunol,* **29** (10): 487-92.

Lund FE, Yu N, Kim KM, Reth M and Howard MC. (1996) 'Signaling through CD38 augments B cell antigen receptor (BCR) responses and is dependent on BCR expression'. *J Immunol,* **157** (4): 1455-67.

Lyons AB. (1999) 'Divided we stand: tracking cell proliferation with carboxyfluorescein diacetate succinimidyl ester'. *Immunol Cell Biol,* **77** (6): 509-15.

Ma S, Turetsky A, Trinh L and Lu R. (2006) 'IFN regulatory factor 4 and 8 promote Ig light chain kappa locus activation in pre-B cell development'. *J Immunol,* **177** (11): 7898-904.

Ma S, Pathak S, Trinh L and Lu R. (2008) 'Interferon regulatory factors 4 and 8 induce the expression of Ikaros and Aiolos to down-regulate pre-B-cell receptor and promote cell-cycle withdrawal in pre-B-cell development'. *Blood,* **111** (3): 1396-403.

Majid A, Lin TT, Best G, Fishlock K, Hewamana S, Pratt G, et al. (2011) 'CD49d is an independent prognostic marker that is associated with CXCR4 expression in CLL'. *Leuk Res,* **35** (6): 750-6.

Malavasi F, Funaro A, Alessio M, DeMonte LB, Ausiello CM, Dianzani U, et al. (1992) 'CD38: a multi-lineage cell activation molecule with a split personality'. *Int J Clin Lab Res,* **22** (2): 73-80.

Malavasi F, Deaglio S, Funaro A, Ferrero E, Horenstein AL, Ortolan E, et al. (2008) 'Evolution and function of the ADP ribosyl cyclase/CD38 gene family in physiology and pathology'. *Physiol Rev,* **88** (3): 841-86.

Malavasi F, Deaglio S, Damle R, Cutrona G, Ferrarini M and Chiorazzi N. (2011) 'CD38 and chronic lymphocytic leukemia: a decade later'. *Blood,* **118** (13): 3470-8.

Mamane Y, Heylbroeck C, Genin P, Algarte M, Servant MJ, LePage C, et al. (1999) 'Interferon regulatory factors: the next generation'. *Gene,* **237** (1): 1-14.

Mankai A, Bordron A, Renaudineau Y, Martins-Carvalho C, Takahashi S, Ghedira I, et al. (2008) 'Purine-rich box-1-mediated reduced expression of CD20 alters rituximab-induced lysis of chronic lymphocytic leukemia B cells'. *Cancer Res,* **68** (18): 7512-9.

Marecki S and Fenton MJ. (2002) 'The role of IRF-4 in transcriptional regulation'. *J Interferon Cytokine Res,* **22** (1): 121-33.

Marti GE, Rawstron AC, Ghia P, Hillmen P, Houlston RS, Kay N, et al. (2005) 'Diagnostic criteria for monoclonal B-cell lymphocytosis'. *Br J Haematol,* **130** (3): 325-32.

Matsuyama T, Grossman A, Mittrucker HW, Siderovski DP, Kiefer F, Kawakami T, et al. (1995) 'Molecular cloning of LSIRF, a lymphoid-specific member of the interferon regulatory factor family that binds the interferon-stimulated response element (ISRE)'. *Nucleic Acids Res,* **23** (12): 2127-36.

Matutes E, Owusu-Ankomah K, Morilla R, Garcia Marco J, Houlihan A, Que TH, et al. (1994) 'The immunological profile of B-cell disorders and proposal of a scoring system for the diagnosis of CLL'. *Leukemia,* **8** (10): 1640-5.

Messmer BT, Albesiano E, Efremov DG, Ghiotto F, Allen SL, Kolitz J, et al. (2004) 'Multiple distinct sets of stereotyped antigen receptors indicate a role for antigen in promoting chronic lymphocytic leukemia'. *J Exp Med,* **200** (4): 519-25.

Messmer BT, Messmer D, Allen SL, Kolitz JE, Kudalkar P, Cesar D, et al. (2005) 'In vivo measurements document the dynamic cellular kinetics of chronic lymphocytic leukemia B cells'. *J Clin Invest,* **115** (3): 755-64.

Mittrucker HW, Matsuyama T, Grossman A, Kundig TM, Potter J, Shahinian A, et al. (1997) 'Requirement for the transcription factor LSIRF/IRF4 for mature B and T lymphocyte function'. *Science,* **275** (5299): 540-3.

Muramatsu M, Kinoshita K, Fagarasan S, Yamada S, Shinkai Y and Honjo T. (2000) 'Class switch recombination and hypermutation require activation-induced cytidine deaminase (AID), a potential RNA editing enzyme'. *Cell,* **102** (5): 553-63.

Nagulapalli S and Atchison ML. (1998) 'Transcription factor Pip can enhance DNA binding by E47, leading to transcriptional synergy involving multiple protein domains'. *Mol Cell Biol,* **18** (8): 4639-50.

Nayar R, Schutten E, Bautista B, Daniels K, Prince AL, Enos M, et al. (2014) 'Graded levels of IRF4 regulate CD8+ T cell differentiation and expansion, but not attrition, in response to acute virus infection'. *J Immunol,* **192** (12): 5881-93.

Nguyen H, Hiscott J and Pitha PM. (1997) 'The growing family of interferon regulatory factors'. *Cytokine Growth Factor Rev,* **8** (4): 293-312.

Nishio M, Endo T, Tsukada N, Ohata J, Kitada S, Reed JC, et al. (2005) 'Nurselike cells express BAFF and APRIL, which can promote survival of chronic lymphocytic leukemia cells via a paracrine pathway distinct from that of SDF-1alpha'. *Blood,* **106** (3): 1012-20.

Ochiai K, Maienschein-Cline M, Simonetti G, Chen J, Rosenthal R, Brink R, et al. (2013) 'Transcriptional regulation of germinal center B and plasma cell fates by dynamical control of IRF4'. *Immunity,* **38** (5): 918-29.

Oscier D, Dearden C, Erem E, Fegan C, Follows G, Hillmen P, et al. (2012) 'Guidelines on the diagnosis, investigation and management of chronic lymphocytic leukaemia'. *Br J Haematol,* **159** (5): 541-64.

Oscier DG, Rose-Zerilli MJ, Winkelmann N, Gonzalez de Castro D, Gomez B, Forster J, et al. (2013) 'The clinical significance of NOTCH1 and SF3B1 mutations in the UK LRF CLL4 trial'. *Blood,* **121** (3): 468-75.

Patten PE, Buggins AG, Richards J, Wotherspoon A, Salisbury J, Mufti GJ, et al. (2008) 'CD38 expression in chronic lymphocytic leukemia is regulated by the tumor microenvironment'. *Blood,* **111** (10): 5173-81.

Pede V, Rombout A, Vermeire J, Naessens E, Vanderstraeten H, Philippe J, et al. (2013) 'Expression of ZAP70 in chronic lymphocytic leukaemia activates NF-kappaB signalling'. *Br J Haematol,* **163** (5): 621-30.

Pepper C, Brennan P, Alghazal S, Ward R, Pratt G, Starczynski J, et al. (2006) 'CD38+ chronic lymphocytic leukaemia cells co-express high levels of ZAP-70 and are functionally distinct from their CD38- counter-parts'. *Leukemia,* **20** (4): 743-4.

Pepper C, Majid A, Lin TT, Hewamana S, Pratt G, Walewska R, et al. (2012) 'Defining the prognosis of early stage chronic lymphocytic leukaemia patients'. *Br J Haematol,* **156** (4): 499-507.

Pernis AB. (2002) 'The role of IRF-4 in B and T cell activation and differentiation'. *J Interferon Cytokine Res,* **22** (1): 111-20.

Pettitt AR, Jackson R, Carruthers S, Dodd J, Dodd S, Oates M, et al. (2012) 'Alemtuzumab in combination with methylprednisolone is a highly effective induction regimen for patients with chronic lymphocytic leukemia and deletion of TP53: final results of the national cancer research institute CLL206 trial'. *J Clin Oncol,* **30** (14): 1647-55.

Pileri SA, Ascani S, Sabattini E, Fraternali-Orcioni G, Poggi S, Piccioli M, et al. (2000) 'The pathologist's view point. Part I--indolent lymphomas'. *Haematologica,* **85** (12): 1291-307.

Pizzolo G, Chilosi M, Ambrosetti A, Semenzato G, Fiore-Donati L and Perona G. (1983) 'Immunohistologic study of bone marrow involvement in B-chronic lymphocytic leukemia'. *Blood,* **62** (6): 1289-96.

Ponader S, Chen SS, Buggy JJ, Balakrishnan K, Gandhi V, Wierda WG, et al. (2012) 'The Bruton tyrosine kinase inhibitor PCI-32765 thwarts chronic lymphocytic leukemia cell survival and tissue homing in vitro and in vivo'. *Blood,* **119** (5): 1182-9.

Pongubala JM, Nagulapalli S, Klemsz MJ, McKercher SR, Maki RA and Atchison ML. (1992) 'PU.1 recruits a second nuclear factor to a site important for immunoglobulin kappa 3' enhancer activity'. *Mol Cell Biol,* **12** (1): 368-78.

Pongubala JM, Van Beveren C, Nagulapalli S, Klemsz MJ, McKercher SR, Maki RA, et al. (1993) 'Effect of PU.1 phosphorylation on interaction with NF-EM5 and transcriptional activation'. *Science,* **259** (5101): 1622-5.

Puente XS, Pinyol M, Quesada V, Conde L, Ordonez GR, Villamor N, et al. (2011) 'Whole-genome sequencing identifies recurrent mutations in chronic lymphocytic leukaemia'. *Nature,* **475** (7354): 101-5.

Puente XS, Bea S, Valdes-Mas R, Villamor N, Gutierrez-Abril J, Martin-Subero JI, et al. (2015) 'Non-coding recurrent mutations in chronic lymphocytic leukaemia'. *Nature,*

Rai KR, Sawitsky A, Cronkite EP, Chanana AD, Levy RN and Pasternack BS. (1975) 'Clinical staging of chronic lymphocytic leukemia'. *Blood,* **46** (2): 219-34.

Ramkumar C, Cui H, Kong Y, Jones SN, Gerstein RM and Zhang H. (2013) 'Smurf2 suppresses B-cell proliferation and lymphomagenesis by mediating ubiquitination and degradation of YY1'. *Nat Commun,* **4** 2598.

Raval A, Tanner SM, Byrd JC, Angerman EB, Perko JD, Chen SS, et al. (2007) 'Downregulation of death-associated protein kinase 1 (DAPK1) in chronic lymphocytic leukemia'. *Cell,* **129** (5): 879-90.

Redondo-Munoz J, Escobar-Diaz E, Samaniego R, Terol MJ, Garcia-Marco JA and Garcia-Pardo A. (2006) 'MMP-9 in B-cell chronic lymphocytic leukemia is up-regulated by alpha4beta1 integrin or CXCR4 engagement via distinct signaling pathways, localizes to podosomes, and is involved in cell invasion and migration'. *Blood,* **108** (9): 3143-51.

Redondo-Munoz J, Ugarte-Berzal E, Garcia-Marco JA, del Cerro MH, Van den Steen PE, Opdenakker G, et al. (2008) 'Alpha4beta1 integrin and 190-kDa CD44v constitute a cell surface docking complex for gelatinase B/MMP-9 in chronic leukemic but not in normal B cells'. *Blood,* **112** (1): 169-78.

Reinherz EL, Kung PC, Goldstein G, Levey RH and Schlossman SF. (1980) 'Discrete stages of human intrathymic differentiation: analysis of normal thymocytes and leukemic lymphoblasts of T-cell lineage'. *Proc Natl Acad Sci U S A,* **77** (3): 1588-92.

Roos G, Krober A, Grabowski P, Kienle D, Buhler A, Dohner H, et al. (2008) 'Short telomeres are associated with genetic complexity, high-risk genomic aberrations, and short survival in chronic lymphocytic leukemia'. *Blood,* **111** (4): 2246-52.

Rosati E, Sabatini R, Rampino G, Tabilio A, Di Ianni M, Fettucciari K, et al. (2009) 'Constitutively activated Notch signaling is involved in survival and apoptosis resistance of B-CLL cells'. *Blood,* **113** (4): 856-65.

Rose DM, Han J and Ginsberg MH. (2002) 'Alpha4 integrins and the immune response'. *Immunol Rev,* **186** 118-24.

Rosenbauer F, Waring JF, Foerster J, Wietstruk M, Philipp D and Horak I. (1999) 'Interferon consensus sequence binding protein and interferon regulatory factor-4/Pip form a complex that represses the expression of the interferon-stimulated gene-15 in macrophages'. *Blood,* **94** (12): 4274-81.

Rosenwald A, Alizadeh AA, Widhopf G, Simon R, Davis RE, Yu X, et al. (2001) 'Relation of gene expression phenotype to immunoglobulin mutation genotype in B cell chronic lymphocytic leukemia'. *J Exp Med,* **194** (11): 1639-47.

Rossi D, Cerri M, Deambrogi C, Sozzi E, Cresta S, Rasi S, et al. (2009a) 'The prognostic value of TP53 mutations in chronic lymphocytic leukemia is independent of Del17p13: implications for overall survival and chemorefractoriness'. *Clin Cancer Res,* **15** (3): 995-1004.

Rossi D, Lobetti Bodoni C, Genuardi E, Monitillo L, Drandi D, Cerri M, et al. (2009b) 'Telomere length is an independent predictor of survival, treatment requirement and Richter's syndrome transformation in chronic lymphocytic leukemia'. *Leukemia,* **23** (6): 1062-72.

Rossi D, Bruscaggin A, Spina V, Rasi S, Khiabanian H, Messina M, et al. (2011) 'Mutations of the SF3B1 splicing factor in chronic lymphocytic leukemia: association with progression and fludarabine-refractoriness'. *Blood,* **118** (26): 6904-8.

Saito M, Gao J, Basso K, Kitagawa Y, Smith PM, Bhagat G, et al. (2007) 'A signaling pathway mediating downregulation of BCL6 in germinal center B cells is blocked by BCL6 gene alterations in B cell lymphoma'. *Cancer Cell,* **12** (3): 280-92.

Santos-Argumedo L, Teixeira C, Preece G, Kirkham PA and Parkhouse RM. (1993) 'A B lymphocyte surface molecule mediating activation and protection from apoptosis via calcium channels'. *J Immunol,* **151** (6): 3119-30.

Sava GP, Speedy HE, Di Bernardo MC, Dyer MJ, Holroyd A, Sunter NJ, et al. (2015) 'Common variation at 12q24.13 (OAS3) influences chronic lymphocytic leukemia risk'. *Leukemia,* **29** (3): 748-51.

Schmid C and Isaacson PG. (1994) 'Proliferation centres in B-cell malignant lymphoma, lymphocytic (B-CLL): an immunophenotypic study'. *Histopathology,* **24** (5): 445-51.

Schmidt D, Wilson MD, Spyrou C, Brown GD, Hadfield J and Odom DT. (2009) 'ChIP-seq: using high-throughput sequencing to discover protein-DNA interactions'. *Methods,* **48** (3): 240-8.

Sciammas R, Shaffer AL, Schatz JH, Zhao H, Staudt LM and Singh H. (2006) 'Graded expression of interferon regulatory factor-4 coordinates isotype switching with plasma cell differentiation'. *Immunity,* **25** (2): 225-36.

Sciammas R, Li Y, Warmflash A, Song Y, Dinner AR and Singh H. (2011) 'An incoherent regulatory network architecture that orchestrates B cell diversification in response to antigen signaling'. *Mol Syst Biol,* **7** 495.

Scielzo C, Apollonio B, Scarfo L, Janus A, Muzio M, Ten Hacken E, et al. (2011) 'The functional in vitro response to CD40 ligation reflects a different clinical outcome in patients with chronic lymphocytic leukemia'. *Leukemia,* **25** (11): 1760-7.

Seifert M, Sellmann L, Bloehdorn J, Wein F, Stilgenbauer S, Durig J, et al. (2012) 'Cellular origin and pathophysiology of chronic lymphocytic leukemia'. *J Exp Med,* **209** (12): 2183-98.

Sellick GS, Goldin LR, Wild RW, Slager SL, Ressenti L, Strom SS, et al. (2007) 'A high-density SNP genome-wide linkage search of 206 families identifies susceptibility loci for chronic lymphocytic leukemia'. *Blood,* **110** (9): 3326-33.

Shaffer AL, Emre NC, Lamy L, Ngo VN, Wright G, Xiao W, et al. (2008) 'IRF4 addiction in multiple myeloma'. *Nature,* **454** (7201): 226-31.

Shaffer AL, Emre NC, Romesser PB and Staudt LM. (2009) 'IRF4: Immunity. Malignancy! Therapy?'. *Clin Cancer Res,* **15** (9): 2954-61.

Shukla V, Ma S, Hardy RR, Joshi SS and Lu R. (2013) 'A role for IRF4 in the development of CLL'. *Blood,* **122** (16): 2848-55.

Shukla V and Lu R. (2014) 'IRF4 and IRF8: Governing the virtues of B Lymphocytes'. *Front Biol (Beijing),* **9** (4): 269-82.

Silvennoinen O, Nishigaki H, Kitanaka A, Kumagai M, Ito C, Malavasi F, et al. (1996) 'CD38 signal transduction in human B cell precursors. Rapid induction of tyrosine phosphorylation, activation of syk tyrosine kinase, and phosphorylation of phospholipase C-gamma and phosphatidylinositol 3-kinase'. *J Immunol,* **156** (1): 100-7.

Slager SL, Goldin LR, Strom SS, Lanasa MC, Spector LG, Rassenti L, et al. (2010) 'Genetic susceptibility variants for chronic lymphocytic leukemia'. *Cancer Epidemiol Biomarkers Prev,* **19** (4): 1098-102.

Slager SL, Rabe KG, Achenbach SJ, Vachon CM, Goldin LR, Strom SS, et al. (2011) 'Genome-wide association study identifies a novel susceptibility locus at 6p21.3 among familial CLL'. *Blood,* **117** (6): 1911-6.

Slager SL, Camp NJ, Conde L, Shanafelt TD, Achenbach SJ, Rabe KG, et al. (2012) 'Common variants within 6p21.31 locus are associated with chronic lymphocytic leukaemia and, potentially, other non-Hodgkin lymphoma subtypes'. *Br J Haematol,* **159** (5): 572-6.

Slager SL, Achenbach SJ, Asmann YW, Camp NJ, Rabe KG, Goldin LR, et al. (2013) 'Mapping of the IRF8 gene identifies a 3'UTR variant associated with risk of chronic lymphocytic leukemia but not other common non-Hodgkin lymphoma subtypes'. *Cancer Epidemiol Biomarkers Prev,* **22** (3): 461-6.

Speedy HE, Sava G and Houlston RS. (2013) 'Inherited susceptibility to CLL'. *Adv Exp Med Biol,* **792** 293-308.

Speedy HE, Di Bernardo MC, Sava GP, Dyer MJ, Holroyd A, Wang Y, et al. (2014) 'A genome-wide association study identifies multiple susceptibility loci for chronic lymphocytic leukemia'. *Nat Genet,* **46** (1): 56-60.

Stacchini A, Aragno M, Vallario A, Alfarano A, Circosta P, Gottardi D, et al. (1999) 'MEC1 and MEC2: two new cell lines derived from B-chronic lymphocytic leukaemia in prolymphocytoid transformation'. *Leuk Res,* **23** (2): 127-36.

Stankovic T, Stewart GS, Fegan C, Biggs P, Last J, Byrd PJ, et al. (2002) 'Ataxia telangiectasia mutated-deficient B-cell chronic lymphocytic leukemia occurs in pregerminal center cells and results in defective damage response and unrepaired chromosome damage'. *Blood,* **99** (1): 300-9.

States DJ, Walseth TF and Lee HC. (1992) 'Similarities in amino acid sequences of Aplysia ADP-ribosyl cyclase and human lymphocyte antigen CD38'. *Trends Biochem Sci,* **17** (12): 495.

Staudt V, Bothur E, Klein M, Lingnau K, Reuter S, Grebe N, et al. (2010) 'Interferon-regulatory factor 4 is essential for the developmental program of T helper 9 cells'. *Immunity,* **33** (2): 192-202.

Stilgenbauer S, Schnaiter A, Paschka P, Zenz T, Rossi M, Dohner K, et al. (2014) 'Gene mutations and treatment outcome in chronic lymphocytic leukemia: results from the CLL8 trial'. *Blood,* **123** (21): 3247-54.

Strati P and Shanafelt T. (2015) 'Monoclonal B-cell lymphocytosis and early stage CLL: diagnosis, natural history, and risk stratification'. *Blood,*

Stratowa C, Loffler G, Lichter P, Stilgenbauer S, Haberl P, Schweifer N, et al. (2001) 'CDNA microarray gene expression analysis of B-cell chronic lymphocytic leukemia proposes potential new prognostic markers involved in lymphocyte trafficking'. *Int J Cancer,* **91** (4): 474-80.

Strefford JC, Kadalayil L, Forster J, Rose-Zerilli MJ, Parker A, Lin TT, et al. (2015) 'Telomere length predicts progression and overall survival in chronic lymphocytic leukemia: data from the UK LRF CLL4 trial'. *Leukemia,*

Su GH, Ip HS, Cobb BS, Lu MM, Chen HM and Simon MC. (1996) 'The Ets protein Spi-B is expressed exclusively in B cells and T cells during development'. *J Exp Med,* **184** (1): 203-14.

Takasawa S, Tohgo A, Noguchi N, Koguma T, Nata K, Sugimoto T, et al. (1993) 'Synthesis and hydrolysis of cyclic ADP-ribose by human leukocyte antigen CD38 and inhibition of the hydrolysis by ATP'. *J Biol Chem,* **268** (35): 26052-4.

Till KJ, Lin K, Zuzel M and Cawley JC. (2002) 'The chemokine receptor CCR7 and alpha4 integrin are important for migration of chronic lymphocytic leukemia cells into lymph nodes'. *Blood,* **99** (8): 2977-84.

Tsuboi K, Iida S, Inagaki H, Kato M, Hayami Y, Hanamura I, et al. (2000) 'MUM1/IRF4 expression as a frequent event in mature lymphoid malignancies'. *Leukemia,* **14** (3): 449-56.

Tsukada N, Burger JA, Zvaifler NJ and Kipps TJ. (2002) 'Distinctive features of "nurselike" cells that differentiate in the context of chronic lymphocytic leukemia'. *Blood,* **99** (3): 1030-7.

Vaisitti T, Aydin S, Rossi D, Cottino F, Bergui L, D'Arena G, et al. (2010) 'CD38 increases CXCL12-mediated signals and homing of chronic lymphocytic leukemia cells'. *Leukemia,* **24** (5): 958-69.

Vaisitti T, Serra S, Pepper C, Rossi D, Laurenti L, Gaidano G, et al. (2012) 'CD38 signals upregulate expression and functions of matrix metalloproteinase-9 in chronic lymphocytic leukemia cells'. *Leukemia,*

Wang L, Lawrence MS, Wan Y, Stojanov P, Sougnez C, Stevenson K, et al. (2011) 'SF3B1 and other novel cancer genes in chronic lymphocytic leukemia'. *N Engl J Med,* **365** (26): 2497-506.

Weilemann A, Grau M, Erdmann T, Merkel O, Sobhiafshar U, Anagnostopoulos I, et al. (2015) 'Essential role of IRF4 and MYC signaling for survival of anaplastic large cell lymphoma'. *Blood,* **125** (1): 124-32.

Wiestner A. (2013) 'Targeting B-Cell receptor signaling for anticancer therapy: the Bruton's tyrosine kinase inhibitor ibrutinib induces impressive responses in B-cell malignancies'. *J Clin Oncol,* **31** (1): 128-30.

Yamagata T, Nishida J, Tanaka S, Sakai R, Mitani K, Yoshida M, et al. (1996) 'A novel interferon regulatory factor family transcription factor, ICSAT/Pip/LSIRF, that negatively regulates the activity of interferon-regulated genes'. *Mol Cell Biol,* **16** (4): 1283-94.

Yang Y, Shaffer AL, 3rd, Emre NC, Ceribelli M, Zhang M, Wright G, et al. (2012) 'Exploiting synthetic lethality for the therapy of ABC diffuse large B cell lymphoma'. *Cancer Cell,* **21** (6): 723-37.

Zenz T, Eichhorst B, Busch R, Denzel T, Habe S, Winkler D, et al. (2010) 'TP53 mutation and survival in chronic lymphocytic leukemia'. *J Clin Oncol,* **28** (29): 4473-9.

Zhang S, Xu J, Wu S, Wang R, Qu X, Yu W, et al. (2013) 'IRF4 promotes cell proliferation by JNK pathway in multiple myeloma'. *Med Oncol,* **30** (2): 594.

Zhu YX, Kortuem KM and Stewart AK. (2013) 'Molecular mechanism of action of immune-modulatory drugs thalidomide, lenalidomide and pomalidomide in multiple myeloma'. *Leuk Lymphoma,* **54** (4): 683-7.

Zucchetto A, Bomben R, Dal Bo M, Bulian P, Benedetti D, Nanni P, et al. (2006) 'CD49d in B-cell chronic lymphocytic leukemia: correlated expression with CD38 and prognostic relevance'. *Leukemia,* **20** (3): 523-5; author reply 28-9.

Zucchetto A, Benedetti D, Tripodo C, Bomben R, Dal Bo M, Marconi D, et al. (2009) 'CD38/CD31, the CCL3 and CCL4 chemokines, and CD49d/vascular cell adhesion molecule-1 are interchained by sequential events sustaining chronic lymphocytic leukemia cell survival'. *Cancer Research,* **69** (9): 4001-9.

Zucchetto A, Vaisitti T, Benedetti D, Tissino E, Bertagnolo V, Rossi D, et al. (2012) 'The CD49d/CD29 complex is physically and functionally associated with CD38 in B-cell chronic lymphocytic leukemia cells'. *Leukemia,* **26** (6): 1301-12.

Zupo S, Rugari E, Dono M, Taborelli G, Malavasi F and Ferrarini M. (1994) 'CD38 signaling by agonistic monoclonal antibody prevents apoptosis of human germinal center B cells'. *Eur J Immunol,* **24** (5): 1218-22.

Zupo S, Isnardi L, Megna M, Massara R, Malavasi F, Dono M, et al. (1996) 'CD38 expression distinguishes two groups of B-cell chronic lymphocytic leukemias with different responses to anti-IgM antibodies and propensity to apoptosis'. *Blood,* **88** (4): 1365-74.